

MASTER THESIS

**On the kinematic processes which can give
rise to the phenomenon of high-rate water
injections into a porous medium.**

Author:
Fokke-Jan SWART

Supervisors:
Prof. Dr. Ruud J. SCHOTTING
Asst. Prof. Dr. Amir RAOOF

*A thesis submitted in fulfilment of the requirements
for the degree of Master of Science*

in the

Environmental Hydrogeology Group
Department of Earth Sciences

August 22, 2014

Abstract

This manuscript is on the phenomenon of high rate water mass injections in to a saturated confined aquifer, in aid of a better understanding of the dewatering methodology known as "Densauginfiltration" (DSI), or less common "Jet Suction Infiltration" (JSI). In this work, of exploratory nature, we present a general conceptual model for this phenomenon, the result of a literature review. Further, based on theoretical considerations on flow and deformation kinematics as well as the derivation of a Lagrangian-Eulerian balance principle, we present six possible fundamental kinematic processes which may underlie the phenomenon. In future research the relevance of these processes can be investigated, for example laboratory experiments, and may uncover the kinematics giving rise to the phenomenon.

Acknowledgements

The final words of this manuscript, displayed at the beginnings. They mark the last moment, before submission, of ponderings on high rate water injections in to an aquifer and the ending of a period of wrestling with many devils and flirting with at least twice as much angels. Although, I am convinced at the moment that essentially it where all flirts with angels and that it is likely a matter of time before I am able to recognize these devils as such. Moreover, my experience so far let me to believe that angels and devils are symmetrical although their equality is not always easy to reveal. It is a matter of perspective, so far I have had the fortunate experience that many of the devils disappear when a level of sufficient understanding was reached.

This is probably the most important concept I have been working with, at least personally, over the last period: perspective. I bumped into it while reviewing the literature for my thesis, in the form of the dynamical perspectives (Newtonian, Lagrangian and Hamiltonian) as well as the observational perspectives (Eulerian and Lagrangian). Without changes in perspective I would probably have not been able to finish this manuscript. For helping me with changing my perspective towards my thesis, in order to be able to finish it, I would like to express my gratitude to Oscar GebSKI, Femke Bosma and my brother Ewoud Swart. They achieved to set a heavy steam engine, rusted by stubbornness, in to motion and eventually let it reach as well as maintain it at full speed.

The inspiring words of my supervisor Ruud Schotting, let me to enrol into the master Environmental Hydrogeology. Consequently without him this manuscript would not have existed at all. Moreover, I may have not been able to awaken in me my interest in hydrogeology and water in general, for which I would like thank him deeply. The second reader of my thesis, Amir Raoof, I confronted with a lot of work in his well deserved holidays. I want to express my gratitude to him for helping me to get through the last bits and pieces as well as letting me know that his door was always open if I wanted to discuss something on MODFLOW.

This manuscript started as an attempt to design an experiment, although I have eventually not succeeded in that, I had the honour to have some invaluable discussions with Pieter Kleingeld. The time was not right jet for me, however he has revealed to me that experimental design is a real art, which I would like to learn definitely more about in the future. I would like to thank him for this perception. Every morning I came at the office, there was the warm welcome by Magreet Evertmam. She assured me that there was always coffee when I needed it and helped me out when I forgot pencils etc., as well as giving me the most beautiful post-its. Without these sticky notes I would have likely been lost in my notes on mathematical derivations and I want to thank her for that.

Besides raising wonderful philosophical discussions, my housemate Gijs as well as my Aikido friend Tunc helped me with digitizing figures and making some three dimensional drawings (although some did not make it to the manuscript because their mathematical treatment became to complex for me). Hence, I want to thank them for preventing that this manuscript became an even more obscure text with only letters and mathematical symbols.

During the course of writing this manuscript, I was fortunate to be allowed into the residences of Marleen and Tessa for some days, to write and contemplate, with which they helped me to dissolve some major writing blockades. Hereby I want to acknowledge their invaluable role. I also want to thank my dear friends Annelies, Elise and Zillah. They became my weekly spirit boosters, who let me grumble and successively let me share a tango dance or a nice walk with them after which I could continue working with full motivation.

The down to earth attitude of my friends Ernest, Lotte and Erica prevented me from drifting to far away on the ocean of my thoughts. In our shared coffee breaks or meals, they turned the tide by exchanging perspectives and holding me mirrors, which let me return back to the coast. I owe you my deep gratitude.

Finally, I would like to acknowledge my "Atlases", my parents who have never neglected to support me, already for twenty-seven years. The last two weeks I worked on this manuscript, they provided me a retreat where I was able to have only one concern, wrapping up this thesis. From a bigger view they provided me with invaluable wisdom, among others that "at the moment you make a decision, it is the best one you are able to make at that time. Don't regret it in the light of later acquired understanding."

Contents

1	Introduction: The phenomenon of high-rate water mass injection in a saturated aquifer.	5
1.1	Demarcating the phenomenon of high rate water mass infiltration in a porous medium. . .	6
1.2	Outline and brief sketch of the scope of this manuscript.	8
1.3	Conceptual model: The porous-medium-injection-well system.	9
1.3.1	A typical injection well & the essence of a DSI injection well.	9
1.3.2	Well entrance velocity: On defining "high" injection rates.	11
1.3.3	Stressing a porous medium by a nonoperating well.	12
1.3.4	Stressing a porous medium by seismic waves.	13
1.3.5	Stressing the fluid phase: Towards validity of well hydraulics.	17
1.3.6	Stressing the fluid phase: Fully versus partially penetrating wells.	20
1.3.7	A conceptual model for high-rate water injection into a PM.	21
1.4	Relevance for society and for understanding the physics underlying the JSI methodology.	23
1.4.1	The relevance of a better understanding of infiltration points for society.	23
1.4.2	The relevance of revisiting a porous medium its mass balance in aid of a better physical understanding of infiltration points.	25
2	A deterministic kinematic model.	29
2.1	Introduction: Kinematics of the phases of a PM	30
2.2	Deterministic variation of a smooth vector field.	31
2.2.1	Introduction: Variation from a norm.	31
2.2.2	The multivariate Taylor series expansion of a vector function.	31
2.2.3	Interpretation of the multivariate Taylor series: An Eulerian kinematic view. . . .	32
2.2.4	The total derivative of the multivariate Taylor series.	35
2.2.5	Section summary: Smooth vector fields & their polynomial variation structure. . .	36
2.3	The fundamental theorem of deformation kinematics.	37
2.3.1	Introduction: Displacements from an Eulerian observational perspective.	37
2.3.2	On the absolutely continuous nature of a displacement field, physically.	38
2.3.3	The polynomial variation structure of a smooth displacement field.	39
2.3.4	The relative displacement near a reference point.	40
2.3.5	The relative velocity near a reference point.	44
2.3.6	Section summary: The fundamental theorem of deformation kinematics.	46
2.4	Conclusion & chapter summary: A deterministic kinematic model.	46
3	A Lagrangian-Eulerian balance principle.	48
3.1	Introduction: A porous medium as an Lagrangian-Eulerian object.	49
3.2	Rate of change of the value of a $1D$ spatial integral: Leibniz's integral rule.	50
3.2.1	Introduction: Variation of an integral.	50
3.2.2	A $1D$ domain in a $1D$ space: General domain variation.	51
3.2.3	The change of the value of an integral: series approximation.	52
3.2.4	A $1D$ domain in a $1D$ space: Average domain variation.	54
3.2.5	Leibniz's integral rule.	55
3.2.6	Conclusion: Rate of change of the value of an $1D$ spatial integral.	56
3.3	Rate of change of the value of $3D$ spatial integrals: Reynolds transport theorem.	56

3.3.1	Introduction: Chain rule representation of the variation of an integral.	56
3.3.2	A 1D domain in a 3D space: General domain variation.	57
3.3.3	A 1D domain in a 3D space: Average domain variation.	59
3.3.4	Generalization of Leibniz's integral rule: A 1D domain in a 3D space.	60
3.3.5	Parallelogramic and a parallelepiped domains: Area & volume elements.	62
3.3.6	Deformation of area & volume elements.	63
3.3.7	Generalization of Leibniz's integral rule: 2D & 3D domains in 3D space.	66
3.3.8	Conclusion: Reynolds transport theorem.	68
3.4	Integrand variation: Eulerian balance principle.	70
3.4.1	Introduction: a physical approach to integrand variation.	70
3.4.2	Control volume analysis & a conservation law.	71
3.4.3	Inward flow in terms of a Flux.	71
3.4.4	Conclusions: Eulerian balance equation & conservation law	72
3.5	An arbitrary dimensional boundary integral.	73
3.5.1	Introduction: One dimensional domains and zero dimensional boundaries.	73
3.5.2	Selecting a domain of integration by a distribution function.	73
3.5.3	Selecting the boundary of a domain of integration through the gradient of the distribution function.	74
3.5.4	The boundary integral over a fixed domain.	75
3.5.5	Conclusion: An arbitrary dimensional boundary integral.	76
3.6	Conclusion & chapter summary: A Lagrangian-Eulerian balance principle.	77
4	Conclusion: Where can the injected water mass go to?	80
4.1	Introduction: Puzzle pieces coming together.	81
4.2	The Lagrangian-Eulerian mass balance over an infinitesimal portion of a porous medium.	81
4.2.1	Introduction: From a change in integral value to a change in mass.	81
4.2.2	Mass integrals for a water saturated porous medium.	82
4.2.3	Boundary velocity and solid flux velocity: A two velocity description of the evolu- tion of the solid mass.	84
4.2.4	The Lagrangian-Eulerian balance principle for the solid mass.	88
4.2.5	The Lagrangian-Eulerian balance principle for the liquid mass.	90
4.2.6	Conclusion: The Lagrangian-Eulerian balance principle for the mass of a porous medium.	92
4.3	Discussion, conclusion and advice on future research.	95
4.3.1	Discussion: On the validity of three adopted assumptions.	95
4.3.2	Conclusion: A porous medium has six elementary kinematic processes at hand to facilitate high rate water injections.	96
4.3.3	Future research: steps which can be taken to obtain a robust experimental design.	98

Chapter 1

Introduction: The phenomenon of high-rate water mass injection in a saturated aquifer.

1.1 Demarcating the phenomenon of high rate water mass infiltration in a porous medium.

The object of study in this manuscript is the phenomenon of a saturated porous medium (PM) subjected to a continuous high rate well injection of water mass. The particular interest in this phenomenon is within the commercial context of "Düsenauginfiltration" (DSI), or jet suction infiltration (JSI), as invented by Werner Wils [126, 127, 36].

The understanding of this phenomenon is still rather premature, hence the character of this research is exploratory. Roughly, from a theoretical perspective, the behaviour of a general PM is captured by the overlap of the theoretical fields of soil, rock and fluid mechanics. This overlap is typically referred to as poromechanics. Classical hydrogeology as well as the more refined Biot's poroelastic theory are special sub fields of poromechanics. From the scarce data there currently is on the subject (e.g [60, 61, 57, 52]), obtained in a JSI setting, there seems to be no convincing trend in for example the type of aquifers in which the phenomenon is observed as well as on the role of heterogeneity and anisotropy in hydrogeological characteristics. In addition there seems to be a strong believe that classical hydrogeological theory does not govern the phenomenon[129]. Consequently, we concluded that more data is required for a meaningful descriptive statistical analysis in order to be of aid in deciding whether we can start investigating the phenomenon from a particular area within the scope of poromechanical theory. As a result, in this manuscript we make a start with exploring the phenomenon theoretically, in a general sense, following the (classical) physical paradigm. The physical paradigm, in general, presupposes that a physical phenomenon can be described by 5 balance principle/equations ([116], p. 36):

- 1.) a mass balance;
- 2.) a linear momentum balance;
- 3.) an angular/rotational momentum balance;
- 4.) an energy balance; and
- 5.) an entropy balance.

Since the theoretical scope of poromechanics is rather large, we are obliged to limit it. We do this based on aquifer characteristics. The PM we consider is unconsolidated¹ confined and saturated at all times. We believe that this demarcation with respect to aquifer type does reduce the complexity significantly, however without obscuring possible fundamental physical processes. The main purpose of the demarcation is to be of aid in clarifying the discussion. As such we expect that the material presented in this manuscript can eventually be readily generalized to other aquifer types. Roughly, we see it as that in this manuscript we construe a colouring picture in section 1.3. The aquifer types are some of the available colours to colour in the picture. However, in this manuscript we will start colouring in larger "patches" relative to the detailed aquifer types.

In following Wils and Hölscher (respectively p. 2 in [127] and p. 17 in [60]), we will subject this PM to injection rates of $Q_{inj} > 40m^3 \cdot hr^{-1}$. We became aware of the fact that the injection rate on its own is rather ambiguous regarding whether it is "high" are not. In subsection 1.3.2 we briefly discuss this issue and propose an alternative discriminator in the form of the well entrance velocity. To resolve the ambiguity for the scope of this manuscript, we consider the injection rate of $40m^3 \cdot hr^{-1}$ as being "high", for injection wells with a screen length of $1m$ a diameter of $160mm$ and a slotted area of $40\%^2$.

From a more abstract point of view, the system we look at is an injection well embedded in a PM (see figure 1.8 and subsection 1.3.7 for more details). Considering the combinatorics of this system, facilitation of a high rate water mass injection maybe a result of convenient PM characteristics and the well characteristics may be negligible. In contrast, it may be completely a function of the characteristics

¹Consolidation in this sense does not refer to the process of soil consolidation, or compaction ([79], section 5.10). Here we interpret it as loose grains, contrasting attached grains (cemented, interlocked, etc.) like in rocks.

²The value of the slotted area we based on the upper limit mentioned on p. 29 in [69] and the discussion on p. 405 of [31]. We haven decided to let the slotted area be as close to the porosity value we will consider for the PM in this manuscript, in contrast to the slotted area of the actual well screen we have at our availability. This well screen has measurements of $1m$ screen length, $160mm$ screen diameter and a slotted area of about 5%.

of the well, irrespective of the PM characteristics. Another possibility is that both the facilitation of a high rate water mass injection is determined by both, PM and well characteristics.

In this manuscript we consider the contribution of the PM to facilitating the high rate injection of water mass, irrespective of the details of the injection well, i.e. we keep the characteristics of the well constant. Moreover, we assume superposable separability of the overall PM-well system, in a PM subsystem surrounding a well subsystem, where we will focus on the PM subsystem. The separability of the PM and the well subsystems will be briefly discussed below (section 1.3) in terms of how a borehole/well can stress a PM.

Neglecting the details of the injection well puts forward that in this manuscript we essentially consider a more general variant of the phenomenon of high injection rates facilitated by a saturated PM: *The phenomenon of high infiltration rates supported by a saturated PM*. Regarding this high infiltration rate phenomenon, in this manuscript we will elaborate on the question:

Where can the injected water mass go to?

Considering the physical paradigm stated above, we will focus on the first balance principle. Moreover, to answer this question we will revisit the kinematics underlying the rather general mass balance principle over a water saturated PM, referred to by Verruijt as the "storage equation" (e.g. see chapter 4 & 5 in [120]):

$$\alpha \frac{\partial \varepsilon}{\partial t} + (\phi \beta_w - (\alpha - \phi \beta_s)) \frac{\partial p}{\partial t} = -\text{div} \left[\frac{K}{\rho_w g} \text{grad} [p] \right]. \quad (1.1)$$

In this equation α is Biot's coefficient, ε is the volumetric strain, ϕ the porosity, β_w and β_s are respectively the compressibility of water and the solid phase, K is the hydraulic conductivity, ρ_w the density of the water, g the gravitational constant, and p the water pressure in the void space³.

An approximate answer to the question can be immediately given from the storage equation. The water can be transported through the PM, as described by the term on the right hand side, or it can be stored in the PM, accounted for by the two terms on the left hand side. However, in this manuscript we aim to be of aid in a deeper understanding of storage mechanisms which may take place in a PM. A better understanding of the storage mechanisms may help to assess the importance of storage mechanisms in facilitating high rate infiltration.

In this manuscript we will give a detailed theoretical re-examination of the derivation of the storage equation starting from the roots, Leibniz integral rule and its physical functioning as a general balance principle. The generality of the balance principle is with respect to the Eulerian and Lagrangian observational perspectives. Moreover, our focus in the examination is on the "shallow" kinematic aspects as opposed to the "deep" dynamical aspects.

The deep dynamical aspects are too complex to consider in this manuscript with sufficient detail. In addition, in the light of the current knowledge regarding the subject, we are inhibited from making a decision on which dynamical aspects to focus on. It is likely that the focus would turn out to be too narrow. Nevertheless, knowledge of the kinematic aspects can be of great value, especially considering that it is the connection between the dynamical aspects and what we observe. Hence, a better understanding of the kinematics may also improve the decision on which dynamical aspects to focus.

In this manuscript, with the kinematic aspects we set a frame in which the dynamic aspects can be inserted through appropriate constitutive equations. We will provide a brief account on the constitutive equations, to provide an overview which may be of aid in future research regarding the phenomenon of high rate water mass injection in to a saturated PM.

³Remark, the volumetric strain term represents the motion of the solid phase. Further, the derivation of this equation given by Verruijt ([120], chapter 4) relies on a geostatic pressure assumption imposed on the generalized Terzaghi's effective stress law. In other words, lithostatic stress state for the solid and hydrostatic stress state for the water,

$$\underline{\sigma}_{tot} = \underline{\sigma}_{eff} + \alpha p \underline{\delta} \rightarrow \sigma_v = \sigma_{eff} + \alpha p. \quad (1.2)$$

In this equation σ_{tot} is the lithostatic stress, p the hydrostatic pressure, σ_{eff} the effective stress acting on the solid grains, α Biot's coefficient and $\underline{\delta}$ the unit tensor.

1.2 Outline and brief sketch of the scope of this manuscript.

This manuscript will be structured as follows. We will continue this introductory chapter with a section in which we present a conceptual model for the phenomenon of a high rate water mass injection in to a PM, the overall system of a PM with a JSI injection well embedded in it. In this section the demarcation of what will be discussed in this manuscript (see former section) will be substantiated by first considering a typical well setup in a PM, followed by a discussion on the meaning of reporting a volumetric injection rate ("well yield") in relation to "high" injection rates. Successively, the impact of a basic injection well on a PM will be treated, essentially we will argue on which processes can occur and which are not accounted for by basic well hydraulics. Most profoundly, stressing of the PM through the casing of the well and the onset of seismic wave phenomena as well as deviations from laminar creep flow, induced by the well, within the PM.

We will conclude the chapter with a discussion on our motivations for being interested in the phenomenon of *a saturated porous medium (PM) subjected to a continuous high rate well injection of water mass*. and the more general phenomenon of *high infiltration rates supported by a saturated PM*. This will be done by first discussing the relevance of the more specific phenomenon to society, viz. its value for the dewatering industry and the artificial recharge industry. Second, we shall briefly elaborate on how we got to the topic, the question of *Where can the injected water mass go to?* as well as the approach to answer the question, the theoretical analysis of the storage equation (the general mass balance principle used in hydrogeology).

The body of this manuscript comprises three chapters. In the second chapter we treat a rather general kinematic model. This model is well known in continuum mechanics and especially in fluid mechanics and may be known as *the fundamental theorem of deformation kinematics*. The model describes a.) rigid translations (global); b.) rigid rotations (global); c.) dilatation (local); and d.) spin/vorticity (local).

The model is founded on the physical concept of a displacement and the mathematical result known as "Taylor's theorem". We will discuss the model from an Eulerian observational perspective and hence in terms of the derived concept of a displacement field. This puts us in the position to describe the kinematics of general objects subjected to a continuous, smooth and slowly varying displacement field. Thus, besides the kinematics of the physical object of a continuum body, we can also discuss the kinematics of a mathematical object such as a domain of integration. As a side result, we discuss in this chapter Taylor's theorem for a vector function, rather at length. This technical result dominates deterministic mathematical physics and we rely on it in the subsequent chapters.

In chapter three we derive a general balance principle, with respect to the Lagrangian and Eulerian observational perspectives. In other words, we will obtain in chapter three a Lagrangian-Eulerian balance principle. A balance principle is in most physical problems the fundamental object and a Lagrangian-Eulerian balance principle seems to be its most general form. We will derive the balance principle by starting from Leibniz's integral rule for differentiation under the integral sign, for one dimensional integrals. From it we will distil the "algorithm", as outlined in [40], of considering the total time derivative of an integral as being composed of a integrand variation contribution as well as a contribution due to varying the domain of integration. From a physical point of view, we associate the integrand variation with an Eulerian perspective and the domain variation with a Lagrangian perspective. Further more, in this chapter we shall generalize Leibniz's integral rule to three dimensions and discuss its connection with Reynold's transport theorem. The major difficulty in the generalization lies in the domain variation contribution. To tackle this difficulty, we will rely on the results of chapter two to discuss the domain deformation/variation. After discussing the integrand variation from a more physical perspective, we conclude by combining our results of the domain and integrand variation and come up with a Lagrangian-Eulerian balance principle.

In the fourth and concluding chapter we will apply the result from chapter three, the Lagrangian-Eulerian balance principle, to the physical quantity of mass. Moreover, the rather theoretical considerations from chapter two and three put us in the position to obtain a rather general mass balance principle. We will obtain this balance principle by first discussing the kinematics of the mass balance principle. Our focus will be on storage mechanisms, hence on the compressibility of the PM its skeleton, the solid phase and the water. Based on this result we will give an answer on the question posed: *Where can the injected water mass go to?* We will finalize this chapter with some ideas for future research, geared towards experimental investigation of the phenomenon of high rate water mass injections into a saturated

1.3 Conceptual model: The porous-medium-injection-well system.

1.3.1 A typical injection well & the essence of a DSI injection well.

From the literature it is known that injection wells are fairly similar in design to extraction wells (e.g. p. 769 in [31], p. 540 in [93] or p. 5 in [72]), though they are more sensitive to failure. Particular clogging of the well screen is a serious problem (e.g. see p. 769 in [31] or p. 5 in [72]).

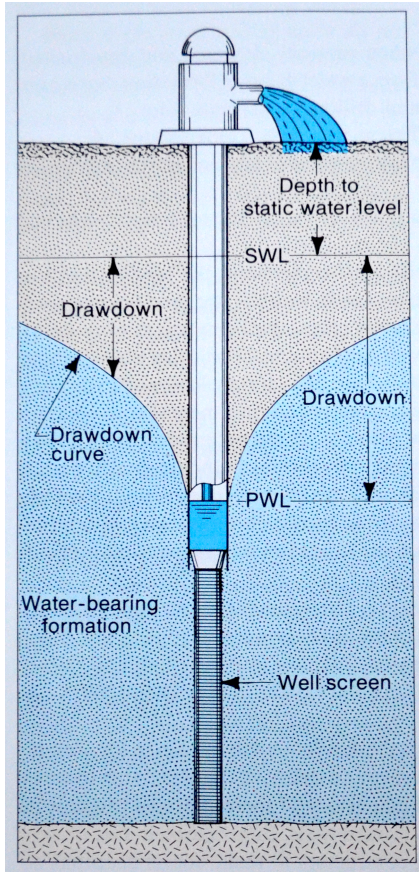
The essence of a theoretical well design for a certain well yield (injection rate or extraction rate), entails hydrogeological and well-construction considerations (e.g. see chapter 13 in [31], chapter 10 in [69], chapter 6 in [93], section 2.3 in [69], or [125]):

- | | | |
|--|---|-------------------|
| <ul style="list-style-type: none"> (1) Lithological facies (distribution of physical parameters of rocks or regolith, p. 376 in [65]) (2) Geochemical facies (distribution of chemical parameters of rocks or regolith) (2) Hydrogeological facies (distribution of hydrogeological parameters) (3) Water mass balance conditions (4) Water chemistry | } | hydrogeological |
| <ul style="list-style-type: none"> (6) Casing diameter (7) Well depth (8) Well screen length and diameter (9) Slot width, length and spacing on the screen. | } | well-construction |

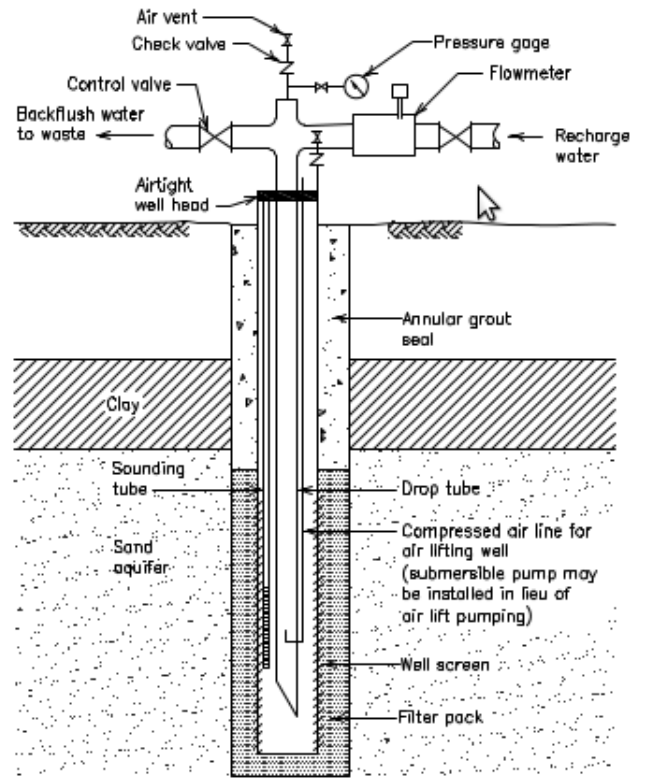
⁴ In this manuscript, the chemical considerations are neglected. Further, note that a practical well design comprises much more detail of which treatment is beyond the scope of this manuscript. The interested reader may consult chapters 12-15 17 & 19 in [31], chapters 18 & 19 in [93], or for a brief overview [125]. Knowledge of the outlined characteristics seems to be sufficient to make theoretical (analytical) well design assessments for a wide variety of wells, at least for the variants governed in the book of Kruseman [69].

A typical conceptual model for a water extraction/pumping well is given on p. 206-207 of [31] and a prototype injection/recharge well is given on p. 547 of [93], which we have included, figures 1.1a and 1.1b.

⁴A facies is a demarcated region with similar characteristics (p. 30 in [27] or p. 19 in [97]). It may be a convenient way to discuss (spatial) heterogeneity, e.g. see p. 196 in [2].



(a) A typical extraction well, p. 206 in [31]



(b) A typical injection well, p. 547 in [93]

Figure 1.1: Two "school examples" of water wells. Figure 1.1a is more theoretically oriented and figure 1.1b is more practically oriented.

According to Driscoll (p. 769 in [31]), the main differences between an extraction and an injection well are the well-construction related characteristics of the entrance velocity and the screen length. The well (or PM) entrance velocity is a parameter to get insight in the dissipation of flow energy due to the well. It can be regarded as a function of the position on the well screen, the slot characteristics (screen open area), as well as length and diameter of the well screen. The theoretical entrance velocity will be discussed in more detail in subsection 1.3.2. Further, for injection wells it is important, given the problem of clogging of the well screen, that the screen open area (which can be obtained from the slot information) as well as the screen length are optimal. In the following we will briefly treat the different well construction characteristics, in the context of a presupposed well yield.

For a confined aquifer, saturated at all times, the thickness of the aquifer is the major factor setting a limit to the length of the well screen. As a rule of thumb, the most optimal screen length is 80 to 90 per cent of the thickness of the confined aquifer (e.g. see p. 433-434 in [31] or p. 29 in [69]). Kruseman ([69], p. 29) makes the remark that this rule of thumb can be also used as a rough validation for the Dupuit/Dupuit-Forchheimer assumption, i.e. that the flow to a well is approximately horizontal (e.g. see section 8.1 in [13]). This assumption underlies most analytical equations for flow towards or away from a well.

The slot characteristics of a screen are predominantly related to the grain size distribution of the aquifer. However, in the analytical well equations this information is not taken in account, it seems to be "implicitly" taken care of by setting it equal to the porosity of the aquifer. The reason for it might be that, slot characteristic considerations, besides matching the porosity, are mainly their in order to prevent the screen from clogging. For the scope of this manuscript slot characteristics are important for the theoretical well entrance velocity, however we consider them to be given. Therefore, a more detailed account on slot characteristics is beyond the scope of this manuscript and we would like to refer the

interested reader to Driscoll ([31], p. 434-447).

The diameter of the well screen seems to be a rather independent factor regarding the hydrogeological characteristic of an aquifer. It can be considered as the factor to fine tune a well design such that the entrance velocity remains below its empirical limit of $0.03m \cdot s^{-1}$ for extraction wells and $0.015m \cdot s^{-1}$ for injection wells ([31], p. 450, p. 769 and appendix 13.I). The screen diameter does affect the well yield, however relatively small in comparison to the length of the screen. As a rule of thumb ([69],p. 29): "Doubling the diameter would only increase the well yield by about 10 per cent, other things being equal."

The essence of a jet suction infiltration well, is that a JSI nozzle is placed in the injection well, just before the well screen. The nozzle constricts the flow through area and the observed effect is that it facilitates larger injection rates. For example see the Potsdam example in [127] (p. 1), where the nozzle constricts the flow area from a diameter of $150mm$ to a diameter of $100mm$. See figure 1.2 for an illustration.

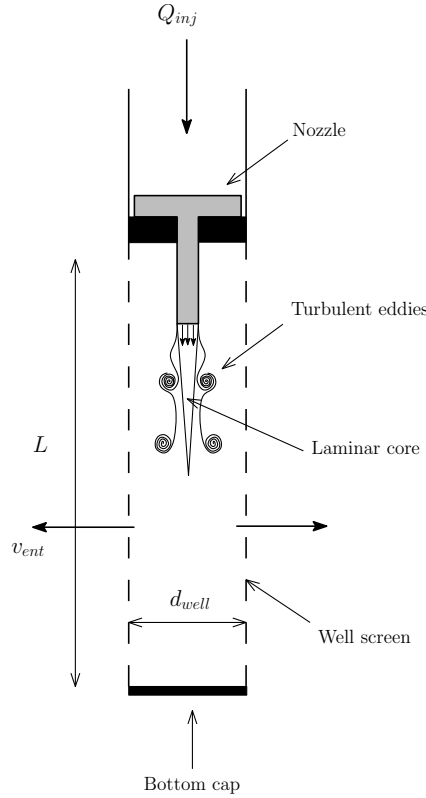


Figure 1.2: A JSI nozzle placed in an injection well, Q_{inj} refers to the injection rate, v_{ent} is the entrance velocity (outflow velocity), L is the screen length, d_{well} the screen diameter and ϕ_{slot} the well screen porosity (slotted fraction). The turbulent eddies together with the laminar core can be interpret as a manifestation of a Kelvin-Helmholtz instability/flow, for example see [68] for a "school example" of flow through a nozzle.

1.3.2 Well entrance velocity: On defining "high" injection rates.

We came aware of the fact that solely giving an injection rate does not necessarily mean that an injection rate is "high". For example, Driscoll reports an injection rate as high as $\approx 170m^3 \cdot hr^{-1}$ ([31], p. 769), without other details. In a similar vein, Wils reports an injection rate as high as $40m^3 \cdot hr^{-1}$ ([127], p. 2). Wils mentions a screen diameter, though it seems also here that more details are lacking. However, comparing the mentioned injection rates, $170m^3 \cdot hr^{-1}$ exceeds by far the rate of $40m^3 \cdot hr^{-1}$ and one may start wondering about what a high injection rate is.

The details about the well mentioned by Driscoll can be found in [72]. This recharge well, located in Nebraska, had a screen length of $24.4m$, a well diameter of $457mm$ and slots having a width of $1.0mm$

([72], p. 33). We were not able to trace back the details of the well belonging to the injection rate given by Wils, though we have found a JSI related "substitute" in the report of Hölscher [60]. The recharge well used by Hölscher, to inject $40m^3 \cdot hr^{-1}$, had a screen length of $2m$, a diameter of $200mm$ and a slot width of $0.5mm$ ([60], p. 16).

To resolve the ambiguity, the theoretical concept of a well entrance velocity can be employed as a discriminating characteristic between "ordinary" and "high" injection rates. The entrance velocity of a well can be regarded as a function of the position on the well screen, the slot characteristics (screen open area), as well as length and diameter of the well screen. However, in practice the average well entrance velocity will suffice. Mathematically the entrance velocity is defined as (e.g. see p. 451 in [31], p. 280 in [93] or [125]),

$$v_{ent} = Q_{inj} / (\phi_{slot}A). \quad (1.3)$$

In this equation Q_{inj} is the injection rate, ϕ_{slot} the fraction of the screen slotted, A the area of the well screen and v_{ent} the entrance velocity (see figure 1.2).

Unfortunately, this requires information about the area of the screen available for flow (ϕ_{slot}), which seems not to be reported in either [60] or [72] (besides the slot width we also need the slot length as well as slot spacing).

Though, to give a rough estimate, recall from above that the screen length is known to be the dominant parameter controlling the entrance velocity, leaving the screen diameter to function as a "smaller scale" refinement parameter. If we suppose both well screens are slotted at the suggested limit, i.e 40 per cent ([69], p. 29), then the respective entrance velocities are $v_{ent} \approx 12.16m \cdot hr^{-1}$ and $v_{ent} \approx 79.58m \cdot hr^{-1}$ for respectively the Nebraska well and Hölscher's well. Consequently, in this light it is clear that Hölscher's well injects water mass under high rates. Note, the entrance velocity for the Nebraska well is below the advised maximum entrance velocity of $54m \cdot hr^{-1}$ (or $0.015m \cdot s^{-1}$ as given by on p. 769 of [31]), whereas the well reported by Hölscher exceeds the maximum velocity. For a discussion on the suggested maximum well entrance velocity see appendix 13.I in [31].

From this brief example we infer that it is important to report the well characteristics in order to compare well injection rates/yields. Solely a yield does not disclose much about the "highness" of a rate. Further it seems to us that the average well entrance velocity is a rather good summary description of a well and that it is of use in comparing well rates/yields. The reason for it being that a.) it captures the mentioned relevant theoretical characteristics of a well, independent of hydrogeological characteristics; b.) it is a relevant measure for both extraction and injection wells (see former subsection); and c.) its "flow through area intensive nature" (e.g. see p. 68 in [13] on intensive and extensive descriptors) suggests its comparative value.

1.3.3 Stressing a porous medium by a nonoperating well.

A borehole with a water well completed in it, may stress a saturated PM, simply by being "present" without operating. Suppose the PM is initially in approximate geostatic equilibrium, i.e. hydrostatic conditions for the water and lithostatic conditions for the solid⁵. The construction of the well stresses the PM, hence may disturb the equilibrium and thus the geostatic state due to that it produces deviatoric stress components.

The continuum mechanical definition of a fluid hinges on that a fluid cannot withstand shear stresses under static conditions (e.g. see section 1.2 in [62], section 9.1 in [79] or section 12.2 in [21]), whereas a solid can. Moreover, in contrast to a solid a fluid does not have a shear strength. As a consequence, as long as a deviatoric stress component exists, it continuously deforms or flows with the purpose of resolving these stresses and a solid appears to do not, like a rigid body. However, according to Heim's rule, at very large, geological time scales a solid may resolve the deviatoric stresses as well. In other words over very long times scales solids exhibit creep flow behaviour. Consequently, the "withstanding" of deviatoric stresses is a relative notion.

According to this definition of a fluid and Heim's rule, the water resolves the deviatoric stress components much quicker than the solid. Consequently, we will eventually have a setting of a PM with

⁵Note, lithostatic conditions for the solid is a rather rough approximation, e.g. see [59] or section 5.1 in [132]. The approximation is known as Heim's rule and is founded on the idea that "... the rock is assumed to behave viscoelastically, according to a Maxwell or Burgers model ..., the stress state will eventually approach a lithostatic condition given sufficient (geological) time" (Heim (1878) on p. 400 in [66] or p. 2 in [132]).

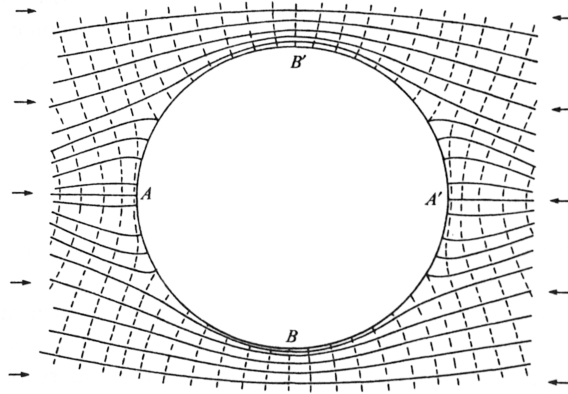


Figure 1.3: This figure originally appeared on p. 269 in [79]:” *Distribution of stress around a borehole. The full and broken lines are the trajectories of the maximum and minimum principal stresses, respectively.*”

a well, where the water retained its hydrostatic state as opposed to the solid, which will likely be left with deviatoric stresses. Besides that, since the solid resolves the deviatoric stresses at such a slow rate (geological times scales) we can regard the solid phase to be in equilibrium with the borehole/well, we will not see it ”creep”, and hence has a shear strength. In addition, liquids and solids have in general a compressive and tensile strength, i.e. they can withstand compressive and tensile stresses.

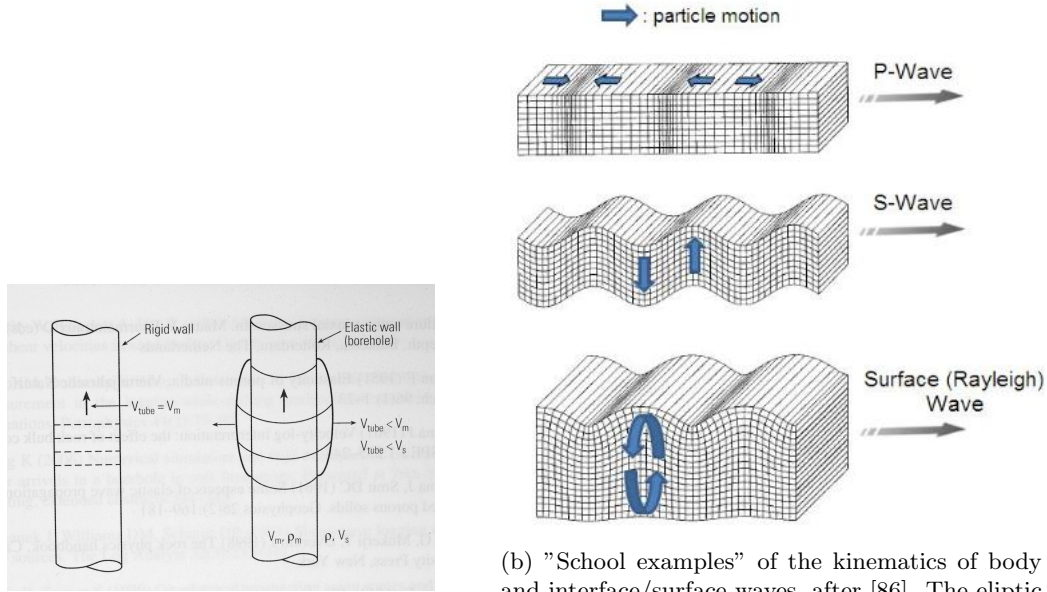
The deviatoric stresses induced by the well/borehole are typically local and the disturbance in the stress field does not penetrate far in to the surrounding solid (e.g. see [59] for a nice explanation). Furthermore, the effect of the borehole on the stress field is the concentration of stresses (e.g. see p. 269 in [79], p. 63 in [99] or [59, 119]), in analogy to the convergence of flow in case of a well in operation. See figure 1.3 for an illustration. Further considerations on the effect of a nonoperating well/borehole on the solid phase of a PM is beyond the scope of this manuscript. The reason for it is that we do not consider in this manuscript explicitly the stress state of the PM before the completion of the well.

1.3.4 Stressing a porous medium by seismic waves.

In basic well hydraulic theory (e.g. see [69, 31, 125, 93]), the effect of a working water well on a PM is as such that it stresses the water phase by applying a pumping pressure to it. The stressing of the water phase in turn stresses the solid phase and hence the PM as a whole. This indirect way of stressing the solid phase is captured theoretically by Terzaghi’s law of effective stress (e.g. see p. 54-55 in [13] or p. 58-59 in [42]) and the response of the solid phase is captured by the strength (static friction) of the solid as well as solid matrix and solid phase compressibility. However, a well in operation can also stress directly the solid phase (superposed on the borehole excavation effect considered above) due to the well bore fluid pressure communicated through the well casing to the PM.

In case that the bore fluid pressure as well as the pore-fluid pressure are sufficiently high, such that the static friction of the solid phase and/or well casing is overcome, deformation occurs. The stressing can be transient or steady. In turn, the transient stressing can be monotonic or fluctuating (”periodic”). In case of periodic stressing the resulting deformation manifests itself as a seismic wave. We regard the transient stressing to be bounded, which implies the monotonic case to be a transition between two constant stressing states and for the periodic case the fluctuation to remain between two extrema. For the scope of this manuscript we set aside the monotonic transient stressing, which can be interpreted as neglecting the details between two successive steady stressing states.

The essence of well casing stressing of the PM is that the casing can dilatate as a result of an imbalance between well bore pressure and lateral earth pressure (e.g. see chapter 1 in [28] or [78, 91]) acting on opposite sides of the casing. In case of constant or quasistatic stressing, the casing simply sets itself to a new equilibrium well radius in accordance to the stress field, elastic and strength properties. The constant stressing effect is analogous to the above mentioned excavating effect. Periodic stressing results in a vibration of the casing, inducing seismic waves, see figure 1.4a for an illustration.



(a) After Ellis ([38], p. 527. Vibration of a borehole motion displayed for the Rayleigh wave is a charge-giving rise to a Lamb wave (low frequency Stoneley wave) characteristic of all interface waves (e.g. see p. 19-20 in [95]).

Figure 1.4: Visualizations of the kinematics of Seismic waves.

In seismology, in general, two classes of waves are recognized (e.g. see section 2.4 and 2.7 in [110], chapter 2 and 8 in [107] or chapter 5 in [4]):

- a.) body-waves (P- & S-waves); and
- b.) surface-, or interface-waves (Rayleigh-, Scholte- & Stoneley-waves [95, 41, 30]).

Surface waves are essentially composite waves arising from interference among the "elementary" body waves (e.g. see p. 10 in [95]). For an illustration of the discriminating kinematics of these main two classes of seismic waves see figure 1.4.

Let us assume that the elastic properties of the PM are homogeneous. From the articles of Crain [24] and Dusseault [34] it seems that the PM-well system can support up to nine different kinds of wave modes. Four of the wave modes may actually reside within the interior of the PM whereas the other five modes are supported by the borehole or they live in the interface zone of the PM and the borehole. Moreover, the four interior modes can have their origin within the borehole, e.g. due to a fluctuating bore fluid pressure, or within the PM due to fluctuating pore fluid pressures. Note, in case of elastic heterogeneity, the PM may support additional interface wave modes (Stoneley).

Biot proved theoretically the possibility of the three elementary waves which could reside within the interior of the PM [14, 15]:

- 1.) a rotational wave (S-wave);
- 2.) a fast dilatational wave (P-wave) progressing through the solid phase;
- 3.) a slow dilatational wave (P-wave) traversing through the fluid phase.

In addition, within the theory developed by de la Cruz and Spanos (e.g. see [25, 26]) there is recognized a fourth wave (e.g. see [34, 35, 43]),

- 4.) a porosity dilatation wave.

It seems that this wave is essentially a Scholte wave, a wave at the interface between a solid and a fluid, at the pore-scale (e.g. for a definition of Scholte waves see [30, 41, 95]). For more information on how the Scholte wave/porosity dilatational wave can be induced by a borehole see [49].

The five remaining waves associated with the borehole are essentially "guided" by the borehole, or borehole-PM interface (e.g. see [22, 24] or section 18.5 in [38]). They are:

- 5.) a surface compressional wave;
- 6.) a shear surface wave (psuedo-Rayleigh wave);
- 7.) a Stoneley wave;
- 8.) a Lamb wave (waterhammer); and
- 9.) a fluid compressional wave (mud wave).

Of these five waves the psuedo-Rayleigh, Stoneley and Lamb wave seem to be of most impact in acoustic borehole logging (e.g. see p. 14-19 in [84], p. 3 in [114]). For an illustration of a typical acoustic waveform from borehole logging see figure 1.5. Remark, regarding interface characteristics they are one and the same, "Stoneley waves" (e.g. see p. 12 in [95], [41, 30]). However, the recognition of Lamb waves can be considered as a refinement, based on frequency. Consequently, in acoustic logging it is customary to refer to Stoneley waves as high frequency solid-solid interface waves and Lamb waves as low frequency solid-solid interface waves (e.g. see [24], p. 525 in [38]).

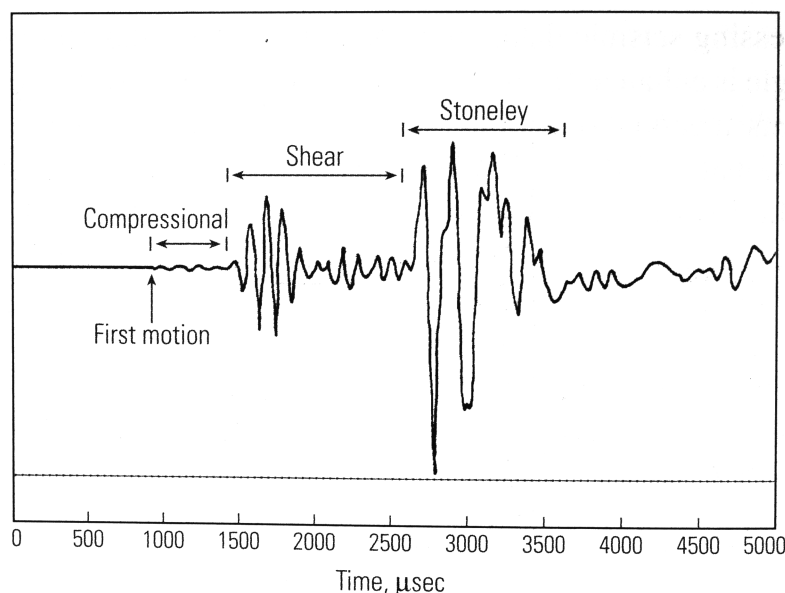


Figure 1.5: A "school example" of an acoustic wave form obtained from borehole logging. The three main wave modes are indicated, after Ellis, p. 520 in [38].

Basic hydrogeological theory neglects the stressing of the PM due to the borehole fluid/casing. This can be interpret as that within the PM-well system the theory demarcates a PM- from a well-subsystem. Besides the effect on the pore fluid pressure due to extracting or injecting water, the systems are then considered as separable and as a first approximation the well-subsystem effects are assumed to be negligible.

The validity of separation of phenomena is in general a matter of scale. Most important would be the magnitude of the deformation as a result of the borehole associated waves, i.e. their amplitude, and the spatial extend of the waves (deformation). Here we discuss briefly only the latter, since to argue on the amplitudes of the waves we have to know the elastic properties and stressing function/source, which is rather specific information and too restrictive for the moment.

Insight in the spatial scale at which the wave phenomena operate can be obtained from the attenuation characteristics of a wave. In general seismic waves damp out, or attenuate in four manners:

$$\begin{array}{ll}
 1.) & \text{geometric spreading} \\
 2.) & \text{scattering} \\
 3.) & \text{multipathing} \\
 4.) & \text{internal friction}
 \end{array}
 \left. \vphantom{\begin{array}{l} 1.) \\ 2.) \\ 3.) \\ 4.) \end{array}} \right\}
 \begin{array}{l}
 \text{elastic} \\
 \\
 \\
 \text{plastic/inelastic}
 \end{array}
 \quad (1.4)$$

Geometric spreading, i.e. the spatial diffusion of seismic energy, is the dominating attenuation mechanism. Scattering and multipathing depend on heterogeneity in the elastic properties of the medium the wave propagates through. For simplicity we assume a homogeneous medium and hence we can neglect them. Internal friction is the result of plastic deformation of the medium due to the wave, which can be thought of in a macroscopic sense due to compressive or shear plastic deformation. Typically shear contributions dominate over compressive contributions and as a first approximation the compressive contribution can be neglected (e.g. see p. 192 in [110] or p. 114 in [107]).

Body and surface waves differ significantly in how they are affected by geometric spreading. Body waves propagate three dimensionally (spherically), hence their energy density decays approximately proportional to r^{-2} and their amplitude to r^{-1} . In contrast, surface waves propagate two dimensionally (cylindrically), therefore their energy density decays approximately proportional to r^{-1} and their amplitude to $r^{-1/2}$ (e.g. see p. section 3.7.2 in [110] or p. 135 in [73]). Hence, surface/interface waves reach deeper in to a medium before they are damped out, at least in the direction of propagation.

The attenuation of the amplitude A of a wave as a result of internal friction can be described by an exponential function, depending on the frequency of the wave ω (higher tortuosity), the distance of propagation from the seismic source r , the propagation velocity (celerity) c and an attenuation strength Q (e.g. see p. 113 in [107], section 3.7.5 in [110], section 5.5 in [4] or section 3.3.2.7 in [73])

$$A(x) = A_0 e^{-\omega r / (2cQ)} \quad (1.5)$$

As stated earlier, the main wave phenomena associated with the existence of a borehole in a PM, hence can affect a PM through the casing, are the P- and S-waves excited within the borehole, which are transmitted to the PM, as well as tube waves in the form of the high frequency Stoneley wave or low frequency Lamb wave. In case of water wells, Lamb waves can be induced by a rapid change in the direction of the water flow in the well bore. This Lamb wave is also known as a "water hammer" (e.g. see [133] or 18.5.2 in [38]). A tube wave is not transmitted to the PM, at least not to the interior, since its direction of propagation is along the PM-well interface. Therefore, the penetration depth of the tube wave is determined by the influence of the amplitude in the direction normal to the direction of propagation and hence the attenuation of the amplitude due to internal friction alone. According to Rauch (p. 12 in [95] or [30]), as a rule of thumb, interface waves in general are attenuated to negligible amplitudes over one wave length⁶. This is in line with the numerical results of Baker (1984), as mentioned on p. 30 in [83], indicating penetration depths of slightly larger than one wave length.

Without attenuation P- and S-waves may penetrate in to the interior of the PM however, geometric spreading and internal friction limit their reach. As a rule of thumb, the penetration depth of the collective of waves used in acoustic logging is about one wavelength of the P -wave, which is according to Paillet on the order of $\sim 50\text{cm}$ ([83], p. 129). Note, as we can see from figure 1.5, interface waves have typically larger amplitudes than body waves. This implies, given that geometric attenuation dominates, that interface waves may penetrate deeper into the PM than body waves. However, dispersive behaviour of the Stoneley- and Lamb-wave seem to confine them to "skin deep" extends (e.g. see p. 154 in [114]). Which may be an explanation for the P-wave penetration depth as defining the range of influence of wave phenomena having their origin within the borehole.

Further treatment of the direct stressing of the PM by an operating well, i.e. by the well casing, is beyond the scope of this manuscript. The purpose of the above is simply to sufficiently substantiate, considering the exploratory nature of this research, the separation of the PM subsystem from the well-subsystem as well as to provide directions in the literature for further research, when of interest. In following the latter, we would like to note that hydrogeological characteristics can considerably affect the attenuation of a seismic wave due to internal friction. For example, the factor describing the strength

⁶Theoretically, based on the exponential form of attenuation due to internal friction an absorption distance can be defined as e^{-1} at which the initial amplitude of a wave is attenuated to roughly 1/3 (e.g. see a. 135 in [73]).

of the attenuation is known to be a proportional to the saturation of the PM, the permeability, effective stress crack density and (grain) cohesiveness of the PM (e.g. see [22], p. 183 in [115], [18, 63]). In addition, the mathematical description of seismic wave phenomena affecting porous media is essentially considered to be governed by Biot’s poroelastic theory [14, 15, 16, 16] and in particular Biot-Rosenbaum theory (e.g. see [113]).

To argue on the separation of the two subsystems, as noted, we should have a sense of scale. In the above we have summarised some rule of thumbs which can be found in the literature, mainly the acoustic logging literature. At best, we can say that whenever our PM is much larger than the wavelengths of the seismic waves generated within the well, then these deformation phenomena have a relative ”skin deep” effect and as a first approximation we disregard them. Unfortunately at the moment we do not know yet something about wave lengths, however as a first estimate we may consider the absolute order of $50cm$. Thus, as long as we do not care about the deformation within the $50cm$ annulus of the well, we can separate the PM from the ”well-casing” effects. For the rest of this manuscript we assume that the transient stressing effects of the PM due to the well casing, if it occurs, are maintained in a negligible small zone around the well.

In the above we have omitted the treatment of wave phenomena in the interior of the PM. We will not consider them here, or in this manuscript, since this research is of exploratory nature and we are concerned with ”extend”/scale. The extends, if they are bounded, can be set by steady state considerations and the wave phenomena occur between the deformation related extends, hence we regard them as a special cases which suit an investigation of ”refinement” nature. Not treating them here, does not affect the accuracy of this manuscript, it is a matter of precision. In contrast, the just presented brief considerations on borehole wave phenomena are relevant. The reason is that we wanted to know, roughly, the implications of narrowing the scope by neglecting casing-stressing of the PM. Neglecting these wave phenomena may affect the accuracy and assuming their irrelevance requires a reasonable explicated assumption. Further more, work regarding deformation due to wave phenomena is done elsewhere (e.g. see [94]). For the rest of this manuscript we will consider a constant stressing of the PM hence we do not consider wave phenomena any further.

1.3.5 Stressing the fluid phase: Towards validity of well hydraulics.

In the former we, among others, argued on the separability of the PM and well subsystem. From the argument it follows that we can consider the systems separable whenever the PM is negligibly affected by the well casing. In other words, stressing of the PM is constraint to increasing the pore pressure. This is what is accounted for in basic well hydraulics, within the scope of hydrogeology.

However, well hydraulics also relies on the assumption that the flow patterns resemble creep flow through the PM, at least on the average, such that Darcy’s law is valid. The implication of assuming creep flow, is such that we deal with the minimum energy dissipation situation regarding flow. This follows from Helmholtz’s minimum energy dissipation theorem which states that ([12], p. 227): ”... *a flow with negligible inertia forces has a smaller total rate of dissipation than any other incompressible flow in the same region with the same values of the velocity vector everywhere on the boundary of the region.*”

From a kinematic point of view, Helmholtz’s theorem can be roughly understood as that creep flow in a PM can be associated with the flow having flow paths with minimal lengths. Different flow patterns, i.e. transitional and turbulent flow are characterized by longer flow paths, due to significant curvature and changes in curvature (tortuosity) of the paths (e.g. see [20, 37, 90, 50]), bounded by the void walls. Consequently, these flows have larger energy dissipation. Theoretically it is described by the concept of ”eddy viscosity”/Reynolds turbulent stresses (e.g. see chapter 11 in [79], chapter 8-10 in [104], [118, 89, 88]). In addition, significant curvature and tortuosity of the void channels induces additional void-wall dissipation of the flow (e.g. see section 6.5 in [3]). In turn, these void space related effects induce larger energy dissipation. Mathematically the latter is often described by the Darcy-Forchheimer flow equation for PM, as long as the flow patterns are laminar (e.g. see section 5.11 in [13] or [50]).

In this manuscript we will adopt a creep flow pattern as a first estimate for flow through a PM, mostly for mathematical convenience. However, we stated above that other flow patterns are associated with higher energy dissipation and therefore require more flow work⁷ to be performed to attain the same

⁷See for a definition of this kind of physical work chapter 6 in [123].

specific discharge through a slab of PM (See figure 1.6 for an illustration). Moreover, for a given void space (flow through geometry) and a given global pressure gradient, deviations from creep flow inhibit water mass injection in a PM, the opposite of what we aim for.

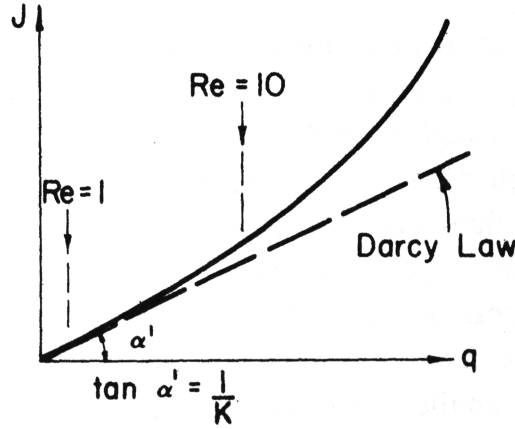


Figure 1.6: "Schematic curve representing experimental relationship between the specific discharge q and the hydraulic gradient J ", after p. 177 in [13].

Since Reynolds experiments (e.g. see section 9.1 in [3] or p. 365 in [79]) it is well known that deviations from a laminar flow pattern, for a given flow geometry, eventually occur when the velocity is increased beyond a certain value⁸, i.e. at some point the laminar flow pattern becomes unstable. Dynamically, this happens when inertial forces grow beyond their negligible status and is customary quantified by the Reynolds number: the ratio of inertial over viscous effects. For water flow through porous media the relation is (e.g. see p. 125 in [13]),

$$Re = \frac{qd\rho_w}{\mu_w}, \quad (1.6)$$

with q being the Darcy flux/specific discharge, ρ_w the density of water, μ_w the dynamic viscosity of water and d the average grain diameter of the solid matrix. It is known from experiments that for PM flow, the laminar creep pattern can be maintained up to a certain value for Re in the range of 1-10 (e.g. see p. 126-127 [13] or [50]). Thus, there is a limiting velocity by which we can transport water through a PM under the most efficient, creep flow conditions. This implies there is an optimal pressure gradient beyond which the proportion of the pressure energy converted in to heat increase relative to the proportion that is used to perform work, i.e. the ratio of pressure gradient over specific discharge increases ([13], p. 177).

Consider Prigrione's principle of minimum rate of entropy production. This principle can be used as a "decision" tool between multiple physical plausible equilibrium states where a system in nonequilibrium may tend to, given a context. It states that the equilibrium state with the smallest rate of entropy production is the one a system tends to [55].

So far we kept the void space fixed, however actually the void space may deform. Suppose the PM is stressed by increasing the global water pressure gradient. If we assume that Prigrione's principle can be validly applied, then the void space will deform if it means that it can transfer to a more efficient equilibrium state given the circumstances. Moreover, under the same boundary conditions, whenever deformation of the PM can drive the system to a state with a lower rate of entropy production it will do so. Suppose that this new equilibrium state comprises a static solid matrix and hence that water flow is the only dynamic process. This implies that the dissipation of energy can be only lower, relative to the former equilibrium state, if the resistance to the flow is smaller and hence that the flow pattern tends to a creep flow pattern (Re decreases).

From this we conclude that the purpose of the deformation of the PM is to minimize the dissipation rate, if Prigrione's principle applies. Hence, besides the mathematical tractability of considering creep

⁸Strictly speaking, the current experience is as such that no flow of water is unconditionally stable.

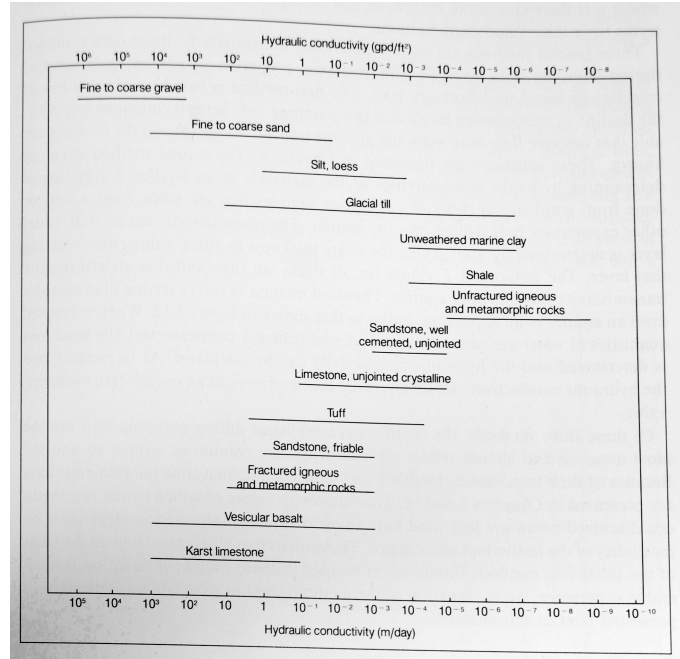


Figure 1.7: Typical hydraulic conductivity values for consolidated and unconsolidated aquifers, after [31], p. 75.

flow, it makes also physical sense to consider this flow pattern. Helmholtz principle and Prigrione's principle dictate that it is the flow pattern a PM system will tend to if it has the choice.

To obtain a rough estimate of the extend from how far a flow pattern may be from Creep flow of water through a PM, consider a synthetic PM of uniform rigid spheres and equation 1.6. The spheres are least economically packed, most efficient regarding porosity, following a cubic packing which is known to have a porosity of $\phi = 47.64\%$ (e.g. see p. 46 in [13]). Note, this packing can be interpreted as a liquefaction limit, a further increase in porosity due to deformation means that the grains become disconnected. Further we aim the PM to resemble as close as possible a "gravel", simply because their hydraulic conductivity values favour water transport (e.g. see figure 1.7). The grain size limit of gravels lie in the range of $d > 2mm$ (e.g. see p. 40 in [13]). We assume the water to have a temperature of $10^\circ C$. Consequently the water has a dynamic viscosity of $\mu_w = 1.31 \cdot 10^{-3} kg \cdot m^{-1} \cdot s^{-1}$ and a density of $\rho_w = 999.70 kg \cdot m^{-3}$. As an estimate of the flow velocity a PM should sustain when it is subject to a high rate injection we take the value for the PM (well) entrance velocity as computed for the Hölischer well in section 1.3.2, i.e. $v = 79.58 m \cdot day^{-1}$. The Reynold's number for this setting is,

$$Re = \frac{v\phi d\rho_w}{\mu_w} = \frac{(79.58/3600) \cdot 47.64 \cdot 2 \cdot 10^{-3} \cdot 999.70}{1.31 \cdot 10^{-3}} \approx 16. \quad (1.7)$$

In the light of the discussion on the onset of turbulent flow patterns over a PM in [50] and section 5.3.1 in [13], it seems that we can conclude that this Reynolds number indicates a nonlinear, "Forchheimer" laminar flow pattern over the PM. Moreover, the value for Re is well below 100 and in the words of Hassanizadeh [50]: "... deviations from Darcy's law have been observed at Reynolds numbers of order 10, experience have indicated that the onset of turbulence occurs at much higher velocities. ... values up to 300 have been reported". Note, this is a maximal value for Re considering that the average PM entrance velocity equals the average velocity over the PM. The entrance velocity is computed for a well screen length of $1m$ (see subsection 1.3.2) and the above situation implies a fully penetrating well screen, it implies a PM of thickness $1m$.

Suppose the above sketched synthetic PM would be able to facilitate the high velocity water transport for a creep flow pattern. Then from Darcy's law and the Kozeny-Carman permeability-porosity relation (e.g. see section 5.10.3 in [13]) we can obtain an estimate of the hydraulic gradient required to drive this flow. Omitting the computational details, the hydraulic gradient would be $J = 0.16 [-]$. From figure 1.7

it can be easily seen that this is the minimum gradient that should be imposed to obtain the desired flow velocity and the actual gradient will be higher since we just concluded that the flow is likely Forchheimer laminar, or at least not Darcy laminar.

1.3.6 Stressing the fluid phase: Fully versus partially penetrating wells.

In the previous two subsections we discussed, among others, on two aspects which underlie basic well hydraulics. The assumption that the casing does not stress the porous medium after it has been developed as well as the validity of Darcy's law, or creep flow through the PM. Based on these considerations we conclude that it is of value to examine the stressing of the PM by stressing the pore fluid through analytical tools of basic well hydraulics. Albeit the likely inaccuracy of Darcy's law, if we consider it in the light of our considerations on the well entrance velocity for JSI injection wells, the fact that the law represents a limit of minimum energy dissipation makes it a valuable reference. Especially in aid of investigating the role of deformation in facilitating the high rate water mass injection in to a PM.

Recalling the exploratory nature of this manuscript we can set aside, for the scope of this manuscript, transient well hydraulics and focus on steady state well hydraulics⁹. We are currently interested in the limits between which phenomena behave. For the situation of the influence of a well casing on the PM, we noted that, in relation to transient deformation, transient effects can be viewed as "in between the limits" effects. Analogous, the analytical steady state equations, (Thiem's, Glee's and Dupuit's equation for respectively confined, leaky and unconfined aquifers [69]) for a given well yield and hydrogeological parameters, result in the maximum corresponding drawdown as well as radius of influence relative to their transient counterparts (Theis's equation, e.g. Neuman-Witherspoon's method [69] and Neuman's equation [82]). The limits of deformation of the piezometric surface.

Moreover, for the scope of this manuscript we consider a continuous water mass injection under constant stressing of the pore fluid, as opposed to the other interesting approach of periodic stressing the pore fluid. From this we anticipate that a PM will settle to a steady state which is of current interest, not the path towards a new steady state.

The way in which a well stresses the fluid phase differs with respect to whether a well fully penetrates the aquifer or only partially. In case of fully penetrating wells, the assumption is typically that the flow to the well is horizontal/radial (Dupuit assumption), whether it is a confined aquifer or an unconfined aquifer ([69], section 3.1 & section 5.2). Note, for unconfined aquifers this is questionable, especially in the neighbourhood of the well. The Dupuit assumption mainly favors mathematical tractability (e.g. see section 8.1 in [13] and chapter 5 in [69]), however in many cases it is also physically sufficiently accurate and precise.

The main difference between fully and partially penetrating wells is that it induces vertical flow in confined aquifers and additional vertical flow in unconfined aquifers. Consequently, from a kinematic perspective, it introduces curvature in the flow paths and hence additional energy dissipation. In addition, a mass balance or more specific the well entrance velocity dictates that the velocity increases in the region of vertical flow: the same amount of water has to flow through a smaller area. From this one may wonder whether the flow pattern may change near the well from creep to transitional or turbulent, as a result of the increase in flow velocity. If so, than there would be additional dissipation of energy. However, experiments have shown (Mogg 1959 in [31], p. 215) that this turbulent head loss near the well is relatively small.

From a dynamic perspective, a consequence of creep flow is that the pressure field over the PM/aquifer is approximate hydrostatic and hence vertically uniform. In case of a fully penetrating well, this uniform pressure field is maintained. However, a partially penetrating well disturbs this uniform field, consistent with the kinematic aspects. Thus, for curving flow paths the dissipation is higher and hence there is an additional pressure drop. Moreover, a partially penetrating well induces a vertical component to the pressure gradient. The dynamical view also reveals that the pressure drop has two contributions, besides the additional dissipation as a result of a longer flow path, extra work (gravitational) should also be performed in order to move a blob from a certain position on the vertical to another position on the vertical¹⁰.

⁹According to Kruseman it steady states are essentially approximations since he states that essentially there only unsteady state flow exists ([69], p. 55)

¹⁰See section 6.2 in [79] for the rather clear "work" interpretation of the energy state of a blob of fluid.

The effect of partially penetration on the flow paths and the pressure field of an aquifer does not extend to infinity, the zone in which the effect is sensed has a radial extend r , from the well, of roughly $r > 2D\sqrt{K_h/K_v}$, with D being the thickness of the aquifer, K_h the horizontal hydraulic conductivity and K_v the vertical hydraulic conductivity (assuming a homogeneous hydraulic conductivity field). Beyond this distance the conditions are "fully penetrating well like".

The effect of partially penetrating wells is of interest since a typical JSI system is essentially a partially penetrating well. Of specific interest is the effect of a vertical contribution to the pressure gradient over the PM and its potential to cause localized deformation of the void space.

Well flow for a fully penetrating well, or more general cylindrical radial flow affects the flow velocity with distance due to one dimensional geometric spreading, analogous to the geometric spreading we considered for seismic waves (see subsection 1.3.4). The flow through area increases with distance from the well and this geometric effect causes the flow velocity to decrease with distance, without energy dissipation (a conservative effect, the energy is diffused). This is closely related to the concept of an influence zone for a well, however this concept entails also a decrease in velocity due to friction (non conservative, energy is dissipated). In case of a partially penetrating well, as a result of the additional vertical pressure gradient there is two dimensional flow (assuming a homogeneous PM). Consequently, the geometric spreading effect is two dimensional and hence the flow velocity decreases faster with (spherical) radial distance from the well than for a fully penetrating well. In general, the geometric spreading affect causes the flow velocity to decrease, in an energy conservative manner. Hence, if a flow pattern adjacent to the well is different from a creep pattern, with distance the flow pattern in the PM tends to a creep flow pattern. Moreover, a non creep flow pattern induced by a well will be local due to the geometric spreading effect.

Partially penetrating wells are rather difficult to model analytically (e.g. see p. 250 in [31] or section 6.9 in [93]). Some authors even advice immediately to rely on numerical modeling of these wells (e.g. section 6.9 in [93]). However, Kruseman ([69]) devotes a whole chapter to analytical and semi-analytical descriptions of partially penetrating wells. Similar, the section Sen ([106], section 8.4) devotes to partially penetrating wells is also rather valuable. The material these two authors cover are susceptible of improving ones intuition regarding partially penetrating wells. A remark we want to make is that the analytical methods given in [69] and [106] are typically in the form of "corrections" to the fully penetrating solutions, i.e. superposition of a partially penetrating effect on a fully penetrating well solution.

1.3.7 A conceptual model for high-rate water injection into a PM.

In this section we presented considerations on:

- 1.) typical characteristics of a theoretical well design;
- 2.) the explication of "high rate" in terms of well/PM entrance velocity;
- 3.) the effect of excavating a borehole on a PM;
- 4.) well case stressing of a PM;
- 5.) inducing seismic wave phenomena;
- 6.) pore fluid stressing of a PM;
- 7.) the physical meaning of creep flow through a PM;
- 8.) the physical purpose of deformation;
- 9.) the effect of partially penetrating well screens on a PM's pore pressure distribution.

Important results that followed from these reflections are that the disturbance of a PM due to the excavation of a borehole are local. From the induction of seismic wave phenomena on a PM by the well casing we inferred that the well case stressing of a PM is a local effect with an extend of one wave length of a P-wave (rule of thumb), roughly on the order of $\sim 50cm$. From minimal energy dissipation considerations, guided by Helmholtz theorem and Prigrione's principle, we deduced that the purpose of

PM deformation is to drive the fluid flow pattern through a PM towards laminar flow and ultimately creep flow. Further more, a very rough assessment is made on the possibility of laminar flow given a high rate PM (well) entrance velocity by computing the Reynolds number for a cubic packing of uniform spheres of the size of a $2mm$. The resulting Reynolds number indicates (nonlinear) laminar "Forchheimer" flow. From reflecting on the effect of partially penetrating well screens on the pore pressure distribution on a PM we inferred that it is a plausible method to constrain PM deformation locally. The locality of PM deformation is of interest regarding the environmental constraints set concerning the JSI application of the high rate water mass injection phenomenon (see subsection 1.4.1). Finally we noted that in case of radial flow the flow velocity decreases with distance from the well due to geometric spreading. This effect is higher for a partially penetrating well, as compared with a fully penetrating well, which is due to that the geometric spreading is two dimensional as opposed to one dimensional (for a homogeneous PM). If around adjacent to a well there is flow pattern different from laminar creep, than the geometric spreading phenomenon bounds this region and transforms the flow patterns, with distance, into a laminar creep pattern.

These results let us construct the conceptual model illustrated in figure 1.8. We take this as a reference, a map to guide research with respect to the phenomenon of high rate water mass injection in to a PM. Note, the model reflects the material we presented in this section and hence, it implicitly indicates that the knowledge regarding seismic wave phenomena within the PM is limited at the moment.

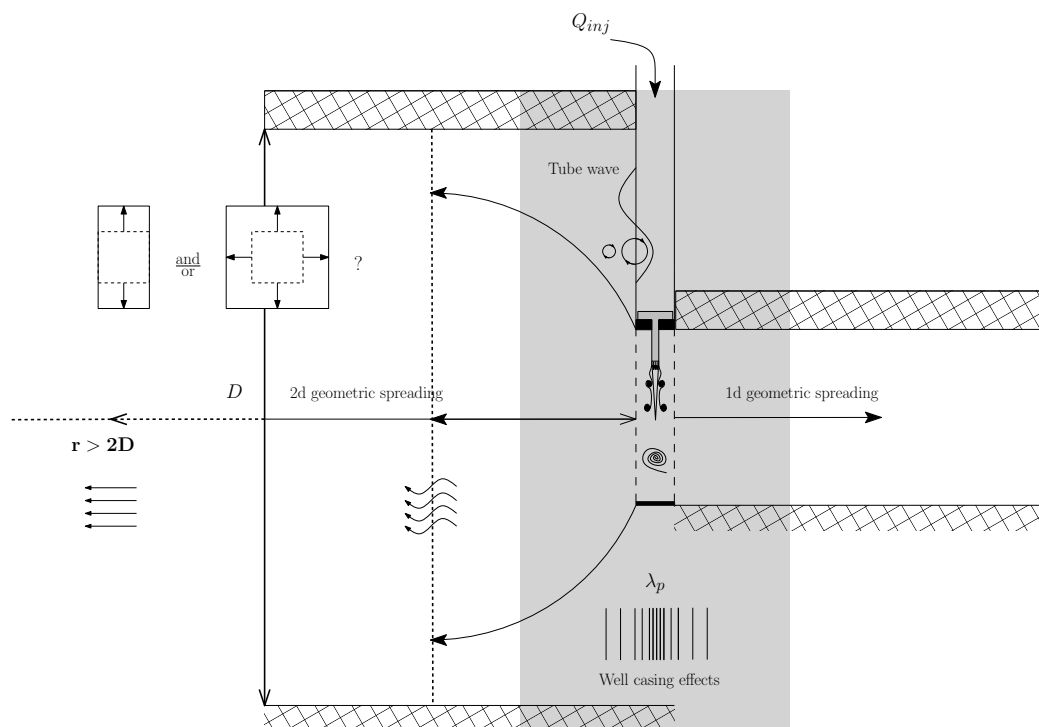


Figure 1.8: A visualisation of the proposed conceptual model to investigate the phenomenon of high rate water mass injections in to a porous medium. The left side is a schematic of a partially penetrating well and the right side of a fully penetrating well. The focus is on the partially penetrating well, for which we indicated different flow patterns and deformation mechanisms, which we hypothesised to occur, as well as the scales at which they are supported. The symbol λ_p refers to the wave length of a P-wave, Q_{inj} to the well injection rate, D to the thickness of the aquifer and r to the (horizontal) radial distance.

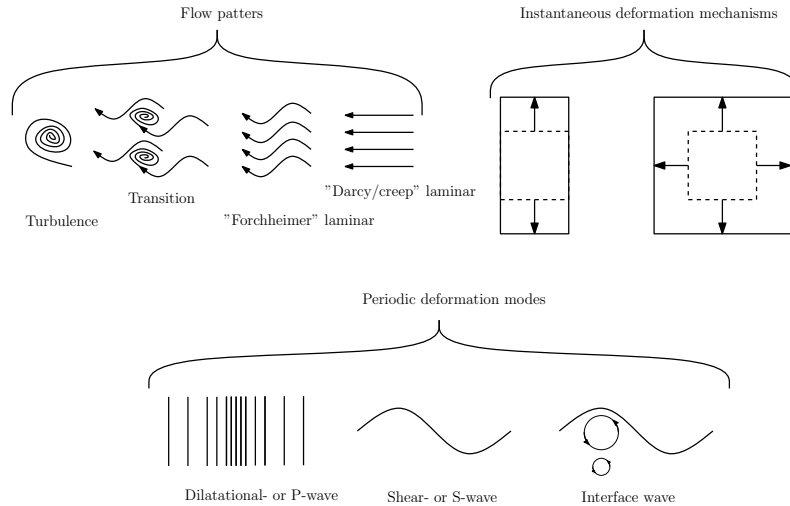


Figure 1.9: Legend for 1.8, explicating the symbols reflecting flow patterns and deformation mechanisms.

For the scope of this manuscript we consider constant water injection as opposed to periodic water injections. The latter is associated with periodic stressing of the PM and hence the possibility of wave phenomena to arise. However, we do not take them in account here, at least not explicitly. In figure 1.8 the well details are omitted for sake of clarity, they can be found in section 1.1 and subsection 1.3.1, especially in figure 1.2.

1.4 Relevance for society and for understanding the physics underlying the JSI methodology.

1.4.1 The relevance of a better understanding of infiltration points for society.

The interest in the phenomenon, "*a saturated porous medium (PM) subjected to a continuous high rate well injection of water mass*", was awoken in industry due to the recurrence of a stuck-pipe phenomenon when drilling boreholes for water wells.

The stuck-pipe phenomenon is characterised by a high suction force which jams the drill string and inhibits the drill from drilling deeper. According to Hölscher ([60], p. 9) it is a common problem in the borehole drilling practice. In the scarce petroleum related literature reviewed, we noticed an analogous phenomenon, known as differential pipe sticking (e.g. see chapter 10 in [102] or [1, 29]). However, currently there seems to be not enough information to assess the equivalence between the two reported stuck pipe phenomena, and hence to "pick the brain of the petroleum engineers".

The drill contractor Werner Wils recognized (e.g. see [36, 52]) that he could take advantage of this differential-pressure stick pipe phenomenon, or actually of the points at which the phenomenon occurs, by injecting water at these points in the subsurface. In practice Wils' idea are reported to work out very well, these "infiltration points" are capable of facilitating the high rate injection¹¹ of water mass in to the saturated zone of the subsurface/aquifer. For example, the Pots dam case, described on p. 1-2 of [126], where they managed to inject water mass in to the subsurface at rates of $40m^3.hr^{-1}$ ¹². For more successful examples see the books of Wils [126, 127] or the article of Ebneith [36]. As a result, a new methodology for artificial well recharge was born and named "Dsensauginfiltration" (DSI) [126, 127, 60, 36] or "jet suction infiltration (JSI) [128].

The basic idea of the JSI methodology is that water is injected through a well at an infiltration point. To take full advantage of the infiltration point a JSI nozzle is installed in the injection well. For

¹¹Remark, above we argued that high rate injections means actually that the infiltration points facilitate high well entrance velocities.

¹²Note, the information is actually incomplete, the screen details of the used injection well should be given in order to assess whether the rate is high or not.

an illustration see figure 1.2 (subsection 1.3.1), it illustrates the prototypical JSI methodology and the system is related to the Glindow JSI/DSI unit. Besides the infiltration point, the nozzle proved its use in practice, for example in the Pots dam case, referred to earlier. Some preliminary research to, among others, the effect of the nozzle can be found in the report of Havik [52].

A particular use of this new artificial recharge methodology is at construction sites. In order to prevent excavations on construction sites from flooding, one has several options, e.g. ([93], chapter 16): a.) open pumping; b.) predrainage; c.) flow cut off; or d.) flow exclusion. The JSI methodology can be employed in case of the first two options. Regarding predrainage the groundwater level has to be lowered to decrease the hydraulic gradient towards the excavations and hence the seepage of groundwater in the excavations. See for an example in the Netherlands the brief informal article [74]. The advantage of predrainage over open pumping is that, the groundwater not necessarily has to come in to direct contact with the atmosphere, which may alter its chemical composition and hence imposes difficulties with successively discharging the pumped water ([93], chapter 13). For the scope of this manuscript we assume predrainage to be the method to prevent flooding, in order to avoid water chemistry related issues. Note, predrainage may be seriously constraint due to environmental regulations, which is typically explicated in terms of a maximum allowed drawdown of the water level or piezometric surface and the extend of the region influenced by drawdown (e.g. see the informal case report [74]).

Through extraction wells, the water table can be sufficiently lowered, however the bottleneck is: *Where to leave the abstracted water?* There are three options to discharge the abstracted water to ([93], chapter 10): 1.) the sewage system; 2.) surface water bodies; or 3.) back in to the ground. Discharging the extracted water in to the sewage system is often limited by governmental regulations. For example, in the Netherlands there is a certain volume of water which can be discharged free of charge. However, when exceeding a certain threshold volume, one has to pay per additional cubical meter, which may render this option eventually rather costly [52]. The second option is often inhibited by environmental regulations regarding the chemical considerations. In general the chemistry of the water to be discharged differs to much from the chemistry of the surface water (e.g. see [112]). Consequently, mixing of the two types of waters can have significant effects on the ecosystem the surface water body is part of. Discharging, or injecting the extracted groundwater back in the ground is free of charge in the Netherlands and the water chemistry of the groundwater body which is recharged differs likely much less in chemical composition¹³. Hence, this suggest that recharging an aquifer with the extracted water is favoured over the other two options, both regarding economical and environmental concerns.

Though, similar to that extracting groundwater is regulated environmentally by limiting the allowed drawdown and the region influenced by drawdown, injecting water in to the ground is limit by the allowed "drawup" and the region influenced by it. This may severely limit the amount of water that can be injected back in to the ground¹⁴. The JSI methodology claims to have negligible environmental disturbances, i.e. the drawup as well as its region of influence is small compared to ordinary well recharge (e.g. see [60, 74]).

The accredited performance of the JSI methodology hinges on whether an infiltration point can be found in the aquifer selected for recharge/injection. Roughly, an infiltration point is a point with a high infiltration capacity, relative to other positions in the aquifer. Currently it seems that locating an infiltration point should be done by trial and error, or more formal an infiltration investigation should be employed from which the existence and the location of an infiltration point can be inferred. A prototypical infiltration investigation is documented in [60] (p. 18-21). The essence of such an infiltration investigation is captured by highly controlled (jet) drilling. Careful observations are made of the behaviour of the drill fluid¹⁵. Predominantly

- 1.) the evolution of the pressure of the drill fluid within the borehole with respect to the advancing bottom of the borehole; and
- 2.) the water balance regarding the borehole (sub) system.

¹³Note, of course it should be assessed whether the chemical composition of the the recharge water and the water of the recharge aquifer are sufficiently similar. However, for the scope of this manuscript we assume this to be the case.

¹⁴To summarize the effect of the a well its yield on the watertable or piezometric surface, the quantitative measures of specific capacity and specific injectivity for respectively extraction and injection wells may be of value. They are defined as yield per drawdown/drawup (e.g. see p. 62 in [80]).

¹⁵For information on jet drilling see e.g. p. 307 in [31], and for more information on drill fluids see e.g. chapter 11.

Regarding the latter one can identify borehole storage, related to the pressure of the drill fluid, and two types of fluxes, a.) a flux upwards to the earth surface, facilitated by the borehole; and b.) a flux in to the surrounding PM, i.e. one takes advantage of the problem of "drill fluid loss". From these observations one may construct an infiltration profile of the drilled subsurface. An infiltration point is marked by a rapid decrease in drill fluid pressure (also providing the suction force which may jam the drill string) and the observed rapid depletion of the drill fluid stored in the borehole, during the drilling.

Whenever it appears that an infiltration point is found, the capacity of the point can be assessed by increasing the water (drill fluid) pumped in to the borehole in order to determine the equilibrium injection rate: "the maximum injection rate for which the water level within the borehole remains constant without a flux towards the earth surface". In other words, the maximum borehole storage is related to the injection rate capacity of the infiltration point.

In summary, the JSI methodology suggests that a PM can facilitate high rate water mass injections. An understanding of this phenomenon is of interest for the artificial recharge industry since it seems that it has the potential to pump large amounts of water in a short time span, relative to conventional well recharge, while minimally affecting the environment. In the more specific context of dewatering it may also be economically advantageous in some countries. For example the Netherlands, where it is the cheapest option to discharge the water from a flooded (construction) site into an aquifer, as long as the environment is not harmed.

The current understanding of infiltration points is too minor in order to predict their occurrence. Which is a major limitation in employing the JSI methodology, currently the only exploitation of the phenomenon of a high rate water mass injection of a PM, we are aware of. Hence, a better understanding of infiltration points is of great value for the commercial application of the JSI methodology, or more general the practice of artificial recharge and dewatering.

Note, infiltrations points are in the scarce literature commonly referred to as DSI/JSI points. However, it is our opinion that this name is incorrect. To us it seems that an infiltration point is a property of the PM/aquifer system and the borehole, irrespective of special DSI/JSI technology which is essentially the nozzle. Accordingly, we define the DSI/JSI methodology as a developed injection well equipped with a JSI nozzle, or other (patentable) high rate facilitating technological attributes.

1.4.2 The relevance of revisiting a porous medium its mass balance in aid of a better physical understanding of infiltration points.

The origin of this thesis was the request to design an experimental apparatus with which the phenomenon of high rate water injection into a PM could be demonstrated in the lab. The aim was that the apparatus could mimic the physical phenomenon induced in the field by a DSI/JSI system, such that the problem could be nearer investigated in the lab. Specifically in aid of the understanding of the occurrence of infiltration points. This practical purpose of the eventual apparatus let us to adopt a normative design approach, as opposed to designing completely from scratch. The norm, or prototype system¹⁶ was set to be the field setting of a JSI (DSI) system. Moreover, we anticipated the apparatus, or analog system/model to resemble as close as possible the setting of a JSI system (see subsection 1.3.7).

Designing an experiment/modelling is essentially about finding out relevant symmetries, i.e. finding the governing characteristics of a phenomenon which render the phenomenon invariant under necessary abstraction¹⁷. Usually an experimental design is framed by three kinds of symmetry considerations, which can be viewed as "nested": geometric symmetry \supset kinematic symmetry \supset dynamic symmetry, which we illustrated in figure 1.10.

¹⁶We adopt here the jargon regarding modelling as used by Bear, chapter 11 in [13].

¹⁷For a nice discussion on symmetry and its use in (scientific) research see [100].

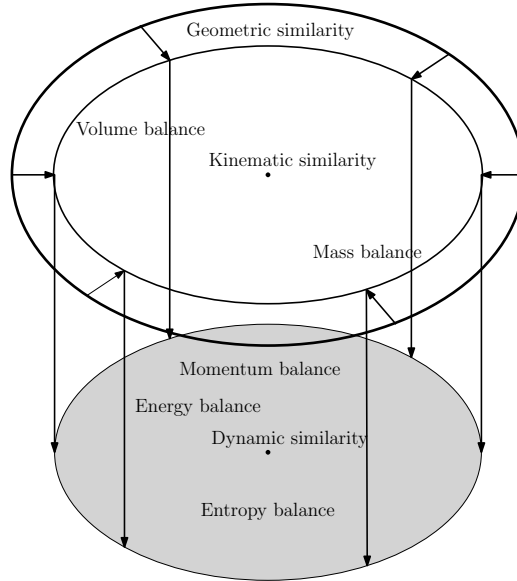


Figure 1.10: A schematic illustration of how geometric, kinematic and dynamic similarity/symmetry considerations are related.

Of particular importance are scaling symmetries, or similarities (e.g. see section 1.3 in [64]). If one is able to fulfil these similarity requirements, then theoretically the model is sound in representing the observed field phenomena (e.g. see chapter 11 in [13], section 3.4 in [79] or section 4.7 in [12]).

Roughly stated, geometric similarity defines the spatial scope of an experiment, i.e. the measurements of an experimental apparatus as well as extends of roughness elements. Dynamic similarity provides energy or force scales¹⁸. Regarding these scales, the scales of the surface forces or pressure/normal- and shear-strain energies are of main importance, since these determine material behaviour. From knowledge of the material behaviour one can infer material properties and hence one can estimate the materials to build the experimental apparatus from. Most importantly, from a robust perspective, the material of which one should construct the experiment-confining frame. This frame should be made of a material which can withstand the maximum expected forces/energies. In addition, from dynamic symmetry one may also infer (deductively) geometric symmetry. Moreover, through geometric and dynamic similarity one can set the extremum scope, or the accuracy of phenomenon. From this scope one can design a robust initial experiment which only needs internal refinement, or precision tweaking to converge to a desired reproduced appearance of the phenomenon of interest. In other words, after geometric and dynamical similarity we can have a closer look on other symmetries.

We view kinematic symmetry literally in between geometric and dynamic symmetry. The main purpose of considerations on kinematic symmetry is to fill up the gaps in the required geometrical and dynamical knowledge. For example, velocity can be viewed as a geometrical extend per time. The connection between kinematics and dynamics can be explicated by noticing that dynamical information is usually summarized in the form of an equation of motion. A general equation of motion is simply a function of geometric and kinematic information (e.g. see chapter 9 in [70] or p. 79 in [96]), with geometric information accounting for potential-energies/configuration effects and the kinematic information governing kinetic-energies/inertial-effects and energy-dissipation/friction. Kinematic considerations can have both deductive as well as considerable inductive inferential power. Regarding the latter its inductive inferential power we assess due to its tractable number of fundamental components (three) scientifically proven and captured in theorems: 1.) Euler's theorem ([44], p. 156) 2.) Chasles' theorem ([44], p. 161) 3.) Helmholtz's fundamental theorem of deformation kinematics (p. 21 in [130] or [53]).

In addition kinematic considerations are of use in validating the workings of an experimental apparatus, since the kinematic characteristics of a phenomenon are the aspects of motion we can directly observe, unlike the dynamical characteristics which can only be observed indirectly.

The understanding of the scales at which a JSI system operates (spatial, velocity and pressure scales)

¹⁸This depends on the mechanical perspective one adopts, a Lagrangian/Hamiltonian or a Newtonian perspective.

seems to be rather poor at the moment, at least insufficient for an experimental design¹⁹. Consequently, we are obliged to infer knowledge about the extremum scales at which a JSI system (likely) works. This knowledge can be acquired in two ways: a.) inference from dynamical considerations (as mentioned above); and through b.) statistical inference. At the moment we do not have sufficient data to conduct a (descriptive) statistical analysis and make estimates of the extremum scales. Hence, we have to rely on dynamical considerations.

The source of dynamical information to tap from is the theory of poromechanics, the overlap of fluid and (solid) deformation mechanics. Let us roughly sketch the scope in five major (binary) considerations. First we should consider whether the current settled/practical part of poromechanical theory at the scale of a porous medium (PM) suffices (which seems to us to be classical hydrogeological theory and Biot's poroelastic theory), viz.

Can we consider the PM scale or do we have to refine to the pore scale? (1.8)

Second, our system (as explained above in section 1.3) comprises a PM in which a well is situated and we can ask ourselves whether we have to consider initially both the PM and the well subsystem or does one of the subsystems dominate the phenomenon? In other words,

Can we focus on the PM and consider only basic well hydraulics? (1.9)

Third, we have PM comprising a solid phase as well as a liquid phase and we may wonder whether the dynamics of one of the phases affects the other, i.e.

Are changes in the phases coupled or uncoupled? (1.10)

A decision on one of these is highly related to whether we can consider,

Quasistatic changes (a sequence of steady states) or transient changes? (1.11)

Fourth, the decision regarding scale is highly affected by the more refined consideration on flow patterns,

Can we expect a specific kind of flow pattern ("Darcy laminar", "Forchheimer laminar", transition or turbulent flow) or do we have to keep all options open? (1.12)

as well as on the kind of solid deformation,

Can we expect a certain type of deformation (elastic, plastic fracture) or not? (1.13)

Fifth and final parameter considerations are of interest, i.e.,

Does heterogeneity and anisotropy play a controlling role for the phenomenon? (1.14)

These considerations span a considerable theoretical scope in which we recognize the current main difficulty, regarding dynamics, to lie in answering question 1.13 and 1.14. In conclusion, the question arises: where to start? Question 1.9 and 1.11 we have argued on theoretically in section 1.3 and concluded that for the scope of this manuscript it seems valid to focus on the PM and quasistatic changes. However, the remaining scope is still of considerable extend.

Fortunately, fluid and solid deformations have the same kinematic foundation and understanding of this kinematic framework may facilitate to demarcate a best estimate starting point. Moreover, it facilitates the gross understanding of two important scope-summarizing graphs in which both kinematic and dynamic characteristics culminate, namely:

- 1.) a friction factor versus Reynolds number graph, summarizing flow patterns;
- 2.) a stress versus strain graph, summarizing general deformation mechanisms.

¹⁹We are only aware of a few field specific scales, documented in [60, 61, 36].

Of course an intuitive jump in the field of poromechanics is also a way to start, however for that to be reliable, sufficient experience is required which the author of this work cannot claim to have.

In summary, a lack of knowledge, or data about the scales at which the JSI system operates suggest that we have to investigate how to acquire the required scales as well as how they scale, from dynamical considerations. However, given the diversity, at least seemingly, of dynamical possibilities, assessing them all would be beyond the scope of this manuscript and we believe to be unnecessary. The reason for it, is that kinematic considerations provide a gross reasoning framework by means we can argue where to take off dynamically. Hence, that is why this manuscript is *on the kinematics of the phenomenon of a saturated porous medium (PM) subjected to a continuous high rate well injection of water mass, with negligible global disturbance of the PM.*

In conclusion, from the four balance equations supposed to govern a physical phenomenon, dynamical characteristics are accounted for by the momentum, energy and entropy balance, whereas the mass balance governs the kinematic characteristics. The general mass balance equation for a PM is typically referred to within the hydrogeological literature as the storage equation. This is the reason why we investigate the kinematics of the phenomenon by means of revisiting the storage equation. From a rigorous derivation of the storage equation we can infer: 1.) the kinematic manifestation that can occur in a PM; 2.) which of these possibilities eventually are accounted for by the storage equation; and 3.) which assumptions are imposed that may have rendered some kinematic manifestations as negligible. This overview is the answer to our posed question,

Where can the injected water mass go to?

Furthermore, from this overview we can establish an overview of the possible dynamic processes, which may be of aid in the symmetry considerations. For example, we may infer whether in the scaled analogue system we have to account for additional smaller scale processes to render the experimental design sound in supporting the phenomenon of interest. In addition from the overview of manifestations we may also infer the possible mechanisms which may play a role in localizing an infiltration point, which is currently characterized kinematically by a high "well entrance velocity" and dynamically by an under-pressure at the instant of localization (see subsection 1.4.1).

Chapter 2

A deterministic kinematic model.

2.1 Introduction: Kinematics of the phases of a PM

In this chapter we are concerned with the mathematical description of relative motion of a multi particle system. This in order to construe a rather general kinematic model with a minimum of physical assumptions. The model has a descriptive purpose concerning the different components of motion of a multi particle system. That is to say, it summarizes the contributions of the different components of motion making up the trace of the motion of the multi particle system:

$$\begin{array}{ll}
 a.) \text{ rigid translation} & \left. \vphantom{a.)} \right\} \textit{ global} \\
 b.) \text{ rigid rotation} & \\
 \\
 b.) \text{ dilatation} & \left. \vphantom{b.)} \right\} \textit{ local} \\
 d.) \text{ spin/vorticity} &
 \end{array} \tag{2.1}$$

Regarding interpretation, an Eulerian perspective is adopted, i.e. an observer distant from the space under consideration (mathematically speaking). The motion of the multi particle system is described relative to two different kinds of reference points: 1.) a point internal to the system; and 2.) a point external to the system. The former is interpreted here as if the focus of the observer moves with the multi particle system.

Mathematically, the motion is described by means of a Taylor series expansion of a displacement function or field. For a Taylor series expansion to be accurate, the function or field has to be absolutely continuous (continuous and smooth). Therefore the model inheres physical assumptions which support the supposition that the trajectory of the motion of an object (e.g. a particle or a system), continuous in time, is absolutely continuous.

In addition, the model describes the trace of motion through addition of the different motive components: "the sum of the components makes the whole". Consequently, the model inheres physical assumptions which support the separation of the components, or the independence of the components regarding order and variation.

The reason for construing a kinematic model for a multi particle system is in order to investigate the possible kinematics of the phases making up a PM. Analysing the phases on their kinematic behaviour, or possible kinematic behaviour can be of a valuable aid in understanding deformation mechanisms and the dynamic aspect of the dissipation of energy in or of a PM. In this manuscript we deal with a simple two phase PM of liquid water saturating a matrix spanned by a solid phase. The kinematics of the liquid phase likely increases our inductive certainty regarding the kind of flow patterns that may exist within the PM ("Darcy/creep" laminar, "Forchheimer" laminar, transition or turbulent). With respect to the solid phase, we likely increase our inductive power regarding the type of deformation which may occur (elastic, plastic or even fracture failure).

Phases are by definition (physical) continuum objects (e.g. see section 1.1 in [12], p. 9 in [87] or section 1.2 in [79]) and we view a continuum object as a specific case of a multi particle system. Namely, a multi particle system which has the mathematical continuum amount of particles. Theoretically this means that the "continuum set" comprises a number of particles equal to the amount of real numbers \aleph (e.g. see p. 16 in [67]). In practice this requirement on the size of the number of particles a system should comprise is relaxed. A multi particle system should appear as a continuum and this manifestation is a function of observation scale. Further considerations on the definition of a (physical) continuum are beyond the scope of this chapter and we would like to refer the interested reader to a.) section 1.2 in [12], section 1.3 in [13], section 1.2 in [79] or section 2.2-3 in [42] for a rather intuitive explanation of a (physical) continuum; and b.) the article of [9] for a more theoretical explanation relating the mathematical to the physical continuum.

We will construe the kinematic model in this chapter by setting the mathematical framework in the following (second) section: the deterministic variation of a continuous and smooth vector field. This entails explicating "relativity", subsequently deriving a Taylor series expansion for a vector function and then considering simplifications of this result by interpreting it in an Eulerian perspective. We conclude the section with a corollary, the total derivative of the Taylor series expansion for a vector function.

In the third section we apply the mathematical framework to the physical concept of a displacement vector to obtain the fundamental theorem of deformation kinematics. This statement, proven by Helmholtz [53] (or see p. 238 in [79] and section 2.3 in [12]), dictates the possible motive contributions

an object its trajectory may be composed off. In the section we define the mathematical concept of a displacement vector, subsequently the Taylor series expansion of the displacement vector and consequently we interpret the Taylor series in terms of the motive contributions: the fundamental theorem of deformation kinematics.

We conclude the chapter with a chapter summary.

2.2 Deterministic variation of a smooth vector field.

2.2.1 Introduction: Variation from a norm.

Consider a vector function, or vector field \mathbf{f} which is an explicit function of the fixed Cartesian coordinates \mathbf{x} and time t , viz.,

$$\mathbf{f} = \mathbf{f}(\mathbf{x}, t). \quad (2.2)$$

At a position $\Delta\mathbf{x}$ way from \mathbf{x} at a later time $t + \Delta t$ we encounter a value $\mathbf{f}(\mathbf{x} + \Delta\mathbf{x}, t + \Delta t)$, and the difference between the two function values is, $\Delta\mathbf{f}(\mathbf{x}, t) = \mathbf{f}(\mathbf{x} + \Delta\mathbf{x}, t + \Delta t) - \mathbf{f}(\mathbf{x}, t)$. Hence, we can write,

$$\mathbf{f}(\mathbf{x} + \Delta\mathbf{x}, t + \Delta t) = \mathbf{f}(\mathbf{x}, t) + \Delta\mathbf{f}(\mathbf{x}, t). \quad (2.3)$$

This equation can be regarded as having three unknowns. Therefore, for the latter equation to be of any use, we should have an equation which defines $\Delta\mathbf{f}(\mathbf{x}, t)$ independent of $\mathbf{f}(\mathbf{x} + \Delta\mathbf{x}, t + \Delta t)$. This equation captures the variation structure of the field, i.e. it states how \mathbf{f} varies when we vary its variables \mathbf{x} and/or t . More general, it states how $\mathbf{f}(\mathbf{x} + \Delta\mathbf{x}, t + \Delta t)$ varies from a norm $\mathbf{f}(\mathbf{x}, t)$.

We will denote the variation structure of a field by $\mathring{\mathbf{f}}$ and write equation 2.3 as,

$$\mathbf{f}(\mathbf{x} + \Delta\mathbf{x}, t + \Delta t) = \mathbf{f}(\mathbf{x}, t) + \mathring{\mathbf{f}}. \quad (2.4)$$

Note, this form can be recognized as similar to a Reynolds decomposition (e.g. see p. 97 in [13], p. 528 in [33] or p. 262 in [104]), commonly used in Turbulent flow analysis. For a Reynolds decomposition the norm is an average value and the variation term is interpreted as the statistical fluctuation.

In this section we determine the variation structure $\mathring{\mathbf{f}}$ in the specific case that the field \mathbf{f} is continuous in its variables \mathbf{x} and t as well as smooth. By virtue of Taylor's theorem (e.g. see chapter 7 in [7] or section 3.2. in [76]) such fields underlie a (multivariate) polynomial variation structure, which can be inferred from a Taylor series expansion around a (reference) point, or norm.

In this section we will derive the multivariate Taylor series expansion for a vector field \mathbf{f} as well as for the derivative field $d\mathbf{f}/dt$, around their respective norms $\mathbf{f}(\mathbf{x}, t)$ and $d\mathbf{f}(\mathbf{x}, t)/dt$. From these series expansions we infer the polynomial variation structure $\mathring{\mathbf{f}}$ and $d\mathring{\mathbf{f}}/dt$. In addition will give an abstract physical interpretation of the series expansion from an Eulerian observation perspective.

2.2.2 The multivariate Taylor series expansion of a vector function.

In the following we will derive the multivariate Taylor series expansion after section 8.18 in [6]. However, we take a more heuristic approach which we hope will favor intuition.

We can obtain the multivariate Taylor series expansion, heuristically, by considering the concept of a "total derivative operator",

$$\frac{d}{dt} = \frac{\partial}{\partial t} + \frac{\partial(\cdot)}{\partial\mathbf{x}} \cdot \frac{d\mathbf{x}}{dt}. \quad (2.5)$$

In the light of this concept we rewrite \mathbf{f} implicitly as,

$$\mathbf{f}(\mathbf{x}, t) = \mathbf{f}(t). \quad (2.6)$$

The (accurate) Taylor expansion of $\mathbf{f}(t + \Delta t)$ around t , given precision Δt , is (e.g. see chapter 7 in [7] or section 3.2. in [76]),

$$\mathbf{f}(t + \Delta t) = \mathbf{f}(t) + \frac{d\mathbf{f}(t)}{dt} \Delta t + \frac{d^2\mathbf{f}(t)}{dt^2} \frac{(\Delta t)^2}{2!} + \mathcal{O}\left((\Delta t)^3\right). \quad (2.7)$$

The total derivative of \mathbf{f} is,

$$\frac{d\mathbf{f}(t)}{dt} = \frac{d\mathbf{f}(\mathbf{x}, t)}{dt} = \frac{\partial\mathbf{f}(\mathbf{x}, t)}{\partial t} + \frac{\partial\mathbf{f}(\mathbf{x}, t)}{\partial\mathbf{x}} \cdot \frac{d\mathbf{x}}{dt}, \quad (2.8)$$

which can be written in a more physical parlance as,

$$\frac{d\mathbf{f}(\mathbf{x}, t)}{dt} = \frac{\partial\mathbf{f}(\mathbf{x}, t)}{\partial t} + \text{grad} [\mathbf{f}(\mathbf{x}, t)] \cdot \frac{d\mathbf{x}}{dt}. \quad (2.9)$$

Substituting the former expression in equation 2.7 yields,

$$\mathbf{f}(t+\Delta t, \mathbf{x}+\Delta\mathbf{x}) = \mathbf{f}(\mathbf{x}, t) + \frac{\partial\mathbf{f}(\mathbf{x}, t)}{\partial t} \Delta t + \frac{\partial\mathbf{f}(\mathbf{x}, t)}{\partial\mathbf{x}} \cdot \frac{d\mathbf{x}}{dt} \Delta t + \frac{d}{dt} \left(\frac{\partial\mathbf{f}(\mathbf{x}, t)}{\partial t} + \frac{\partial\mathbf{f}(\mathbf{x}, t)}{\partial\mathbf{x}} \cdot \frac{d\mathbf{x}}{dt} \right) \frac{(\Delta t)^2}{2!} + \mathcal{O} \left((\Delta t)^3, (\Delta\mathbf{x})^3 \right). \quad (2.10)$$

The first factor of the fourth term on the right hand side of equation 2.10 can be nearer refined to,

$$\frac{\partial^2}{\partial t^2} (\mathbf{f}(\mathbf{x}, t)) + \frac{\partial^2}{\partial t \partial \mathbf{x}} (\mathbf{f}(\mathbf{x}, t)) \cdot \frac{d\mathbf{x}}{dt} + \frac{\partial^2 \mathbf{f}(\mathbf{x}, t)}{\partial \mathbf{x} \partial t} \cdot \frac{d\mathbf{x}}{dt} + \left(\frac{\partial^2 \mathbf{f}(\mathbf{x}, t)}{\partial \mathbf{x}^2} \cdot \frac{d\mathbf{x}}{dt} \right) \cdot \frac{d\mathbf{x}}{dt} + \frac{\partial \mathbf{f}(\mathbf{x}, t)}{\partial \mathbf{x}} \cdot \frac{d^2 \mathbf{x}}{dt^2}. \quad (2.11)$$

The fourth term can be recognized as the "Hessian matrix" term over the spatial coordinates (e.g. see p. 399 in [109], p. 212 in [76] or p. 308 in [6]). The Hessian matrix results from the gradient of the gradient of a function. Since the considered function is the vector function $\mathbf{f}(\mathbf{x}, t)$, the Hessian matrix is a third order tensor. If we substitute the refined expression 2.11 in equation 2.10 we obtain,

$$\begin{aligned} \mathbf{f}(t + \Delta t, \mathbf{x} + \Delta\mathbf{x}) &= \mathbf{f}(\mathbf{x}, t) \\ &+ \frac{\partial\mathbf{f}(\mathbf{x}, t)}{\partial t} \Delta t + \frac{\partial^2}{\partial t^2} (\mathbf{f}(\mathbf{x}, t)) \frac{(\Delta t)^2}{2!} \\ &+ \frac{\partial\mathbf{f}(\mathbf{x}, t)}{\partial\mathbf{x}} \cdot \frac{d\mathbf{x}}{dt} \Delta t + \left(\frac{\partial^2 \mathbf{f}(\mathbf{x}, t)}{\partial \mathbf{x}^2} \cdot \frac{d\mathbf{x}}{dt} \right) \cdot \frac{d\mathbf{x}}{dt} \frac{(\Delta t)^2}{2!} \\ &+ \frac{\partial^2}{\partial t \partial \mathbf{x}} (\mathbf{f}(\mathbf{x}, t)) \cdot \frac{d\mathbf{x}}{dt} \frac{(\Delta t)^2}{2!} + \frac{\partial^2 \mathbf{f}(\mathbf{x}, t)}{\partial \mathbf{x} \partial t} \cdot \frac{d\mathbf{x}}{dt} \frac{(\Delta t)^2}{2!} \\ &+ \frac{\partial \mathbf{f}(\mathbf{x}, t)}{\partial \mathbf{x}} \cdot \frac{d^2 \mathbf{x}}{dt^2} \frac{(\Delta t)^2}{2!} \\ &+ \mathcal{O} \left((\Delta t)^3 \right). \end{aligned} \quad (2.12)$$

This result is what we will refer to in this manuscript as the multivariate Taylor series expansion of a vector function. From expression 2.4 (subsection 2.2.1) it follows that the polynomial variation structure we are after is,

$$\begin{aligned} \hat{\mathbf{f}} &= + \frac{\partial\mathbf{f}(\mathbf{x}, t)}{\partial t} \Delta t + \frac{\partial^2}{\partial t^2} (\mathbf{f}(\mathbf{x}, t)) \frac{(\Delta t)^2}{2!} \\ &+ \frac{\partial\mathbf{f}(\mathbf{x}, t)}{\partial\mathbf{x}} \cdot \frac{d\mathbf{x}}{dt} \Delta t + \left(\frac{\partial^2 \mathbf{f}(\mathbf{x}, t)}{\partial \mathbf{x}^2} \cdot \frac{d\mathbf{x}}{dt} \right) \cdot \frac{d\mathbf{x}}{dt} \frac{(\Delta t)^2}{2!} \\ &+ \frac{\partial^2}{\partial t \partial \mathbf{x}} (\mathbf{f}(\mathbf{x}, t)) \cdot \frac{d\mathbf{x}}{dt} \frac{(\Delta t)^2}{2!} + \frac{\partial^2 \mathbf{f}(\mathbf{x}, t)}{\partial \mathbf{x} \partial t} \cdot \frac{d\mathbf{x}}{dt} \frac{(\Delta t)^2}{2!} \\ &+ \frac{\partial \mathbf{f}(\mathbf{x}, t)}{\partial \mathbf{x}} \cdot \frac{d^2 \mathbf{x}}{dt^2} \frac{(\Delta t)^2}{2!} \\ &+ \mathcal{O} \left((\Delta t)^3 \right). \end{aligned} \quad (2.13)$$

Notice, the two terms on the fourth row are similar except for the order of differentiation. From mathematics it is known that when one of the mixed second order partial derivatives is continuous in the neighbourhood of (\mathbf{x}, t) , they are equal (e.g. see p. 948 [5] or p. 255 in [6]),

$$\frac{\partial^2 \mathbf{f}(\mathbf{x}, t)}{\partial \mathbf{x} \partial t} = \frac{\partial^2 \mathbf{f}(\mathbf{x}, t)}{\partial t \partial \mathbf{x}}. \quad (2.14)$$

Since we assumed that \mathbf{f} is smooth, we can validly adopt this equality and may write the above equations 2.12 and 2.13 in a more compact form.

2.2.3 Interpretation of the multivariate Taylor series: An Eulerian kinematic view.

In the former subsection we have tacitly adopted a voyeuristic perspective, or Eulerian observational perspective: *an outside observer looking at a distant to the space Ω with the embedded function \mathbf{f} and a focal area which shifts position at a rate $d\mathbf{x}/dt$.* We illustrated this in figure 2.1.

Alternatively, one may view Ω and \mathbf{f} from a Lagrangian observational perspective: a "nigh" observer riding on the back of a point particle traversing the embedded function. See for an illustration figure 2.2. Defined as such, it can be shown that the Eulerian and Lagrangian perspectives are similar through a translation transformation. This connection we will consider nearer in section 2.3 where the translation transformation is captured by a displacement vector. In the following we remain with the Eulerian observational perspective.

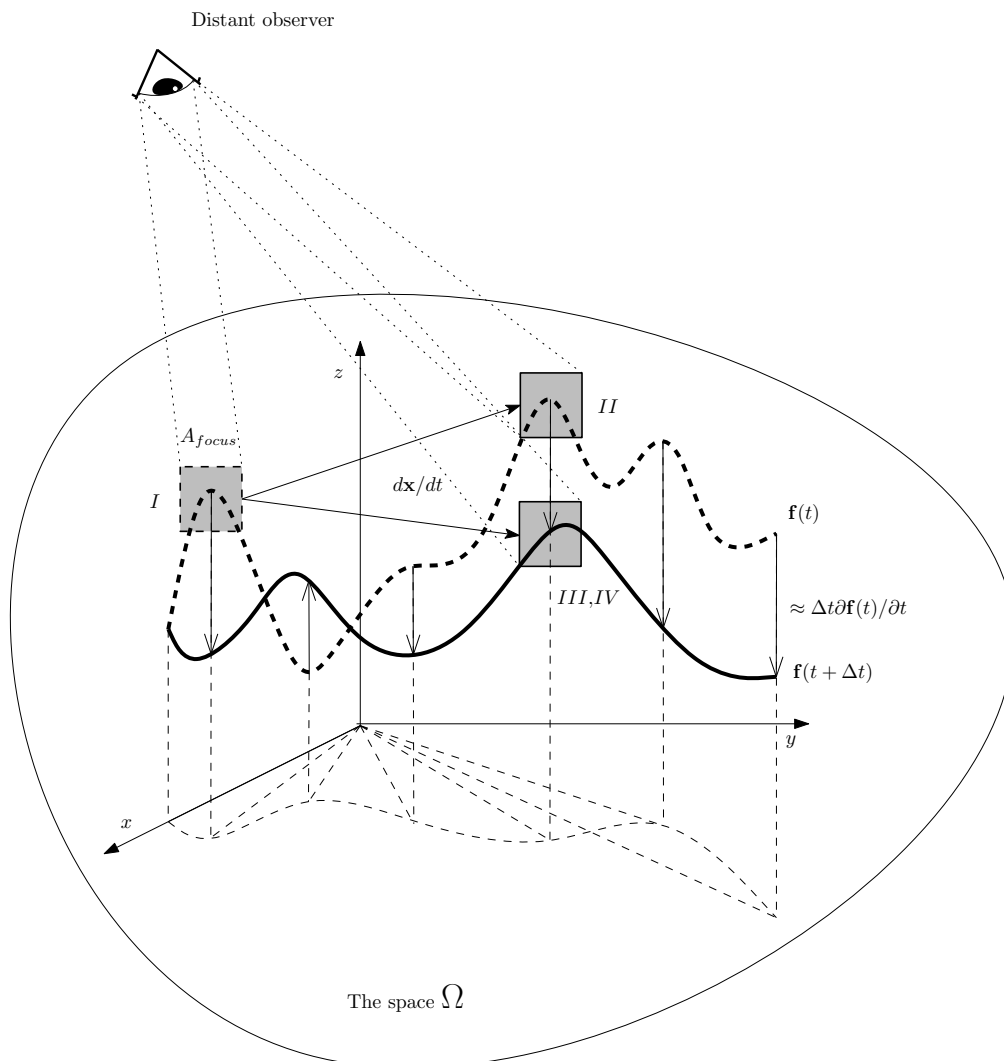


Figure 2.1: A distant observer looking at a function f embedded in a three dimensional space Ω and having an focal area A_{focus} . The roman numerals correspond to four of the five scenarios mentioned in the text.

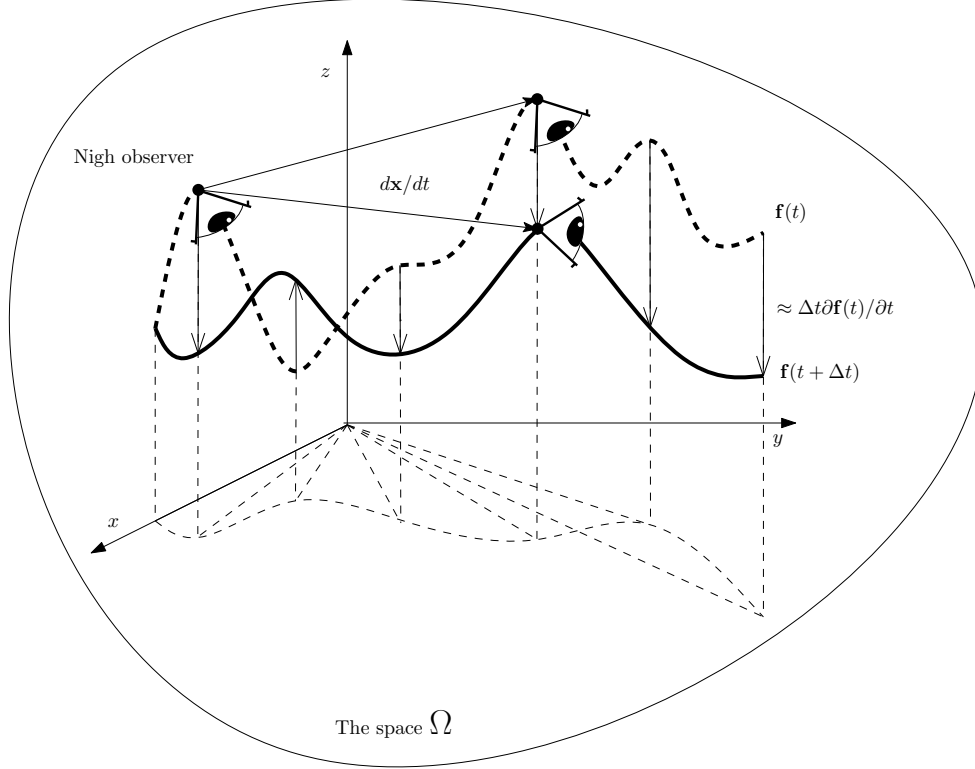


Figure 2.2: A "nigh" observer sitting on a particle traversing the function f embedded in a three dimensional space Ω .

Consider equation 2.12,

$$\begin{aligned}
 \mathbf{f}(\mathbf{x} + \Delta \mathbf{x}, t + \Delta t) &= \mathbf{f}(\mathbf{x}, t) \\
 &+ \frac{\partial \mathbf{f}(\mathbf{x}, t)}{\partial t} \Delta t + \frac{\partial^2}{\partial t^2} (\mathbf{f}(\mathbf{x}, t)) \frac{(\Delta t)^2}{2!} \\
 &+ \frac{\partial \mathbf{f}(\mathbf{x}, t)}{\partial \mathbf{x}} \cdot \frac{d\mathbf{x}}{dt} \Delta t + \left(\frac{\partial^2 \mathbf{f}(\mathbf{x}, t)}{\partial \mathbf{x}^2} \cdot \frac{d\mathbf{x}}{dt} \right) \cdot \frac{d\mathbf{x}}{dt} \frac{(\Delta t)^2}{2!} \\
 &+ \frac{\partial^2}{\partial t \partial \mathbf{x}} (\mathbf{f}(\mathbf{x}, t)) \cdot \frac{d\mathbf{x}}{dt} \frac{(\Delta t)^2}{2!} + \frac{\partial^2 \mathbf{f}(\mathbf{x}, t)}{\partial \mathbf{x} \partial t} \cdot \frac{d\mathbf{x}}{dt} \frac{(\Delta t)^2}{2!} \\
 &+ \frac{\partial \mathbf{f}(\mathbf{x}, t)}{\partial \mathbf{x}} \cdot \frac{d^2 \mathbf{x}}{dt^2} \frac{(\Delta t)^2}{2!} \\
 &+ \mathcal{O}((\Delta t)^3).
 \end{aligned} \tag{2.15}$$

In the light of the Eulerian perspective multiple scenarios can be recognized of different complexity. For simplicity, let us assume for the following discussion that the third order contributions are negligibly small and that our focus does not accelerate. The latter, in order to avoid unwanted fictitious inertial effects which not have anything to do with the space (they are "subjective"). Hence, we do not take in account the last two lines of equation 2.15. Consequently, we end up with a set of five different scenarios: I.) a static focal area with a time-explicit varying function; II.) a stationary function with a wandering focal area; III.) a wandering focal area interfering with a time-explicit varying function; IV.) a wandering focal area non interfering with a time-explicit varying function; and V.) the local linear approximation for sufficiently small precision in time.

Consider first that during an observation the embedded function may change with time, while we keep our focus fixed. In this scenario, $\frac{d\mathbf{x}}{dt} = 0$ and equation 2.15 is reduced to,

$$\mathbf{f}(\mathbf{x} + \Delta \mathbf{x}, t + \Delta t) = \mathbf{f}(\mathbf{x}, t) + \frac{\partial \mathbf{f}(\mathbf{x}, t)}{\partial t} \Delta t + \frac{\partial^2}{\partial t^2} (\mathbf{f}(\mathbf{x}, t)) \frac{(\Delta t)^2}{2!} \tag{2.16}$$

We can relax this fixation and let our focal area wander at a steady pace. While changing our focus and hence the view, the embedded function itself may remain static or the function may change. In the scenario where the function itself remains static, the partial derivatives with respect to time are zero and

equation 2.15 will become,

$$\mathbf{f}(\mathbf{x} + \Delta\mathbf{x}, t + \Delta t) = \mathbf{f}(\mathbf{x}, t) + \frac{\partial\mathbf{f}(\mathbf{x}, t)}{\partial\mathbf{x}} \cdot \frac{d\mathbf{x}}{dt} \Delta t + \left(\frac{\partial^2\mathbf{f}(\mathbf{x}, t)}{\partial\mathbf{x}^2} \cdot \frac{d\mathbf{x}}{dt} \right) \cdot \frac{d\mathbf{x}}{dt} \frac{(\Delta t)^2}{2!} \quad (2.17)$$

For the scenario that the function does change, we have to include the second line as well as the cross terms of the fourth line of equation 2.15. The terms on the fourth line account for the inseparable contribution to the apparent change in \mathbf{f} by simultaneously varying \mathbf{f} and \mathbf{x} . The equation reduces to,

$$\begin{aligned} \mathbf{f}(\mathbf{x} + \Delta\mathbf{x}, t + \Delta t) &= \mathbf{f}(\mathbf{x}, t) \\ &+ \frac{\partial\mathbf{f}(\mathbf{x}, t)}{\partial t} \Delta t + \frac{\partial^2}{\partial t^2} (\mathbf{f}(\mathbf{x}, t)) \frac{(\Delta t)^2}{2!} \\ &+ \frac{\partial\mathbf{f}(\mathbf{x}, t)}{\partial\mathbf{x}} \cdot \frac{d\mathbf{x}}{dt} \Delta t + \left(\frac{\partial^2\mathbf{f}(\mathbf{x}, t)}{\partial\mathbf{x}^2} \cdot \frac{d\mathbf{x}}{dt} \right) \cdot \frac{d\mathbf{x}}{dt} \frac{(\Delta t)^2}{2!} \\ &+ \frac{\partial^2}{\partial t\partial\mathbf{x}} (\mathbf{f}(\mathbf{x}, t)) \cdot \frac{d\mathbf{x}}{dt} \frac{(\Delta t)^2}{2!} + \frac{\partial^2\mathbf{f}(\mathbf{x}, t)}{\partial\mathbf{x}\partial t} \cdot \frac{d\mathbf{x}}{dt} \frac{(\Delta t)^2}{2!} \end{aligned} \quad (2.18)$$

As special case of this scenario is the situation in which the inseparable contributions are negligibly small. In other words, the variation of \mathbf{f} is independent of the variation in \mathbf{x} . Hence, both equations 2.15 and 2.18 reduce to,

$$\begin{aligned} \mathbf{f}(\mathbf{x} + \Delta\mathbf{x}, t + \Delta t) &= \mathbf{f}(\mathbf{x}, t) \\ &+ \frac{\partial\mathbf{f}(\mathbf{x}, t)}{\partial t} \Delta t + \frac{\partial^2}{\partial t^2} (\mathbf{f}(\mathbf{x}, t)) \frac{(\Delta t)^2}{2!} \\ &+ \frac{\partial\mathbf{f}(\mathbf{x}, t)}{\partial\mathbf{x}} \cdot \frac{d\mathbf{x}}{dt} \Delta t + \left(\frac{\partial^2\mathbf{f}(\mathbf{x}, t)}{\partial\mathbf{x}^2} \cdot \frac{d\mathbf{x}}{dt} \right) \cdot \frac{d\mathbf{x}}{dt} \frac{(\Delta t)^2}{2!} \end{aligned} \quad (2.19)$$

In the specific situation that we can consider a very small precision $\Delta t \ll 1$, terms multiplied with $(\Delta t)^2$ become vanishingly small and we end up with the local linear approximation,

$$\mathbf{f}(\mathbf{x} + \Delta\mathbf{x}, t + \Delta t) = \mathbf{f}(\mathbf{x}, t) + \frac{\partial\mathbf{f}(\mathbf{x}, t)}{\partial t} \Delta t + \frac{\partial\mathbf{f}(\mathbf{x}, t)}{\partial\mathbf{x}} \cdot \frac{d\mathbf{x}}{dt} \Delta t \quad (2.20)$$

This approximation becomes exact (fully accurate) when we consider infinitesimal precision. In other words, from very small down to infinitesimal precision, a function its behaviour is (locally) linear and its arguments can be varied sequentially, or independently to yield an accurate result.

2.2.4 The total derivative of the multivariate Taylor series.

Consider the total derivative of a vector function $d\mathbf{f}/dt$. Similar to \mathbf{f} , we are interested in the variation structure of this derivative field $d\mathbf{f}/dt$. Moreover, we suppose it is possible that we can predict $d\mathbf{f}(\mathbf{x} + \Delta\mathbf{x}, t + \Delta t)/dt$ from a relation similar in form like equation 2.4, i.e.,

$$\frac{d\mathbf{f}(\mathbf{x} + \Delta\mathbf{x}, t + \Delta t)}{dt} = \frac{d\mathbf{f}(\mathbf{x}, t)}{dt} + \frac{\dot{d}\mathbf{f}}{dt}, \quad (2.21)$$

and we are interested in $\frac{\dot{d}\mathbf{f}}{dt}$, in the specific case that the derivative-field is continuous in \mathbf{x} and t as well as that it varies smoothly.

To obtain an expression for the variation term $\frac{\dot{d}\mathbf{f}}{dt}$, we may follow the same steps like we did for \mathbf{f} above or simply substitute for each \mathbf{f} in equation 2.12 the function $d\mathbf{f}/dt$. Alternatively, we may take the total derivative of equation 2.12. If we pursue the latter approach (in line with [98], p. 96), we obtain,

$$\begin{aligned} \frac{d}{dt} (\mathbf{f}(t + \Delta t, \mathbf{x} + \Delta\mathbf{x})) &= \frac{d\mathbf{f}(\mathbf{x}, t)}{dt} \\ &+ \frac{d}{dt} \left(\frac{\partial\mathbf{f}(\mathbf{x}, t)}{\partial t} \Delta t \right) + \frac{d}{dt} \left(\frac{\partial^2}{\partial t^2} (\mathbf{f}(\mathbf{x}, t)) \frac{(\Delta t)^2}{2!} \right) \\ &+ \frac{d}{dt} \left(\frac{\partial\mathbf{f}(\mathbf{x}, t)}{\partial\mathbf{x}} \cdot \frac{d\mathbf{x}}{dt} \Delta t \right) + \frac{d}{dt} \left(\left(\frac{\partial^2\mathbf{f}(\mathbf{x}, t)}{\partial\mathbf{x}^2} \cdot \frac{d\mathbf{x}}{dt} \right) \cdot \frac{d\mathbf{x}}{dt} \frac{(\Delta t)^2}{2!} \right) \\ &+ \frac{d}{dt} \left(\frac{\partial^2}{\partial t\partial\mathbf{x}} (\mathbf{f}(\mathbf{x}, t)) \cdot \frac{d\mathbf{x}}{dt} \frac{(\Delta t)^2}{2!} \right) + \frac{d}{dt} \left(\frac{\partial^2\mathbf{f}(\mathbf{x}, t)}{\partial\mathbf{x}\partial t} \cdot \frac{d\mathbf{x}}{dt} \frac{(\Delta t)^2}{2!} \right) \\ &+ \frac{d}{dt} \left(\frac{\partial\mathbf{f}(\mathbf{x}, t)}{\partial\mathbf{x}} \cdot \frac{d^2\mathbf{x}}{dt^2} \frac{(\Delta t)^2}{2!} \right) \\ &+ \mathcal{O} \left((\Delta t)^3, (\mathbf{x})^3 \right). \end{aligned} \quad (2.22)$$

This expression can be refined in a straight forward manner by working out the total derivatives, in a similar vein to what we did in order to obtain the expression 2.12. However, for the scope of this manuscript it suffices that we consider the local linear approximation to $d\mathbf{f}(t + \Delta t, \mathbf{x} + \Delta\mathbf{x})/dt$ and subsequently obtain,

$$\begin{aligned} \frac{d}{dt} (\mathbf{f}(t + \Delta t, \mathbf{x} + \Delta\mathbf{x})) &\approx \frac{d\mathbf{f}(\mathbf{x}, t)}{dt} + \frac{d}{dt} \left(\frac{\partial\mathbf{f}(\mathbf{x}, t)}{\partial t} \Delta t \right) + \frac{d}{dt} \left(\frac{\partial\mathbf{f}(\mathbf{x}, t)}{\partial \mathbf{x}} \cdot \frac{d\mathbf{x}}{dt} \Delta t \right) \\ &= \frac{\partial\mathbf{f}(\mathbf{x}, t)}{\partial t} + \frac{\partial\mathbf{f}(\mathbf{x}, t)}{\partial \mathbf{x}} \cdot \frac{d\mathbf{x}}{dt} + \frac{\partial^2\mathbf{f}(\mathbf{x}, t)}{\partial t^2} \Delta t \\ &\quad + \frac{\partial^2\mathbf{f}(\mathbf{x}, t)}{\partial \mathbf{x} \partial t} \cdot \frac{d\mathbf{x}}{dt} \Delta t + \frac{\partial^2\mathbf{f}(\mathbf{x}, t)}{\partial t \partial \mathbf{x}} \cdot \frac{d\mathbf{x}}{dt} \Delta t \\ &\quad + \left(\frac{\partial^2\mathbf{f}}{\partial \mathbf{x}^2} \cdot \frac{d\mathbf{x}}{dt} \right) \cdot \frac{d\mathbf{x}}{dt} \Delta t + \frac{\partial\mathbf{f}(\mathbf{x}, t)}{\partial t} \cdot \frac{d^2\mathbf{x}}{dt^2} \Delta t. \end{aligned} \quad (2.23)$$

Notice, the two terms on the third row of this equation are similar except for the order of differentiation. From mathematics it is known that when one of the mixed second order partial derivatives is continuous in the neighbourhood of (\mathbf{x}, t) , they are equal (e.g. see p. 948 [5] or p. 255 in [6]),

$$\frac{\partial^2\mathbf{f}(\mathbf{x}, t)}{\partial \mathbf{x} \partial t} = \frac{\partial^2\mathbf{f}(\mathbf{x}, t)}{\partial t \partial \mathbf{x}}. \quad (2.24)$$

Since we assumed that \mathbf{f} is smooth, we can validly adopt this equality and end up with the more compact result,

$$\begin{aligned} \frac{d}{dt} (\mathbf{f}(t + \Delta t, \mathbf{x} + \Delta\mathbf{x})) &\approx \frac{\partial\mathbf{f}(\mathbf{x}, t)}{\partial t} + \frac{\partial\mathbf{f}(\mathbf{x}, t)}{\partial \mathbf{x}} \cdot \frac{d\mathbf{x}}{dt} + \frac{\partial^2\mathbf{f}(\mathbf{x}, t)}{\partial t^2} \Delta t \\ &\quad + 2 \frac{\partial^2\mathbf{f}(\mathbf{x}, t)}{\partial \mathbf{x} \partial t} \cdot \frac{d\mathbf{x}}{dt} \Delta t + \left(\frac{\partial^2\mathbf{f}}{\partial \mathbf{x}^2} \cdot \frac{d\mathbf{x}}{dt} \right) \cdot \frac{d\mathbf{x}}{dt} \Delta t + \frac{\partial\mathbf{f}(\mathbf{x}, t)}{\partial t} \cdot \frac{d^2\mathbf{x}}{dt^2} \Delta t \end{aligned} \quad (2.25)$$

or in a more physical parlance,

$$\begin{aligned} \frac{d}{dt} (\mathbf{f}(t + \Delta t, \mathbf{x} + \Delta\mathbf{x})) &\approx \frac{\partial\mathbf{f}(\mathbf{x}, t)}{\partial t} + \text{grad} [\mathbf{f}(\mathbf{x}, t)] \cdot \frac{d\mathbf{x}}{dt} + \frac{\partial^2\mathbf{f}(\mathbf{x}, t)}{\partial t^2} \Delta t + 2 \text{grad} \left[\frac{\partial\mathbf{f}(\mathbf{x}, t)}{\partial t} \right] \cdot \frac{d\mathbf{x}}{dt} \Delta t \\ &\quad + \left(\text{grad} [\text{grad} [\mathbf{f}(\mathbf{x}, t)]] \cdot \frac{d\mathbf{x}}{dt} \right) \cdot \frac{d\mathbf{x}}{dt} \Delta t + \frac{\partial\mathbf{f}(\mathbf{x}, t)}{\partial t} \cdot \frac{d^2\mathbf{x}}{dt^2} \Delta t. \end{aligned} \quad (2.26)$$

The above two equations are representations of the Taylor series expansion of the derivative field, truncated down to the second order. Since the first two terms in these equations resemble the total derivative (equation 2.8), we can see from these equations that the variation structure we are after is approximately,

$$\frac{d\mathbf{f}}{dt} \approx \frac{\partial^2\mathbf{f}(\mathbf{x}, t)}{\partial t^2} \Delta t + 2 \frac{\partial^2\mathbf{f}(\mathbf{x}, t)}{\partial \mathbf{x} \partial t} \cdot \frac{d\mathbf{x}}{dt} \Delta t + \left(\frac{\partial^2\mathbf{f}}{\partial \mathbf{x}^2} \cdot \frac{d\mathbf{x}}{dt} \right) \cdot \frac{d\mathbf{x}}{dt} \Delta t + \frac{\partial\mathbf{f}(\mathbf{x}, t)}{\partial t} \cdot \frac{d^2\mathbf{x}}{dt^2} \Delta t \quad (2.27)$$

The considerations presented in subsection 2.2.3 on interpreting equation 2.12 can be also applied to equation 2.25 above. Hence, we do not repeat it here. Though, recall that within subsection 2.2.3 we assumed that "our focus does not accelerate", i.e. $\frac{d^2\mathbf{x}}{dt^2} = 0$, and that the reason for it is that a non-zero acceleration would give rise to unwanted fictitious/apparent effects which have nothing to do with the object in the space we are observing. This same assumption we apply to equation 2.25 and consequently we obtain the general result we will built on further in this manuscript,

$$\begin{aligned} \frac{d}{dt} (\mathbf{f}(t + \Delta t, \mathbf{x} + \Delta\mathbf{x})) &\approx \frac{\partial\mathbf{f}(\mathbf{x}, t)}{\partial t} + \frac{\partial\mathbf{f}(\mathbf{x}, t)}{\partial \mathbf{x}} \cdot \frac{d\mathbf{x}}{dt} + \frac{\partial^2\mathbf{f}(\mathbf{x}, t)}{\partial t^2} \Delta t \\ &\quad + 2 \frac{\partial^2\mathbf{f}(\mathbf{x}, t)}{\partial \mathbf{x} \partial t} \cdot \frac{d\mathbf{x}}{dt} \Delta t + \left(\frac{\partial^2\mathbf{f}}{\partial \mathbf{x}^2} \cdot \frac{d\mathbf{x}}{dt} \right) \cdot \frac{d\mathbf{x}}{dt} \Delta t \end{aligned} \quad (2.28)$$

2.2.5 Section summary: Smooth vector fields & their polynomial variation structure.

In this section we obtained the Taylor series expansion for a continuous and smooth vector function/field \mathbf{f} (equation 2.12 in subsection 2.2.2) as well as its associated derivative field $d\mathbf{f}/dt$ (equation 2.25 in subsection 2.2.4). In the light of the Reynolds decomposition, we argued that the Taylor series can be viewed as being composed from a normative function value attributed to the position (\mathbf{x}, t) and a polynomial variation structure (equation 2.4 in subsection 2.2.1). Together they provide an alternative representation of a function value of f at an arbitrary distance and time $(\mathbf{x} + \Delta\mathbf{x}, t + \Delta t)$, away from the norm.

The general case, that we want to represent a function value f at an arbitrary distance and time away from the norm requires an infinite order polynomial to be accurate and precise. However, such a representation is intractable and we discussed five approximations, in the light of a Eulerian kinematic perspective (subsection 2.2.3). Especially the local linear approximation (equation 2.20) is convenient due to 1.) its independent nature regarding the variation of the variables, 2.) a tractable number of linear terms, and 3.) in the limit of infinitesimal precision $\Delta\mathbf{x}, \Delta t \rightarrow 0$ it is known to be accurate. This approximation will be relied on heavily in the rest of this manuscript.

2.3 The fundamental theorem of deformation kinematics.

2.3.1 Introduction: Displacements from an Eulerian observational perspective.

Let us adopt a Eulerian kinematic perspective, i.e. we are a distant observer and our focus wanders over the points \mathbf{x} (See for more information subsection 2.2.3). We define over Ω a displacement field \mathbf{u} . The displacement field entails the information where a particle will be displaced to, \mathbf{r} , when it visits an arbitrary position \mathbf{x} at an arbitrary time t ,

$$\mathbf{r}(\mathbf{x}, t) = \mathbf{x} + \mathbf{u}(\mathbf{x}, t), \quad \mathbf{x}, \mathbf{r} \in \Omega. \quad (2.29)$$

1

The displacement value $\mathbf{u}(\mathbf{x}, t)$ is attached to the position \mathbf{x} and is instantaneously attained by a particle visiting it. Reordering the latter equation let us define the displacement vector as,

$$\mathbf{u}(\mathbf{x}, t) = \mathbf{r}(\mathbf{x}, t) - \mathbf{x} = \hat{\mathbf{n}}_{\mathbf{u}}(\mathbf{x}, t)\Delta x(\mathbf{x}, t). \quad (2.30)$$

In words, "a step in the space Ω of magnitude Δx and in the direction of $\hat{\mathbf{n}}_{\mathbf{u}}$." The direction in which the step is taken as well as the magnitude may differ with position \mathbf{x} and time t .

From equation 2.30 we define heuristically the velocity as the rate of displacement,

$$\lim_{\Delta t \rightarrow 0} \frac{\mathbf{u}(\mathbf{x}, \tau)}{\Delta t} = \hat{\mathbf{n}}(\mathbf{x}, \tau) \lim_{\Delta t \rightarrow 0} \frac{\Delta x(\mathbf{x}, \tau)}{\Delta t} = \mathbf{v}(\mathbf{x}, \tau). \quad (2.31)$$

We interpret Δt as the duration in which the particle fulfils its displacement and τ as the time parameter related to changes in the fields \mathbf{u} and $\hat{\mathbf{n}}$. It is of course the similar time as t , however for clarity we separate them. We will consider the definition of \mathbf{v} nearer in subsection 2.3.5.

Note, we tacitly assumed a stationary displacement field, i.e. the direction and the magnitude of the displacement attributed with the position \mathbf{x} do not change with time. Alternatively we can now define the displacement as,

$$\mathbf{u}(\mathbf{x}, t) = \mathbf{v}(\mathbf{x}, t)\Delta t. \quad (2.32)$$

At an arbitrary moment in time, the displacement at a point \mathbf{x} is $\mathbf{u}(\mathbf{x}, t)$ and for a neighbouring point $\mathbf{x} + \Delta\mathbf{x}$ it is $\mathbf{u}(\mathbf{x} + \Delta\mathbf{x}, t)$. We may wonder if the displacement values are fully correlated, i.e. whether we can describe the displacement at $\mathbf{x} + \Delta\mathbf{x}$ in terms of the ("normative") displacement at a point \mathbf{x} .

Let us define the relative displacement of $\mathbf{x} + \Delta\mathbf{x}$ with respect to \mathbf{x} as,

$$\Delta_{\mathbf{x}}\mathbf{u} = \mathbf{u}(\mathbf{x} + \Delta\mathbf{x}, t) - \mathbf{u}(\mathbf{x}, t). \quad (2.33)$$

If we rewrite this expression in the form,

$$\mathbf{u}(\mathbf{x} + \Delta\mathbf{x}, t) = \mathbf{u}(\mathbf{x}, t) + \hat{\mathbf{u}}, \quad (2.34)$$

¹This equation can be considered as relating the Eulerian to the Lagrangian observational perspective. The position \mathbf{r} can be interpret as the position of the point particle on which a nigh observer sits as illustrated in figure 2.1 (subsection 2.2.3). The position \mathbf{x} can be interpret as the position of the center of focus of the distant observer. In this light, the displacement vector \mathbf{u} expresses the mutual distance. Note, it is customary to be more specific regarding \mathbf{x} , namely to specify a fixed focus and let it be a point within this focus. Moreover, to let \mathbf{x} be the initial position of the particle $\mathbf{x} = \mathbf{r}(\mathbf{x}, t_0)$.

it becomes clear that, in line with subsection 2.2.1, whenever the displacement values for the different points are fully correlated, the relative displacement (the variation term) is some deterministic function of $\mathbf{u}(\mathbf{x})$.

In the former section we considered the Taylor series expansion of a vector field/function. By virtue of Taylor's theorem, it is an accurate representation of a vector function whenever it is smooth. In continuum mechanics it is presupposed to be that the displacement (vector) field is smooth, at least, over a continuum object (e.g. see chapter 7 in [79], chapter 4 in [62], chapter 2 in [21], chapter 3 in [98] or chapter 4 in [8]).

In this section we will assume an absolute continuous displacement field and subject it to a Taylor series expansion in order to investigate its variation structure. However, first we will briefly discuss the absolute continuous nature of the displacement field, physically. Second, we will obtain the Taylor series representation for the displacement field. Third, we shall examine the variation structure on the different kinds of motion it describes. The same we will do, fourth, for the associated velocity field and finally we conclude with the fundamental theorem of deformation kinematics and argue on its wider applicability.

2.3.2 On the absolutely continuous nature of a displacement field, physically.

To make amenable why continuum mechanics may presuppose a continuous displacement field, consider first that when a rigid object moves without being stopped. It can be argued physically from scatter theory (e.g. see section 1.27 in [103], section 3.11 in [44] or [23]) that its trajectory is essentially absolutely continuous. Alternatively, it seems to follow from the presuppositions:

- 1.) time is continuous;
- 2.) a particle is conserved at all times; and
- 3.) a particle its velocity is finite (in classical mechanical systems it is even smaller than the finite speed of light).

These presuppositions suggest that whenever a particle its motion is continuous in time, its trajectory is absolutely continuous, i.e. continuous as well as smooth.

The trajectory of a single rigid object in a space can be interpret as the displacement function of the object, or a "sample" of a displacement field defined over the space. When a continuum object moves then, according to the argument on absolute continuity, each constituent particle of the continuum follows an absolutely continuous trajectory. In turn we can interpret each trajectory as a "sample" from a displacement field. For a multi particle system/continuum we should add another presupposition to the ones given above:

- 4.) two or more particles cannot visit the same position at the same time (i.e. phase space trajectories cannot cross).

Second, in case of a stationary displacement field, the trajectory of the constituents cannot cross², since if they do it means that there is a double point in the field (the point of crossing), which violates the assumption of determinism. For a continuum, embedded in a stationary displacement field, the constituents can be infinitesimally close to each other. Two infinitesimally distant constituents follow each an absolutely continuous path, i.e. the displacement along the trajectory varies continuously and smooth. That we can make the distant between two constituents arbitrary small (for a continuum) suggests continuity in displacement between trajectories. Though, the nature of the continuity is not necessarily smooth, at least not in the magnitude of the displacement³.

Third, to argue on the absolute continuous nature of the transition between two displacement values belonging to two infinitesimally close trajectories, we rely on dynamical considerations, as opposed to the kinematic considerations given above. From a phenomenological dynamic perspective, the constituent particles may interact through attractive, repulsive and collisional interactions (e.g. see section 1.1 in [12]

²Note, this is actually suggested by Bernoulli's streamline theorem, e.g. see p. 9 in [3].

³The absolutely continuous nature of the direction of the displacement one can argue about, since trajectories cannot cross for a stationary field setting and therefore placing a constraint on converging behaviour. Diverging behaviour suggest eventual violation of the definition of a continuum, i.e. two constituent particles who relatively diverge, initially arbitrary/infinitesimally close, give rise to vacuous regions.

or section 1.2 [101]). These interactions are responsible for correlated motion between the constituent particles and hence for an absolute continuous transition between two displacement values on different trajectories. For the different phases (gas, liquid or solid) typically a different interaction may dominate the correlation and different assumptions are in need to validate the presupposition of an absolutely continuous displacement field. In case of liquid and solid phases, of interest in this manuscript, it is common to consider that the attractive and repulsive interaction dominate (e.g. see section 18.2 in [131]). Due to their presence we state that the portion of the displacement field "sampled" by a continuum object is at least absolutely continuous.

2.3.3 The polynomial variation structure of a smooth displacement field.

If the displacement field is continuous and varies smoothly over Ω , by virtue of Taylor's theorem, the relative displacement can be written, with full accuracy, in terms of the "precision" $\Delta \mathbf{x}$ and the set of partial derivatives (with respect to \mathbf{x}) of \mathbf{u} around the point (\mathbf{x}, t) (e.g. see subsection 2.2.2). Hence, in the light of equation 2.12 subsection 2.2.2, we can obtain the polynomial expression,

$$\mathbf{u}(\mathbf{x} + \Delta \mathbf{x}, t) = \mathbf{u}(\mathbf{x}, t) + \frac{\partial \mathbf{u}(\mathbf{x}, t)}{\partial \mathbf{x}} \cdot \Delta \mathbf{x} + \left(\frac{\partial^2 \mathbf{u}(\mathbf{x}, t)}{\partial \mathbf{x}^2} \cdot \Delta \mathbf{x} \right) \cdot \frac{\Delta \mathbf{x}}{2!} + \mathcal{O}((\Delta \mathbf{x})^3). \quad (2.35)$$

In a more physical parlance this equation becomes,

$$\mathbf{u}(\mathbf{x} + \Delta \mathbf{x}, t) = \mathbf{u}(\mathbf{x}, t) + \text{grad}[\mathbf{u}(\mathbf{x}, t)] \cdot \Delta \mathbf{x} + \text{grad}(\text{grad}[\mathbf{u}(\mathbf{x}, t)] \cdot \Delta \mathbf{x}) \cdot \frac{\Delta \mathbf{x}}{2!} + \mathcal{O}((\Delta \mathbf{x})^3). \quad (2.36)$$

Local linear approximations, i.e. truncated Taylor series down to the first order derivatives, are ubiquitous in physics. The local linear approximation of this equation is,

$$\mathbf{u}(\mathbf{x} + \Delta \mathbf{x}, t) \approx \mathbf{u}(\mathbf{x}, t) + \text{grad}[\mathbf{u}(\mathbf{x}, t)] \cdot \Delta \mathbf{x}. \quad (2.37)$$

The accuracy of this approximation is determined by the magnitude of $\Delta \mathbf{x}$ and it becomes an exact relation for infinitesimal precision (e.g. see subsection 2.2.3).

Note, in the above we kept the time parameter fixed, however considering equation 2.12 from subsection 2.2.2, we can obtain the more general multivariate Taylor series expansion,

$$\begin{aligned} \mathbf{u}(t + \Delta t, \mathbf{x} + \Delta \mathbf{x}) &= \mathbf{u}(\mathbf{x}, t) \\ &+ \frac{\partial \mathbf{u}(\mathbf{x}, t)}{\partial t} \Delta t + \frac{\partial^2}{\partial t^2} (\mathbf{u}(\mathbf{x}, t)) \frac{(\Delta t)^2}{2!} \\ &+ \frac{\partial \mathbf{u}(\mathbf{x}, t)}{\partial \mathbf{x}} \cdot \frac{d\mathbf{x}}{dt} \Delta t + \left(\frac{\partial^2 \mathbf{u}(\mathbf{x}, t)}{\partial \mathbf{x}^2} \cdot \frac{d\mathbf{x}}{dt} \right) \cdot \frac{d\mathbf{x}}{dt} \frac{(\Delta t)^2}{2!} \\ &+ \frac{\partial^2}{\partial t \partial \mathbf{x}} (\mathbf{u}(\mathbf{x}, t)) \cdot \frac{d\mathbf{x}}{dt} \frac{(\Delta t)^2}{2!} + \frac{\partial^2 \mathbf{u}(\mathbf{x}, t)}{\partial \mathbf{x} \partial t} \cdot \frac{d\mathbf{x}}{dt} \frac{(\Delta t)^2}{2!} \\ &+ \frac{\partial \mathbf{u}(\mathbf{x}, t)}{\partial \mathbf{x}} \cdot \frac{d^2 \mathbf{x}}{dt^2} \frac{(\Delta t)^2}{2!} \\ &+ \mathcal{O}((\Delta t)^3). \end{aligned} \quad (2.38)$$

expressing spatial and temporal correlation/dependence in terms of a polynomial. On the right hand side, except for the implicit third and higher order term, the terms on the first and third line resemble equation 2.35. The second line accounts for the variation in time and the fourth and the fifth line account for the simultaneous variation of both time and space (see subsection 2.2.3).

In this section we will consider a stationary displacement field. Hence, we will not discuss this multivariate Taylor series expansion of the displacement function $\mathbf{u}(\mathbf{x} + \Delta \mathbf{x}, t + \Delta t)$ further. Remark, if we imagine that a space Ω is equipped with a stationary displacement function, then the physical implication of this assumption is that we suppose global mechanical equilibrium. In other words, there is no net force acting on the Ω .

In the scope of this section we will assume that a local linear approximation of the displacement function $\mathbf{u}(\mathbf{x} + \Delta \mathbf{x}, t)$ suffices. Hence, in the following subsections we will built further on equation 2.37. In that case the variation structure of the displacement field in the neighbourhood of a point $\mathbf{u}(\mathbf{x}, t)$ is given by the displacement gradient $\text{grad}[\mathbf{u}(\mathbf{x}, t)]$, i.e.

$$\mathring{\mathbf{u}} = \Delta \mathbf{u}(\mathbf{x}, t) = \text{grad}[\mathbf{u}(\mathbf{x}, t)] \cdot \Delta \mathbf{x}. \quad (2.39)$$

2.3.4 The relative displacement near a reference point.

Consider a continuum body \mathcal{B} , e.g. the body construed of two "beach balls" and a "connector" in figure 2.3, wandering through the Cartesian space Ω . The region \mathcal{B} occupies in Ω is given by its volume $V(\mathcal{B})$. Define over Ω a displacement field \mathbf{u} . The points making up the volume $V(\mathcal{B})$ are subjected to this displacement field and consequently a point initially at a position $\mathbf{x} \in \Omega$ is taken to $\mathbf{r}(\mathbf{x}, t)$, i.e.

$$\mathbf{r}(\mathbf{x}, t) = \mathbf{x} + \mathbf{u}(\mathbf{x}, t). \quad (2.40)$$

The displacement field dictates the kinematic behaviour of \mathcal{B} , which entails the collective displacement of the continuum set as a whole as well as the individual motion of each constituent of the set. The former is conveniently discussed in terms of the "center of mass" of the set and the latter in terms of relative displacements, commonly relative to the center of mass.

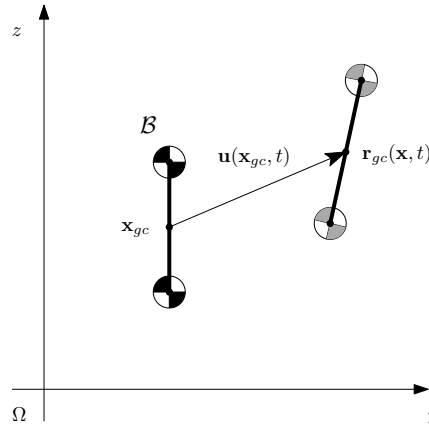


Figure 2.3: The dumbbell like continuum object \mathcal{B} composed of two beach balls and a connector. The dumbbell with the gray beach balls represents \mathcal{B} at a latter time than with the black beach balls.

The relative displacement of two arbitrary constituent-points on \mathcal{B} , e.g. the centers of the beach balls which occupy initially \mathbf{x} and $\mathbf{x} + \Delta\mathbf{x}$ in Ω , can be described by the results obtained in the former subsection 2.3.3. In other words, at an arbitrary moment in time, the variation structure of the displacement field $\mathbf{u}(\mathbf{x}, t)$ describes how the two material-points are displaced relatively to each other,

$$\mathbf{r}(\mathbf{x} + \Delta\mathbf{x}, t) - \mathbf{r}(\mathbf{x}, t) = \Delta\mathbf{x} + \Delta\mathbf{u}(\mathbf{x}, t). \quad (2.41)$$

Let us assume that the variation structure $\Delta\mathbf{u}(\mathbf{x}, t)$ is linear, or at least that it is locally linear and that the particles are at time t sufficiently close to each other. Hence, from subsection 2.3.3 we can use equation 2.37,

$$\mathbf{u}(\mathbf{x} + \Delta\mathbf{x}, t) \approx \mathbf{u}(\mathbf{x}, t) + \text{grad}[\mathbf{u}(\mathbf{x}, t)] \cdot \Delta\mathbf{x}. \quad (2.42)$$

In case that the displacement field is uniform, the gradient of the field vanishes and it results that both material points are displaced an equal amount and in the same direction. There is no relative displacement between the material points, i.e. these two points behave rigidly relative to each other. Hence, we can interpret the first term on the right hand side as describing the rigid-translational contribution to the displacement of $\mathbf{x} + \Delta\mathbf{x}$ relative to \mathbf{x} . See for an illustration figure 2.4.

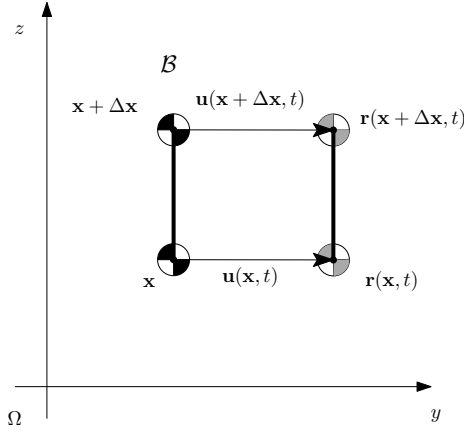
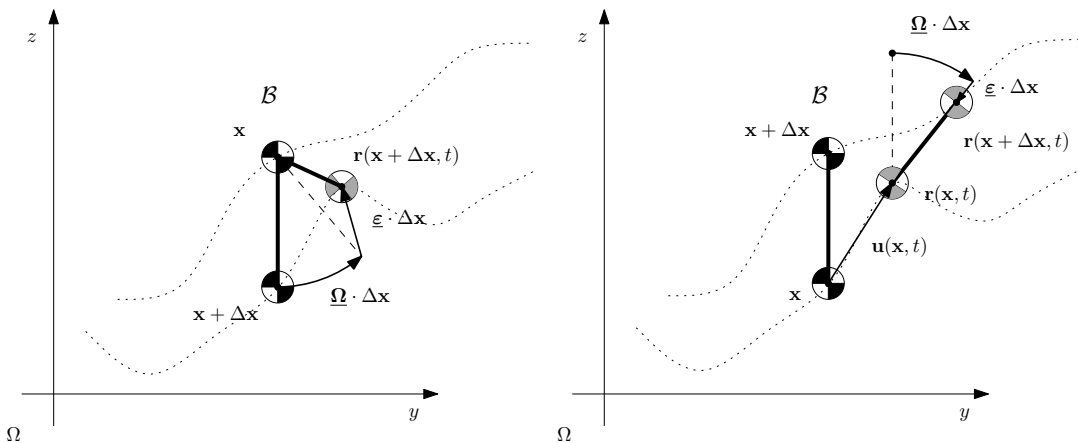


Figure 2.4: A uniform translation of the object \mathcal{B} .

From tensor theory it is known that any second order tensor can be decomposed into a symmetric and an antisymmetric tensor (e.g. see p. 503 in [17]). This is achieved by adding and subtracting the transpose of the tensor multiplied by a half, and subsequent reordering. Since the displacement gradient is a second order tensor, we can refine equation 2.42 to,

$$\begin{aligned}
 \mathbf{u}(\mathbf{x} + \Delta \mathbf{x}, t) &\approx \mathbf{u}(\mathbf{x}, t) + \text{grad}[\mathbf{u}(\mathbf{x}, t)] \cdot \Delta \mathbf{x} + \frac{1}{2} (\text{grad}[\mathbf{u}(\mathbf{x}, t)])^T \cdot \Delta \mathbf{x} - \frac{1}{2} (\text{grad}[\mathbf{u}(\mathbf{x}, t)])^T \cdot \Delta \mathbf{x} \\
 &= \mathbf{u}(\mathbf{x}, t) + \frac{1}{2} \left(\text{grad}[\mathbf{u}(\mathbf{x}, t)] - (\text{grad}[\mathbf{u}(\mathbf{x}, t)])^T \right) \cdot \Delta \mathbf{x} + \frac{1}{2} \left(\text{grad}[\mathbf{u}(\mathbf{x}, t)] + (\text{grad}[\mathbf{u}(\mathbf{x}, t)])^T \right) \cdot \Delta \mathbf{x} \\
 &= \mathbf{u}(\mathbf{x}, t) + \underline{\Omega} \cdot \Delta \mathbf{x} + \underline{\varepsilon} \cdot \Delta \mathbf{x}.
 \end{aligned} \tag{2.43}$$

In this equation $\underline{\varepsilon}$ is the symmetric part and describes an infinitesimal stretch or squeeze of the point initially at $\mathbf{x} + \Delta \mathbf{x}$ away from or towards \mathbf{x} . Consequently it is known as the infinitesimal strain tensor. The antisymmetric $\underline{\Omega}$ part describes an infinitesimal relative displacement of the point initially at $\mathbf{x} + \Delta \mathbf{x}$ over a circular arc with radius $\Delta \mathbf{x}$ and center \mathbf{x} , i.e. an infinitesimal rotation of the point $\mathbf{x} + \Delta \mathbf{x}$ around the point \mathbf{x} . Hence, it is known as the infinitesimal rotation tensor. An illustration of the complete motion of \mathcal{B} is given in 2.5b.



(a) The motion of \mathcal{B} as described by the sequence of: 1.) an infinitesimal rotation and 2.) an infinitesimal dilatation. (b) The motion of \mathcal{B} as described by the sequence of: 1.) a translation, 2.) an infinitesimal rotation and 3.) an infinitesimal dilatation.

Figure 2.5: The motion of a dumbbell shaped object \mathcal{B} as described by infinitesimal strain theory.

The interpretations of $\underline{\varepsilon}$ and $\underline{\Omega}$ may be more clearly seen from their matrix formulations, which are,

$$\underline{\varepsilon} = \begin{pmatrix} \frac{\partial u_x}{\partial x} & \frac{1}{2} \left(\frac{\partial u_x}{\partial y} + \frac{\partial u_y}{\partial x} \right) & \frac{1}{2} \left(\frac{\partial u_x}{\partial z} + \frac{\partial u_z}{\partial x} \right) \\ \frac{1}{2} \left(\frac{\partial u_y}{\partial x} + \frac{\partial u_x}{\partial y} \right) & \frac{\partial u_y}{\partial y} & \frac{1}{2} \left(\frac{\partial u_y}{\partial z} + \frac{\partial u_z}{\partial y} \right) \\ \frac{1}{2} \left(\frac{\partial u_z}{\partial x} + \frac{\partial u_x}{\partial z} \right) & \frac{1}{2} \left(\frac{\partial u_z}{\partial y} + \frac{\partial u_y}{\partial z} \right) & \frac{\partial u_z}{\partial z} \end{pmatrix} \quad (2.44)$$

and

$$\underline{\Omega} = \begin{pmatrix} 0 & \frac{1}{2} \left(\frac{\partial u_x}{\partial y} - \frac{\partial u_y}{\partial x} \right) & \frac{1}{2} \left(\frac{\partial u_x}{\partial z} - \frac{\partial u_z}{\partial x} \right) \\ \frac{1}{2} \left(\frac{\partial u_y}{\partial x} - \frac{\partial u_x}{\partial y} \right) & 0 & \frac{1}{2} \left(\frac{\partial u_y}{\partial z} - \frac{\partial u_z}{\partial y} \right) \\ \frac{1}{2} \left(\frac{\partial u_z}{\partial x} - \frac{\partial u_x}{\partial z} \right) & \frac{1}{2} \left(\frac{\partial u_z}{\partial y} - \frac{\partial u_y}{\partial z} \right) & 0 \end{pmatrix}. \quad (2.45)$$

The interpretation of the infinitesimal strain tensor is relatively straight forward, though if desired one may consult for example chapter 7 in [79] or chapter 4 in [62]. The interpretation of $\underline{\Omega}$ describing infinitesimal rotations is a little bit more obscure.

To make the interpretation more amenable, note that each derivative in the tensor can be recognized to be a form of the goniometric formula $\tan(\gamma)$, with γ being the respective "Euler angle" (e.g. see figure 2.6). In other words, we can write the infinitesimal rotation tensor as,

$$\begin{aligned} \underline{\Omega} &= \begin{pmatrix} 0 & \frac{1}{2} \left(\frac{\partial u_x}{\partial y} - \frac{\partial u_y}{\partial x} \right) & \frac{1}{2} \left(\frac{\partial u_x}{\partial z} - \frac{\partial u_z}{\partial x} \right) \\ \frac{1}{2} \left(\frac{\partial u_y}{\partial x} - \frac{\partial u_x}{\partial y} \right) & 0 & \frac{1}{2} \left(\frac{\partial u_y}{\partial z} - \frac{\partial u_z}{\partial y} \right) \\ \frac{1}{2} \left(\frac{\partial u_z}{\partial x} - \frac{\partial u_x}{\partial z} \right) & \frac{1}{2} \left(\frac{\partial u_z}{\partial y} - \frac{\partial u_y}{\partial z} \right) & 0 \end{pmatrix} \\ &= \begin{pmatrix} 0 & \frac{1}{2} (\tan(\gamma_{yx}) - \tan(\gamma_{xy})) & \frac{1}{2} (\tan(\gamma_{zx}) - \tan(\gamma_{xz})) \\ \frac{1}{2} (\tan(\gamma_{xy}) - \tan(\gamma_{yx})) & 0 & \frac{1}{2} (\tan(\gamma_{zy}) - \tan(\gamma_{yz})) \\ \frac{1}{2} (\tan(\gamma_{xz}) - \tan(\gamma_{zx})) & \frac{1}{2} (\tan(\gamma_{yz}) - \tan(\gamma_{zy})) & 0 \end{pmatrix}. \end{aligned} \quad (2.46)$$

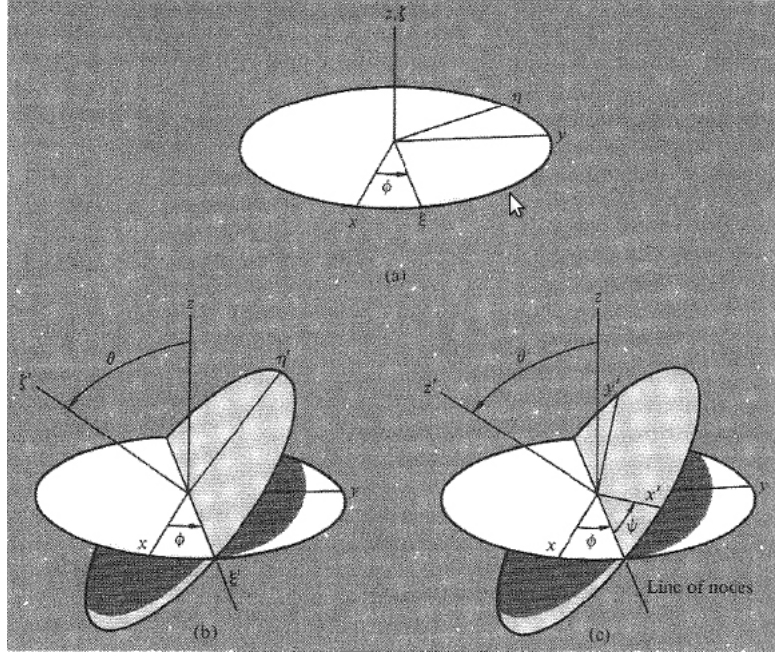


Figure 2.6: Visualisation of the Euler angles, after p. 152 in [44]. The average angles ω_{xy} , ω_{zx} and ω_{zy} are respectively referred to in the figure by ϕ , θ and ψ .

It is known from mathematics that for very small angles γ ,

$$\tan(\gamma) \approx \gamma, \quad (2.47)$$

which is often referred to as the small angle approximation. If we define an average angle as,

$$\omega_{ji} = \frac{1}{2} (\gamma_{ji} - \gamma_{ij}), \quad (2.48)$$

then we can rewrite $\underline{\Omega}$ as,

$$\begin{aligned} \underline{\Omega} &= \begin{pmatrix} 0 & \frac{1}{2} (\tan(\gamma_{yx}) - \tan(\gamma_{xy})) & \frac{1}{2} (\tan(\gamma_{zx}) - \tan(\gamma_{xz})) \\ \frac{1}{2} (\tan(\gamma_{xy}) - \tan(\gamma_{yx})) & 0 & \frac{1}{2} (\tan(\gamma_{zy}) - \tan(\gamma_{yz})) \\ \frac{1}{2} (\tan(\gamma_{xz}) - \tan(\gamma_{zx})) & \frac{1}{2} (\tan(\gamma_{yz}) - \tan(\gamma_{zy})) & 0 \end{pmatrix} \\ &\approx \begin{pmatrix} 0 & \frac{1}{2} (\gamma_{yx} - \gamma_{xy}) & \frac{1}{2} (\gamma_{zx} - \gamma_{xz}) \\ \frac{1}{2} (\gamma_{xy} - \gamma_{yx}) & 0 & \frac{1}{2} (\gamma_{zy} - \gamma_{yz}) \\ \frac{1}{2} (\gamma_{xz} - \gamma_{zx}) & \frac{1}{2} (\gamma_{yz} - \gamma_{zy}) & 0 \end{pmatrix} \\ &= \begin{pmatrix} 0 & \omega_{yx} & \omega_{zx} \\ \omega_{xy} & 0 & \omega_{zy} \\ \omega_{xz} & \omega_{yz} & 0 \end{pmatrix}. \end{aligned} \quad (2.49)$$

If we imagine a point on a circle with radius r , if we rotate the point over an angle θ radians then the point traversed a circular arc of length

$$s = r\theta. \quad (2.50)$$

Note that this product is analogous to the tensor-vector product

$$\underline{\Omega} \cdot \Delta \mathbf{x}. \quad (2.51)$$

Thus, the antisymmetric part of the displacement gradient describes infinitesimal displacements along a circular arc.

The infinitesimal straining displacements as well as the infinitesimal rotational displacements we defined in the above in a local sense with respect to the space Ω , or relative to the scale of the position vector connecting the origin of the space and the (geometric) center of the body \mathcal{B} . In contrast, we defined the displacements globally with respect to the scale of the body, $\Delta \mathbf{x}$. In addition we can define both kinds of displacements globally with respect to the space as well as locally with respect to the scale of the "beach balls". The form of the mathematical description of the displacements does not change for that, i.e. it remain two tensors multiplied by a difference vector.

To define the infinitesimal rotational and straining displacements, we essentially imagine the whole object \mathcal{B} to be concentrated on its geometric center \mathbf{x}_{gc} and consider the relative displacement between \mathbf{x}_{gc} and the origin of the space $\mathbf{0}$. The refined local linear approximation for this situation is,

$$\begin{aligned} \mathbf{u}(\mathbf{x}_{gc}, t) &\approx \mathbf{u}(\mathbf{0}, t) + \text{grad} [\mathbf{u}(\mathbf{0}, t)] \cdot \mathbf{x}_{gc} \\ &= \mathbf{u}(\mathbf{0}, t) + \underline{\Omega}(\mathbf{0}, t) \cdot \mathbf{x}_{gc} + \underline{\varepsilon}(\mathbf{0}, t) \cdot \mathbf{x}_{gc}. \end{aligned} \quad (2.52)$$

The first term on the right hand side describes the translational displacement of the combined system of the origin and \mathcal{B} , relative to an observer. However, we assume the origin to be fixed, at least relative to the observed, hence,

$$\mathbf{u}(\mathbf{0}, t) = 0. \quad (2.53)$$

Then, in the context of spherical coordinates, the term $\underline{\varepsilon}(\mathbf{0}, t) \cdot \mathbf{x}_{gc}$ can be interpret as describing a displacement in the radial direction with the azimuthal and zenithal angles kept fixed. In other words, it describes how \mathbf{x}_{gc} changes from orbit (two dimensional) or a spherical shell (three dimensional) around $\mathbf{0}$. The rotational term $\underline{\Omega}(\mathbf{0}, t) \cdot \mathbf{x}_{gc}$ describes the position of \mathbf{x}_{gc} along such an orbit or shell. For an illustration see figure 2.7.

Continuing this line, we can write the local displacement of \mathcal{B} with respect to $\mathbf{0}$ in terms of the relative displacement between \mathbf{x}_{gc} and the beach balls at \mathbf{x} and $\mathbf{x} + \Delta \mathbf{x}$. Since, for both relative displacement the idea is similar, we will only consider the relative displacement between the beach ball at \mathbf{x} and \mathbf{x}_{gc} . The associated local linear approximation for \mathbf{x} is,

$$\mathbf{u}(\mathbf{x}, t) \approx \mathbf{u}(\mathbf{x}_{gc}, t) + \underline{\Omega}(\mathbf{x}_{gc}, t) \cdot (\mathbf{x} - \mathbf{x}_{gc}) + \underline{\varepsilon}(\mathbf{x}_{gc}, t) \cdot (\mathbf{x} - \mathbf{x}_{gc}). \quad (2.54)$$

The interpretation is similar to above, in the context of spherical coordinates, however now orbits or shells are centred around \mathbf{x}_{gc} , instead of $\mathbf{0}$.

The local motion with respect to \mathbf{x}_{gc} or the local motion of \mathcal{B} can be imagined to be the rotation and dilatation of the beach ball. We will not explicate it here mathematically, since the idea is similar to the above only with \mathbf{x} as the center of the orbits or shells describing the global motion of the beach ball, or the local motion of \mathcal{B} .

Note, the global motion of \mathcal{B} comprises a translation of its geometric center \mathbf{x}_{gc} , which can be refined in terms of a relative motion with respect to the origin of the space $\mathbf{0}$ describing its "straight line" displacement in the radial direction by $\underline{\varepsilon}(\mathbf{0}, t)$ and its curving/tortuous displacement by $\underline{\Omega}(\mathbf{0}, t)$. The local motion of \mathcal{B} over the scale $\mathbf{x} - \mathbf{x}_{gc}$ describes the dilatation of \mathcal{B} by $\underline{\varepsilon}(\mathbf{x}_{gc}, t)$ and the spin of \mathbf{x} around \mathbf{x}_{gc} by $\underline{\Omega}(\mathbf{x}_{gc}, t)$. Moreover, if we substitute equation 2.52 in expression 2.54 we obtain the motion of the point \mathbf{x}

$$\mathbf{u}(\mathbf{x}, t) \approx \mathbf{u}(\mathbf{0}, t) + \underline{\Omega}(\mathbf{0}, t) \cdot \mathbf{x}_{gc} + \underline{\varepsilon}(\mathbf{0}, t) \cdot \mathbf{x}_{gc} + \underline{\Omega}(\mathbf{x}_{gc}, t) \cdot (\mathbf{x} - \mathbf{x}_{gc}) + \underline{\varepsilon}(\mathbf{x}_{gc}, t) \cdot (\mathbf{x} - \mathbf{x}_{gc}). \quad (2.55)$$

For an illustration of this final result, with $\mathbf{u}(\mathbf{0}, t) = 0$, see 2.7.

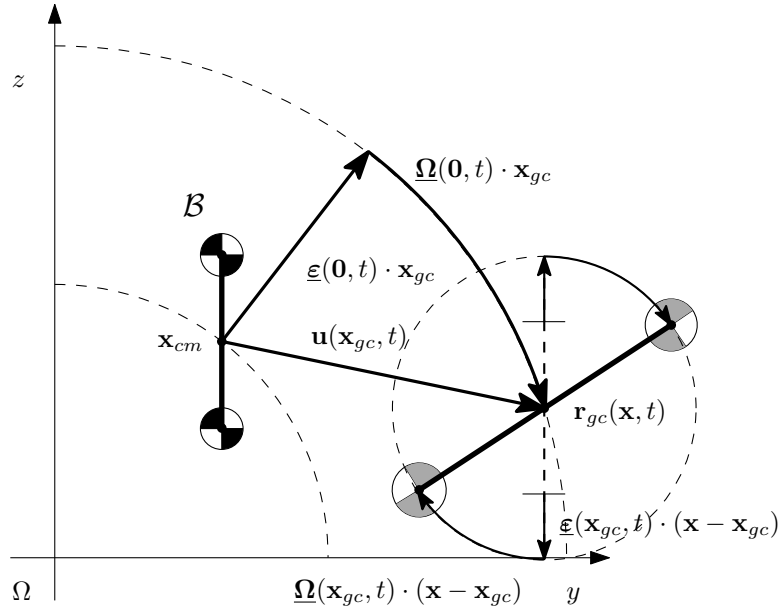


Figure 2.7: Global and local infinitesimal motion of a dumbbell shaped object \mathcal{B} .

2.3.5 The relative velocity near a reference point.

So far we have considered the displacement of an object \mathcal{B} and its constituent points. In the introduction of this section (subsection 2.3.1) we heuristically defined a rate of displacement as

$$\mathbf{v}(\mathbf{x}, \tau) = \lim_{\Delta t \rightarrow 0} \frac{\mathbf{u}(\mathbf{x}, \tau)}{\Delta t}, \quad (2.56)$$

with τ representing the time parameter accounting for the change in the displacement field and t being associated with the duration in which a displacement is fulfilled. However, both parameters are associated with the same time, they simply refer to different mechanisms which we explicate as such.

From an Eulerian perspective, the rate of displacement is attached to a position \mathbf{x} in a space Ω . It can be interpreted as the instantaneous velocity a particle attains when it visits the position \mathbf{x} . However, in general it is only a partial contribution to the velocity of the particle. To see, consider figure 2.8 which suggests that we can define the velocity of a particle by using equation 2.41 and 2.56 as well as the directional derivative. Thus,

$$\begin{aligned} \lim_{\Delta t \rightarrow 0} \frac{\mathbf{r}(\mathbf{x}, t + \Delta t) - \mathbf{r}(\mathbf{x}, t)}{\Delta t} &= \frac{\partial \mathbf{r}(\mathbf{x}, t)}{\partial t} \\ &= \lim_{\Delta t \rightarrow 0} \frac{\mathbf{r}(\mathbf{x}, t) - \mathbf{x}}{\Delta t} + \lim_{\Delta t \rightarrow 0} \frac{\mathbf{u}(\mathbf{x} + \mathbf{u}(\mathbf{x}, \tau), \tau) - \mathbf{u}(\mathbf{x}, \tau)}{\Delta t} \\ &= \mathbf{v}(\mathbf{x}, t) + \frac{\partial \mathbf{u}(\mathbf{x}, \tau)}{\partial \mathbf{x}} \cdot \mathbf{v}(\mathbf{x}, \tau) \\ &= d\mathbf{u}(\mathbf{x}, \tau)/dt. \end{aligned} \quad (2.57)$$

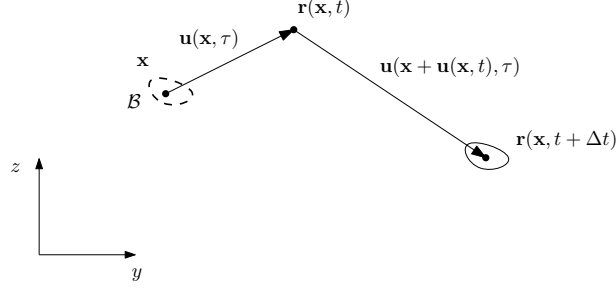


Figure 2.8: Two successive displacements for an object \mathcal{B} .

From this equation we can infer the definition for the rate of displacement, or strain rate as,

$$\mathbf{v}(\mathbf{x}, \tau) = \frac{\partial \mathbf{u}(\mathbf{x}, \tau)}{\partial t}. \quad (2.58)$$

In a similar vein like in the former subsection we can consider the different kinds of motion near a reference point \mathbf{x} , close enough such that the local linear approximation suffices. Therefore we start with equation 2.41, slightly rewrite it in analogy with 2.30 and then take the partial derivative with respect to time, which yields,

$$\frac{\partial}{\partial t} [\mathbf{r}(\mathbf{x} + \Delta \mathbf{x}, t) - (\mathbf{x} + \Delta \mathbf{x})] = \frac{\partial}{\partial t} [\mathbf{r}(\mathbf{x}, t) - \mathbf{x}] + \frac{\partial}{\partial t} [\Delta \mathbf{u}(\mathbf{x}, t)]. \quad (2.59)$$

This expression states that we can infer the velocity of a particle visiting $\mathbf{x} + \Delta \mathbf{x}$ from a knowledge of the velocity a particle would attain at \mathbf{x} .

From equation 2.42 we know that we can rewrite the relative displacement (second term on the right hand side of the latter equation) as the gradient of the displacement field around the point \mathbf{x} . Hence, we obtain,

$$\mathbf{v}(\mathbf{x} + \Delta \mathbf{x}, t) = \mathbf{v}(\mathbf{x}, t) + \frac{\partial}{\partial t} \text{grad} [\mathbf{u}(\mathbf{x}, t)] \cdot \Delta \mathbf{x} = \mathbf{v}(\mathbf{x}, t) + \text{grad} [\mathbf{v}(\mathbf{x}, t)] \cdot \Delta \mathbf{x}. \quad (2.60)$$

Since the displacement field is stationary, the gradient of \mathbf{u} does not change with time which allows us to interchange the gradient with the partial derivative. The latter equation for the rate of displacement is analogous to equation 2.55 for displacements.

The considerations we gave in the former subsection (subsection 2.3.4) for different modes of displacement of two points on a continuum body \mathcal{B} as well as locality also apply to equation 2.60. The reason is simply mathematical equivalence, we have only to keep in mind of the physical difference between a displacement and the rate of displacement. Consequently, we will not go through the programme again, we simply state here the two most important results:

- 1.) the motion of a point on a continuum object, relative to another point on the object; and
- 2.) the motion of a point on a continuum object, relative to a point external to the object.

Thus, we imagine a continuum body \mathcal{B} and highlight two points on the body, e.g. \mathbf{x}_{gc} and \mathbf{x} . The point \mathbf{x} can execute three kinds of motion relative to the geometric center \mathbf{x}_{gc} of \mathcal{B} : a.) a translational motion, b.) a straining motion, and/or c.) a rotational motion. If we suppose that the displacement gradients are very small (infinitesimal strain assumption), then we can describe this mathematically as,

$$\mathbf{v}(\mathbf{x} + \Delta \mathbf{x}, t) \approx \mathbf{v}(\mathbf{x}, t) + \underline{\boldsymbol{\Omega}}(\mathbf{x}, t) \cdot \delta \mathbf{x} + \underline{\boldsymbol{\epsilon}}(\mathbf{x}, t) \cdot \delta \mathbf{x}, \quad (2.61)$$

where we consider it to be understood that $\underline{\boldsymbol{\Omega}}(\mathbf{x}, t)$ and $\underline{\boldsymbol{\epsilon}}(\mathbf{x}, t)$ represent now respectively the infinitesimal rate of rotation and the strain rate tensor.

In case of an external reference point, e.g. the origin $\mathbf{0}$ of the space Ω through which \mathcal{B} wanders, then \mathcal{B} can execute four modes of relative motion: a.) a translation, b.) a rotation, c.) a vibration/dilatation, and/or d.) a spin/vorticity. The former two modes are global with respect to the space and the latter

two are local with respect to the space (see figure 2.7 for an illustration). Mathematically the relative motion of \mathbf{x} can be described as,

$$\mathbf{v}(\mathbf{x}, t) \approx \underbrace{\underline{\boldsymbol{\varepsilon}}(\mathbf{0}, t) \cdot \mathbf{x}_{gc}}_{\text{translation}} + \underbrace{\underline{\boldsymbol{\Omega}}(\mathbf{0}, t) \cdot \mathbf{x}_{gc}}_{\text{rotation}} + \underbrace{\underline{\boldsymbol{\varepsilon}}(\mathbf{x}_{gc}, t) \cdot (\mathbf{x} - \mathbf{x}_{gc})}_{\text{vibration/dilatation}} + \underbrace{\underline{\boldsymbol{\Omega}}(\mathbf{x}_{gc}, t) \cdot (\mathbf{x} - \mathbf{x}_{gc})}_{\text{spin/vorticity}}. \quad (2.62)$$

2.3.6 Section summary: The fundamental theorem of deformation kinematics.

In the above section we have considered relative displacements and rates of displacements of an object \mathcal{B} . We have shown that a general relative displacement or rate of displacement can be considered to be composed out of three, or four modes of motion, depending on whether the reference point lies on \mathcal{B} or external to it. In case of an external reference point, the modes are:

$$\left. \begin{array}{l} 1.) \text{ a translation,} \\ 2.) \text{ a rotation,} \\ 3.) \text{ a vibration/dilatation,} \\ 4.) \text{ a spin/vorticity,} \end{array} \right\} \begin{array}{l} \text{Object global} \\ \text{Object local} \end{array} \quad (2.63)$$

In the situation when we have a reference point internal to \mathcal{B} , then we have solely the translation, vibration/dilatation and the spin/vorticity (object local rotation). This result, of that a general motion can be decomposed in essentially three different contributions, can be referred to as the fundamental theorem of deformation kinematics (e.g. see [130]) and first proven by von Helmholtz [53] in the context of fluid flow.

We arrived at this result by supposing a continuous, smooth and slowly varying displacement field. These assumptions put us in the position to start with the local linear approximation of a displacement value at a position sufficiently near to a reference position. Then, by refining the displacement gradient in a symmetric and antisymmetric part we revealed the rotational and dilatational contributions to motion. Additional, considerations on relative global and local motion, to the object and the space in which the object resides, give rise to distinction between a global rotation and a spin/vorticity.

Recall from subsection 2.2.3 the definitions for the Lagrangian and Eulerian observational perspectives. In the light of these definitions, the case of an internal reference point can be paired up with the Lagrangian perspective and the situation of an external reference point can be associated with an Eulerian perspective. This suggest that if we are a "neigh observer" riding the back of \mathcal{B} , we would not notice whether the path along we translate would curve or not. For this to be amenable, the rate of curvature has to be small with respect to the extend of the translational displacements. Moreover, the displacement field (or rate of displacement/velocity field) should vary slowly, i.e. $\text{grad}[\mathbf{u}] \ll 1$, which is what we have presupposed, in the form of the infinitesimal strain assumption, throughout this section.

This suggests that the global rotation with respect to the space-object is actually a scale artefact, which is also how we unfold its existence in subsection 2.3.4. Moreover, we obtained the fundamental theorem for the motion of a point \mathbf{x} on \mathcal{B} relative to the geometric center \mathbf{x}_{gc} of \mathcal{B} , and subsequently we refined the translational term by inserting the fundamental theorem for \mathbf{x}_{gc} relative to the origin $\mathbf{0}$ of the space Ω . In this spirit, it is possible to construe complex kinematic descriptions through reapplication of the theorem of deformation kinematics, which is also the motivation to define the concept of vorticity as an average rotation (see for example p. 81-82 in [12] for more information).

2.4 Conclusion & chapter summary: A deterministic kinematic model.

In this chapter we considered the kinematics of an object \mathcal{B} traversing a space Ω . We have derived the mathematical explication of Helmholtz's fundamental theorem of deformation kinematics in subsection 2.3.4, which states that an object its motion is essentially a composition of three modes of motion: a.) a rigid translational motion; b.) a rigid spinning motion; and c.) a dilatational motion. In this subsection we have also considered briefly the importance of the observation scale when considering the motion of an object, in terms of the relative notions of global and local motion. The rigid spinning motion and the

dilatational motion we designated as local modes of motion. The translational motion we equipped with the notion of global.

In section 2.2 we treated the mathematical details of Taylor's theorem in the context of a vector field. We considered it in a frame analogous to a Reynolds decomposition: a field value is the sum of a reference value plus a deviation. Whereas in a Reynolds decomposition the deviation is explicated probabilistically, here the deviation accounts for the deterministic variation of the displacement field, at least in a sufficiently small neighbourhood around the reference value. The mathematical explication of Helmholtz's fundamental theorem we derived from the local linear approximation of a Taylor series representation of the displacement field. Consequently, the deviation describes the variation in displacement, or the relative displacement between the reference value and the considered field value.

We introduced the notions of globality and locality by considering different reference points in line with the two observational perspectives, Lagrangian versus Eulerian (the perspectives we explained in subsection 2.2.3). Moreover, we considered a reference point external to the object \mathcal{B} as well as a reference point internal to \mathcal{B} .

As a result of the continuous and smooth displacement field driving the motion, which we argued on in subsection 2.3.2, Taylor's theorem can be validly applied and we can look at the displacement field through the glasses of differential calculus. Differential calculus relies on the conceptual model that a curve, or surface can be described as a composition of straight line elements. With this conceptual image in mind, at the small, or local scale the translational motion is what it is referred to: a straight line motion. However, at the global scale the translational motion can be regarded as an averaged straight line motion and at intermediate scales, in between the local and global scale, besides a translational motion there can be also a rotational motion describing the curvature in the path of an object. Consequently, we concluded that in general an objects motion comprises four modes of motion, the two local modes mentioned earlier and a global translation as well as a global rotation. The two global modes are viewed as a refinement of an average global translation. The global rotation is not a new mode of motion, essentially it is a scale artefact. Note, there is no limit in considering different scales in the same spirit we just did, e.g. viewing the local motions in turn as relative global manifestations and in the other direction the global motions as relative local manifestations. Consequently, very complex kinematic descriptions can be construed, though the key idea does not differ.

The kinematic model we presented in this chapter seems to be valid for the kinematic description of all sorts of objects wandering through space, which we tried to reveal by adopting an Eulerian observational perspective. However, the model relies on that one can define a continuous smooth and slowly varying displacement field over the space in which the objects resides. The continuous and smooth assumptions assure that Taylor's theorem can be employed and hence that we can infer in a deterministic manner relative motions between a reference point/object and an other point/object. The assumption of slow variation of the displacement field (infinitesimal strain assumption) we imposed tacitly in subsection 2.3.4 and will get back to in chapter 3. The assumption allows us to decompose the motion of an object additively. In other words, that the motion of an object is essentially the sum of a translation, rotation and dilatation.

Chapter 3

A Lagrangian-Eulerian balance principle.

3.1 Introduction: A porous medium as an Lagrangian-Eulerian object.

In the coming chapter we will derive a Lagrangian-Eulerian (L-E) balance principle. This in order to describe in a rather general manner, mathematically, the evolution of the mass enclosed within a deformable porous medium (PM). Although off course the L-E balance principle can also be applied to other physical quantities of interest. Fundamental to the derivation is Leibniz's integral rule, which can be regarded as the decomposition of the (total) rate of change of the value of an integral in to an integrand variation and a domain-boundary variation contribution. In this chapter it functions as the abstract "hat stand" on which we can hang physical ideas to render it a balance principle as encountered in physics. For the physical attributes to hang on the stand, we mainly tap from the deformation kinematics considerations from chapter 2, in order to describe the deformation of the boundary of the domain of integration. Moreover, here we apply the results presented in that chapter.

We will generalize Leibniz's integral rule and derive Reynold's transport theorem as its generalization regarding a three dimensional domain of integration embedded in a three dimensional space. This generalization entails the conversion of boundary integrals to relative volume integrals, or vice versa. From Leibniz's integral rule we obtain a simple visual interpretation which we will associate with Reynolds transport theorem as its underlying general conceptual model. This model shows clearly how the Eulerian observational perspective can be interpret as a physical refinement of the contribution to the change in the value of the integral due to integrand variation and that the Lagrangian observational perspective is simply the contribution due to domain variation.

In addition we will discuss in this chapter boundary integrals, inspired by the article of [45]. This discussion suggests an abstract frame underlying the physical concept of a flux. Consequently, we can present a consistent general balance principle with respect to dimensions, at least regarding one, two and three dimensional (physical) spaces.

It is customary in physical analysis to employ either an analysis from a Lagrangian or else from an Eulerian observational perspective. Lagrangian and Eulerian in this sense have slightly different meanings then how we defined them in subsection 2.2.3: two mathematical perspectives between which one can change, without altering the content, through a (symmetry) transformation in the form of the displacement vector. In physical practice the perspectives are usually defined more strict. The Eulerian perspective is genuine understood to be equipped with the physical constraint of volume conservation and hence often referred to as a control volume perspective. The Lagrangian perspective is typically associated with particle conservation. These constraints render the perspectives to become mutually asymmetrical, at least not any more under the transformation of the displacement vector, simply because physically one considers two different things.

Fluid flow is typically described from an Eulerian point of view, where the analysis is performed within a fixed control volume (volume conservation). The deformation of solids is usually considered in a Lagrangian perspective by tracking a fixed set of mass particles (particle conservation). For examples, see section 2.1 in [12], section 4.1.3 and 6.3 in [13] or section 8.1.2 in [42]). This approach is also prevailing in hydrogeology, i.e. in describing the behaviour of a porous medium (PM). Heuristically speaking, dilatation is often discussed in an Lagrangian particle conservative setting and flow in an Eulerian volume conservative setting. Consequently, when a phase can flow as well as that it can be compressed or expanded it comprises characteristics of both perspectives.

A PM is a mixture of at least a solid and a fluid phase which are in basic hydrogeological theory regarded as being incompressible (e.g. see p. 205 in [13]). However, the PM itself can be compressible due to compressibility of the matrix spanned by the solid phase, i.e. the reordering of the solid grains (e.g. see section 2.7 in [13]). As a logical result the composite PM entails characteristics of both a Lagrangian and an Eulerian perspective and in line with the above, the solid phase is viewed from a Lagrangian particle conservative perspective and the fluid phase from an Eulerian volume conservative perspective. Note, in this sense the solid phase, at least the backbone of the matrix functions as a material boundary, or material defining boundary.

In addition, the water table in unconfined aquifers can also be denoted as a material boundary, a common explication encountered in the literature considering analytical expression for flow towards a well (e.g. see [82, 81]). Moreover, in a partially saturated PM, neglecting residual water and deformation of the solid matrix, the volume of water can be abstracted as a balloon which expands and contracts

depending on the volume of water stored within an under saturated PM control volume (fixed). Although the water itself we consider still as incompressible, the volume it occupies dilates due to flow across its boundaries: it shows both Lagrangian and Eulerian characteristics.

Both these two examples, are common in hydrogeology and have their overlap in the storage of water. The Lagrangian particle conservative view is employed in describing this storage mechanism, whether it is associated with the motion of a material boundary in the form of the solid matrix, the water interface or, less commonly, the compression of the solid and water phase. In this manuscript we are concerned with storage mechanisms and how they may play a role in the phenomenon of a high rate injection of water mass in a PM. Moreover, in this manuscript we aim to give a rigorous overview of storage mechanisms we can (theoretically) occur in a PM, as revealed from kinematic considerations. This for the purpose of answering the question: "Where can the injected water mass go to?" Consequently, we believe it is of interest to define, in a rather rigorous manner, a balance principle in which Lagrangian and Eulerian characteristics coexist, with a purely Eulerian control volume analysis as well as a Lagrangian particle tracking analysis as special cases.

We will derive in this chapter the three dimensional L-E balance principle by first considering the mathematical essence of a balance principle in one dimension. In other words, Leibniz's integral rule for the variation of an (one dimensional) integral. This relatively simple case puts forward a simple conceptual model and facilitates with relative ease interpretation of the mathematics. Successively, Leibniz's integral rule will be generalized for one and three dimensional domains embedded in three dimensional space. We will do this by first considering the mathematical description and deformation of parallelograms and parallelepipeds, the basic two and three dimensional domains underlying the conceptual ideas of integral calculus. Subsequently Leibniz's integral rule can be generalized relatively straight forward to three dimensional domains, as well as that we can establish its connection with Reynolds transport theorem. Furthermore, a brief treatment of an Eulerian fixed control volume analysis will be presented. With these physical considerations we can refine the integrand variation term which appears in Leibniz's integral rule/Reynolds transport theorem. Before concluding this chapter, we derive a general expression for a boundary integral, general with respect to dimension. This result is tacitly used through out this chapter. Finally we will end this chapter with a summary as well as a presentation of the Lagrangian-Eulerian balance principle: *The mathematical result of Reynolds transport theorem with a refinement of its integrand variation term, based on physical grounds.*

3.2 Rate of change of the value of a 1D spatial integral: Leibniz's integral rule.

3.2.1 Introduction: Variation of an integral.

Imagine an arbitrary spatial integral,

$$F(D, t) = \int_D f(\mathbf{x}, t) d\mathbf{V}. \quad (3.1)$$

The value of the integral $F(D, t)$ can change due to three kinds of variables/contributions:

- 1.) a change in the integrand f , while keeping the domain of integration fixed;
- 2.) a change in the domain of the integration D , while maintaining the integrand fixed; or
- 3.) varying simultaneously the integrand and the domain of integration.

For the specific case of only one spatial dimension, the domain $D = D_x$ is constrained to be a line element demarcating a region in the Cartesian space $\Omega = \mathbb{R}$. Let us make explicit that the variation in D_x is dependent on time, i.e. $D_x = D_x(t)$.

The one dimensional domain can be described by means of an interval,

$$D_x(t) = [x_a(t), x_b(t)], \quad (3.2)$$

with $x_a(t)$ and $x_b(t)$ representing the end/boundary points of the line element. Consequently, we can write equation 3.1 as,

$$F(x_a(t), x_b(t), t) = \int_{x_a(t)}^{x_b(t)} f(x, t) dx. \quad (3.3)$$

Note, we associate the interval with the domain of focus of an outside observer (see subsection 2.2.3), to avoid confusion, in the light of equation 3.32, $x(t)$ is associated with x and not with $r(t)$ (the position of an object wandering through Ω). Further, remark that it seems that an essential difference between one dimensional and higher dimensional integrals is that the boundary ∂D of the domain of a one dimensional integral is not connected, it are two isolated points.

Consider figure 3.1, which displays five different possible contributions to a change in the value of a one dimensional integral. Contribution *II* is of the kind mentioned under item 1 and the contributions *III* and *IV* are of the type described under item 2. The contributions *V* and *VI* are the "simultaneous changes", item 3.

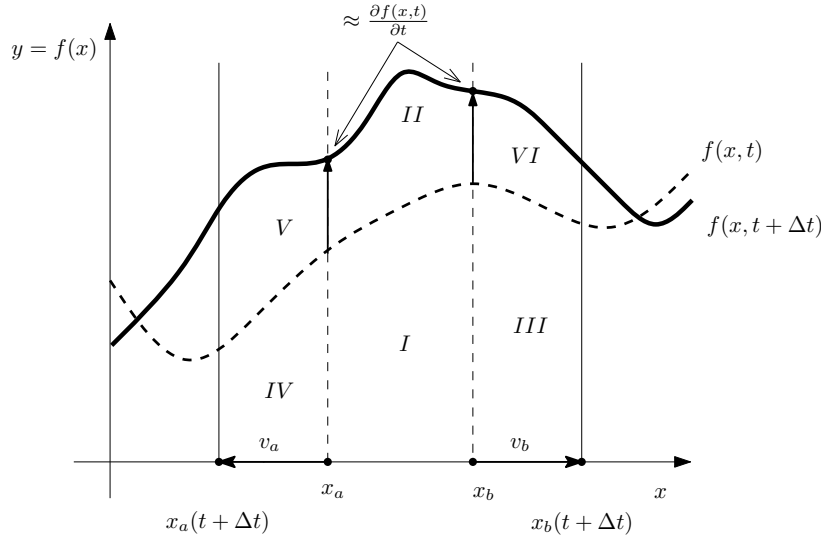


Figure 3.1: The variation of an integral for an expanding domain and time explicit varying integrand f . The different contributions are labelled by roman numerals, with *III* and *IV* accounting for domain variation effects, *II* for integrand variation effects and *V* as well as *VI* for simultaneous domain and integrand variation effects. The symbols v_a and v_b are the velocities of the boundary points x_a and x_b respectively, whereas $\frac{\partial f(x,t)}{\partial t}$ is the "average" velocity/rate with which the function f changes over the interval Δt .

In this section we will derive Leibniz's integral rule which explicates the rate of change of a one dimensional integral. We will do this through a sequential approximation to the change in the value of an integral and transform this sequence into the common representation of Leibniz's integral rule with the use of the calculus theorems: 1.) Taylor's theorem; 2.) the mean value theorem; and 3.) the intermediate value theorem.

3.2.2 A 1D domain in a 1D space: General domain variation.

Regarding the changes in the value of integral due to a change in $D_x(t)$, the possibilities are that, a.) the lower boundary x_a changes, while keeping the upper boundary x_b fixed; b.) x_b changes, while maintaining x_a constant; or c.) x_a and x_b change simultaneously.

The resulting effect of changes in the position of the boundary points can cause the domain of integration to (see section 2.3),

- 1.) translate,
- 2.) dilatate, i.e. compress or stretch, or

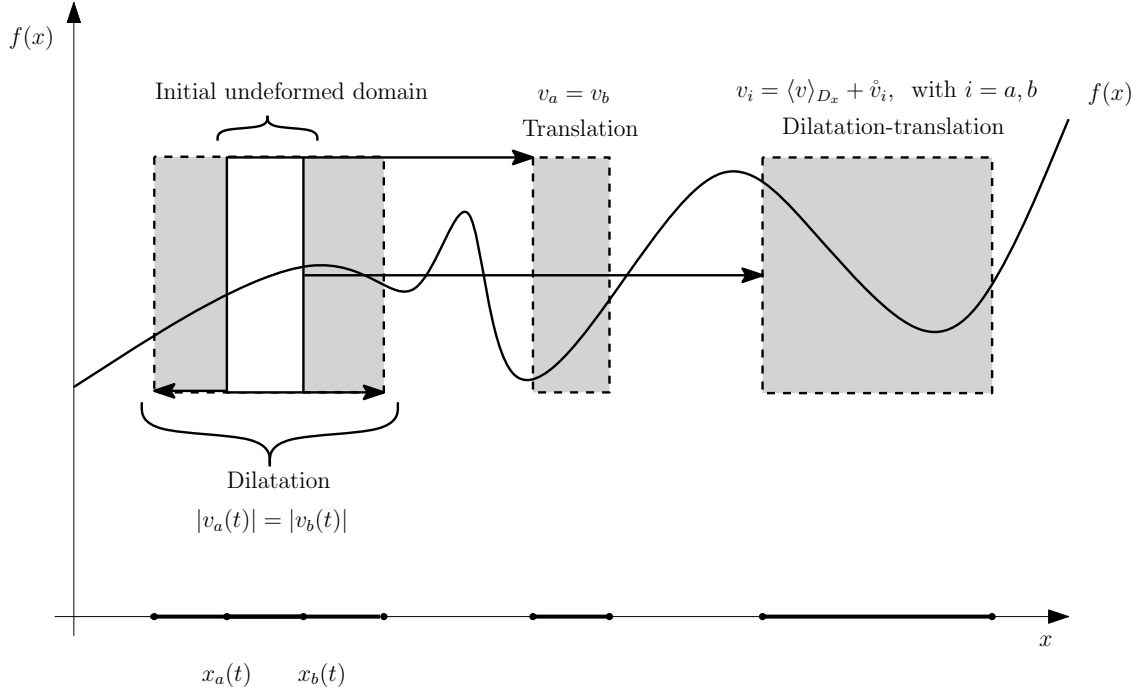


Figure 3.2: The three modes of domain variation.

3.) a combination of both,

which we illustrated in figure 3.2.

The lower boundary $x_a(t)$ can be displaced with a velocity $v_a(t)$ and end up at $x_a(t + \Delta t) = x_a(t) + v_a(t)\Delta t$. Similar, the upper boundary can change from position $x_b(t)$ to $x_b(t + \Delta t) = x_b(t) + v_b(t)\Delta t$. In the specific case that both displacements are equal in magnitude as well as direction, the changes in the position of the boundaries has the net effect of a translation of the domain. Mathematically, for a pure translation of D_x we should have,

$$v_a = v_b. \quad (3.4)$$

In contrast, when the displacements are both equal in magnitude though opposite in direction, will cause the domain to dilatate. This pure dilatation of D_x can be summarized symbolically as,

$$|v_a| = |v_b|, \quad \text{with} \quad v_a \neq v_b. \quad (3.5)$$

Different magnitudes and/or directions of the displacements results in a combination of translation and dilatation. This can be described conveniently in terms of statistics, by expressing the displacement of each of the boundary points in terms of a domain average velocity and a variational term (i.e. a Reynolds decomposition),

$$v_i = \langle v_x \rangle_{D_x} + \hat{v}_i, \quad \text{with} \quad i = a, b. \quad (3.6)$$

The average represents the translational contribution and the variation the dilatational contribution. Moreover,

$$|v_a| \neq |v_b|, \quad \text{with} \quad v_i = \langle v \rangle_{D_x} + \hat{v}_i, \quad i = a, b.. \quad (3.7)$$

3.2.3 The change of the value of an integral: series approximation.

Let us define a general change in the value of the integral,

$$F(x_a(t), x_b(t), t) = \int_{x_a(t)}^{x_b(t)} f(x, t) dx, \quad (3.8)$$

in a time interval Δt as,

$$\Delta F(x_a(t), x_b(t), t) = F(x_a(t + \Delta t), x_b(t + \Delta t), t + \Delta t) - F(x_a(t), x_b(t), t). \quad (3.9)$$

Reconsider figure 3.1. The change in the value of the integral can be approximately described through the sum of a sequence, or series of partial changes. From the former subsection we know that in the sequence we can discriminate among domain, integrand and simultaneous domain-integrand variation related partial changes. The series approximation entails solely the domain and integrand variation and different sequences may yield different series and hence values ΔF . In other words, in general there is no order independence among the partial changes in a sequence due to simultaneous variation of the domain and integrand (covariation). See figure 3.3 for an illustration of two possible series approximations.

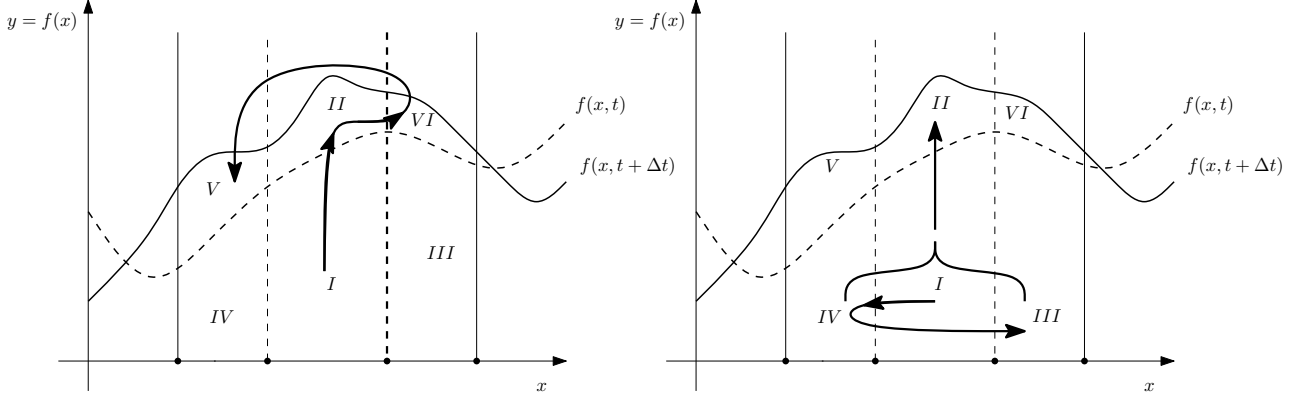


Figure 3.3: Two series approximations to a finite change in the value of an integral $\Delta F(x_a(t), x_b(t), t)$.

Let us consider one such a sequence, which starts with the partial changes related to the domain variation. For example the sequence starting with the partial change due to contribution *IV*,

$$IV = F(x_a(t + \Delta t), x_b(t), t) - F(x_a(t), x_b(t), t), \quad (3.10)$$

and then a partial change due to contribution *III*,

$$III = F(x_a(t + \Delta t), x_b(t + \Delta t), t) - F(x_a(t + \Delta t), x_b(t), t). \quad (3.11)$$

Finally we have the partial change associated with the integrand variation $II + V + VI$, i.e.,

$$II + V + VI = F(x_a(t + \Delta t), x_b(t + \Delta t), t + \Delta t) - F(x_a(t + \Delta t), x_b(t + \Delta t), t). \quad (3.12)$$

We can rewrite equation 3.9 by adding twice "zero" and obtain a series representation. By choosing the "zeros" well, we can write the equation in terms of the just suggested sequence of partial changes, i.e.,

$$\begin{aligned} \Delta F(x_a(t), x_b(t), t) &\approx \underbrace{F(x_a(t + \Delta t), x_b(t + \Delta t), t + \Delta t) - F(x_a(t + \Delta t), x_b(t + \Delta t), t)}_{II+V+VI} \\ &\quad + \underbrace{F(x_a(t + \Delta t), x_b(t + \Delta t), t) - F(x_a(t + \Delta t), x_b(t), t)}_{III} \\ &\quad + \underbrace{F(x_a(t + \Delta t), x_b(t), t) - F(x_a(t), x_b(t), t)}_{IV} \end{aligned} \quad (3.13)$$

The approximation symbol in the latter equation may seem confusing since mathematically one can argue, by noting that adding zero should not change anything, that there should be an equality symbol. However, the approximation sign is there to remind us that the additive sequence itself is an approximate expansion of ΔF .

If we assume that the changes are sufficiently smooth in time, we can subject the first two terms in the latter expression to Taylor's theorem (see section 2.2)¹. Let us successively truncate it down to the first order derivative (local linear approximation) to obtain the "local time variation" term,

$$F(x_a(t + \Delta t), x_b(t + \Delta t), t + \Delta t) - F(x_a(t + \Delta t), x_b(t + \Delta t), t) \approx \Delta t \frac{\partial}{\partial t} F(x_a(t + \Delta t), x_b(t + \Delta t), t), \quad (3.14)$$

Note, alternatively we could have considered the terms in the light of the definition of a partial derivative, which would tantamount to the same thing.

Substituting for every F its integral representation and applying some integral algebra we can obtain,

$$\begin{aligned} \Delta F(x_a(t), x_b(t), t) &\approx \Delta t \frac{\partial}{\partial t} \int_{x_a(t+\Delta t)}^{x_b(t+\Delta t)} f(x, t) dx \\ &+ \int_{x_a(t+\Delta t)}^{x_b(t+\Delta t)} f(x, t) dx - \int_{x_a(t+\Delta t)}^{x_b(t)} f(x, t) dx \\ &- \int_{x_b(t)}^{x_a(t+\Delta t)} f(x, t) dx - \int_{x_a(t)}^{x_b(t)} f(x, t) dx \\ &= \Delta t \frac{\partial}{\partial t} \int_{x_a(t+\Delta t)}^{x_b(t+\Delta t)} f(x, t) dx \\ &+ \int_{x_b(t)}^{x_b(t+\Delta t)} f(x, t) dx \\ &- \int_{x_a(t)}^{x_a(t+\Delta t)} f(x, t) dx \end{aligned} \quad (3.15)$$

The last two integrals on the right hand side explicate the contributions *III* and *IV* in figure 3.1 and the first "linear extrapolation" integral the contribution *II* + *V* + *VI*.

3.2.4 A 1D domain in a 1D space: Average domain variation.

The last two integrals in equation 3.15 can be conveniently rewritten with the use of the mean value theorem for integrals (e.g. see section 3.19 in [7] or section 6.6 in [5]), which states that whenever a function g is continuous on its interval of integration $[a, b]$,

$$\int_a^b g(x) dx = g(x^*)(b - a). \quad (3.16)$$

By virtue of the intermediate value theorem (e.g. see p. 154 in [5] or p. 144 in [7]) $g(x^*)$ equals the average of $g(x)$,

$$g(x^*) = \frac{1}{b - a} \int_a^b g(x) dx = \langle g \rangle_{(b-a)}. \quad (3.17)$$

Considering equation 3.15 in the light of the mean and intermediate value theorem we obtain the following approximation of a finite change in the value of the integral,

$$\begin{aligned} \Delta F(x_a(t), x_b(t), t) &\approx \Delta t \frac{\partial}{\partial t} \int_{x_a(t+\Delta t)}^{x_b(t+\Delta t)} f(x, t) dx \\ &+ \langle f(t) \rangle_{\Delta x_b(t)} \Delta x_b(t) \\ &- \langle f(t) \rangle_{\Delta x_a(t)} \Delta x_a(t) \end{aligned} \quad (3.18)$$

Employing the average representation we circumvent the details over the parts of the domain of integration affected by dilatation, while the dilatation occurs. In words, while the domain varies/deforms its boundaries experience solely a uniform/homogenized integrand field (See figure 3.4 for an illustration).

¹The same can be done with the other terms, assuming that the changes in F are sufficiently smooth in space. However, for convenience we will leave them for the moment as they are.

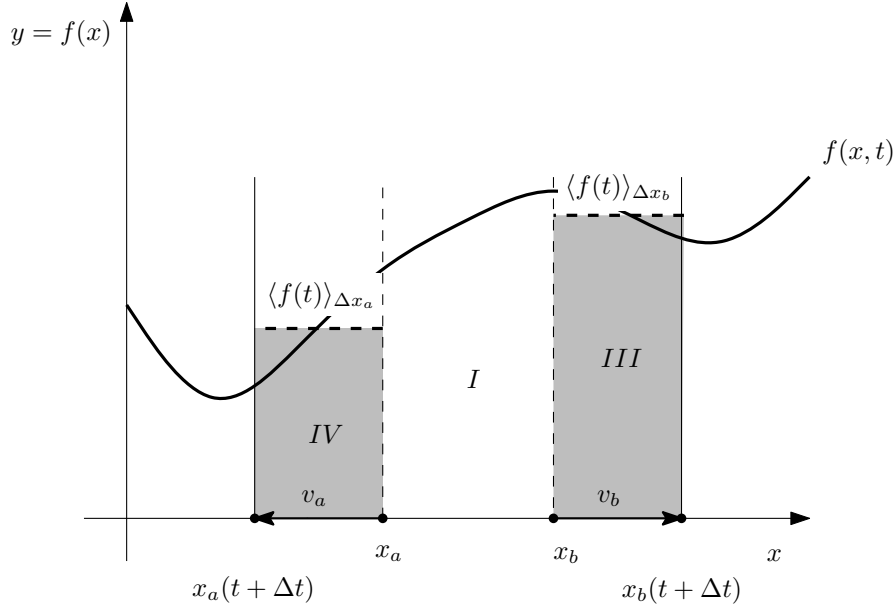


Figure 3.4: Visualization of the two average terms in equation 3.18.

3.2.5 Leibniz's integral rule.

In a heuristic manner we can obtain from the approximation to a finite change, an exact expression for an infinitesimal change.

To obtain the infinitesimal change dF , we divide both sides of the latter equation by Δt and take the limit of $\Delta t \rightarrow 0$, viz.,

$$\begin{aligned} \lim_{\Delta t \rightarrow 0} \frac{\Delta F(x_a(t); x_b(t); t)}{\Delta t} &= \lim_{\Delta t \rightarrow 0} \frac{\partial}{\partial t} \int_{x_a(t+\Delta t)}^{x_b(t+\Delta t)} f(x, t) dx \\ &+ \lim_{\Delta t \rightarrow 0} \langle f(t) \rangle_{\Delta x_b(t)} \frac{\Delta x_b(t)}{\Delta t} \\ &- \lim_{\Delta t \rightarrow 0} \langle f(t) \rangle_{\Delta x_a(t)} \frac{\Delta x_a(t)}{\Delta t}. \end{aligned} \quad (3.19)$$

Evaluating the limits yields an expression for the rate of change²,

$$\begin{aligned} \frac{d}{dt} F(x_a(t), x_b(t), t) &= \frac{d}{dt} \int_{x_a(t)}^{x_b(t)} f(x, t) dx \\ &= \frac{\partial}{\partial t} \int_{x_a(t)}^{x_b(t)} f(x, t) dx + f(x_b(t), t) \frac{dx_b(t)}{dt} - f(x_a(t), t) \frac{dx_a(t)}{dt}. \end{aligned} \quad (3.20)$$

This equation is known as Leibniz (one-dimensional) integral rule, or "Leibniz's rule for differentiating under the integral sign". The exactness of the integral rule can be made amenable from figure 3.1. Whenever, $\Delta x, \Delta t \ll 1$ the simultaneous domain-integrand variation contributions V and VI become vanishingly small.

The fundamental theorem of calculus part II, states that,

$$\frac{d}{dx} \left[\int_a^x f(t) dt \right] = f(x), \quad (3.21)$$

whenever f is a continuous function on its domain of integration (e.g. p. 422 in [5]). In the light of this theorem, the first factors of the last two terms of Leibniz's integral rule (equation 3.20) can be rewritten as,

$$f(x_b(t), t) = \frac{\partial}{\partial x_b} \left[\int_{x_a(t)}^{x_b(t)} f(x, t) dx \right], \quad (3.22)$$

²Note, from an Eulerian perspective, Δx should be essentially interpret as the displacement the point $x(t)$ undergoes in a duration Δt . In this view, v_a is the displacement rate associated with the point $x(t)$. The smaller we take the duration, the smaller the portion of Δx traversed. Consequently, the limit $\Delta t \rightarrow 0$ can be interpret as making the "sample domain" Δx to take the average over infinitesimally small, i.e. so small that it essentially entails only the single point $x(t)$. Hence, $\langle f(t) \rangle_{\Delta x}$ becomes $f(x_a, t)$.

and

$$f(x_a(t), t) = \frac{\partial}{\partial x_a} \left[\int_{x_b(t)}^{x_a(t)} f(x, t) dx \right]. \quad (3.23)$$

Substituting these two expressions into Leibniz's integral rule yields,

$$\begin{aligned} \frac{d}{dt} F(x_a(t), x_b(t), t) &= \frac{\partial}{\partial t} \int_{x_a(t)}^{x_b(t)} f(x, t) dx + f(x_b(t), t) \frac{dx_b(t)}{dt} - f(x_a(t), t) \frac{dx_a(t)}{dt} \\ &= \frac{\partial}{\partial t} \int_{x_a(t)}^{x_b(t)} f(x, t) dx + \frac{\partial}{\partial x_b} \left[\int_{x_a(t)}^{x_b(t)} f(x, t) dx \right] \frac{dx_b(t)}{dt} + \frac{\partial}{\partial x_a} \left[\int_{x_a(t)}^{x_b(t)} f(x, t) dx \right] \frac{dx_a(t)}{dt}. \end{aligned} \quad (3.24)$$

In turn we can rewrite the last row as,

$$\frac{d}{dt} F(x_a(t), x_b(t), t) = \frac{\partial}{\partial t} F(x_a(t), x_b(t), t) + \frac{\partial}{\partial x_b} F(x_a(t), x_b(t), t) \frac{dx_b(t)}{dt} + \frac{\partial}{\partial x_a} F(x_a(t), x_b(t), t) \frac{dx_a(t)}{dt}, \quad (3.25)$$

which we can recognize as Leibniz's chain rule.

Related, we have the local linear form for an infinitesimal change in F ,

$$dF(x_a(t), x_b(t), t) = \frac{\partial}{\partial t} F(x_a(t), x_b(t), t) dt + \frac{\partial}{\partial x_b} F(x_a(t), x_b(t), t) \frac{dx_b(t)}{dt} dt + \frac{\partial}{\partial x_a} F(x_a(t), x_b(t), t) \frac{dx_a(t)}{dt} dt. \quad (3.26)$$

and an alternative for the finite change expression 3.18, the local linear approximation,

$$\Delta F(x_a(t), x_b(t), t) \approx \frac{\partial}{\partial t} F(x_a(t), x_b(t), t) \Delta t + \frac{\partial}{\partial x_b} F(x_a(t), x_b(t), t) \frac{dx_b(t)}{dt} \Delta t + \frac{\partial}{\partial x_a} F(x_a(t), x_b(t), t) \frac{dx_a(t)}{dt} \Delta t. \quad (3.27)$$

3.2.6 Conclusion: Rate of change of the value of an 1D spatial integral.

Leibniz's integral rule (equation 3.20) or its chain rule variant (equation 3.25), expresses the rate of change of the value of a one dimensional integral. The first term on the right hand side of both equations expresses the contribution due to the integrand variation and the other two terms due to the domain variation. The rate expression shows that we can separate integrand and domain variation.

We obtained the integral rule by a series approximation, a sequence of independent partial changes, due to either integrand variation or else domain variation (subsection 3.2.3). For a finite change in the integral value such a sequence is an approximation since, the sequence does not contain terms accounting for simultaneous variation of the domain and the integrand and hence also not for dependence in the order in which the partial changes appear in the sequence. The order dependence is an approximation artefact related to the precision of the approximation, since the assumption that the integrand is a smooth function in space and time renders the order of differentiation interchangeable (Recall section 2.2).

In contrast to the finite change, at the infinitesimal (precision) level, the contributions due to simultaneous variation of the domain and the integrand vanish and the series approximation becomes exact (subsection 3.2.5). An infinitesimal change in the value of an integral is due to separate contributions of integrand and domain variation.

Note, to obtain Leibniz's integral rule we expressed the domain variation integrals in their average representation. Hence, the rule is not concerned with the details of how the value of the integral changes while the domain of integrations deforms. Of interest is the value of the integral before (prior) and after (posterior) the deformation of the domain (subsection 3.2.4). This can be interpreted physically as a quasistatic approach.

3.3 Rate of change of the value of 3D spatial integrals: Reynolds transport theorem.

3.3.1 Introduction: Chain rule representation of the variation of an integral.

In the former subsection the foundations were laid down such that we are now in the position to generalize Leibniz's integral rule for a one dimensional integral, obtained in subsection 3.2.5, for three dimensional integrals. This generalization is commonly known in the literature as Reynolds transport theorem.

In subsection 3.2.3 we stated that a change in the value of a one dimensional integral ΔF can be approximated by the sum of a contribution due to the variation of the integrand and a contribution resulting from the variation of the domain. In the current section we are concerned with generalizing the contribution due to the variation of the domain. Recall from this subsection equation 3.15,

$$\Delta F(x_a(t), x_b(t), t) \approx \Delta t \frac{\partial}{\partial t} \int_{x_a(t+\Delta t)}^{x_b(t+\Delta t)} f(x, t) dx + \int_{x_b(t)}^{x_b(t+\Delta t)} f(x, t) dx - \int_{x_a(t)}^{x_a(t+\Delta t)} f(x, t) dx. \quad (3.28)$$

The contribution due to the domain variation can be rewritten in terms of two integrals defined over the whole domain, as opposed to the two integrals in the latter equation, which are solely over the fringes of the domain. In other words, in the former section we actually accounted for the domain variation implicitly by considering variation in the boundary of the domain. In this section we will account for the domain variation explicitly.

The starting point for this is that we rewrite expression 3.28 by adding "zero" to the boundary variation terms, i.e.,

$$\begin{aligned} \int_{x_b(t)}^{x_b(t+\Delta t)} f(x, t) dx - \int_{x_a(t+\Delta t)}^{x_a(t+\Delta t)} f(x, t) dx + \int_{x_a(t)}^{x_b(t)} f(x, t) dx - \int_{x_a(t)}^{x_b(t)} f(x, t) dx \\ = \\ \int_{x_a(t+\Delta t)}^{x_b(t+\Delta t)} f(x, t) dx - \int_{x_a(t)}^{x_b(t)} f(x, t) dx. \end{aligned} \quad (3.29)$$

From subsection 3.2.2 we know that the first integrand on the right hand side differs from the second one in that the domain may have been dilatated, translated or a combination of both. In chapter 2 we considered how to account for these motions mathematically. We will obtain the desired generalization of Leibniz's integral rule by combining the results from the former section with those from chapter 2. Moreover, in this section we will show that equation 3.28 can be written as,

$$\begin{aligned} \Delta F(D_x(t), t) &\approx \Delta t \frac{\partial}{\partial t} \int_{x_a(t+\Delta t)}^{x_b(t+\Delta t)} f(x, t) dx + \int_{D_x(t+\Delta t)} f(x, t) dx - \int_{D_x(t)} f(x, t) dx \\ &\approx \Delta t \frac{\partial}{\partial t} F(D_x(t), t) + \Delta t \frac{\partial}{\partial D_x(t)} F(D_x(t), t) \cdot \frac{d}{dt} D_x(t), \end{aligned} \quad (3.30)$$

and hence, that Leibniz's integral rule can be written in the form of Leibniz's chain rule,

$$\frac{d}{dt} F(D_x(t), t) = \frac{\partial}{\partial t} F(D_x(t), t) + \frac{\partial}{\partial D_x(t)} F(D_x(t), t) \cdot \frac{d}{dt} D_x(t). \quad (3.31)$$

This differential form will be central in this section and we will generalize it to one, two and three dimensional domains embedded in a three dimensional space. The latter case being Reynold's transport theorem.

Physical space is three dimensional and hence of particular use is a balance principle in three dimensions. Consequently mathematical descriptions of physical phenomena make use of integrand fields and domains of integration defined over/embedded in three dimensional spaces. Therefore we want to extend the simple model (figure 3.1) for the variation of a one dimensional integral to three dimensional integrals.

In this section we will consider first the generalization of Leibniz's integral rule for one dimensional domains embedded in a three dimensional space. The programme entails relating the change in the integral due to a change in the domain of integration to the displacement of the domain, followed by its average representation and finally conclude by revealing the connection with Leibniz's integral rule. Second we will treat the mathematical description of parallelogramic and parallelepiped domains and their infinitesimal deformation. These pave the ground for, three, considering the generalization of Leibniz's integral rule for three dimensional domains and how this result is related to Reynolds transport theorem.

3.3.2 A 1D domain in a 3D space: General domain variation.

Suppose the domain $D_{\mathbf{x}}$ is deformed during the time interval $[t, t + \Delta t]$, due to a smooth displacement field \mathbf{u} defined over Ω . From equation 2.40 in section 2.3 we know that the new position of each point in $D_{\mathbf{x}}$ posterior to the deformation is given by,

$$\mathbf{r}(t) = \mathbf{x} + \mathbf{u}(\mathbf{x}, t). \quad (3.32)$$

The positions $\mathbf{r}(t)$ make up the posterior domain of integration $D_{\mathbf{r}}(t)$.

We can construe a prior and a posterior integral,

$$\int_{D_{\mathbf{x}}} f(\mathbf{x}, t) d\mathbf{x}, \quad (3.33)$$

and

$$\int_{D_{\mathbf{r}(t)}} f(\mathbf{r}(t), t) d\mathbf{r}. \quad (3.34)$$

The change in the value of the integral due to the deformation/domain variation is,

$$F(D_{\mathbf{r}(t)}, t) - F(D_{\mathbf{x}}, t) = \int_{D_{\mathbf{r}(t)}} f(\mathbf{r}(t), t) d\mathbf{r} - \int_{D_{\mathbf{x}}} f(\mathbf{x}, t) d\mathbf{x}. \quad (3.35)$$

Assuming a stationary displacement field we can write, in a heuristic manner, the total derivative of equation 3.32 as,

$$d\mathbf{r}(t) = d\mathbf{x} + d\mathbf{u}(\mathbf{x}, t) = d\mathbf{x} + \frac{\partial \mathbf{u}(\mathbf{x}, t)}{\partial \mathbf{x}} \cdot d\mathbf{x}. \quad (3.36)$$

With this expression as well as equation 3.32 we can rewrite equation 3.35, as,

$$\begin{aligned} \int_{D_{\mathbf{r}(t)}} f(\mathbf{r}(t), t) d\mathbf{r} - \int_{D_{\mathbf{x}}} f(\mathbf{x}, t) d\mathbf{x} &= \int_{D_{\mathbf{x}}} f(\mathbf{x} + \mathbf{u}(\mathbf{x}, t), t) d\mathbf{x} + \int_{D_{\mathbf{x}}} f(\mathbf{x} + \mathbf{u}(\mathbf{x}, t), t) \frac{\partial \mathbf{u}(\mathbf{x}, t)}{\partial \mathbf{x}} \cdot d\mathbf{x} \\ &\quad - \int_{D_{\mathbf{x}}} f(\mathbf{x}, t) d\mathbf{x}. \end{aligned} \quad (3.37)$$

The definition of the partial directional derivative is,

$$\lim_{h \rightarrow 0} \frac{f(\mathbf{x} + h\hat{\mathbf{n}}, t) - f(\mathbf{x}, t)}{h} = \frac{\partial f(\mathbf{x}, t)}{\partial \mathbf{x}} \cdot \hat{\mathbf{n}}. \quad (3.38)$$

Recognizing that $h\hat{\mathbf{n}} = \mathbf{u}(\mathbf{x}, t)$, we can infer the approximation,

$$f(\mathbf{x} + \mathbf{u}(\mathbf{x}, t), t) \approx f(\mathbf{x}, t) + \frac{\partial f(\mathbf{x}, t)}{\partial \mathbf{x}} \cdot \mathbf{u}(\mathbf{x}, t). \quad (3.39)$$

Substituting the latter expression for the integrand f in the first and the second integral on the right hand side of equation 3.37, yields

$$\begin{aligned} \int_{D_{\mathbf{r}(t)}} f(\mathbf{r}(t), t) d\mathbf{r} - \int_{D_{\mathbf{x}}} f(\mathbf{x}, t) d\mathbf{x} &\approx \int_{D_{\mathbf{x}}} \left[\frac{\partial f(\mathbf{x}, t)}{\partial \mathbf{x}} \cdot \mathbf{u}(\mathbf{x}, t) \right] \cdot d\mathbf{x} + \int_{D_{\mathbf{x}}} f(\mathbf{x}, t) \frac{\partial \mathbf{u}(\mathbf{x}, t)}{\partial \mathbf{x}} \cdot d\mathbf{x} \\ &\quad + \int_{D_{\mathbf{x}}} \frac{\partial f(\mathbf{x}, t)}{\partial \mathbf{x}} \cdot \mathbf{u} \frac{\partial \mathbf{u}(\mathbf{x}, t)}{\partial \mathbf{x}} \cdot d\mathbf{x} \end{aligned} \quad (3.40)$$

In the light of section 2.3, we can interpret the first term on the right hand side as accounting for, the changes in the value of the integral due to changes in the integrand as a result of the translations of the infinitesimal subdomains $d\mathbf{x}$. The second term on the right hand side accounts for the changes due to rotations and dilatations (strain) of the infinitesimal subdomains, without encountering spatial variation in the integrand while being deformed. The third term is a hybrid, it accounts for spatial variation in the integrand when the infinitesimal domains are subjected to translational, as well as rotational and dilatational deformations.

In subsection 3.3.6 we considered the infinitesimal strain assumption. Besides its role in the latter expression, it can help to simplify equation 3.40. If we suppose that the gradient of the integrand f is very small and in addition adopt the infinitesimal strain assumption, products of the gradient of f and the displacement gradient yield negligible/vanishing contributions. Hence, the last "crossterm" integral in equation 3.40 vanishes and we end up with,

$$\int_{D_{\mathbf{r}(t)}} f(\mathbf{r}(t), t) d\mathbf{r} - \int_{D_{\mathbf{x}}} f(\mathbf{x}, t) d\mathbf{x} \approx \int_{D_{\mathbf{x}}} \left[\frac{\partial f(\mathbf{x}, t)}{\partial \mathbf{x}} \cdot \mathbf{u}(\mathbf{x}, t) \right] \cdot d\mathbf{x} + \int_{D_{\mathbf{x}}} f(\mathbf{x}, t) \frac{\partial \mathbf{u}(\mathbf{x}, t)}{\partial \mathbf{x}} \cdot d\mathbf{x}. \quad (3.41)$$

3.3.3 A 1D domain in a 3D space: Average domain variation.

Suppose we are not interested in the details of how the infinitesimal sub domains $d\mathbf{x}$ are displaced and deformed, of interest is the deformation of the domain $D_{\mathbf{x}}$ as a whole. Moreover, we do not care about the possible curving of D_x due to the displacement field and consider only rigid translation and rotation as well as dilatation of D_x . These effects are captured by the average behaviour of the domain variation on the change in integral value.

To obtain a representation in terms of averages, let us rewrite the two integrals on the right hand side of equation 3.41 by virtue of the product rule for the gradient, in reverse,

$$\int_{D_{\mathbf{x}}} \left[\frac{\partial f(\mathbf{x}, t)}{\partial \mathbf{x}} \cdot \mathbf{u}(\mathbf{x}, t) \right] \cdot d\mathbf{x} + \int_{D_{\mathbf{x}}} f(\mathbf{x}, t) \frac{\partial \mathbf{u}(\mathbf{x}, t)}{\partial \mathbf{x}} \cdot d\mathbf{x} = \int_{D_{\mathbf{x}}} \frac{\partial}{\partial \mathbf{x}} [f(\mathbf{x}, t) \mathbf{u}(\mathbf{x}, t)] \cdot d\mathbf{x}. \quad (3.42)$$

Then, by multiplying by "one" we can express the latter integral in terms of the domain average, of the gradient of the product, i.e.,

$$\frac{D_{\mathbf{x}}}{D_{\mathbf{x}}} \int_{D_{\mathbf{x}}} \frac{\partial}{\partial \mathbf{x}} [f(\mathbf{x}, t) \mathbf{u}(\mathbf{x}, t)] \cdot d\mathbf{x} = \left\langle \frac{\partial}{\partial \mathbf{x}} [f(\mathbf{x}, t) \mathbf{u}(\mathbf{x}, t)] \right\rangle_{D_{\mathbf{x}}} D_{\mathbf{x}}. \quad (3.43)$$

The obtained average is not very elaborating, and a more insightful representation of it can be obtained by applying an averaging theorem, developed by Slattery ([108]) and Whitaker ([124]), which states that for a sufficiently smooth function/field g we can write the average of the gradient of g as (e.g. see [108, 124, 45, 58]),

$$\left\langle \frac{\partial}{\partial \mathbf{x}} g \right\rangle_V = \frac{\partial}{\partial \mathbf{x}} \langle g \rangle_V + \frac{1}{V} \int_A g \hat{\mathbf{n}} dA. \quad (3.44)$$

Employing this theorem we can rewrite equation 3.43 as,

$$\left\langle \frac{\partial}{\partial \mathbf{x}} [f(\mathbf{x}, t) \mathbf{u}(\mathbf{x}, t)] \right\rangle_{D_{\mathbf{x}}} D_{\mathbf{x}} = \frac{\partial}{\partial \mathbf{x}} [\langle f(\mathbf{x}, t) \mathbf{u}(\mathbf{x}, t) \rangle_{D_{\mathbf{x}}}] D_{\mathbf{x}} + \sum_i^2 f(\mathbf{x}_i, t) \mathbf{u}(\mathbf{x}_i, t) \cdot \hat{\mathbf{n}}(\mathbf{x}_i). \quad (3.45)$$

The last term in this equation is a "zero dimensional boundary" integral, which follows nicely from Gray's derivation of the averaging theorem ([45]). It will be explained in section 3.5.

Substituting the last equation, in the light of equation 3.43 and 3.42, for the right hand side of equation 3.41 we obtain,

$$\int_{D_{\mathbf{r}(t)}} f(\mathbf{r}(t), t) d\mathbf{r} - \int_{D_{\mathbf{x}}} f(\mathbf{x}, t) d\mathbf{x} \approx \frac{\partial}{\partial \mathbf{x}} [\langle f(\mathbf{x}, t) \mathbf{u}(\mathbf{x}, t) \rangle_{D_{\mathbf{x}}}] D_{\mathbf{x}} + \sum_i^2 f(\mathbf{x}_i, t) \mathbf{u}(\mathbf{x}_i, t) \cdot \hat{\mathbf{n}}(\mathbf{x}_i). \quad (3.46)$$

The average of a product can be decomposed in the product of the averages and their covariance (e.g. see p. 10 in [47]). Hence, we can refine the latter equation as,

$$\begin{aligned} \int_{D_{\mathbf{r}(t)}} f(\mathbf{r}(t), t) d\mathbf{r} - \int_{D_{\mathbf{x}}} f(\mathbf{x}, t) d\mathbf{x} &\approx \frac{\partial}{\partial \mathbf{x}} [\langle f(\mathbf{x}, t) \mathbf{u}(\mathbf{x}, t) \rangle_{D_{\mathbf{x}}}] D_{\mathbf{x}} + \sum_i^2 f(\mathbf{x}_i, t) \mathbf{u}(\mathbf{x}_i, t) \cdot \hat{\mathbf{n}}(\mathbf{x}_i). \\ &= \frac{\partial}{\partial \mathbf{x}} [\langle f(\mathbf{x}, t) \rangle_{D_{\mathbf{x}}} \langle \mathbf{u}(\mathbf{x}, t) \rangle_{D_{\mathbf{x}}}] D_{\mathbf{x}} + \frac{\partial}{\partial \mathbf{x}} \left[\left\langle \mathring{f}(\mathbf{x}, t) \mathring{\mathbf{u}}(\mathbf{x}, t) \right\rangle_{D_{\mathbf{x}}} \right] D_{\mathbf{x}} \\ &\quad + \sum_i^2 f(\mathbf{x}_i, t) \mathbf{u}(\mathbf{x}_i, t) \cdot \hat{\mathbf{n}}(\mathbf{x}_i). \end{aligned} \quad (3.47)$$

Successively, applying the product rule for differentiation to the first term on the second row, we can obtain,

$$\begin{aligned} \int_{D_{\mathbf{r}(t)}} f(\mathbf{r}(t), t) d\mathbf{r} - \int_{D_{\mathbf{x}}} f(\mathbf{x}, t) d\mathbf{x} &\approx \frac{\partial}{\partial \mathbf{x}} [\langle f(\mathbf{x}, t) \rangle_{D_{\mathbf{x}}}] D_{\mathbf{x}} \langle \mathbf{u}(\mathbf{x}, t) \rangle_{D_{\mathbf{x}}} + \frac{\partial}{\partial \mathbf{x}} [\langle \mathbf{u}(\mathbf{x}, t) \rangle_{D_{\mathbf{x}}}] D_{\mathbf{x}} \langle f(\mathbf{x}, t) \rangle_{D_{\mathbf{x}}} \\ &\quad + \frac{\partial}{\partial \mathbf{x}} \left[\left\langle \mathring{f}(\mathbf{x}, t) \mathring{\mathbf{u}}(\mathbf{x}, t) \right\rangle_{D_{\mathbf{x}}} \right] D_{\mathbf{x}} + \sum_i^2 f(\mathbf{x}_i, t) \mathbf{u}(\mathbf{x}_i, t) \cdot \hat{\mathbf{n}}(\mathbf{x}_i). \end{aligned} \quad (3.48)$$

The covariance term $\left\langle \mathring{f}(\mathbf{x}, t) \mathring{\mathbf{u}}(\mathbf{x}, t) \right\rangle_{D_{\mathbf{x}}}$ accounts for the dependence among the two quantities. The factors $\mathring{f}(\mathbf{x}, t)$ and $\mathring{\mathbf{u}}(\mathbf{x}, t)$ are the deviatoric quantities in a Reynolds decomposition. Hence, the covariance accounts for smaller than domain scale effects. Moreover, the covariance term expresses how varying one of the quantities affects the other, on the average. In our case we may interpret the term

as accounting for how on the average the deformation of a infinitesimal sub domain $d\mathbf{x}$ influences the value for f .

From these considerations we infer that the covariance term is the statistical representation of the cross term in equation 3.40 of subsection 3.3.2. Except for the last "boundary" term, this last result appears practically similar in form to this equation.

In subsection 3.3.2 we regarded the cross term vanishingly small, in the light of the assumptions of very small displacement gradients (infinitesimal strain assumption) and gradients of f . In other words, there is no dependence among the two variables. Logically, the covariance term then also vanishes and we arrive at,

$$\int_{D_{\mathbf{r}(t)}} f(\mathbf{r}(t), t) d\mathbf{r} - \int_{D_{\mathbf{x}}} f(\mathbf{x}, t) d\mathbf{x} \approx \frac{\partial}{\partial \mathbf{x}} [\langle f(\mathbf{x}, t) \rangle_{D_{\mathbf{x}}}] D_{\mathbf{x}} \langle \mathbf{u}(\mathbf{x}, t) \rangle_{D_{\mathbf{x}}} + \frac{\partial}{\partial \mathbf{x}} [\langle \mathbf{u}(\mathbf{x}, t) \rangle_{D_{\mathbf{x}}}] D_{\mathbf{x}} \langle f(\mathbf{x}, t) \rangle_{D_{\mathbf{x}}} + \sum_i^2 f(\mathbf{x}_i, t) \mathbf{u}(\mathbf{x}_i, t) \cdot \hat{\mathbf{n}}(\mathbf{x}_i). \quad (3.49)$$

Analogous to our interpretation of equation 3.40 in subsection 3.3.2, the first term on the right hand side of the latter equation accounts for the change of the integrand f , at the scale of the (prior) domain $D_{\mathbf{x}}$, as a result of a "rigid" translation of the domain as a whole.

The gradient factor in the second term on the right hand side expresses a possible "rigid" rotation of $D_{\mathbf{x}}$ as well as the average straining of $D_{\mathbf{x}}$ while being "rigidly" displaced. The second term measures the effect of these two deformation mechanisms on the change in the value of the integral, while "assuming" that the (average) integrand, as initially defined over $D_{\mathbf{x}}$, does not change.

Considering the third term, the scalar product between the displacement vector and the orientation of the respective boundary point (zero dimensional boundary element) can be interpreted as the component of the displacement in the direction of the orientation of the boundary points. It describes the dilatation of the domain in the absence of a rigid translation and rotation of $D_{\mathbf{x}}$.

In figure 3.5 we tried to illustrate the different components of the domain variation of a line domain $D_{\mathbf{x}}$ embedded in a multidimensional space. It is similar to figure 3.1 in which we tried to capture the combined domain and integrand variation for $D_{\mathbf{x}}$ embedded in a one dimensional space.

3.3.4 Generalization of Leibniz's integral rule: A 1D domain in a 3D space.

Let us return to the more implicit equation 3.40. From it we can obtain the rate of change for the integral $\int_{D_{\mathbf{x}}} f(\mathbf{x}, t) d\mathbf{x}$ with respect to time, due to changes in the domain of integration (time implicit changes). Therefore we divide the equation by Δt and subsequently take the limit $\Delta t \rightarrow 0$,

$$\lim_{\Delta t \rightarrow 0} \frac{1}{\Delta t} \left[\int_{D_{\mathbf{r}(t)}} f(\mathbf{r}(t), t) d\mathbf{r} - \int_{D_{\mathbf{x}}} f(\mathbf{x}, t) d\mathbf{x} \right] = \frac{\partial}{\partial D_{\mathbf{x}}} \left[\int_{D_{\mathbf{x}}} f(\mathbf{x}, t) d\mathbf{x} \right] \frac{dD_{\mathbf{x}}}{dt} \approx \lim_{\Delta t \rightarrow 0} \frac{1}{\Delta t} \int_{D_{\mathbf{x}}} \left[\frac{\partial f(\mathbf{x}, t)}{\partial \mathbf{x}} \cdot \mathbf{u}(\mathbf{x}, t) \right] \cdot d\mathbf{x} + \lim_{\Delta t \rightarrow 0} \frac{1}{\Delta t} \int_{D_{\mathbf{x}}} f(\mathbf{x}, t) \frac{\partial \mathbf{u}(\mathbf{x}, t)}{\partial \mathbf{x}} \cdot d\mathbf{x}. \quad (3.50)$$

Recall, the integrand $f(\mathbf{x}, t)$ is kept fixed with respect to time, i.e. no time explicit changes. For the two integrals on the right hand side the domain is the domain prior to the deformation, i.e. relatively "fixed with time". Hence, we can take the factor $1/\Delta t$ under the integral sign and rewrite our equation in terms of the velocity of the displacement, or strain-rates (e.g. subsection 2.3.5),

$$\frac{\partial}{\partial D_{\mathbf{x}}} \left[\int_{D_{\mathbf{x}}} f(\mathbf{x}, t) d\mathbf{x} \right] \frac{dD_{\mathbf{x}}}{dt} \approx \int_{D_{\mathbf{x}}} \left[\frac{\partial f(\mathbf{x}, t)}{\partial \mathbf{x}} \cdot \mathbf{v}(\mathbf{x}, t) \right] \cdot d\mathbf{x} + \int_{D_{\mathbf{x}}} f(\mathbf{x}, t) \frac{\partial \mathbf{v}(\mathbf{x}, t)}{\partial \mathbf{x}} \cdot d\mathbf{x}. \quad (3.51)$$

Thus, considering equation 3.31, equation 3.51 provides us with a more explicit expression for the general domain variation term $\frac{\partial}{\partial D} F(D(t), t) \frac{dD}{dt}$, in the specific case of a one dimensional domain $D_{\mathbf{x}}$ embedded in a three dimensional space Ω .

The counter part of equation 3.51 in terms of averages can be obtained by simply applying the averaging paradigm employed above to this rate formulation. Alternatively, since the averages are all taken over the relatively fixed in time domain $D_{\mathbf{x}}$, we can directly divide equation 3.49 by Δt and take the limit of $\Delta t \rightarrow 0$, which yields,

$$\frac{\partial}{\partial D_{\mathbf{x}}} \left[\int_{D_{\mathbf{x}}} f(\mathbf{x}, t) d\mathbf{x} \right] \frac{dD_{\mathbf{x}}}{dt} \approx \frac{\partial}{\partial \mathbf{x}} [\langle f(\mathbf{x}, t) \rangle_{D_{\mathbf{x}}}] D_{\mathbf{x}} \langle \mathbf{v}(\mathbf{x}, t) \rangle_{D_{\mathbf{x}}} + \frac{\partial}{\partial \mathbf{x}} [\langle \mathbf{v}(\mathbf{x}, t) \rangle_{D_{\mathbf{x}}}] D_{\mathbf{x}} \langle f(\mathbf{x}, t) \rangle_{D_{\mathbf{x}}} + \sum_i^2 f(\mathbf{x}_i, t) \mathbf{v}(\mathbf{x}_i, t) \cdot \hat{\mathbf{n}}(\mathbf{x}_i). \quad (3.52)$$

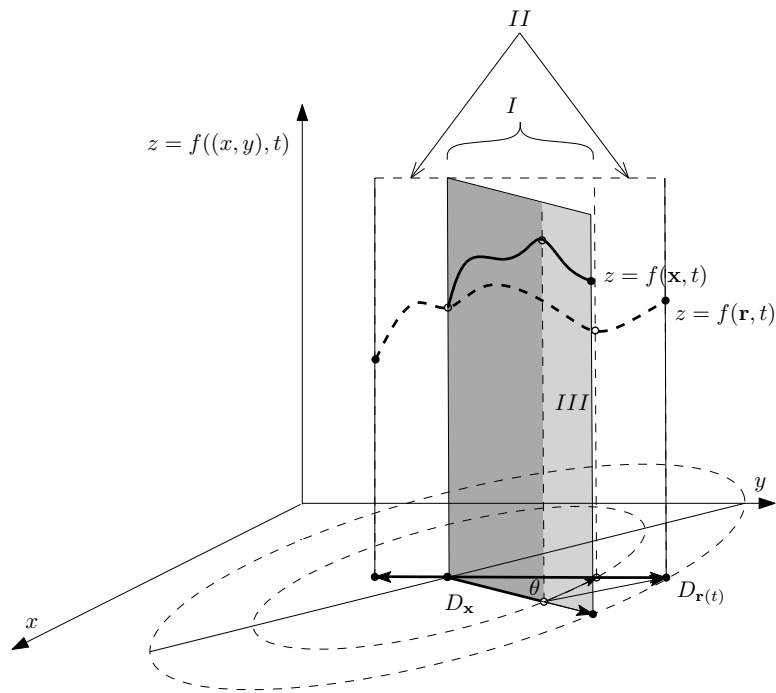


Figure 3.5: The change in the value of an integral over a one dimensional line domain embedded three dimensional space. The numerals correspond with the terms on the right hand side of equation 3.49. We illustrated the change in the value of the integral due to dilatation of the domain without a change in its orientation, captured by *III*. In addition we tried to illustrate the advective change in the value of the integral without domain dilatation, captured by *I*. The contribution due to *II* reflects the change in the value of the integral due to dilatation of the domain while changing its orientation.

Let us revisit equation 3.31 and consider its variant for our one dimensional line domain embedded in three dimensional space,

$$\frac{d}{dt}F(D_{\mathbf{x}}(t), t) \approx \frac{\partial}{\partial t}F(D_{\mathbf{x}}(t), t) + \frac{\partial F(D_{\mathbf{x}}(t), t)}{\partial D_{\mathbf{x}}} \frac{dD_{\mathbf{x}}(t)}{dt}. \quad (3.53)$$

Substituting the obtained expression for the rate of domain variation, equation 3.52, and the integral expression for the integrand variation in the latter equation we obtain,

$$\begin{aligned} \frac{d}{dt}F(D_{\mathbf{x}}(t), t) \approx & \frac{\partial}{\partial t} \int_{D_{\mathbf{x}}} f(\mathbf{x}, t) d\mathbf{x} + \sum_i^2 f(\mathbf{x}_i, t) \mathbf{v}(\mathbf{x}_i, t) \cdot \hat{\mathbf{n}}(\mathbf{x}_i) \\ & + \frac{\partial}{\partial \mathbf{x}} [\langle \mathbf{v}(\mathbf{x}, t) \rangle_{D_{\mathbf{x}}}] D_{\mathbf{x}} \langle f(\mathbf{x}, t) \rangle_{D_{\mathbf{x}}} + \frac{\partial}{\partial \mathbf{x}} [\langle f(\mathbf{x}, t) \rangle_{D_{\mathbf{x}}}] D_{\mathbf{x}} \langle \mathbf{v}(\mathbf{x}, t) \rangle_{D_{\mathbf{x}}}. \end{aligned} \quad (3.54)$$

We obtained Leibniz's integral rule for a one dimensional domain embedded in a one dimensional space, in subsection 3.2.5, and it is given by,

$$\frac{d}{dt}F(x_a(t), x_b(t), t) = \frac{\partial}{\partial t} \int_{x_a(t)}^{x_b(t)} f(x, t) dx + f(x_b(t), t) \frac{dx_b(t)}{dt} - f(x_a(t), t) \frac{dx_a(t)}{dt}. \quad (3.55)$$

From the striking similarity between the first rows of last two equations as well as from the considerations given above which make the additional terms in equation 3.54 amenable, we conclude that equation 3.54 is the generalization of Leibniz's integral rule for a one dimensional domain embedded in a multidimensional space. Within figure 3.5 we illustrated our interpretation of the two additional terms, which makes clear that they account for effects associated with three dimensional space.

This derivation suggests that Leibniz's integral rule is essentially an expression relating the total variation of the value of an integral to a contribution due to integrand variation and a contribution as a result of the average domain variation.

3.3.5 Parallelogramic and a parallelepiped domains: Area & volume elements.

A domain in a one dimensional space can only have only one "shape", a line element. In contrast there is no definite shape for one, two or three dimensional domains embedded in a three dimensional space. However, considering the definition of the Riemann integral (e.g. see chapter 5 in [76], chapter 11 in [6], chapter 15 in [5]), smooth shaped domains can be viewed as being composed, at the infinitesimal level, out of parallelogramic and parallelepiped domains. This suggests that from considerations over infinitesimal rectangular and parallelepiped domains we can infer results valid for arbitrary shaped smooth domains. Consequently, this is the shape of the domain we consider in our analyse,

Imagine an empty oriented volume, or volume element $\delta\mathbf{V}$ in the Cartesian space Ω , e.g. like in figure 3.6b. The volume has a parallelepiped shape and is spanned by the difference vectors $\Delta\mathbf{x}_a$, $\Delta\mathbf{x}_b$ and $\Delta\mathbf{x}_c$, hence we define the volume element as the triple scalar product (e.g. see p. 278 [17] or p. 18 in [8]),

$$\delta\mathbf{V} = \Delta\mathbf{x}_c \cdot \Delta\mathbf{x}_a \otimes \Delta\mathbf{x}_b. \quad (3.56)$$

A surface/areal element, e.g. the base of the parallelepiped, can be defined as,

$$\delta\mathbf{A} = \Delta\mathbf{x}_a \otimes \Delta\mathbf{x}_b. \quad (3.57)$$

Furthermore, the magnitude, or the volume of $\delta\mathbf{V}$ can be expressed as,

$$|\delta\mathbf{V}| = \delta V = |\Delta\mathbf{x}_c \cdot \Delta\mathbf{x}_a \otimes \Delta\mathbf{x}_b|. \quad (3.58)$$

The scalar product yields a scalar, hence the oriented volume and the magnitude are similar except possibly by a minus sign. The magnitude, or area of $\delta\mathbf{A}$ is,

$$|\delta\mathbf{A}| = \delta A = |\Delta\mathbf{x}_a \otimes \Delta\mathbf{x}_b|, \quad (3.59)$$

or the determinant of the cross product.

In following equation 3.56 and 3.57 we can define heuristically a (empty) differential volume element $d\mathbf{V}$ in terms of the infinitesimal difference vectors $d\mathbf{x}_a$, $d\mathbf{x}_b$ and $d\mathbf{x}_c$ (e.g. p. 50 in [8]),

$$d\mathbf{V} = d\mathbf{x}_c \cdot d\mathbf{x}_a \otimes d\mathbf{x}_b, \quad (3.60)$$

and a differential surface element,

$$d\mathbf{A} = d\mathbf{x}_a \otimes d\mathbf{x}_b. \quad (3.61)$$

A vector can be factorised in its magnitude and a unit vector expressing its orientation as well as direction. Accordingly, we can factorise the finite and infinitesimal area element as well as volume element, viz.

$$\delta\mathbf{A} = \hat{\mathbf{e}}_a \otimes \hat{\mathbf{e}}_b \Delta x_a \Delta x_b = \hat{\mathbf{n}}_A \delta A, \quad (3.62)$$

$$d\mathbf{A} = \hat{\mathbf{e}}_a \otimes \hat{\mathbf{e}}_b dx_a dx_b = \hat{\mathbf{n}}_A dA, \quad (3.63)$$

$$\delta\mathbf{V} = \hat{\mathbf{e}}_c \cdot (\hat{\mathbf{e}}_a \otimes \hat{\mathbf{e}}_b) \Delta x_c \Delta x_a \Delta x_b = \hat{\mathbf{e}}_c \cdot (\hat{\mathbf{e}}_a \otimes \hat{\mathbf{e}}_b) \delta V, \quad (3.64)$$

and,

$$d\mathbf{V} = \hat{\mathbf{e}}_c \cdot (\hat{\mathbf{e}}_a \otimes \hat{\mathbf{e}}_b) dx_c dx_a dx_b = \hat{\mathbf{e}}_c \cdot (\hat{\mathbf{e}}_a \otimes \hat{\mathbf{e}}_b) dV, \quad (3.65)$$

with the triple product $\hat{\mathbf{e}}_c \cdot \hat{\mathbf{e}}_a \otimes \hat{\mathbf{e}}_b$ being minus or plus one.

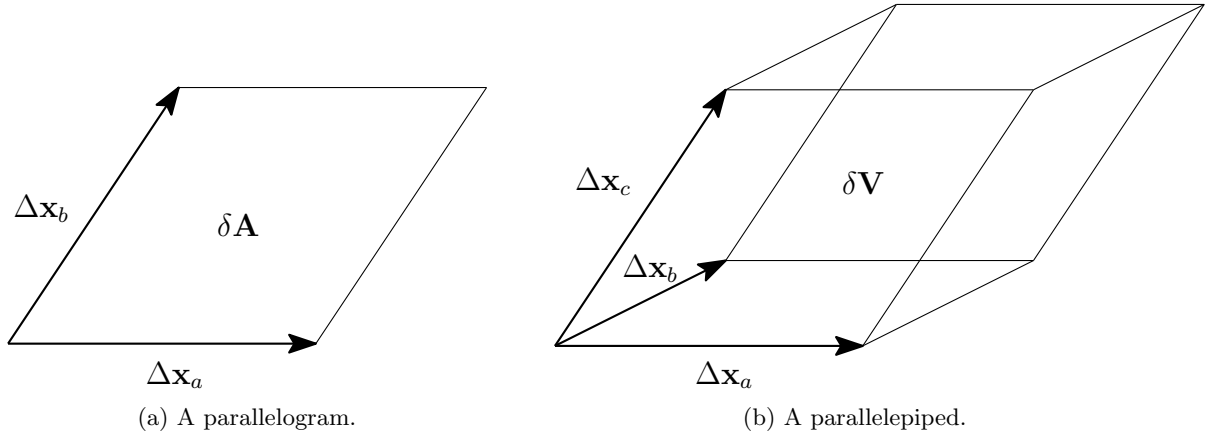


Figure 3.6: A basic area & volume element.

3.3.6 Deformation of area & volume elements.

Suppose we define a (stationary) displacement field \mathbf{u} over Ω which affects the volume element $\delta\mathbf{V}$, i.e. the boundary points defining $\delta\mathbf{V}$ are instantaneous displaced. From section 2.3 we know that under the influence of the displacement field the volume element may be translated (global effect), rotated and/or distorted/strained (local effects).

To see what happens to the volume element, on the scale of the volume element, recall the equations 2.40 and 2.42,

$$\mathbf{r}(\mathbf{x}, t) = \mathbf{x} + \mathbf{u}(\mathbf{x}, t). \quad (3.66)$$

and

$$\mathbf{u}(\mathbf{x} + \Delta\mathbf{x}, t) \approx \mathbf{u}(\mathbf{x}, t) + \frac{\partial \mathbf{u}(\mathbf{x}, t)}{\partial \mathbf{x}} \cdot \Delta\mathbf{x}. \quad (3.67)$$

The former equation can be interpreted, in the context of the volume element, as that a boundary point of $\delta\mathbf{V}$ initially at \mathbf{x} is displaced an amount of $\mathbf{u}(\mathbf{x}, t)$ and ends up at $\mathbf{r}(\mathbf{x}, t)$. The latter equation states that, in case of a smooth displacement field \mathbf{u} , the relative displacement of a boundary point occupying initially the position $\mathbf{x} + \Delta\mathbf{x}$, relative to a boundary point initially at position \mathbf{x} , can be approximated by $\frac{\partial \mathbf{u}(\mathbf{x}, t)}{\partial \mathbf{x}} \cdot \Delta\mathbf{x}$.

Let \mathbf{x} and $\mathbf{x} + \Delta\mathbf{x}_a$ be the two vertices through which we can define the difference vector, or oriented line element $\Delta\mathbf{x}_a$ being the edge of the parallelogram or parallelepiped (see figure 3.6). In the light of equations 3.66 and 3.67 we can then define the configuration of the line element after the effect of the displacement field (posterior line element) as,

$$\mathbf{r}(\mathbf{x} + \Delta\mathbf{x}_a, t) - \mathbf{r}(\mathbf{x}, t) = \Delta\mathbf{x}_a + \Delta\mathbf{u}(\mathbf{x}, t) \approx \Delta\mathbf{x}_a + \frac{\partial \mathbf{u}(\mathbf{x}, t)}{\partial \mathbf{x}} \cdot \Delta\mathbf{x}_a. \quad (3.68)$$

Substitution of $\Delta \mathbf{x}_b$ and $\Delta \mathbf{x}_c$ for $\Delta \mathbf{x}_a$ yields the expressions for the other line elements spanning the parallelogram as well as the parallelepiped.

In following equation 3.66, let us label a volume its state prior to a deformation by \mathbf{x} and its posterior state by \mathbf{r} . Subsequently, we can define what happens to the areal element as a response to the displacement field,

$$\delta \mathbf{A}_{\mathbf{r}} \approx \left[\Delta \mathbf{x}_a + \frac{\partial \mathbf{u}(\mathbf{x}, t)}{\partial \mathbf{x}} \cdot \Delta \mathbf{x}_a \right] \otimes \left[\Delta \mathbf{x}_b + \frac{\partial \mathbf{u}(\mathbf{x}, t)}{\partial \mathbf{x}} \cdot \Delta \mathbf{x}_b \right], \quad (3.69)$$

and what the effect is upon a volume element,

$$\delta \mathbf{V}_{\mathbf{r}} \approx \left[\Delta \mathbf{x}_c + \frac{\partial \mathbf{u}(\mathbf{x}, t)}{\partial \mathbf{x}} \cdot \Delta \mathbf{x}_c \right] \cdot \left[\Delta \mathbf{x}_a + \frac{\partial \mathbf{u}(\mathbf{x}, t)}{\partial \mathbf{x}} \cdot \Delta \mathbf{x}_a \right] \otimes \left[\Delta \mathbf{x}_b + \frac{\partial \mathbf{u}(\mathbf{x}, t)}{\partial \mathbf{x}} \cdot \Delta \mathbf{x}_b \right]. \quad (3.70)$$

Alternatively, these equations can be written in terms of the deformation gradient tensor $\underline{\mathbf{F}}$ (e.g. section 2.5 in [21], section 3.3 in [98] or section 1.4 in [117]), respectively,

$$\begin{aligned} \delta \mathbf{A}_{\mathbf{r}} &\approx \left[\left(\underline{\boldsymbol{\delta}} + \frac{\partial \mathbf{u}(\mathbf{x}, t)}{\partial \mathbf{x}} \right) \cdot \Delta \mathbf{x}_a \right] \otimes \left[\left(\underline{\boldsymbol{\delta}} + \frac{\partial \mathbf{u}(\mathbf{x}, t)}{\partial \mathbf{x}} \right) \cdot \Delta \mathbf{x}_b \right] \\ &= \left[\underline{\mathbf{F}} \cdot \Delta \mathbf{x}_a \right] \otimes \left[\underline{\mathbf{F}} \cdot \Delta \mathbf{x}_b \right], \end{aligned} \quad (3.71)$$

and,

$$\begin{aligned} \delta \mathbf{V}_{\mathbf{r}} &\approx \left[\left(\underline{\boldsymbol{\delta}} + \frac{\partial \mathbf{u}(\mathbf{x}, t)}{\partial \mathbf{x}} \right) \cdot \Delta \mathbf{x}_c \right] \cdot \left[\left(\underline{\boldsymbol{\delta}} + \frac{\partial \mathbf{u}(\mathbf{x}, t)}{\partial \mathbf{x}} \right) \cdot \Delta \mathbf{x}_a \right] \otimes \left[\left(\underline{\boldsymbol{\delta}} + \frac{\partial \mathbf{u}(\mathbf{x}, t)}{\partial \mathbf{x}} \right) \cdot \Delta \mathbf{x}_b \right] \\ &= + \left[\underline{\mathbf{F}} \cdot \Delta \mathbf{x}_c \right] \cdot \left[\underline{\mathbf{F}} \cdot \Delta \mathbf{x}_a \right] \otimes \left[\underline{\mathbf{F}} \cdot \Delta \mathbf{x}_b \right], \end{aligned} \quad (3.72)$$

with $\underline{\boldsymbol{\delta}}$ representing the Kronecker delta tensor.

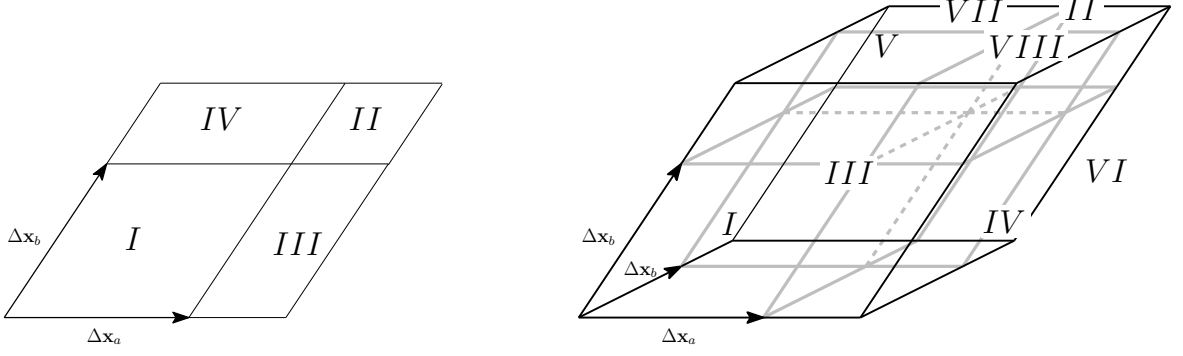
As dictated by the distributive properties of the scalar and the vector product we can rewrite the right hand side of expression 3.69 as,

$$\begin{aligned} \left[\Delta \mathbf{x}_a + \frac{\partial \mathbf{u}(\mathbf{x}, t)}{\partial \mathbf{x}} \cdot \Delta \mathbf{x}_a \right] \otimes \left[\Delta \mathbf{x}_b + \frac{\partial \mathbf{u}(\mathbf{x}, t)}{\partial \mathbf{x}} \cdot \Delta \mathbf{x}_b \right] &= \Delta \mathbf{x}_a \otimes \Delta \mathbf{x}_b + \left(\frac{\partial \mathbf{u}(\mathbf{x}, t)}{\partial \mathbf{x}} \cdot \Delta \mathbf{x}_a \right) \otimes \left(\frac{\partial \mathbf{u}(\mathbf{x}, t)}{\partial \mathbf{x}} \cdot \Delta \mathbf{x}_b \right) \\ &\quad + \left(\frac{\partial \mathbf{u}(\mathbf{x}, t)}{\partial \mathbf{x}} \cdot \Delta \mathbf{x}_a \right) \otimes \Delta \mathbf{x}_b + \Delta \mathbf{x}_a \otimes \left(\frac{\partial \mathbf{u}(\mathbf{x}, t)}{\partial \mathbf{x}} \cdot \Delta \mathbf{x}_b \right) \end{aligned} \quad (3.73)$$

and of equation 3.70 as,

$$\begin{aligned} &\left[\Delta \mathbf{x}_c + \frac{\partial \mathbf{u}(\mathbf{x}, t)}{\partial \mathbf{x}} \cdot \Delta \mathbf{x}_c \right] \cdot \left[\Delta \mathbf{x}_a + \frac{\partial \mathbf{u}(\mathbf{x}, t)}{\partial \mathbf{x}} \cdot \Delta \mathbf{x}_a \right] \otimes \left[\Delta \mathbf{x}_b + \frac{\partial \mathbf{u}(\mathbf{x}, t)}{\partial \mathbf{x}} \cdot \Delta \mathbf{x}_b \right] \\ &= \\ &\Delta \mathbf{x}_c \cdot \Delta \mathbf{x}_a \otimes \Delta \mathbf{x}_b + \frac{\partial \mathbf{u}(\mathbf{x}, t)}{\partial \mathbf{x}} \cdot \Delta \mathbf{x}_c \cdot \left(\frac{\partial \mathbf{u}(\mathbf{x}, t)}{\partial \mathbf{x}} \cdot \Delta \mathbf{x}_a \right) \otimes \left(\frac{\partial \mathbf{u}(\mathbf{x}, t)}{\partial \mathbf{x}} \cdot \Delta \mathbf{x}_b \right) \\ &+ \Delta \mathbf{x}_c \cdot \Delta \mathbf{x}_a \otimes \left(\frac{\partial \mathbf{u}(\mathbf{x}, t)}{\partial \mathbf{x}} \cdot \Delta \mathbf{x}_b \right) + \Delta \mathbf{x}_c \cdot \left(\frac{\partial \mathbf{u}(\mathbf{x}, t)}{\partial \mathbf{x}} \cdot \Delta \mathbf{x}_a \right) \otimes \Delta \mathbf{x}_b + \frac{\partial \mathbf{u}(\mathbf{x}, t)}{\partial \mathbf{x}} \cdot \Delta \mathbf{x}_c \cdot \Delta \mathbf{x}_a \otimes \Delta \mathbf{x}_b \\ &+ \Delta \mathbf{x}_c \cdot \left(\frac{\partial \mathbf{u}(\mathbf{x}, t)}{\partial \mathbf{x}} \cdot \Delta \mathbf{x}_a \right) \otimes \left(\frac{\partial \mathbf{u}(\mathbf{x}, t)}{\partial \mathbf{x}} \cdot \Delta \mathbf{x}_b \right) + \frac{\partial \mathbf{u}(\mathbf{x}, t)}{\partial \mathbf{x}} \cdot \Delta \mathbf{x}_c \cdot \Delta \mathbf{x}_a \otimes \left(\frac{\partial \mathbf{u}(\mathbf{x}, t)}{\partial \mathbf{x}} \cdot \Delta \mathbf{x}_b \right) \\ &\quad + \frac{\partial \mathbf{u}(\mathbf{x}, t)}{\partial \mathbf{x}} \cdot \Delta \mathbf{x}_c \cdot \left(\frac{\partial \mathbf{u}(\mathbf{x}, t)}{\partial \mathbf{x}} \cdot \Delta \mathbf{x}_a \right) \otimes \Delta \mathbf{x}_b. \end{aligned} \quad (3.74)$$

For a parallelogram or parallelepiped embedded in a dilatational displacement field, these two expressions simply state how the initial area or volume element, represented by the two first terms on the right hand side as padded with respectively three parallelogramic and seven parallelepiped contributions, as drawn in figure 3.7.



(a) Dilatation of a parallelogram. The roman numerals correspond to the terms on the right hand side of equation 3.73.

(b) Dilatation of a parallelepiped. The roman numerals correspond to the terms on the right hand side of equation 3.74.

Figure 3.7: Dilatation of a basic area & volume element.

Recall that in this manuscript we assume that objects rotate and strain in such a manner that we can describe them by infinitesimal strain theory. Infinitesimal strain theory relies on the assumption that the displacement gradients are small, i.e. $|\text{grad}[\mathbf{u}]| \ll 1$ (e.g. see section 3.5 in [98]). Consequently, products of displacement gradients become negligibly small, which can be clearly seen from the heuristic geometrical argument illustrated in figure 3.7: when $|\text{grad}[\mathbf{u}]| \rightarrow \ll 1$, the parallelogram represented by the second term on the first row equation 3.73 and the parallelepipeds associated with the terms on the fourth row of equation 3.74 as well as the second term on the second row "shrink much faster" than the other contributions.

Thus, in the specific case of infinitesimal strains, equation 3.73 reduces to,

$$\begin{aligned} \left[\Delta \mathbf{x}_a + \frac{\partial \mathbf{u}(\mathbf{x}, t)}{\partial \mathbf{x}} \cdot \Delta \mathbf{x}_a \right] \otimes \left[\Delta \mathbf{x}_b + \frac{\partial \mathbf{u}(\mathbf{x}, t)}{\partial \mathbf{x}} \cdot \Delta \mathbf{x}_b \right] &= \Delta \mathbf{x}_a \otimes \Delta \mathbf{x}_b \\ &+ \left(\frac{\partial \mathbf{u}(\mathbf{x}, t)}{\partial \mathbf{x}} \cdot \Delta \mathbf{x}_a \right) \otimes \Delta \mathbf{x}_b + \Delta \mathbf{x}_a \otimes \left(\frac{\partial \mathbf{u}(\mathbf{x}, t)}{\partial \mathbf{x}} \cdot \Delta \mathbf{x}_b \right) \end{aligned} \quad (3.75)$$

and equation 3.74 to,

$$\begin{aligned} \delta \mathbf{V}_r &= \left[\Delta \mathbf{x}_c + \frac{\partial \mathbf{u}(\mathbf{x}, t)}{\partial \mathbf{x}} \cdot \Delta \mathbf{x}_c \right] \cdot \left[\Delta \mathbf{x}_a + \frac{\partial \mathbf{u}(\mathbf{x}, t)}{\partial \mathbf{x}} \cdot \Delta \mathbf{x}_a \right] \otimes \left[\Delta \mathbf{x}_b + \frac{\partial \mathbf{u}(\mathbf{x}, t)}{\partial \mathbf{x}} \cdot \Delta \mathbf{x}_b \right] \\ &= \Delta \mathbf{x}_c \cdot \Delta \mathbf{x}_a \otimes \Delta \mathbf{x}_b \\ &+ \Delta \mathbf{x}_c \cdot \Delta \mathbf{x}_a \otimes \left(\frac{\partial \mathbf{u}(\mathbf{x}, t)}{\partial \mathbf{x}} \cdot \Delta \mathbf{x}_b \right) + \Delta \mathbf{x}_c \cdot \left(\frac{\partial \mathbf{u}(\mathbf{x}, t)}{\partial \mathbf{x}} \cdot \Delta \mathbf{x}_a \right) \otimes \Delta \mathbf{x}_b + \frac{\partial \mathbf{u}(\mathbf{x}, t)}{\partial \mathbf{x}} \cdot \Delta \mathbf{x}_c \cdot \Delta \mathbf{x}_a \otimes \Delta \mathbf{x}_b \end{aligned} \quad (3.76)$$

The commonly used expression for the deformed areal element is known as Nanson's formula ((e.g. see p. 75 in [98] or p. 384 in [56]). It can be obtained by factorising equation 3.69 and employing the vector identity,

$$B^T (B \hat{\mathbf{e}}_x \otimes B \hat{\mathbf{e}}_y) = |B| \hat{\mathbf{e}}_x \otimes \hat{\mathbf{e}}_y, \quad (3.77)$$

viz.,

$$\begin{aligned} \delta \mathbf{A}_r &\approx [\underline{\mathbf{F}} \cdot \Delta \mathbf{x}_a] \otimes [\underline{\mathbf{F}} \cdot \Delta \mathbf{x}_b] \\ &= (\underline{\mathbf{F}} \cdot \hat{\mathbf{e}}_a \otimes \underline{\mathbf{F}} \cdot \hat{\mathbf{e}}_b) \Delta x_a \Delta x_b \\ &= |\underline{\mathbf{F}}| \underline{\mathbf{F}}^{-T} \cdot (\hat{\mathbf{e}}_a \otimes \hat{\mathbf{e}}_b) \delta A. \end{aligned} \quad (3.78)$$

The commonly encountered expression for the deformed volume element can be obtained in the light of the vector identities,

$$A \cdot (B \otimes C) = B \cdot (C \otimes A) = C \cdot (A \otimes B), \quad (3.79)$$

and

$$(A \cdot D) (B \otimes C) + (B \cdot D) (C \otimes A) + (C \cdot D) (A \otimes B) = (A \cdot (B \otimes C)) D. \quad (3.80)$$

With these two identities equation 3.76 can be casted in the form (e.g. see section 2.5 in [21], section 3.3 in [98]),

$$\begin{aligned} \delta \mathbf{V}_r &= \Delta \mathbf{x}_c \cdot \Delta \mathbf{x}_a \otimes \Delta \mathbf{x}_b + \frac{\partial \mathbf{u}(\mathbf{x}, t)}{\partial \mathbf{x}} (\Delta \mathbf{x}_c \cdot \Delta \mathbf{x}_a \otimes \Delta \mathbf{x}_b) \\ &= \underline{\mathbf{F}} (\Delta \mathbf{x}_c \cdot \Delta \mathbf{x}_a \otimes \Delta \mathbf{x}_b). \end{aligned} \quad (3.81)$$

Then, from the factorisation of the scalar triple product (equation 3.64) we obtain the familiar expression,

$$\begin{aligned}\delta\mathbf{V}_r &= \underline{\mathbf{F}}(\hat{\mathbf{e}}_c \cdot \hat{\mathbf{e}}_a \otimes \hat{\mathbf{e}}_b) \Delta x_c \Delta x_a \Delta x_b \\ &= |\underline{\mathbf{F}}| \Delta x_c \Delta x_a \Delta x_b.\end{aligned}\quad (3.82)$$

Note, $|\underline{\mathbf{F}}| = \left| \frac{\partial \mathbf{u}(\mathbf{x}, t)}{\partial \mathbf{x}} \right| = J$, which is known as the Jacobian determinant.

The analogous expression for the deformed infinitesimal areal element as well as a volume element are respectively,

$$d\mathbf{A}_r \approx |\underline{\mathbf{F}}| \underline{\mathbf{F}}^{-T} \cdot (\hat{\mathbf{e}}_a \otimes \hat{\mathbf{e}}_b) dA. \quad (3.83)$$

and

$$d\mathbf{V}_r \approx |\underline{\mathbf{F}}| dx_c dx_a dx_b. \quad (3.84)$$

Through integration we can relate the prior infinitesimal area and volume element to the posterior finite area and volume element. In addition considering averages the link between the prior and posterior finite elements can be established. Hence we have for the area element,

$$\delta\mathbf{A}_r = \delta\mathbf{A}_x \langle |\underline{\mathbf{F}}| \underline{\mathbf{F}}^{-T} \rangle = \frac{\delta\mathbf{A}_x}{\delta\mathbf{A}_x} \int_{\delta\mathbf{A}_x} |\underline{\mathbf{F}}| \underline{\mathbf{F}}^{-T} \cdot d\mathbf{A}_x, \quad (3.85)$$

and for the volume element,

$$\delta\mathbf{V}_r = \delta\mathbf{V}_x \langle \underline{\mathbf{F}} \rangle = \frac{\delta\mathbf{V}_x}{\delta\mathbf{V}_x} \int_{\delta\mathbf{V}_x} \underline{\mathbf{F}} \cdot d\mathbf{V}_x. \quad (3.86)$$

For the respective area and volume we have,

$$\delta A_r = A_x \langle |\underline{\mathbf{F}}| \underline{\mathbf{F}}^{-T} \cdot \hat{\mathbf{n}} \rangle = \frac{\delta A_x}{\delta A_x} \int_{\delta A_x} |\underline{\mathbf{F}}| \underline{\mathbf{F}}^{-T} \cdot \hat{\mathbf{n}}(\mathbf{x}) dA_x, \quad (3.87)$$

and

$$\delta V_r = \delta V_x \langle \underline{\mathbf{F}} \rangle = \frac{\delta V_x}{\delta V_x} \int_{\delta V_x} \underline{\mathbf{F}} dV_x. \quad (3.88)$$

Note, recall equation 3.37 from subsection 3.3.2. From it we can clearly see that the analogous integrals relating the infinitesimal line domains in three dimensional space to the prior and posterior line element,

$$\begin{aligned}\delta\mathbf{r}(\mathbf{x}, t) &= \int_{\delta\mathbf{x}} \left[\underline{\boldsymbol{\delta}} + \frac{\partial \mathbf{u}(\mathbf{x}, t)}{\partial \mathbf{x}} \right] \cdot d\mathbf{x} \\ &= \frac{\delta\mathbf{x}}{\delta\mathbf{x}} \int_{\delta\mathbf{x}} \underline{\mathbf{F}} \cdot d\mathbf{x} = \delta\mathbf{x} \langle \underline{\mathbf{F}} \rangle\end{aligned}\quad (3.89)$$

and,

$$\begin{aligned}\delta r(\mathbf{x}, t) &= \delta x \langle \underline{\mathbf{F}} \cdot \hat{\mathbf{n}}(\mathbf{x}) \rangle \\ &= \frac{\delta x}{\delta x} \int_{\delta x} \underline{\mathbf{F}} \cdot \hat{\mathbf{n}}(\mathbf{x}) dx\end{aligned}\quad (3.90)$$

These expressions show that the infinitesimal deformation of an one, two or three dimensional domain are completely controlled by the deformation gradient tensor $\underline{\mathbf{F}}$.

3.3.7 Generalization of Leibniz's integral rule: 2D & 3D domains in 3D space.

The result from subsection 3.3.4, i.e. the generalization of Leibniz's integral rule for a one dimensional domain, in the form of a line element, embedded in a three dimensional space can be further generalized to a two or three dimensional domain, respectively $D_{\mathbf{A}} = \delta\mathbf{A}$ and $D_{\mathbf{V}} = \delta\mathbf{V}$, embedded in a three dimensional space.

This can be done rather straightforward, by going again through the derivation presented in subsections 3.3.2-3.3.4, though this time with the prior and posterior deformation integrals (3.33 and 3.34) replaced by prior and posterior deformation integrals over two and three dimensional domains.

The programme of the presented derivation entails essentially that we separate the integrand from the domain variation and consequently rewrite the domain variation contribution by:

- 1.) rewriting the integral over the posterior domain of integration in an integral over the prior domain of integration;

- 2.) considering the resulting equation in the light of the directional derivative of the gradient of the integrand with the displacement vector;
- 3.) letting the terms explicating the interdependent integrand and domain variation vanish by imposing a.) the infinitesimal strain assumption, as well as b.) the assumption that the gradient of the integrand is very small;
- 4.) employing the product rule in reverse to obtain a single integral over a gradient of the product of the integrand and the displacement vector;
- 5.) rewriting the resulting integral of the gradient, through the average theorem of Slattery and Whitaker, in order to obtain a representation of the average deformation of the domain which includes the "characteristic" boundary integral of Leibniz's integral rule.

The generalization for a two dimensional domain seems to be, at least at a first sight, slightly more complex if we simply compare the three kinds of integrals for the three different dimensional domains, given in subsection 3.3.6,

$$\delta \mathbf{r}(\mathbf{x}, t) = \delta \mathbf{x} \langle \underline{\mathbf{F}} \rangle = \frac{\delta \mathbf{x}}{\delta \mathbf{x}} \int_{\delta \mathbf{x}} \underline{\mathbf{F}} \cdot d\mathbf{x}, \quad (3.91)$$

$$\delta \mathbf{A}_r = \delta \mathbf{A}_x \langle |\underline{\mathbf{F}}| \underline{\mathbf{F}}^{-T} \rangle = \frac{\delta \mathbf{A}_x}{\delta \mathbf{A}_x} \int_{\delta \mathbf{A}_x} |\underline{\mathbf{F}}| \underline{\mathbf{F}}^{-T} \cdot d\mathbf{A}_x, \quad (3.92)$$

and

$$\delta \mathbf{V}_r = \delta \mathbf{V}_x \langle \underline{\mathbf{F}} \rangle = \frac{\delta \mathbf{V}_x}{\delta \mathbf{V}_x} \int_{\delta \mathbf{V}_x} \underline{\mathbf{F}} \cdot d\mathbf{V}_x. \quad (3.93)$$

Due to the factor $|\underline{\mathbf{F}}| \underline{\mathbf{F}}^{-T}$, the directional derivative formulation, under step two of reformulating the domain variation, requires additional considerations. These considerations are beyond the scope of this manuscript, among others since the three dimensional domain generalization is of interest in this manuscript. The interested reader may consult Flanders [40] for the generalization for two dimensional domains, derived in terms of differential forms.

For the three dimensional domain $\delta \mathbf{V}_x$ we have the prior integral,

$$\int_{\delta \mathbf{V}_x} f(\mathbf{x}, t) d\mathbf{V}_x, \quad (3.94)$$

and the posterior integral,

$$\int_{\delta \mathbf{V}_r} f(\mathbf{x}, t) d\mathbf{V}_r. \quad (3.95)$$

From subsection 3.3.6 we know that the representation of the two posterior integrals in terms of the prior domains are,

$$\int_{\delta \mathbf{V}_r} f(\mathbf{x}, t) d\mathbf{V}_r = \int_{\delta \mathbf{V}_x} f(\mathbf{x} + \mathbf{u}(\mathbf{x}, t), t) \underline{\mathbf{F}} d\mathbf{V}_x. \quad (3.96)$$

We defined in subsection 3.3.2 the directional derivative (equation 3.38) and used it to approximate $f(\mathbf{x} + \mathbf{u}(\mathbf{x}, t), t)$ by a linear extrapolation from $f(\mathbf{x}, t)$ (equation 3.39), i.e.

$$f(\mathbf{x} + \mathbf{u}(\mathbf{x}, t), t) \approx f(\mathbf{x}, t) + \frac{\partial f(\mathbf{x}, t)}{\partial \mathbf{x}} \cdot \mathbf{u}(\mathbf{x}, t). \quad (3.97)$$

Recall that, $\underline{\mathbf{F}} = \underline{\boldsymbol{\delta}} + \frac{\partial}{\partial \mathbf{x}} \mathbf{u}(\mathbf{x}, t)$. Then, by combining the linear extrapolation with equation 3.96 we can define the domain variation for the three dimensional integral,

$$\begin{aligned} \int_{\delta \mathbf{V}_r} f(\mathbf{x}, t) d\mathbf{V}_r - \int_{\delta \mathbf{V}_x} f(\mathbf{x}, t) d\mathbf{V}_x &= \int_{\delta \mathbf{V}_x} f(\mathbf{x} + \mathbf{u}(\mathbf{x}, t), t) \underline{\mathbf{F}} \cdot d\mathbf{V}_x - \int_{\delta \mathbf{V}_x} f(\mathbf{x}, t) d\mathbf{V}_x \\ &= \int_{\delta \mathbf{V}_x} \frac{\partial f(\mathbf{x}, t)}{\partial \mathbf{x}} \cdot \mathbf{u}(\mathbf{x}, t) \underline{\boldsymbol{\delta}} \cdot d\mathbf{V}_x + \int_{\delta \mathbf{V}_x} f(\mathbf{x}, t) \frac{\partial \mathbf{u}(\mathbf{x}, t)}{\partial \mathbf{x}} \cdot d\mathbf{V}_x \\ &\quad + \int_{\delta \mathbf{V}_x} \frac{\partial f(\mathbf{x}, t)}{\partial \mathbf{x}} \cdot \mathbf{u}(\mathbf{x}, t) \frac{\partial \mathbf{u}(\mathbf{x}, t)}{\partial \mathbf{x}} \cdot d\mathbf{V}_x. \end{aligned} \quad (3.98)$$

Imposing the assumption of infinitesimal strains and the assumption that the gradient of the integrand is very small, renders the last "cross term" integral negligible. The product of the displacement vector

$\mathbf{u}(\mathbf{x}, t)$ and the unit tensor $\underline{\delta}$ is simply the displacement vector itself. Then, if we in addition consider the product rule of differentiation, the latter equation becomes,

$$\begin{aligned} \int_{\delta V_r} f(\mathbf{x}, t) d\mathbf{V}_r - \int_{\delta V_x} f(\mathbf{x}, t) d\mathbf{V}_x &\approx + \int_{\delta V_x} \frac{\partial f(\mathbf{x}, t)}{\partial \mathbf{x}} \cdot \mathbf{u}(\mathbf{x}, t) \cdot d\mathbf{V}_x + \int_{\delta V_x} f(\mathbf{x}, t) \frac{\partial \mathbf{u}(\mathbf{x}, t)}{\partial \mathbf{x}} \cdot d\mathbf{V}_x \\ &= \int_{\delta V_x} \frac{\partial}{\partial \mathbf{x}} [f(\mathbf{x}, t) \mathbf{u}(\mathbf{x}, t)] \cdot d\mathbf{V}_x. \end{aligned} \quad (3.99)$$

Rewriting the integral of the gradient in terms of an average (i.e. by virtue of the mean and intermediate value theorem), and setting it in the light of the averaging theorem (equation 3.44 in subsection 3.3.3) of Slattery ([108]) and Whitaker ([124]),

$$\left\langle \frac{\partial}{\partial \mathbf{x}} g \right\rangle_V = \frac{\partial}{\partial \mathbf{x}} \langle g \rangle_V + \frac{1}{V} \int_A g \hat{\mathbf{n}} dA, \quad (3.100)$$

we obtain,

$$\begin{aligned} \int_{\delta V_r} f(\mathbf{x}, t) d\mathbf{V}_r - \int_{\delta V_x} f(\mathbf{x}, t) d\mathbf{V}_x &\approx \frac{\delta \mathbf{V}_x}{\delta \mathbf{V}_x} \int_{\delta V_x} \frac{\partial}{\partial \mathbf{x}} [f(\mathbf{x}, t) \mathbf{u}(\mathbf{x}, t)] \cdot d\mathbf{V}_x \\ &= \delta \mathbf{V}_x \frac{\partial}{\partial \mathbf{x}} \langle f(\mathbf{x}, t) \mathbf{u}(\mathbf{x}, t) \rangle_{\delta V_x} + \int_{\delta A_x} f(\mathbf{x}, t) \mathbf{u}(\mathbf{x}, t) \cdot d\mathbf{A}_x. \end{aligned} \quad (3.101)$$

Decomposing the average of the product into the product of the averages and a covariance term, of which the latter vanishes since we argued in subsection 3.3.2 that it is the statistical representation of the cross term integral in equation 3.98, yields,

$$\begin{aligned} \int_{\delta V_r} f(\mathbf{x}, t) d\mathbf{V}_r - \int_{\delta V_x} f(\mathbf{x}, t) d\mathbf{V}_x &\approx \delta \mathbf{V}_x \langle \mathbf{u}(\mathbf{x}, t) \rangle_{\delta V_x} \frac{\partial}{\partial \mathbf{x}} \langle f(\mathbf{x}, t) \rangle_{\delta V_x} + \langle f(\mathbf{x}, t) \rangle_{\delta V_x} \delta \mathbf{V}_x \frac{\partial}{\partial \mathbf{x}} \langle \mathbf{u}(\mathbf{x}, t) \rangle_{\delta V_x} \\ &\quad + \int_{\delta A_x} f(\mathbf{x}, t) \mathbf{u}(\mathbf{x}, t) \cdot d\mathbf{A}_x. \end{aligned} \quad (3.102)$$

This equation is similar to equation 3.49 in subsection 3.3.3 for a one dimensional domain embedded in three dimensional space. The individual terms can be interpreted in the same manner as described in that subsection and we will not repeat it here.

The rate form of this equation can be obtained by dividing the equation by Δt and subsequently taking the limit $\Delta t \rightarrow 0$. Since the derivation parallels the treatment of the one dimensional domain in subsections 3.3.2-3.3.4, we simply state the result here,

$$\begin{aligned} \frac{\partial}{\partial \delta \mathbf{V}_x} \left[\int_{\delta V_x} f(\mathbf{x}, t) d\mathbf{V}_x \right] \frac{d\delta \mathbf{V}_x}{dt} &\approx \delta \mathbf{V}_x \langle \mathbf{v}(\mathbf{x}, t) \rangle_{\delta V_x} \frac{\partial}{\partial \mathbf{x}} \langle f(\mathbf{x}, t) \rangle_{\delta V_x} + \delta \mathbf{V}_x \langle f(\mathbf{x}, t) \rangle_{\delta V_x} \frac{\partial}{\partial \mathbf{x}} \langle \mathbf{v}(\mathbf{x}, t) \rangle_{\delta V_x} \\ &\quad + \int_{\delta A_x} f(\mathbf{x}, t) \mathbf{v}(\mathbf{x}, t) \cdot d\mathbf{A}_x. \end{aligned} \quad (3.103)$$

In following, e.g. equation 3.53 in subsection 3.3.4, we combine the domain variation with the integrand variation to arrive at,

$$\begin{aligned} \frac{d}{dt} \int_{\delta V_x} f(\mathbf{x}, t) d\mathbf{V}_x &\approx \frac{\partial}{\partial t} \int_{\delta V_x} f(\mathbf{x}, t) d\mathbf{V}_x + \int_{\delta A_x} f(\mathbf{x}, t) \mathbf{v}(\mathbf{x}, t) \cdot d\mathbf{A}_x \\ &\quad + \delta \mathbf{V}_x \langle \mathbf{v}(\mathbf{x}, t) \rangle_{\delta V_x} \frac{\partial}{\partial \mathbf{x}} \langle f(\mathbf{x}, t) \rangle_{\delta V_x} + \delta \mathbf{V}_x \langle f(\mathbf{x}, t) \rangle_{\delta V_x} \frac{\partial}{\partial \mathbf{x}} \langle \mathbf{v}(\mathbf{x}, t) \rangle_{\delta V_x} \end{aligned} \quad (3.104)$$

Based on similarity in form with equation 3.53 in subsection 3.3.4 and equation 3.25 in subsection 3.2.5, as well as similarity in meaning, we conclude that this is a generalization of Leibniz's integral rule for three dimensional domains embedded in a three dimensional space.

3.3.8 Conclusion: Reynolds transport theorem.

The generalization of Leibniz's integral rule for three dimensional domains can be obtained in a slightly different manner than presented above, however it requires another physical assumption about the nature of the determinant of the deformation gradient.

From subsection 3.3.5 we know that $\delta \mathbf{V}_x$ is an oriented, or, more precisely, a directed volume, with its direction explicated by a minus or a plus "charge". If we follow Reddy (p. 74 [98]) and assume that the mutual direction of the line elements is preserved under deformation, it follows that the directed volumes are all positive since the determinant of the deformation gradient is positive $|\mathbf{F}| > 0$. This assumption seems to be a logical consequence of the infinitesimal strain assumption.

Adopting this assumption, yields the equality 3.82 given in subsection 3.3.6,

$$d\mathbf{V}_r = \mathbf{F} d\mathbf{V}_x = \mathbf{F} (\hat{\mathbf{e}}_c \cdot \hat{\mathbf{e}}_a \otimes \hat{\mathbf{e}}_b) dV_x = |\mathbf{F}| dV_x. \quad (3.105)$$

Considering the determinant $|\mathbf{F}|$ in the light of the infinitesimal strain assumption (terms which entail products of displacement gradients vanish) yields,

$$|\mathbf{F}| \approx \left(1 + \frac{\partial}{\partial \mathbf{x}} \cdot \mathbf{u}(\mathbf{x}, t)\right). \quad (3.106)$$

From these results we can rewrite equation 3.98 into,

$$\begin{aligned} \int_{\delta V_{\mathbf{r}}} f(\mathbf{x}, t) d\mathbf{V}_{\mathbf{r}} - \int_{\delta V_{\mathbf{x}}} f(\mathbf{x}, t) d\mathbf{V}_{\mathbf{x}} &= \int_{\delta V_{\mathbf{x}}} f(\mathbf{x} + \mathbf{u}(\mathbf{x}, t), t) |\mathbf{F}| dV_{\mathbf{x}} - \int_{\delta V_{\mathbf{x}}} f(\mathbf{x}, t) dV_{\mathbf{x}} \\ &= \int_{\delta V_{\mathbf{x}}} \frac{\partial f(\mathbf{x}, t)}{\partial \mathbf{x}} \cdot \mathbf{u}(\mathbf{x}, t) \cdot dV_{\mathbf{x}} + \int_{\delta V_{\mathbf{x}}} f(\mathbf{x}, t) \left(\frac{\partial}{\partial \mathbf{x}} \cdot \mathbf{u}(\mathbf{x}, t)\right) \cdot dV_{\mathbf{x}} \\ &\quad + \int_{\delta V_{\mathbf{x}}} \frac{\partial f(\mathbf{x}, t)}{\partial \mathbf{x}} \cdot \mathbf{u}(\mathbf{x}, t) \left(\frac{\partial}{\partial \mathbf{x}} \cdot \mathbf{u}(\mathbf{x}, t)\right) \cdot dV_{\mathbf{x}}. \end{aligned} \quad (3.107)$$

Continuing with imposing the assumption that the gradient of f is very small as well as dividing by Δt and taking the limit of $\Delta t \rightarrow 0$, yields an expression for the rate of change of the value of the integral due to domain variation,

$$\frac{\partial}{\partial \mathbf{x}} \left(\int_{\delta V_{\mathbf{x}}} f(\mathbf{x}, t) dV_{\mathbf{x}} \right) \frac{d}{dt} \delta V_{\mathbf{x}}(t) \approx \int_{\delta V_{\mathbf{x}}} \frac{\partial}{\partial \mathbf{x}} (f(\mathbf{x}, t)) \cdot \mathbf{v}(\mathbf{x}, t) \cdot dV_{\mathbf{x}} + \int_{\delta V_{\mathbf{x}}} f(\mathbf{x}, t) \left(\frac{\partial}{\partial \mathbf{x}} \cdot \mathbf{v}(\mathbf{x}, t)\right) \cdot dV_{\mathbf{x}}. \quad (3.108)$$

Finally, combining this expression for the domain variation with the expression of the integrand variation yields,

$$\frac{d}{dt} \int_{\delta V_{\mathbf{x}}} f(\mathbf{x}, t) dV_{\mathbf{x}} = \frac{\partial}{\partial t} \int_{\delta V_{\mathbf{x}}} f(\mathbf{x}, t) dV_{\mathbf{x}} + \int_{\delta V_{\mathbf{x}}} \frac{\partial}{\partial \mathbf{x}} (f(\mathbf{x}, t)) \cdot \mathbf{v}(\mathbf{x}, t) \cdot dV_{\mathbf{x}} + \int_{\delta V_{\mathbf{x}}} f(\mathbf{x}, t) \left(\frac{\partial}{\partial \mathbf{x}} \cdot \mathbf{v}(\mathbf{x}, t)\right) \cdot dV_{\mathbf{x}} \quad (3.109)$$

This variant of Leibniz's integral rule for a three dimensional domain is the common form encountered in the continuum mechanical literature and genuine known as Reynolds transport theorem (e.g. see p. 85 in [8], p. 74 in [13], p. 74 in [12], p. 578 in [76], [40], p. 169 in [98], p. 206 [3]).

The final result of the former subsection 3.3.7 is Leibniz's integral rule for three dimensional domains in the form,

$$\begin{aligned} \frac{d}{dt} \int_{\delta V_{\mathbf{x}}} f(\mathbf{x}, t) d\mathbf{V}_{\mathbf{x}} &\approx \frac{\partial}{\partial t} \int_{\delta V_{\mathbf{x}}} f(\mathbf{x}, t) d\mathbf{V}_{\mathbf{x}} + \int_{\delta \mathbf{A}_{\mathbf{x}}} f(\mathbf{x}, t) \mathbf{v}(\mathbf{x}, t) \cdot d\mathbf{A}_{\mathbf{x}} \\ &\quad + \delta \mathbf{V}_{\mathbf{x}} \langle \mathbf{v}(\mathbf{x}, t) \rangle_{\delta V_{\mathbf{x}}} \frac{\partial}{\partial \mathbf{x}} \langle f(\mathbf{x}, t) \rangle_{\delta V_{\mathbf{x}}} + \delta \mathbf{V}_{\mathbf{x}} \langle f(\mathbf{x}, t) \rangle_{\delta V_{\mathbf{x}}} \frac{\partial}{\partial \mathbf{x}} \langle \mathbf{v}(\mathbf{x}, t) \rangle_{\delta V_{\mathbf{x}}} \end{aligned} \quad (3.110)$$

If we impose the assumption that the (mutual) direction of line elements in the domain are preserved under deformation and keeping in mind the infinitesimal strain assumption, we obtain,

$$\begin{aligned} \frac{d}{dt} \int_{\delta V_{\mathbf{x}}} f(\mathbf{x}, t) dV_{\mathbf{x}} &\approx \frac{\partial}{\partial t} \int_{\delta V_{\mathbf{x}}} f(\mathbf{x}, t) dV_{\mathbf{x}} + \int_{\delta \mathbf{A}_{\mathbf{x}}} f(\mathbf{x}, t) \mathbf{v}(\mathbf{x}, t) \cdot d\mathbf{A}_{\mathbf{x}} \\ &\quad + \delta V_{\mathbf{x}} \langle \mathbf{v}(\mathbf{x}, t) \rangle_{\delta V_{\mathbf{x}}} \frac{\partial}{\partial \mathbf{x}} \langle f(\mathbf{x}, t) \rangle_{\delta V_{\mathbf{x}}} + \delta V_{\mathbf{x}} \langle f(\mathbf{x}, t) \rangle_{\delta V_{\mathbf{x}}} \frac{\partial}{\partial \mathbf{x}} \cdot \langle \mathbf{v}(\mathbf{x}, t) \rangle_{\delta V_{\mathbf{x}}}. \end{aligned} \quad (3.111)$$

Consequently we can conclude that Reynolds transport theorem and the form of Leibniz's integral rule for three dimensional domains derived in the former subsection are equivalent under the assumption that mutual directions of line elements within the domain of interest are preserved. The two equations 3.109 and 3.111 differ only in their representation. However, the form in terms of average domain variation reveals clearer the connection with Leibniz's integral rule as well as that it explicates the kinds of deformation which may possibly affect the value of an integral through the domain at the scale of "observation".

In the following we will continue with Reynolds transport theorem, among others since it is the representation of Leibniz's integral rule for three dimensional domains which is customary in continuum mechanics. For an illustration of Reynolds transport theorem see figure 3.8.

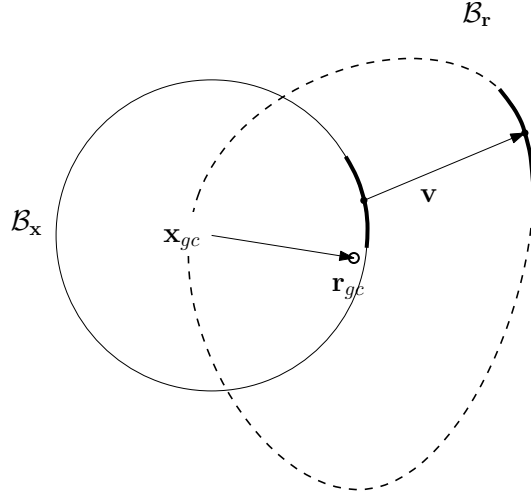


Figure 3.8: A visual interpretation of the domain variation described by Reynolds transport theorem, with \mathcal{B}_x representing the domain prior to deformation and \mathcal{B}_r the domain posterior to deformation.

3.4 Integrand variation: Eulerian balance principle.

3.4.1 Introduction: a physical approach to integrand variation.

Consider the one dimensional integral,

$$F(D_x, t) = \int_{D_x} f(x, t) dx. \quad (3.112)$$

From section 3.2 we know that the value of this integral may vary due to, 1.) variation of the integrand f , and/or 2.) variation of the domain of integration D_x . We concluded that at the infinitesimal level the integrand variation and domain variation can be separated, without approximation error and that we can write the rate of change of the value of an integrand as (equation 3.31),

$$\frac{d}{dt} F(D_x(t), t) = \frac{\partial}{\partial t} F(D_x(t), t) + \frac{\partial}{\partial D_x} F(D_x(t), t) \frac{dD_x(t)}{dt}. \quad (3.113)$$

In this section we adopt this mathematical picture, though in its more general form,

$$\frac{d}{dt} F(D(t), t) = \frac{\partial}{\partial t} F(D(t), t) + \frac{\partial}{\partial D} F(D(t), t) \frac{dD(t)}{dt}. \quad (3.114)$$

In section 3.2 and 3.3 our focus was on the kinematic causes underlying the domain variation and the respective contribution to the change in the value of the integral. The kinematic causes emerged essentially from rewriting the integral in a more revealing form, with the aid of mathematical concepts (most profoundly, Taylor's theorem, mean value theorem and the intermediate value theorem). The results we interpreted more or less physically, however it did not alter the mathematics. The essence was mathematical. Further considerations on the causes underlying the domain variation (e.g. dynamic causes) are beyond the scope of this chapter.

In this section we consider the causes underlying the variation of the integrand f . Our approach to the integrand variation differs from our treatments of the variation of the domain in the sense that the causal mechanisms underlying integrand variation are physical in essence. Moreover, we will consider the integrand variation in the light of the widely used Eulerian control volume analysis (e.g. see chapter 6 in [13], section 3.2 in [12], section 5.9 in [39]).

In an Eulerian control volume analysis the domain of integration is kept fixed, in position as well as magnitude, hence for the scope of this section we do not have to worry about domain variation³. The control volume is arbitrary in shape and its content of the control volume may change. The latter is what the integrand variation describes and what we will elaborate on in this section.

³Alternatively we can interpret it as that our area of focus remains stationary like considered in subsection 2.2.3

3.4.2 Control volume analysis & a conservation law.

Consider figure 3.9 illustrating a control volume analysis. According to the figure, a change in F due to variation of f on D may be the result of a flow of the quantity F in and/or out of D . In addition, the quantity F may be produced and/or consumed within D . Consequently, the change in F in the time interval $[t, t + \Delta t]$ can be represented as a balance equation over D ,

$$F(D, t + \Delta t) - F(D, t) = F_{in}(\partial D, t, \Delta t) - F_{out}(\partial D, t, \Delta t) + F_{prod.}(D, t, \Delta t) - F_{consum.}(D, t, \Delta t). \quad (3.115)$$

To provide a more elaborate mathematical expressions for $F_{prod.}$ and $F_{consum.}$ means that we have to postulate some function Q_{in} and Q_{out} or a resultant function $Q_{res} = Q_{in} - Q_{out}$. In turn we can analyse its behaviour upon integrand and domain variation, i.e. according to our approximation of a finite change (equation 3.31, subsection 3.3.1)

$$\Delta Q_{res} = \Delta t \frac{\partial}{\partial t} Q_{res} + \Delta t \frac{\partial}{\partial D} Q_{res} \frac{dD}{dt}. \quad (3.116)$$

In this subsection we consider a fixed domain and hence the latter term vanishes. To really provide new information on Q_{res} , we have to become rather specific in what kind of function, which is beyond the scope of this subsection.

Therefore, for the following we assume that the production and consumption term vanish, i.e. they balance each other or they are zero each. This means that F is conserved and this more specific case of the latter equation can be denoted as a conservation law for F ,

$$F(D, t + \Delta t) - F(D, t) = F_{in}(\partial D, t, \Delta t) - F_{out}(\partial D, t, \Delta t). \quad (3.117)$$

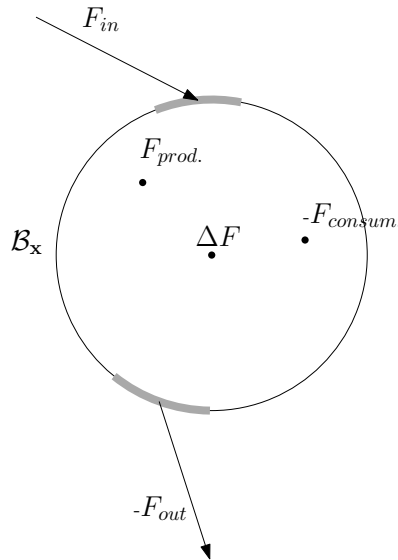


Figure 3.9: A simple control volume analysis over a fixed circular domain.

3.4.3 Inward flow in terms of a Flux.

The flow of F in and/or out of a domain is typically described mathematically as being proportional to the integrand function f , which we interpreted as a density, multiplied by a flow through area A and the perpendicular component of a displacement \mathbf{u} (see figure 3.10). Thus for the inward flow,

$$F_{in} \propto f u \cos(\alpha) A = f \mathbf{u} \cdot (-\hat{\mathbf{n}}) A, \quad (3.118)$$

with $-\hat{\mathbf{n}}$ being the outward unit vector explicating the orientation of the area A . More precise, the factor $f \mathbf{u}$ may be actually an average value defined over the area A . Moreover, $f = f(\mathbf{x})$ and $\mathbf{u} = \mathbf{u}(\mathbf{x})$ with $\mathbf{x} \in A \subset D$. Consequently we can define the inward flow as,

$$\begin{aligned} F_{in} &= \langle f \mathbf{u} \rangle_A \cdot (-\hat{\mathbf{n}}) A \\ &= \int_A f(\mathbf{x}) \mathbf{u}(\mathbf{x}) \cdot d\mathbf{A}. \end{aligned} \quad (3.119)$$

This equation still defines a special case, since we tacitly assumed A to be a planar area for which $\hat{\mathbf{n}}$ is the same for each infinitesimal constituent $dA = \hat{\mathbf{n}}dA$. Genuinely, this unit vector is the average orientation defined over A , hence we can refine the former equation to,

$$\begin{aligned} F_{in} &= \langle f\mathbf{u} \rangle_A \cdot -\langle \hat{\mathbf{n}} \rangle_A A \\ &= \int_A f(\mathbf{x})\mathbf{u}(\mathbf{x}) \cdot -\hat{\mathbf{n}}(\mathbf{x})dA. \end{aligned} \quad (3.120)$$

Note, this refinement states that the composite variable $f(\mathbf{x})\mathbf{u}(\mathbf{x})$ and $\hat{\mathbf{n}}(\mathbf{x})$ vary independently at the scale of A , which can be interpret as that we imagine our A to be a window frame which does not disturb the displacement field.

The displacement can be interpreted as the displacement of point objects carrying F , from "initial" positions which coincide with/lie on the area A (see section 2.3 for more information). Displacements can be thought of as occurring in the time interval $[t, t + \Delta t]$. Hence we may write the displacement in terms of a velocity,

$$\mathbf{u}(\mathbf{x}) = \mathbf{v}(\mathbf{x})\Delta t. \quad (3.121)$$

In addition, the displacement and hence the velocity may vary with time, as well as the value of f on A , i.e. $\mathbf{u} = \mathbf{u}(\mathbf{x}, t)$, $\mathbf{v} = \mathbf{v}(\mathbf{x}, t)$ and $f = f(\mathbf{x}, t)$. From this it follows that the product $f(\mathbf{x})\mathbf{u}(\mathbf{x}) = f(\mathbf{x})\mathbf{v}(\mathbf{x})\Delta t$ is genuine the time average,

$$\langle f(\mathbf{x})\mathbf{v}(\mathbf{x}) \rangle_{\Delta t} \Delta t = \frac{\Delta t}{\Delta t} \int_t^{t+\Delta t} f(\mathbf{x}, t)\mathbf{v}(\mathbf{x}, t)dt, \quad \text{with } \mathbf{x} \in A. \quad (3.122)$$

Remark, for the scope of this subsection we assume a fixed control volume, hence $\hat{\mathbf{n}}(\mathbf{x})$ is time independent.

Suppose we are not interested in the details of f and \mathbf{v} , at A , over $[t, t + \Delta t]$ (in line with subsection 3.2.4). In this light, equation 3.120 can be refined sufficiently to,

$$F_{in} = \langle \langle f\mathbf{v}_{in} \rangle_{\Delta t} \rangle_A \Delta t \cdot \langle \hat{\mathbf{n}} \rangle_A A = \int_A \langle f(\mathbf{x})\mathbf{v}_{in}(\mathbf{x}) \rangle_{\Delta t} \Delta t \cdot \hat{\mathbf{n}}(\mathbf{x})dA. \quad (3.123)$$

An alternative representation of this result can be obtained in terms of a flux \mathbf{q}_{in} . A flux can be defined mathematically by dividing the latter equation by $\Delta t\hat{\mathbf{n}}A$ and subsequently take the limit of $\Delta t \rightarrow 0$ and $A \rightarrow 0$, i.e.,

$$q_{F,in}(\mathbf{x}, t)\hat{\mathbf{n}}(\mathbf{x}) = \lim_{\Delta A \rightarrow 0} \left[\lim_{\Delta t \rightarrow 0} \frac{F_{in}}{\Delta t\hat{\mathbf{n}}A} \right] = \lim_{\Delta A \rightarrow 0} \left[\lim_{\Delta t \rightarrow 0} (\langle \langle f\mathbf{v} \rangle_{\Delta t} \rangle_A \cdot \hat{\mathbf{n}}) \hat{\mathbf{n}} \right] = (f(\mathbf{x}, t)\mathbf{v}_{in}(\mathbf{x}, t) \cdot \hat{\mathbf{n}}) \hat{\mathbf{n}}. \quad (3.124)$$

In words, a flux $\mathbf{q}_{F,in} = q_{F,in}\hat{\mathbf{n}}$ is an amount of a quantity F passing through a "point" \mathbf{x} ($A \rightarrow 0$) in a certain instant of time ($t \rightarrow t$) in the direction of $\hat{\mathbf{n}}(\mathbf{x})$.

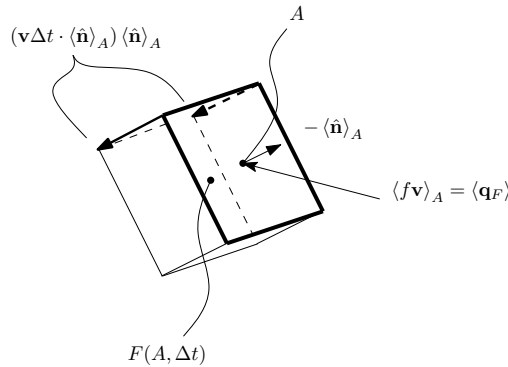


Figure 3.10: Illustration of a flux through a square area.

3.4.4 Conclusions: Eulerian balance equation & conservation law

In the above we considered everything in terms of the inward flow F_{in} , however the same mathematical representation is valid for the outward flow. The differences are physical: a.) the minus sign in front of

F_{out} accounts for the difference in direction relative to the area; b.) the magnitude of the inward and outward flow velocity may differ; as well as c.) the boundaries of the domains over which the flows are defined.

Consequently we can rewrite our expression for the conservation law (equation 3.117) as,

$$\begin{aligned} F(D, t + \Delta t) - F(D, t) &= F_{in}(\partial D, t, \Delta t) - F_{out}(\partial D, t, \Delta t) \\ &= \Delta t \int_{A_{in}} \langle f(\mathbf{x}) \mathbf{v}_{in}(\mathbf{x}) \rangle_{\Delta t} \cdot \hat{\mathbf{n}}(\mathbf{x}) dA - \Delta t \int_{A_{out}} \langle f(\mathbf{x}) \mathbf{v}_{out}(\mathbf{x}) \rangle_{\Delta t} \cdot \hat{\mathbf{n}}(\mathbf{x}) dA. \end{aligned} \quad (3.125)$$

Dividing both sides of this equation by Δt and subsequently taking the limit $\Delta t \rightarrow 0$, we obtain,

$$\frac{\partial}{\partial t} F(D, t) = \int_{A_{in}} f(\mathbf{x}, t) \mathbf{v}_{in}(\mathbf{x}, t) \cdot \hat{\mathbf{n}}(\mathbf{x}) dA - \int_{A_{out}} f(\mathbf{x}, t) \mathbf{v}_{out}(\mathbf{x}, t) \cdot \hat{\mathbf{n}}(\mathbf{x}) dA. \quad (3.126)$$

Whenever the areas over which we integrate are similar, we can lump F_{in} and F_{out} together in a resultant flow over the boundary ∂D of the domain as a whole.

The resultant rate of flow can be expressed as,

$$\begin{aligned} \frac{\partial}{\partial t} F_{res}(\partial D, t) &= \lim_{\Delta t \rightarrow 0} \Delta t \int_{\partial D} [\langle f(\mathbf{x}) \mathbf{v}_{in}(\mathbf{x}) \rangle - \langle f(\mathbf{x}) \mathbf{v}_{out}(\mathbf{x}) \rangle] \cdot \hat{\mathbf{n}}(\mathbf{x}) dA \\ &= \int_{\partial D} f(\mathbf{x}, t) [\mathbf{v}_{in}(\mathbf{x}, t) - \mathbf{v}_{out}(\mathbf{x}, t)] \cdot \hat{\mathbf{n}}(\mathbf{x}) dA \\ &= \int_{\partial D} \mathbf{q}_{F,res}(\mathbf{x}, t) \cdot \hat{\mathbf{n}}(\mathbf{x}) dA. \end{aligned} \quad (3.127)$$

Consequently, the rate form of the conservation law (equation 3.117) can be alternatively expressed as,

$$\frac{\partial}{\partial t} F(D, t) = \int_{\partial D} f(\mathbf{x}, t) \mathbf{v}_{res}(\mathbf{x}, t) \cdot \hat{\mathbf{n}}(\mathbf{x}) dA = \int_{\partial D} \mathbf{q}_{F,res}(\mathbf{x}, t) \cdot \hat{\mathbf{n}}(\mathbf{x}) dA. \quad (3.128)$$

Finally, a general Eulerian balance equation can be written as,

$$\begin{aligned} F(D, t + \Delta t) - F(D, t) &= Q_{res}(D, t, \Delta t) + \Delta t \int_{\partial} \langle f(\mathbf{x}) \mathbf{v}_{res}(\mathbf{x}) \rangle_{\Delta t} \cdot \hat{\mathbf{n}}(\mathbf{x}) dA \\ &= \Delta t \int_D s(\mathbf{x}, t) \gamma_s(\mathbf{x}) dV + \Delta t \int_{\partial D} \mathbf{q}_{F,res}(\mathbf{x}, t) \cdot \hat{\mathbf{n}}(\mathbf{x}) dA. \end{aligned} \quad (3.129)$$

The fifth term is the integral form of the resultant production term, in which s represents a source function and γ_s the distribution function of "point sources".

3.5 An arbitrary dimensional boundary integral.

3.5.1 Introduction: One dimensional domains and zero dimensional boundaries.

Consider the expressions we derived in the former subsection for the resultant flow over a domain D ,

$$F_{res}(\partial D, t, \Delta t) = \Delta t \int_{\partial D} \langle f(\mathbf{x}, t) \mathbf{v}_{res}(\mathbf{x}, t) \rangle_{\Delta t} \cdot \hat{\mathbf{n}}(\mathbf{x}) dA = \Delta t \int_{\partial D} \langle \mathbf{q}_{F,res}(\mathbf{x}, t) \rangle_{\Delta t} \cdot \hat{\mathbf{n}}(\mathbf{x}) dA. \quad (3.130)$$

For one dimensional domains (non looping) it may seem awkward to define the flow crossing the domain boundary in terms of a boundary integral, since what are the boundary integrals for zero dimensional domain?

Briefly we have seen already boundary integrals for a zero dimensional domain. They pop up in the derivation of Leibniz's integral rule for one dimensional domains, i.e. in subsection ?? and ?. In this section we will define them nearer. Moreover, we will define boundary integrals in a general manner through distribution functions, which are defined by Gray [46] as a series of unit step functions or boxcar functions.

3.5.2 Selecting a domain of integration by a distribution function.

The unit step function in a one-dimensional space, also known as the Heaviside function, is defined as,

$$H(x - x_n) = \begin{cases} 1 & \text{if } x \geq x_n \\ 0 & \text{if } x < x_n \end{cases}. \quad (3.131)$$

From the unit step function we can define the boxcar function as (e.g. see [122]),

$$B(x|l, h, c) = h \left[H(x - c + \frac{1}{2}l) - H(x - c - \frac{1}{2}l) \right], \quad (3.132)$$

which is a rectangle function of length l , height h and centred around c . The multidimensional boxcar function can be defined as,

$$B(\mathbf{x}) = \begin{cases} h & \text{if } \mathbf{x} \in D \\ 0 & \text{if } \mathbf{x} \notin D \end{cases}, \quad (3.133)$$

with D being some rectangular shaped domain centred around a point c . The unit height boxcar function can be thought of as the basic building block of the distribution function [46].

A distribution function can be defined as[46, 51],

$$\gamma = \gamma(\mathbf{x}, t) = \begin{cases} 1 & \text{if } \mathbf{x} \in D \\ 0 & \text{if } \mathbf{x} \notin D \end{cases}, \quad (3.134)$$

with D being a domain in an arbitrary dimensional space thought of as being composed out of infinitesimal cubical domains⁴, or boxcar functions.

The Heaviside function can be thought of as the more specific one-dimensional variant of the distribution function. For the scope of this manuscript, the distribution function can be interpreted simply as a manner to demarcate a domain in the space of interest through binary labelling.

3.5.3 Selecting the boundary of a domain of integration through the gradient of the distribution function.

The derivative of the Heaviside function $H(x - x_n)$, is by definition the unit impulse, or Dirac delta function⁵

$$\frac{d}{dx}H(x - x_n) = \delta(x - x_n). \quad (3.135)$$

The Dirac delta function can be used through integration to "select" discrete points from space (e.g. see chapter 11 in [17] or chapter 14 in [109]) and from the latter equation it can be seen why we are interested in it: the delta function picks out the boundary point of the Heaviside function ("Heaviside domain").

A one dimensional distribution function can be thought of as a more complex domain construed from a series of Heaviside functions[46]. It follows from the linear property of the derivative that the derivative of a one dimensional distribution function is a sum of delta functions, describing the boundary points. Thus,

$$\frac{d\gamma(x)}{dx} = \sum_i \delta(x - x_{n,i}). \quad (3.136)$$

This idea of selecting boundary points of domains in one dimension can be generalized to more dimensions through the distribution function. Moreover, according to Gray ([45]) the delta function series describing the set of boundary points of a three dimensional domain can be obtained by taking the gradient of a three dimensional distribution function,

$$\frac{\partial\gamma(\mathbf{x})}{\partial\mathbf{x}} = \sum_i -\hat{\mathbf{n}}_i \delta(\mathbf{x} - \mathbf{x}_{n,i}). \quad (3.137)$$

In this equation $\hat{\mathbf{n}}_i$ is the unit outward vector expressing the "orientation" of the boundary point $\mathbf{x}_{n,i}$. This follows from the concept of a directional derivative, since the directional derivative yields a vector which is perpendicular to an iso-surface (e.g. see p. 293 in [17]) and a boundary can be thought of as being an iso-surface. From this we can infer that the orientation of the gradient vector can be interpreted as the average orientation of the set of boundary points.

⁴This is the conceptual idea behind integration, e.g. see chapter 1 in [7], chapter 5 in [76] or chapter 15 in [5].

⁵The Dirac delta function is a so called generalized function. One way to define it is through a boxcar function with $h = \frac{1}{2l}$ and taking the limit of the boxcar function of $l \rightarrow 0$ (e.g. see chapter 14 in [109]).

3.5.4 The boundary integral over a fixed domain.

Now we are in the position to define boundary integrals. For that, consider an arbitrary dimensional volume integral like,

$$F(D) = \int_D f(\mathbf{x})dV, \quad (3.138)$$

with dV an arbitrary dimensional volume. The related boundary integral can be defined as,

$$F(\partial D) = \int_{\partial D} f(\mathbf{x})d\mathbf{A}, \quad (3.139)$$

with $d\mathbf{A}$ being understood as a general infinitesimal boundary element. An alternative representation of the volume integral can be given through the distribution function⁶. In other words, instead of defining the integral over a domain D , we express the domain information through the distribution function and define the integral over e.g. the whole space Ω in which D is embedded (e.g. see [51]),

$$F(D) = \int_{\Omega} f(\mathbf{x})\gamma(\mathbf{x})dV. \quad (3.140)$$

We heuristically express the variation of $F(D)$ with respect to changing the domain D as,

$$\frac{\partial}{\partial D}F(D) = \frac{\partial}{\partial \mathbf{x}}F(D) = \int_{\Omega} \frac{\partial}{\partial \mathbf{x}} [f(\mathbf{x})\gamma(\mathbf{x})] dV = 0. \quad (3.141)$$

The interchangement of the differentiation and integration is allowed since the domain of integration Ω is fixed⁷. The value is zero since we stated above that we consider a fixed control volume/domain.

According to the product rule of differentiation we can rewrite this equation as,

$$\frac{\partial}{\partial \mathbf{x}}F(D) = \int_{\Omega} \frac{\partial}{\partial \mathbf{x}} [f(\mathbf{x})] \gamma(\mathbf{x})dV + \int_{\Omega} f(\mathbf{x}) \frac{\partial}{\partial \mathbf{x}} [\gamma(\mathbf{x})] dV. \quad (3.142)$$

Thus, the variation in F due to a change in the domain D comprises a contribution due to a change in the encountered integrand function \mathbf{f} as well as due to change in the distribution function.

In the light of equation 3.137 we can express this equation in the form,

$$\frac{\partial}{\partial \mathbf{x}}F(D) = \int_{\Omega} \frac{\partial}{\partial \mathbf{x}} [f(\mathbf{x})] \gamma(\mathbf{x})dV - \int_{\Omega} f(\mathbf{x}) \left[\sum_i \mathbf{n}_i \delta(\mathbf{x} - \mathbf{x}_{n,i}) \right] dV. \quad (3.143)$$

By virtue of the linear property of integration, the last integral of this equation is simply a sum of integrals.

For convenience, suppose the integral is a three dimensional integral. From the definition of the multidimensional Dirac delta function (e.g. see p. 210 in [109] or p. 456 in [17]) combined with the definition of the infinitesimal volume (see subsection ??), we can write the sum of integrals as,

$$- \int_{\Omega} f(\mathbf{x}) \left[\sum_i \hat{\mathbf{n}}_i \delta(\mathbf{x} - \mathbf{x}_{n,i}) \right] dV = - \sum_i \int_{\Omega} f(x, y, z) \hat{\mathbf{n}}_i \delta(x - x_{n,i}) \delta(y - y_{n,i}) \delta(z - z_{n,i}) dx dy dz = - \sum_i f(\mathbf{x}_{n,i}) \hat{\mathbf{n}}_i. \quad (3.144)$$

This resulting sum of point values is simply the net contribution to $F(D)$ from the boundary. Suppose we partition this boundary in finite boundary elements of magnitude δA , consequently we can rewrite the sum in terms of "partition" averages which yields,

$$- \sum_j \langle f(\mathbf{x}_{c,j}) \rangle \langle \hat{\mathbf{n}}_j \rangle \delta A, \quad (3.145)$$

with $\mathbf{x}_{c,j}$ the centroid of the j th partition, and $\langle \hat{\mathbf{n}}_j \rangle$ the average orientation of the partition "attached" to $\mathbf{x}_{c,j}$. Note, we assume that f and $\hat{\mathbf{n}}$ can vary independently, simply because f is a scalar.

⁶Remark the similarity with the concept of an integral over an elementary region, e.g. as defined on p. 342 in [76].

⁷A similar argument like we used in subsection ?? for interchanging the partial differentiation with respect to time and integration.

In the light of the definition of a Riemann integral (e.g. see p. 408 in [5]), whenever we have an infinite set of boundary points we can define a boundary integral as,

$$-\lim_{N \rightarrow \infty} \sum_j^N \langle f(\mathbf{x}_{c,j}) \rangle \langle \hat{\mathbf{n}}_j \rangle \delta A = - \int_{\partial D} f(\mathbf{x}) \hat{\mathbf{n}}(\mathbf{x}) dA. \quad (3.146)$$

Note, this expression is consistent with equation 3.144.

With the latter expression we can write equation 3.143 in the form,

$$\frac{\partial}{\partial \mathbf{x}} F(D) = \int_{\Omega} \frac{\partial}{\partial \mathbf{x}} [f(\mathbf{x})] \gamma(\mathbf{x}) dV - \int_{\Omega} f(\mathbf{x}) \left[\sum_i \mathbf{n}_i \delta(\mathbf{x} - \mathbf{x}_{n,i}) \right] dV = \int_{\Omega} \frac{\partial}{\partial \mathbf{x}} [f(\mathbf{x})] \gamma(\mathbf{x}) dV - \int_{\partial D} f(\mathbf{x}) \hat{\mathbf{n}}(\mathbf{x}) dA. \quad (3.147)$$

In the specific case that we have a two dimensional domain, embedded in a two dimensional space, the infinitesimal "volume element" is $dA = dx dy$, the corresponding one dimensional boundary element is ds . Substituting this into the last equation yields,

$$\frac{\partial}{\partial \mathbf{x}} F(D) = \int_{\Omega} \frac{\partial}{\partial \mathbf{x}} [f(\mathbf{x})] \gamma(\mathbf{x}) dA - \int_{\Omega} f(\mathbf{x}) \left[\sum_i \mathbf{n}_i \delta(\mathbf{x} - \mathbf{x}_{n,i}) \right] dA = \int_{\Omega} \frac{\partial}{\partial \mathbf{x}} [f(\mathbf{x})] \gamma(\mathbf{x}) dA - \int_{\partial D} f(\mathbf{x}) \hat{\mathbf{n}}(\mathbf{x}) ds. \quad (3.148)$$

For a one dimensional domain, embedded in a one dimensional space, we obtain,

$$\frac{\partial}{\partial \mathbf{x}} F(D) = \int_{\Omega} \frac{\partial}{\partial \mathbf{x}} [f(\mathbf{x})] \gamma(\mathbf{x}) dx - \int_{\Omega} f(\mathbf{x}) \left[\sum_i \mathbf{n}_i \delta(\mathbf{x} - \mathbf{x}_{n,i}) \right] dx = \int_{\Omega} \frac{\partial}{\partial \mathbf{x}} [f(\mathbf{x})] \gamma(\mathbf{x}) dx - \sum_i f(x_{n,i}) \hat{\mathbf{n}}_i. \quad (3.149)$$

From the systematics in these three, two and one dimensional cases as well as equation ?? we conclude that a general oriented boundary element can be defined as,

$$d\mathbf{A} = -\hat{\mathbf{n}}_i \delta(\mathbf{x} - \mathbf{x}_{n,i}) dV, \quad (3.150)$$

and that an arbitrary dimensional boundary integral can be defined as an integral over the domain,

$$-\int_{\partial D} d\mathbf{A} = - \int_D \sum_i \hat{\mathbf{n}}_i \delta(\mathbf{x} - \mathbf{x}_{n,i}) dV. \quad (3.151)$$

As a corollary, since for the scope of this section $\partial/\partial \mathbf{x} F(D) = 0$ we can make the statement,

$$-\int_{\Omega} \frac{\partial}{\partial \mathbf{x}} [f(\mathbf{x})] \gamma(\mathbf{x}) dV = \int_D \frac{\partial}{\partial \mathbf{x}} f(\mathbf{x}) dV = + \int_{\partial D} f(\mathbf{x}) \hat{\mathbf{n}}(\mathbf{x}) dA, \quad (3.152)$$

in which we can recognize the traits of Green's and Gauss' theorem, which will be the case when the integrand function is a vector function (e.g. see section 9 in [17] or chapter 8 in [76]).

3.5.5 Conclusion: An arbitrary dimensional boundary integral.

In this section we have elaborated on the boundary integral. The central concept from which we defined the boundary integral is the derivative of a distribution function. This derivative is in general a sum of oriented Dirac delta functions, each centred around a point of the boundary of the domain "selected" by the distribution function. The orientation of the Dirac delta function is expressed as a unit vector and interpreted as the outward normal (with respect of the domain) of the boundary point.

The emergence of the orientation of the Dirac delta function may be the most mysterious. It is heuristically introduced in analogy with the directional derivative and how it can be considered to define unit normal vectors to iso-surfaces. A boundary can be interpret as an iso-surface.

With the use of the definition of the Riemann integral, we have argued that the arbitrary dimensional "volume" integral of the sum of oriented Dirac delta functions is equal to boundary integral, i.e. (equation 3.151),

$$-\int_{\partial D} d\mathbf{A} = - \int_D \sum_i \hat{\mathbf{n}}_i \delta(\mathbf{x} - \mathbf{x}_{n,i}) dV, \quad (3.153)$$

with the minus sign being present due to that the unit vectors are pointing outward of the domain.

3.6 Conclusion & chapter summary: A Lagrangian-Eulerian balance principle.

In this chapter we derived a Lagrangian Eulerian (L-E) balance principle, centred around a mathematical expression for the "total" time rate of change of the value of an integral (one dimensional integrals are considered in section 3.2 and three dimensional integrals in section 3.3),

$$\frac{d}{dt}F(D, t) = \frac{d}{dt} \int_D f(\mathbf{x}, t) d\mathbf{x}. \quad (3.154)$$

The rate of change of the value of an integral can be decomposed as the sum of a contribution due to integrand variation as well as a contribution as a result of domain variation. One way to show this is by applying Leibniz's chain rule applied to the "anti derivative" function F (see the subsections 3.3.1-3.3.4),

$$\frac{d}{dt}F(D, t) = \frac{\partial}{\partial t}F(D, t) + \frac{\partial}{\partial D}F(D, t) \frac{d}{dt}D. \quad (3.155)$$

The integrand variation accounts for the time explicit changes in the integrand and how this affects the value of an integral. The domain variation accounts for the "advective" changes of the domain and how it affects the portion of the integrand function sampled. In addition it describes how the dilatation of the domain, i.e. expansion or compression of the portion of the integrand function sampled, affects the evolution of the value of an integral.

Expression 3.155 focusses on the domain as a whole. However, a domain can be considered as being defined by its boundary and therefore one can emphasize the deformation of the boundary as opposed to the domain as a whole. The latter seems to be the common approach to obtain Leibniz's integral rule (see section 3.2), suggesting a variant of equation 3.155,

$$\frac{d}{dt}F(\partial D, t) = \frac{\partial}{\partial t}F(\partial D) + \frac{\partial}{\partial(\partial D)}F(\partial D, t) \frac{d}{dt}(\partial D). \quad (3.156)$$

Note, we refer with ∂D to the boundary of the domain D . In this chapter we switched from the "boundary focus" approach to the domain focus approach, among others to establish the connection with Reynolds transport theorem, for which it is customary to obtain it with a domain focus (e.g. see p. 85 in [8], p. 74 in [13], p. 74 in [12], p. 578 in [76], [40], p. 169 in [98], a. 206 [3]). The connection between the two approaches we put forward in subsection 3.3.1. From the results presented in subsection 3.3.8 it seems that we can conclude that the the domain approach is less obscure, i.e. more revealing than the boundary approach, at least regarding average domain variation effects. The separation of the total rate of change of the value of an integral in integrand and domain variation contributions essentially emerged by mathematical revelation and for intuitive purposes we attributed them with kinematic (physical) interpretations (see subsection 3.4.1).

We approached the generalization of Leibniz's integral rule to the variation of an integral over a one dimensional domain embedded in a three dimensional space, by focussing on the domain (see subsection 3.3.4). From this derivation we concluded that a "five step" programme can be used to generalize Leibniz's integral rule (see subsection 3.3.7), which we successfully employed to derive the generalization of the integral rule for three dimensional domains embedded in three dimensional spaces.

For the above to be valid, it has been shown that we should assume the integrand f to be continuous, smooth and slowly varying with respect to its variables \mathbf{x} and t . We attributed the variation in the domain of the integral to a displacement field $\mathbf{u}(\mathbf{x}, t)$. Which in turn should also be continuous, smooth and slowly varying (infinitesimal strain assumption). The consequence of the absolutely continuous assumption (continuous and smooth) is that we can employ Taylor's theorem (as discussed in chapter 2) as well as that second order terms, i.e. terms involving products of $\Delta \mathbf{x}$ and Δt , become vanishingly small in the infinitesimal limit. Analogous, the slowly varying field assumptions renders cross terms involving products of the gradients of f and \mathbf{u} to be negligibly small. A small corollary to the infinitesimal strain assumption, i.e. that the mutual orientation of "material lines" within the integral domain remains conserved (also known as the admissibility assumption e.g. see p. 2 in [92], p. 245 in [98], p. 83 in [8] and especially the intuitive account in [19]), assures us that we do not have to worry about the sign of the determinant of the deformation gradient (see subsection 3.3.6). In addition, an implication of that the

two fields of interest are slowly varying is that from the deformation modes the domain can be subjected to, solely the dilatation of the domain contributes to the rate of change of the value of an integral (see subsection 3.3.7).

To obtain the L-E balance principle we refined the integrand variation contribution by essentially physical considerations (see subsection 3.4.1), based on a Eulerian control volume analysis (see section 3.4). The refinement consists out of writing the integrand variation in terms of a time averaged resultant flux over the boundaries of the control volume (domain of integration) and a resultant time averaged production within the control volume. The time average is with respect to the time scale in which the change of the value of the integral takes place.

Combining this physical motivated refinement of the integrand variation with the mathematical motivated refinement of the total derivative of the value of an integral yields the L-E balance principle. Moreover, the time rate of change of the value of F in its well known "Reynolds transport theorem" form is (see subsection 3.3.8),

$$\frac{d}{dt} \int_{V(t)} f(\mathbf{x}, t) dV = \int_{V(t)} \frac{\partial}{\partial t} f(\mathbf{x}, t) dV + \int_{V(t)} \frac{\partial}{\partial \mathbf{x}} \cdot (f(\mathbf{x}, t) \mathbf{v}_{\partial V}(\mathbf{x}, t)) dV. \quad (3.157)$$

The refinement of the integrand variation term in a resultant production and flux contribution is given by,

$$\int_{V(t)} \frac{\partial}{\partial t} f(\mathbf{x}, t) dV = - \int_{\partial V(t)} f(\mathbf{x}, t) \mathbf{v}_f(\mathbf{x}, t) \hat{\mathbf{n}}_A(\mathbf{x}) dA + \int_{V(t)} s(\mathbf{x}, t) \gamma_s(\mathbf{x}) dV. \quad (3.158)$$

With s being a "source" function and γ_s the distribution function associated with "point sources".

Substituting this refinement in equation 3.157 while having Gauss' divergence theorem in the back of our mind, let us to formulate a L-E balance principle for F in terms of f ,

$$\int_{V(t)} \frac{\partial}{\partial t} f(\mathbf{x}, t) dV = - \int_{\partial V(t)} f(\mathbf{x}, t) \mathbf{v}_{rel}(\mathbf{x}, t) \hat{\mathbf{n}}_A(\mathbf{x}) dA + \int_{V(t)} s(\mathbf{x}, t) \gamma_s(\mathbf{x}) dV - \int_{\partial V(t)} f(\mathbf{x}, t) \mathbf{v}_{\partial V}(\mathbf{x}, t) \hat{\mathbf{n}}_A(\mathbf{x}) dA \quad (3.159)$$

with \mathbf{v}_{rel} being the relative velocity of the flux of f with respect to the boundary, i.e.,

$$\mathbf{v}_{rel}(\mathbf{x}, t) = \mathbf{v}_f(\mathbf{x}, t) - \mathbf{v}_{\partial V}(\mathbf{x}, t). \quad (3.160)$$

This result seems to be similar to the result presented by Wu ([130], p. 24), with the difference being that he puts the emphasize on the flux and in our derivation we focussed on the deformation of the domain of integration.

The differential form of the L-E balance equation is,

$$\frac{\partial}{\partial t} f(\mathbf{x}, t) = -\text{div} [f(\mathbf{x}, t) \mathbf{v}_{rel}(\mathbf{x}, t)] + -\text{div} [f(\mathbf{x}, t) \mathbf{v}_{\partial V}(\mathbf{x}, t)] + s(\mathbf{x}, t) \gamma_s(\mathbf{x}). \quad (3.161)$$

We interpret this equation as the description of the time rate of change of a (density) quantity f within a deformable control volume V . The rate of change is due to

- a.) translation and normal-strain deformation of V ,
- b.) a (relative) surface flux of f over the boundary of V , and
- c.) possible sources/sinks in V .

A L-E conservation principle, follows by setting the production term s to zero. Furthermore, by setting $\mathbf{v}_{\partial V} = 0$, which implies that \mathbf{v}_{rel} becomes \mathbf{v}_f , it seems that we obtain the general balance principle as presented in section 4.2 of [13]. Hence, we conclude that this balance principle is a special case of our L-E balance principle derived in this chapter. A visual interpretation of the L-E balance principle is given in figure 3.11.

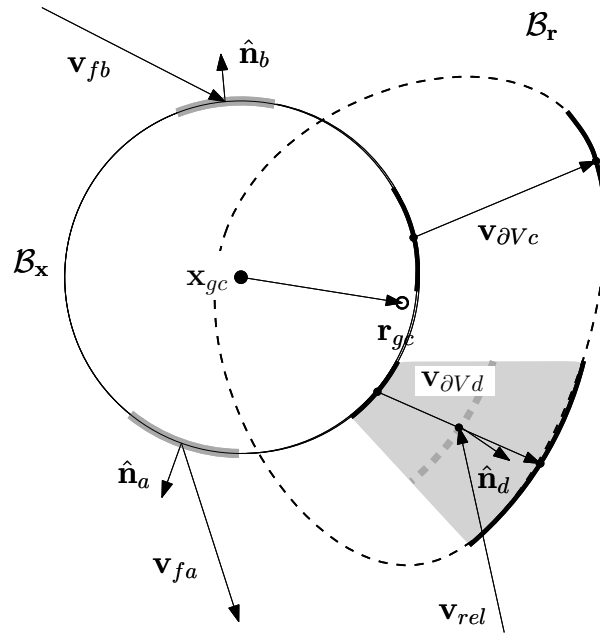


Figure 3.11: The Lagrangian-Eulerian balance principle, a combination of Reynolds transport theorem and a Eulerian control volume analysis. A domain/volume \mathcal{B}_x is deformed to \mathcal{B}_r . The velocities $\mathbf{v}_{\partial V}$ refer to the local velocity of the boundary, \mathbf{v}_f refers to the velocity of the "substance" f and the relative velocity \mathbf{v}_{rel} is defined as the difference between the velocity of the substance and the velocity of the boundary (locally).

As a final remark, in section 3.5 we derived an expression for a general boundary integral, with respect to (integer) dimension of aid in the understanding of zero boundary integrals and their representation. In the light of this discussion we conclude that the two domain variation terms appearing in Leibniz's integral rule are essentially a zero dimensional boundary integral. Consequently, this improved understanding seems to strengthen the connection between Leibniz's integral rule and Reynolds transport theorem as well as that it facilitates the connection between balance considerations in one dimension and their three dimensional counterpart.

Chapter 4

Conclusion: Where can the injected water mass go to?

4.1 Introduction: Puzzle pieces coming together.

In this chapter the results from the foregoing chapters are attributed with a hydrogeological context. In this manuscript the interest is to understand where the water mass, injected under high rate conditions into a PM, finds its "residence". In this chapter we elaborate on the possibilities where the water can go to. We will do this by applying the L-E conservation principle developed in chapter 3 to the mass of a saturated PM, viz. we will derive a L-E conservation principle for the mass of the solid phase as well as one for the water. Their combination yields the L-E conservation principle for a saturated PM. We view the application of the L-E conservation principle as the theoretical tracing of the mass of a PM.

As we stated in the introduction of this manuscript (section 1.1), in general a mass balance over an arbitrary volume dictates that the mass can be a.) stored within the PM, or b.) transported through it. In this chapter we will investigate whether we can acquire a deeper understanding regarding these two possibilities. Moreover, this is the concluding chapter of this manuscript. With the knowledge acquired from the aforementioned investigation we are in the position to give an answer on the research question posed.

In the second section of this chapter we will derive the L-E conservation principle for the mass of a PM. The programme is straightforward, we shall discuss, or interpret the integrand function, the domain of integration and the velocity terms appearing in the L-E conservation principle for each of the PM's constituent phases individually. Finally we will combine them and discuss how the two phases interact kinematically. In the third and final section of this chapter, and hence of this manuscript as a whole, we will discuss some identified weak spots in this manuscript, i.e. we debate some questionable assumptions. Subsequently we will present our final conclusion of this manuscript, viz. we will answer the posed research question in the light of the conducted research. Finally we will end this manuscript with our advice for future research in aid of understanding the phenomenon of high rate water mass injection within a saturated PM, with the focus on the steps we believe will lead to the construction of a successful lab experiment.

4.2 The Lagrangian-Eulerian mass balance over an infinitesimal portion of a porous medium.

4.2.1 Introduction: From a change in integral value to a change in mass.

In this section we will apply the rather abstract Lagrangian-Eulerian (L-E) balance principle obtained in chapter 3 to the physical quantity of mass, the mass of a porous medium (PM). Our PM is a two phase mixture comprising a solid phase functioning as a matrix which consequently spans a void space. The other phase is liquid water, saturating the void space, see for an illustration figure 4.1.

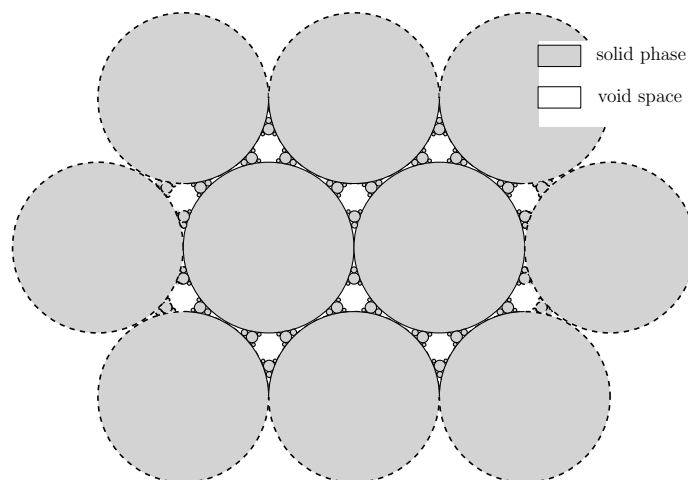


Figure 4.1: Visual interpretation of a porous medium. The dashed boundary expresses the implicit continuation of the PM.

The mass of a PM is the sum of the masses of its constituent phases, here the mass of the solid and the mass of the water,

$$m_{pm} = m_s + m_w. \quad (4.1)$$

This simple expression states that the mass balance for the PM can be considered as the linear superposition of the mass balances for the solid and the liquid phase. Consequently, in this section we will obtain the L-E balance principle expressions for the solid as well as the liquid mass and subsequently the L-E balance principle for the PM as a whole.

A mass balance principle will essentially give an answer on our question posed in the introduction (section 1.1): *"Where can the injected water mass go to?"* We have also mentioned there that a mass balance principle for a PM, e.g. the storage equation 1.1, states that the water mass can go in to storage or be transported through the PM, in the absence of water wells which may function as a source or sink. In chapter 3 we have shown that the Lagrangian-Eulerian (L-E) balance principle dictates that a quantity enclosed by a certain volume may change due to:

- | | | | |
|-----|--|---|---------------------|
| (a) | Dilatative and translational deformation of the bounding volume; | } | Boundary variation |
| (b) | A flux of the quantity crossing the volume its boundary; | | |
| (c) | Production or consumption of the quantity within the volume. | } | Integrand variation |

By applying the L-E balance principle to the solid and fluid phase their masses, enclosing the PM volume we will obtain the palette of storage and "through transport" mechanisms which theoretically can occur in a water saturated PM.

However, note that the balance principle presented here is rather "shallow" regarding mechanical considerations, the only information we can obtain from it is of kinematic nature (see figure 1.10 in subsection 1.4.2). The reason behind this is given in subsection 1.4.2, where we argued on the approach to first setup a kinematic frame, based on the believed, relative, robustness with respect to dynamic considerations.

First we will briefly discuss the definition of a density and we will define the mass density at the infinitesimal PM-/REV-scale. In other words, we will have a closer look at the meaning of the integrand function which appears in the L-E balance principle and we will discuss its application in the context of the mass of a PM. Second, we will discuss on the meaning of the flux and the boundary velocity, appearing in the L-E balance principle, in the context of a PM. Third, we shall combine these considerations with the L-E balance principle and derive a balance principle for the solid mass as well as, fourth, for the liquid mass. We will conclude, fifth, with combining the balance principles for the masses of the solid and liquid phase to obtain the L-E balance principle for a PM.

4.2.2 Mass integrals for a water saturated porous medium.

In chapter 3 we spoke of an integrand function f and the corresponding value for an arbitrary dimensional integral,

$$F = \int_V f dV. \quad (4.2)$$

Mathematically and physically, the function f can be referred to as a density. The more general mathematical definition, typically appearing in measure theory is beyond the scope of this manuscript. In physics a density ρ_F is a limiting ratio of a physical quantity F over its enclosing volume, with the limit approaching an infinitesimal volume dV . In continuum mechanics, this infinitesimal limit is the "extrapolated limit" with the infinitesimal volume being a representative volume (p. 20 and p. 68 in [13], p. 5 in [12] and section 2.2-2.3 in [42]). Thus,

$$\rho_F = \lim_{V \rightarrow dV} \frac{F}{V}. \quad (4.3)$$

A visual interpretation of the extrapolated limit is given in figure 4.2.

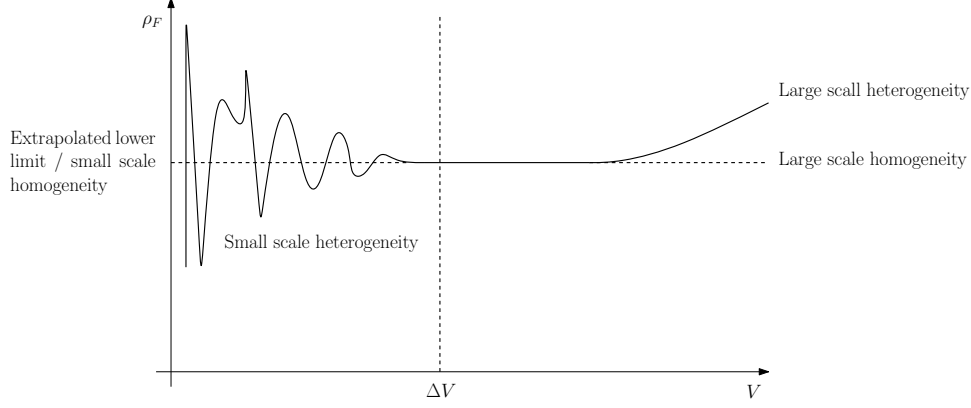


Figure 4.2: The physical definition of a density, redrawn after p. 5 in [12] and p. 17 in [13].

Subsequently, we can define a spatial average density as,

$$\langle \rho_F \rangle_V = \frac{F}{V} = \frac{1}{V} \int_V \rho_F dV. \quad (4.4)$$

In these equations ρ_F is simply a more specific integrand function f , i.e. we equipped the abstract function f with a physical meaning. In case that the physical quantity F is mass m , we obtain,

$$\rho_m = \lim_{V \rightarrow \Delta V} \frac{m}{V}, \quad (4.5)$$

and,

$$\langle \rho_m \rangle_V = \frac{m}{V} = \frac{1}{V} \int_V \rho_m dV. \quad (4.6)$$

As noted in the former subsection, we imagine a PM occupying a volume V_{pm} . Let the volume being occupied by a solid and a liquid water phase,

$$V_{pm} = V_s + V_w. \quad (4.7)$$

The solid mass enclosed by V_s is $m_s(V_s(t), t)$. We regard it as the value of the integral,

$$m_s(V_s(t), t) = \int_{V_s(t)} \rho_s(\mathbf{x}, t) dV, \quad (4.8)$$

with ρ_s being the solid mass density.

Of interest in this manuscript are phenomena which manifest themselves at the scale of a PM as opposed to the scale of its constituents. Hence, smaller scale phenomena at the level of the PM its constituents we neglect: "we will integrate with respect to dV_{pm} ". We assume dV_{pm} to be a representative elementary volume (REV). Elaborating on the concept of an REV is beyond the scope of this manuscript, we would like to refer the interested reader to e.g. p. [13] (p. 15), [12] (p. 4) as well as [42] (section 2.2-3) for an explanation in a rather intuitive manner, and to [9] for a more theoretical explanation.

In the light of the conceptualization of measuring a physical quantity (e.g. see p. 208 in [85] or p. 1 in [111]), the idea is that our physical quantities of interest are "measured" at the scale of δV_{pm} and hence are average values over δV_{pm} . In following Hassanizadeh ([51]), we can rewrite equation 4.8 to match this view by using the distribution function (section 3.5 for more information) and obtain,

$$\begin{aligned} m_s(V_{pm}(t), t) &= \int_{V_s(t)} \rho_s(\mathbf{x}, t) dV = \int_{V_{pm}(t)} \left[\frac{1}{\delta V_{pm}} \int_{\delta V_{pm}(t)} \rho_s(\mathbf{x}, t) \gamma_s(\mathbf{x}, t) dV \right] dV, \\ &= \int_{V_{pm}(t)} \rho_b(\mathbf{x}, t) dV. \end{aligned} \quad (4.9)$$

In this equation ρ_b is the average of ρ_s over the domain δV_{pm} , also referred to as the (dry) bulk density. An alternative, slightly more informative, representation can be obtained by multiplying by "one",

$$\int_{V_{pm}(t)} \left[\frac{\delta V_s}{\delta V_{pm}} \frac{1}{\delta V_s} \int_{\delta V_{pm}(t)} \rho_s(\mathbf{x}, t) \gamma_s(\mathbf{x}, t) dV \right] dV, = \int_{V_{pm}(t)} \phi_s \langle \rho_s(\mathbf{x}, t) \rangle_{\delta V_s} dV_{pm}, \quad (4.10)$$

which puts forward,

$$\rho_b = \phi_s \langle \rho_s \rangle_{\delta V_s}. \quad (4.11)$$

In these equations ϕ_s is the volume fraction of the solid phase, defined in equation 4.10 as,

$$\phi_s = \frac{\delta V_s}{\delta V_{pm}}. \quad (4.12)$$

The representation on the right hand side of expression 4.11 we will adopt for the scope of this manuscript. For convenience we will drop the "average brackets" and consider it to be understood that ρ_s is the average of the solid mass density at the scale of dV_s , which we can infer from measuring ϕ_s and ρ_b at the scale of dV_{pm} . Thus,

$$m_s(V_{pm}(t), t) = \int_{V_{pm}(t)} \phi_s(\mathbf{x}, t) \rho_s(\mathbf{x}, t) dV \quad (4.13)$$

In a similar vein we can write the water mass m_w enclosed by the volume V_w as an integral over the smallest scales,

$$m_w(V_w(t), t) = \int_{V_w(t)} \rho_w(\mathbf{x}, t) dV, \quad (4.14)$$

as well as over the smallest PM scales, of interest here,

$$m_w(V_{pm}(t), t) = \int_{V_{pm}(t)} \phi_w(\mathbf{x}, t) \rho_w(\mathbf{x}, t) dV. \quad (4.15)$$

Recall the volume balance, equation 4.7. Dividing by V_{pm} and reordering yields,

$$\langle \phi \rangle = \frac{V_v}{V_{pm}} = 1 - \frac{V_s}{V_{pm}} = 1 - \langle \phi_s \rangle, \quad (4.16)$$

a relation between the solid volume and the void volume fraction. The volume fractions can be interpreted, in following the above, as average volumetric densities, e.g. for the void volume we have,

$$\phi = \lim_{V_{pm} \rightarrow \delta V_{pm}} \frac{V_v}{V_{pm}}, \quad (4.17)$$

which is known as the volumetric porosity. In this manuscript we consider a saturated PM. Hence, in the light of our definition of ϕ , we can set ϕ_w equal to ϕ . Consequently, equation 4.16 can be interpreted as the relation between the volume fractions of water and the solid phase. Note, the volume fractions are essentially scale artefacts.

4.2.3 Boundary velocity and solid flux velocity: A two velocity description of the evolution of the solid mass.

The boundary of our PM ∂V_{pm} may be some fictitious demarcation, which defines our area of focus or control volume (e.g. see p. 184 in [42]). Alternatively, we can let the boundary of the PM be defined quasi-physically, i.e. being an actual material boundary. Since the solid phase functions as the matrix of the PM, we can argue that its external boundary, or the convex hull of the solid phase is the boundary of the PM and hence defines the volume of the PM, V_{pm} . In figure 4.3 we illustrated this idea for a volume dV_{pm} .

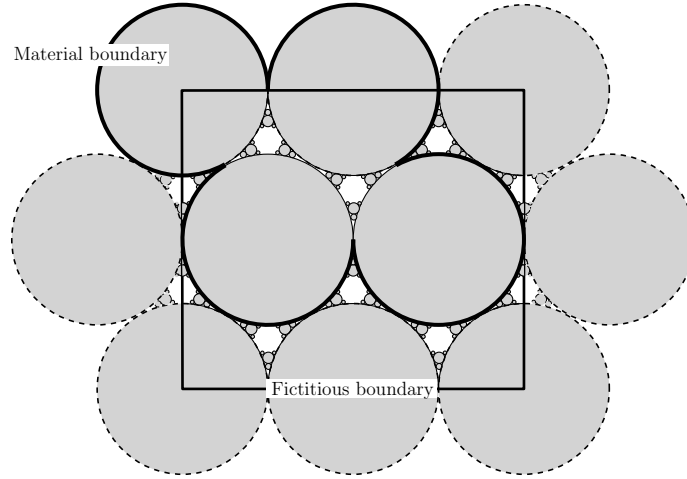


Figure 4.3: A porous medium with a rectangular demarcation, which we interpret as a fictitious boundary, and a demarcation following some of the grains, which we view as a material boundary.

We can refine the solid matrix, which we denote by the set of material points M , and view it as the union of a backbone, or (morphological) skeleton, referred to by the subset S , and a residual matrix M_{res} . Thus,

$$M = S \cup M_{res}. \quad (4.18)$$

See figure 4.4 for a visual interpretation. We interpretate S and M_{res} by analogy with the game Jenga. Jenga is game in which one initially has a tower/stack construed from wooden blocks [105]:

"The blocks are stacked in levels of three placed next to each other along their long sides and at a right angle to the previous level.... Jenga consists of taking one block on a turn from any level of the tower (except the one below an incomplete top level),"

As long as the skeleton of the stack of blocks remains intact, the tower will not collapse and the convex hull spanned by it remains intact. In other words, the shape/volume of the tower is maintained. However, blocks which do not belong to the skeleton may be removed, and we regard them as belonging to the residual matrix M_{res} .

Within the context of the solid matrix of a PM, M_{res} is that part of the solid mass which may be transported in or out of V_{pm} , defined by the convex hull of S , without that the shape of V_{pm} changes, at least approximately (see figure 4.4). However, the porosity ϕ defined for V_{pm} can change. Whenever V_{pm} changes, the skeleton spanning V_{pm} deforms. In the light of the infinitesimal strain assumption, this means that V_{pm} dilatates (see figure 4.4).

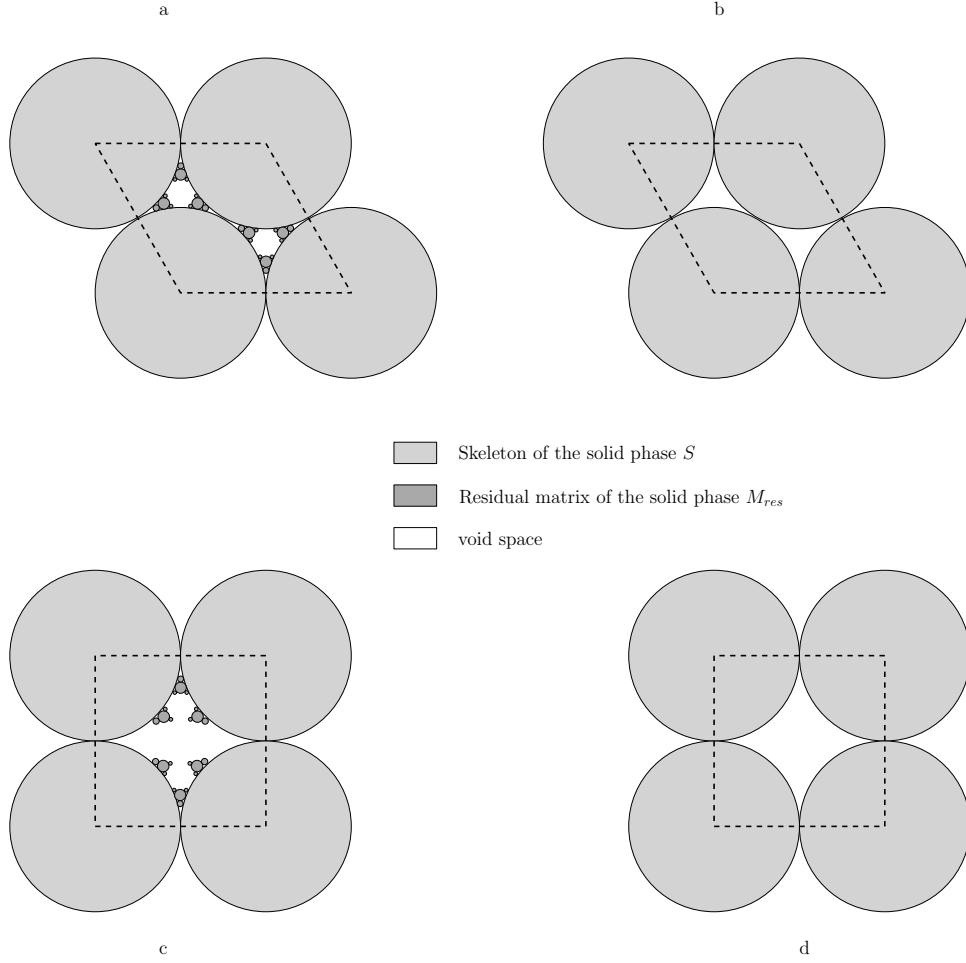


Figure 4.4: The solid matrix of a porous medium: a.) demarcation of the skeleton S and the residual matrix M_{res} ; b.) the porous medium after the M_{res} flushed away; c.) solely deformation of S , from a hexagonal to a square packing, or "from a parallelogram to a cube"; d.) the porous medium after the deformation of S and the M_{res} being flushed away.

The velocities of the particles making up the skeleton $S \subset M$ we associate with the velocity of the boundary of the PM volume, which we denote by $\mathbf{v}_{\partial V}$. The velocities of the particles giving rise to the residual matrix $M_{res} \subset M$ we interpret as the "absolute" flux velocity \mathbf{v}_s (see section 3.6). Further, we can associate the average velocity of S with the volume average velocity and attribute it to the geometric center. We refer to this average velocity by \mathbf{v}_{gc} and it captures the advection of the PM volume.

As illustrated in figure 4.4, we can abstract the solid matrix, for mathematical convenience, to a parallelogram in two dimensions. However, let us consider a three dimensional abstraction of the analogous rhombohedral packing and cubic packing, which is a parallelepiped. From subsection 3.3.5 we know that we can express the parallelepiped mathematically by,

$$V = \Delta x_c [\Delta x_a \Delta x_b \sin(\gamma_{ab})] \cos(\gamma_{c(ab)}) = \Delta \mathbf{x}_c \cdot \Delta \mathbf{x}_a \otimes \Delta \mathbf{x}_b. \quad (4.19)$$

In subsection 3.3.6 we derived an expression for the deformation of a parallelepiped shaped volume. We founded the expression on a local linear approximation to the relative displacement of the difference vectors spanning the volume. The expression underlies four important assumptions:

- 1.) the integrand and displacement field vary continuously and smoothly¹;
- 2.) the integrand and displacement field vary slowly (infinitesimal strain assumption);

¹A prerequisite for the valid application Taylors' theorem and therefore the local linear approximation.

- 3.) the mutual direction of the spanning vectors remains conserved (local admissibility assumption)
- 4.) the displacement field is stationary.

After some algebraic manipulations by means of two vector identities we obtained an expression relating an (relatively) undeformed volume $V_{\mathbf{x}}$ to its deformed counterpart $V_{\mathbf{r}}$ by the determinant of the deformation gradient tensor $|\underline{\mathbf{F}}|$,

$$\underbrace{\Delta \mathbf{r}_c \cdot \Delta \mathbf{r}_a \otimes \Delta \mathbf{r}_b}_{V_{\mathbf{r}}} \approx \underbrace{|\underline{\boldsymbol{\delta}} + \text{grad } \mathbf{u}|}_{|\underline{\mathbf{F}}|} \underbrace{\Delta \mathbf{x}_c \cdot \Delta \mathbf{x}_a \otimes \Delta \mathbf{x}_b}_{V_{\mathbf{x}}}. \quad (4.20)$$

Subsequently we have an expression which provides a clear physical interpretation of the determinant of the deformation gradient (e.g. see p. 83 [8]),

$$\frac{V_{\mathbf{r}}}{V_{\mathbf{x}}} \approx |\underline{\mathbf{F}}|. \quad (4.21)$$

Thus, $|\underline{\mathbf{F}}|$ is the first order approximation to the ratio of a volume prior to deformation over the same volume after the deformation and hence can be interpret as measuring the dilatation of the volume.

For infinitesimal volumes the first order approximations, equation 4.20 and 4.21, become exact, which yields,

$$dV_{\mathbf{r}} = |\underline{\mathbf{F}}| dV_{\mathbf{x}}, \quad (4.22)$$

and,

$$\frac{dV_{\mathbf{r}}}{dV_{\mathbf{x}}} = |\underline{\mathbf{F}}|. \quad (4.23)$$

Note, the left hand side of the latter expression should not be interpret as a derivative term.

An implication of the infinitesimal strain assumption is that the determinant of the deformation gradient can be approximated as (see subsection 3.3.8),

$$|\underline{\mathbf{F}}| \approx (1 + \text{div } \mathbf{u}). \quad (4.24)$$

With this result, we can write equation 4.21 and 4.22 as respectively,

$$\frac{\Delta V}{V_{\mathbf{x}}} \approx \text{div } [\mathbf{u}], \quad (4.25)$$

and

$$\frac{d(dV)}{dV_{\mathbf{x}}} = \text{div } [\mathbf{u}]. \quad (4.26)$$

Physically, these expressions state that the divergence of a displacement field can be interpreted as the relative/normalized change in volume as a result of the deformation.

To describe the kinematics of a fluid we are interest in the strain rate. The reason for it is roughly that a fluid when in motion deforms continuously and the displacements become to large to keep track off. Hence, measuring the strain per time makes the description more tractable. To obtain the analogous expressions for 4.22 and 4.26 in terms of the strain rate², as dictated by equation 2.57 in subsection 2.3.5 we can take the "material" time derivative of these two equations.

Thus, for equation 4.22 we have,

$$\frac{d}{dt} (dV_{\mathbf{r}}) = \frac{d}{dt} (|\underline{\mathbf{F}}|) dV_{\mathbf{x}}. \quad (4.27)$$

In which we "assumed" that the prior volume is relatively fixed with respect to the posterior volume.

The derivative of the determinant of the deformation gradient is given by (e.g. see p. 84 in [8] or p. 175 in [21]) as,

$$\frac{d}{dt} (|\underline{\mathbf{F}}|) = \frac{d}{dt} (\text{div } [\mathbf{u}]) |\underline{\mathbf{F}}|. \quad (4.28)$$

²We immediately pursue the description at the infinitesimal level since the finite level can be obtained in a similar manner and the infinitesimal level is of actual interest in this chapter.

In subsection 2.3.5 we argued that the displacement gradient is independent of the "travel time" t , which we interpreted, for clarity, as a "different time" than the time associated with the possible evolution of the displacement field. Hence, we may interchange the gradient with the time derivative. Consequently, we can obtain an expression for the evolution of the posterior volume,

$$\frac{d}{dt} (dV_r) = \text{div} [\mathbf{v}] |\mathbf{E}| dV_x. \quad (4.29)$$

By imposing the infinitesimal strain assumption ($\text{grad } \mathbf{u} \ll 1$), according to equation 4.24, we can rewrite the last expression as,

$$\frac{d}{dt} (dV_r) = \text{div} [\mathbf{v}] (1 + \text{div} [\mathbf{u}]) dV_x = \left(\text{div} [\mathbf{v}] + \underbrace{\text{div} [\mathbf{v}] \text{div} [\mathbf{u}]}_{\approx 0} \right) dV_x \approx \text{div} [\mathbf{v}] dV_x. \quad (4.30)$$

Analogous to the interpretation of equation 4.26, this equation is often used to attribute the divergence of a velocity field with a physical interpretation, namely as the relative rate of change of a volume, or the relative rate of dilatation (e.g. p. 296 in [76], p. 30 [62] or p. 73 [13]),

$$\frac{1}{dV_x} \frac{d}{dt} (dV_r) \approx \text{div} [\mathbf{v}]. \quad (4.31)$$

From the discussion in section 2.3 on the deformation of a parallelepiped, we may say that the variation of the boundary/skeleton velocity with respect to the velocity of the geometric center is captured by the gradient of the boundary velocity. However, in the light of the considerations above, equation 4.31, we can state that whenever the divergence of the boundary velocities is non-zero the PM volume dilatates, i.e.,

$$\text{div} [\mathbf{v}_{\partial V}] \approx \frac{1}{dV_{pm,x}} \frac{d}{dt} dV_{pm,r}. \quad (4.32)$$

In other words, the relevant variation of the boundary velocity is governed by the divergence. Note, in general we do not expect a PM to actual advect, i.e. a V_{gc} can be merely associated as a side effect of a dilatation whenever the V_{pm} is severely anisotropically squeezed or expanded.

As long as the relative velocity of the surface flux with respect to the velocity of the boundary $\mathbf{v}_{rel} = \mathbf{v}_s - \mathbf{v}_{\partial V}$ is non zero, then solid material may diffuse away from V_{pm} or concentrate within it. We are not necessarily interested in the actual fate of the particles comprising M_{res} . Hence, they may be conveniently viewed from an Eulerian observational perspective. In contrast we are interested in the fate of the particles of the set S and therefore a Lagrangian attitude towards them suits. Note, this is actually (tacitly) assumed in the derivation of the Lagrangian-Eulerian balance principle in chapter 3, or actually one can argue that we defined the Lagrangian and Eulerian observational perspectives as such.

4.2.4 The Lagrangian-Eulerian balance principle for the solid mass.

Consider the mass of the solid of a PM, in integral form defined over the scale of dV_{pm} , i.e.,

$$m_s(V_{pm}(t), t) = \int_{V_{pm}(t)} \phi_s(\mathbf{x}, t) \rho_s(\mathbf{x}, t) dV_{pm}. \quad (4.33)$$

The time rate of change of the mass is,

$$\frac{d}{dt} (m_s(V_{pm}(t), t)) = \frac{d}{dt} \int_{V_{pm}(t)} \phi_s(\mathbf{x}, t) \rho_s(\mathbf{x}, t) dV_{pm}. \quad (4.34)$$

In chapter 3 we developed the mathematical tool to deal with the rate of change of the value of the integral and based on it we formulated a L-E conservation principle. The L-E principle describes, *the rate of change of the value of the integral per infinitesimal portion of the domain is due to explicit time variation of the integrand and translational as well as dilatational deformation of the domain of integration as a result of a stationary displacement field.*

Applying the L-E conservation principle to the mass of solids of a PM per dV_{pm} , yields the differential equation,

$$\frac{\partial}{\partial t} (\phi_s \rho_s) = -\text{div} [\phi_s \rho_s \mathbf{v}_{rel}] - \text{div} [\phi_s \rho_s \mathbf{v}_{\partial V}]. \quad (4.35)$$

Mathematically, for this equation to be valid the fields ϕ_s , ρ_s , \mathbf{v}_{rel} and $\mathbf{v}_{\partial V}$ should be continuous, smooth and slowly varying, at least in space (see chapter 3 for details). The rough physical image this equation describes is that of an infinitesimal PM which is an open system, with respect to solid mass, with a deformable domain. As a consequence of the assumptions of slowly varying fields, the deformations which can affect m_s are translations as well as dilatations. In principle, the space in which the PM resides is in global mechanical equilibrium, i.e. the velocity fields are stationary or they instantaneously adjust to a new mechanical equilibrium, when perturbed.

More specific, the first term at the right hand side is the flux of solid mass crossing the boundary of the PM and the second term accounts for the variation in the domain of the PM. We defined in section 3.4 the product of the variables within the flux term essentially as a time averaged value, defined over the course of the possible domain variation. In addition, regarding the domain variation, or boundary variation we assumed a stationary displacement-rate field and hence a constant boundary velocity, at least over the course of the deformation (see section 3.3). Alternatively it can be thought of as a time averaged value.

We noted in the prior subsection that the solid mass functions as a matrix M and that we can define the physical boundary of a PM to be the convex hull of the skeleton S of this matrix. As a result we associated the boundary velocity $\mathbf{v}_{\partial V}$ with the solid mass velocities over the skeleton and the relative velocity \mathbf{v}_{rel} with the solid mass velocities over the residual matrix M_{res} . The residual portion of the mass may change due to that solid mass diffuses away or concentrate around this skeleton.

Through the product rule for differentiation we can expand equation 4.35 and separate effects due to variations in the density of the solid mass as well as the solid volume fraction. This yields,

$$\rho_s \frac{\partial \phi_s}{\partial t} + \phi_s \frac{\partial \rho_s}{\partial t} = -\rho_s \cdot \text{div} [\phi_s \mathbf{v}_{rel,s}] - \phi_s \mathbf{v}_{rel,s} \cdot \text{grad} [\rho_s] - \rho_s \mathbf{v}_{\partial V} \cdot \text{grad} [\phi_s] - \phi_s \mathbf{v}_{\partial V} \cdot \text{grad} [\rho_s] - \phi_s \rho_s \text{div} [\mathbf{v}_{\partial V}]. \quad (4.36)$$

Recall that $\mathbf{v}_{rel,s}$ is defined as $\mathbf{v}_{rel,s} = \mathbf{v}_s - \mathbf{v}_{\partial V}$, in which we interpret \mathbf{v}_s as the velocity of the solid phase in general.

By combining the two density gradient terms and in addition through using the definition of the total derivative, we can rewrite this last equation as,

$$\begin{aligned} \rho_s \frac{\partial \phi_s}{\partial t} + \rho_s \mathbf{v}_{\partial V} \cdot \text{grad} [\phi_s] + \phi_s \frac{\partial \rho_s}{\partial t} + \phi_s \mathbf{v}_s \cdot \text{grad} [\rho_s] &= \rho_s \frac{d}{d_{\partial V} t} \phi_s + \phi_s \frac{d}{d_s t} \rho_s \\ &= -\rho_s \text{div} [\phi_s \mathbf{v}_{rel,s}] - \rho_s \phi_s \text{div} [\mathbf{v}_{\partial V}]. \end{aligned} \quad (4.37)$$

The subscripts of the total derivatives indicate the associated convective velocities. For the purpose of interpretation it is convenient to rewrite this expression as,

$$\frac{1}{\phi_s^\#} \frac{d}{d_{\partial V} t} \phi_s = -\frac{1}{\rho_s^\#} \frac{d}{d_s t} \rho_s - \frac{1}{\phi_s^\#} \text{div} [\phi_s \mathbf{v}_{rel,s}] - \text{div} [\mathbf{v}_{\partial V}]. \quad (4.38)$$

In the latter equation we explicated by the superscript # ("behind bars") the fact that the density and volume fraction in front of the derivatives are "fixed" values, at least relatively for the scope of a "deformation time step".

Written as such, equation 4.38 expresses three different mechanisms by which the solid volume fraction in a volume dV_{pm} can change. As a result of pairing the time partial of the solid volume fraction with the convective term proportional to the boundary velocity, the total derivative of the solid volume fraction should be interpret in a Lagrangian manner. The convective part describes the relative change in the volume fraction due to advection/translation of the PM volume. The advective velocity is considered to be a global and temporal constant, hence it is equal to the velocity of the geometric center of dV_{pm} and can be interpret as such. The local time part measures the change in volume fraction at the expense of the other possible phases enclosed by dV_{pm} or at the expense of the environment, surrounding this infinitesimal system.

The "expense" is explicated by the three terms on the right hand side. The total derivative of the solid-mass density describes the compressibility of the solid phase (Lagrangian in nature). In following equation

4.32 (subsection 4.2.3), the divergence of the boundary velocity term we interpret in a Lagrangian manner and hence it reflects the dilatation of dV_{pm} , as a result of the dilatation of the skeleton of the solid matrix (solid phase itself being incompressible). The divergence of the product of the volume fraction and the relative velocity can be viewed as an Eulerian term describing the average incompressible solid mass flux crossing the boundary of dV_{pm} , for the scope of a possible deformation. For an illustration of these interpretative considerations see figure 4.5.

Note, in case the relative velocity is zero, i.e. there is no flux of solid mass crossing the boundary, as well as the solid phase itself is incompressible, equation 4.35 reduces to equation 8.42 mentioned on p. 185 in [42].

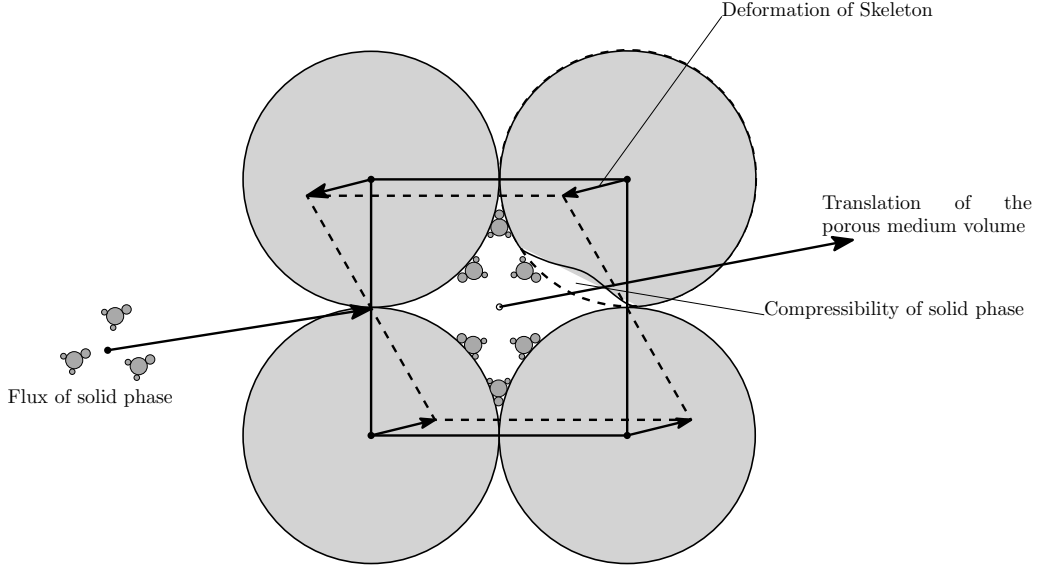


Figure 4.5: A visual interpretation of the Lagrangian-Eulerian balance principle applied to the solid phase of a porous medium. The figure describes the different contributions to a change in the solid volume fraction enclosed by a volume of porous medium.

4.2.5 The Lagrangian-Eulerian balance principle for the liquid mass.

In roughly the same manner like for the solid mass, we can apply the L-E conservation principle to the water mass in a PM. For that we define the water mass integral at the scale dV_{pm} as,

$$m_w(V_{pm}(t), t) = \int_{V_{pm}(t)} \phi_w \rho_w(\mathbf{x}, t) dV_{pm}, \quad (4.39)$$

and the rate of change of the water mass as,

$$\frac{d}{dt}(m_w(V_{pm}(t), t)) = \frac{d}{dt} \int_{V_{pm}(t)} \phi_w(\mathbf{x}, t) \rho_w(\mathbf{x}, t) dV_{pm}. \quad (4.40)$$

Note, we deal in this manuscript with a water saturated PM, hence we can set ϕ_w equal to the porosity ϕ .

Consequently, the L-E balance principle for the water mass over an infinitesimal PM volume dV_{pm} can be written as,

$$\frac{\partial}{\partial t} \phi \rho_w = -\text{div}[\phi \rho_w \mathbf{v}_{rel,w}] - \text{div}[\phi \rho_w \mathbf{v}_{\partial V}]. \quad (4.41)$$

In turn, we can interpret the first term on the right hand side as the time averaged water mass flux crossing the boundary of the PM. In the two former subsections (4.2.3 and 4.2.4) we related the boundary to the solid material making up the skeleton of the PM. Therefore the relative velocity is defined as, $\mathbf{v}_{rel,w} = \mathbf{v}_w - \mathbf{v}_{\partial V}$, the diffusive water-velocity.

In contrast to the balance principle for the solid mass, we interpret the second term as describing the variation of the domain of the water phase dV_w , for the scope of dV_{pm} . In other words, the boundary velocity in the second term describes the velocity of the boundary of the water volume enclosed by the PM. Since we deal with a saturated PM, which we tacitly assumed to be saturated at all times, the boundary velocity of the water phase can be interpreted as the velocity of the solid-water interface \mathbf{v}_{ws} . To explicate this interpretation we write equation 4.41 as,

$$\frac{\partial}{\partial t} \phi \rho_w = -\text{div} [\phi \rho_w \mathbf{v}_{rel,w}] - \text{div} [\phi \rho_w \mathbf{v}_{ws}]. \quad (4.42)$$

We can rewrite the latter equation, like we did for the solid phase balance principle, by employing the product rule for differentiation, the definition of the total derivative and combining the two density gradient terms, which yields,

$$\begin{aligned} \rho_w \frac{\partial}{\partial t} \phi + \rho_w \mathbf{v}_{ws} \cdot \text{grad} [\phi] + \phi \frac{\partial}{\partial t} \rho_w + \phi \mathbf{v}_w \cdot \text{grad} [\rho_w] &= \rho_w \frac{d}{d_{ws}t} \phi + \phi \frac{d}{d_wt} \rho_w \\ &= -\rho_w \text{div} [\phi \mathbf{v}_{rel,w}] - \phi \rho_w \text{div} [\mathbf{v}_{ws}]. \end{aligned} \quad (4.43)$$

In turn, we can divide both sides by the density and the volume fraction, to obtain,

$$\frac{1}{\phi\#} \frac{d}{d_{ws}t} \phi = -\frac{1}{\rho_w\#} \frac{d}{d_wt} \rho_w - \frac{1}{\phi\#} \text{div} [\phi \mathbf{v}_{rel,w}] - \text{div} [\mathbf{v}_{ws}]. \quad (4.44)$$

Just like in equation 4.38, # explicates a relatively fixed value.

The last equation states that the total change in the porosity of dV_{pm} is governed by three different mechanisms. The total derivative of the porosity can be interpreted in a Lagrangian manner. Its convective part describes the change in the porosity due to a translation of the water volume, for the scope of the dV_{pm} . The advective velocity is considered to be a global and temporal constant. If there is actual variation over the volume, then it can be interpreted as a volume averaged velocity. In both cases it can be associated with the geometric center of the water volume present in dV_{pm} . Recall, we deal with a PM which is saturated at all times. As a result, this velocity is equal to the volume averaged velocity of the solid phase, i.e. for the scope of the PM volume $\mathbf{v}_{ws} = \mathbf{v}_s$. In case that the solid phase and the void space are well mixed, as a result also the solid phase and the saturating water are well mixed. Consequently, the geometric center of the solid phase and the fluid phase enclosed within dV_{pm} fall together and the velocities are not only equal in magnitude and direction, they can be also interpreted as "acting" on the same position. The well mixed assumption is implied by the supposition that dV_{pm} is an REV (see subsection 4.2.2).

The local time part of the total derivative of the porosity describes the change at the expense of the other possible phases enclosed within dV_{pm} , here solely the solid phase, as well as indirectly due to dilatation of the dV_{pm} . In turn, this "expense" is explicated by the three terms on the right hand side of equation 4.44. The total derivative of the water mass density describes the compressibility of the water phase (Lagrangian nature). The divergence of the velocity of the water-solid interface can be viewed as the dilatation of the solid matrix as well as the solid phase and the corresponding internal flow of water to maintain a saturated PM (Lagrangian nature). In line with the above discussion, we can consider \mathbf{v}_{ws} as \mathbf{v}_s although in that case the term should be multiplied by minus one (opposite "direction" of the normal vector at the water-solid interface). The divergence of the product of the porosity and the relative velocity can be interpreted as an Eulerian term describing the average flux of incompressible water crossing the boundary of the PM. For an illustration of these interpretative considerations see figure 4.6.

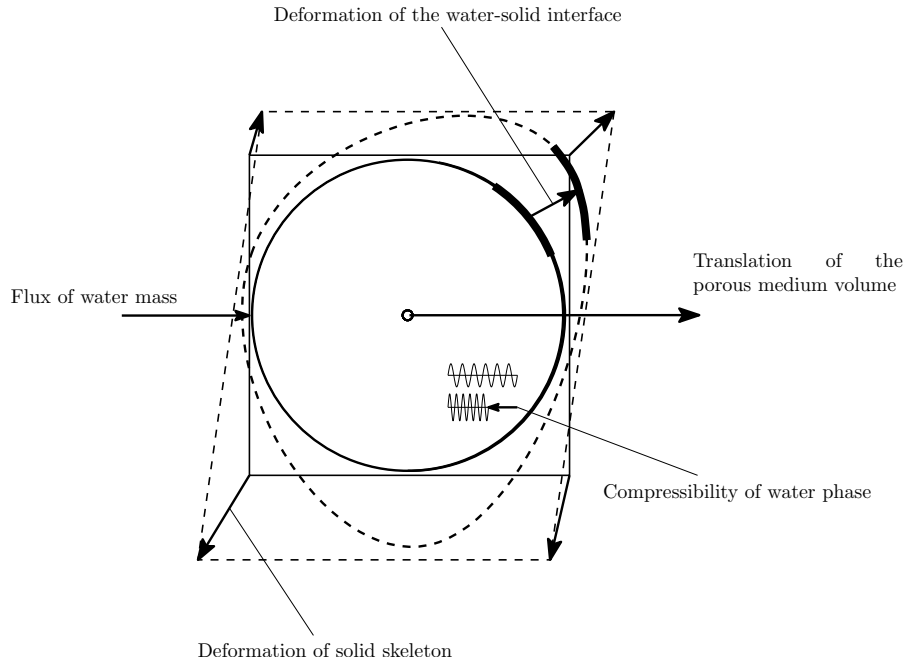


Figure 4.6: A visual interpretation of the Lagrangian-Eulerian balance principle applied to the water mass of a porous medium. The figure describes the different contributions to a change in the (saturated) porosity of the porous medium. The bounding parallelograms are analogous to the parallelograms in figure 4.5, they explicate the deformation of the PM due to the dilatation of the solid skeleton. The round shapes reflect the water mass volume ("balloon"). The solid lines indicate undeformed volumes and the dashed lines deformed volumes.

4.2.6 Conclusion: The Lagrangian-Eulerian balance principle for the mass of a porous medium.

In the previous subsections we applied the Lagrangian-Eulerian (L-E) conservation principle to an infinitesimal porous medium (PM) volume, comprising 1.) a solid phase spanning a matrix and 2.) water saturating the resulting void space. In the subsections 4.2.2 and 4.2.3 we paved the ground by attributing the fundamental mathematical constituents with a physical interpretation. In the former subsection we discussed the role of the integrand function as a physical density defined over a representative elementary volume (REV). Consequently, very brief, volume averaging was brought to the attention and put forward additional parameters, volume fractions, which we denoted as scale artefacts. These volume fractions are of major importance since they explicate the (kinematic) coupling between the solid and the water phase at the scale of averaging, here the REV. In the latter subsection we considered the meaning of the boundary and the flux velocity in case of the solid phase. We discussed fictitious and material boundaries as well as the relation between dilatation and the divergence of a velocity. The latter can be established when adopting a Lagrangian "particle conservative" view.

In the following two subsections 4.2.4 and 4.2.5 the pieces were put together and we obtained two L-E mass conservation principles, one for each constituent phase of the PM. The equations we interpreted with the relative change in volume fraction being central. Consequently, each conservation principle put forward explicitly four possible mechanisms which could cause the volume fraction to change with time (explicitly), in general,

- a.) a Lagrangian term describing the translation of the bounding volume of the phase;
- b.) a Lagrangian term describing the incompressible contribution to the deformation of the bounding volume of the phase;
- c.) a Lagrangian term describing the compressibility of the phase;
- d.) an Eulerian term describing the mass flux of the phase crossing the boundary of the PM boundary.

In the light of chapter 3, mathematically speaking, the first pair governs the domain variation and the second pair the integrand variation.

We associated the boundary of the PM with the material boundary spanned by the skeleton of the solid matrix, i.e. the convex hull of the skeleton. This volume is also (mathematically) an upper bound, bounding the solid phase constituent of the PM. For the water phase, since it saturates the PM, we interpret the boundary as the solid-water interface and the boundary velocity accordingly. The boundary of the PM is also an upper bound for the water phase. Moreover, the essential difference between the boundary considered explicitly in the solid mass conservation principle is that it bounds the PM mixture, whereas the boundary in the water mass conservation principle bounds the actual water phase (it is the least upper bound, e.g. see p. 44 in [7]). Less abstract, we interpret the water volume as a balloon which cannot extend beyond the boundaries of the PM.

In the introduction of this chapter we stated that the mass of the water saturated PM is,

$$m_{pm} = m_s + m_w. \quad (4.45)$$

The local time rate of m_{pm} , in integral form can therefore be written as (see subsection 4.2.2 and section 3.6),

$$\int_{V_{pm}(t)} \frac{\partial}{\partial t} \rho_{pm} dV_{pm} = \int_{V_{pm}(t)} \frac{\partial}{\partial t} \phi_s \rho_s dV_{pm} + \int_{V_{pm}(t)} \frac{\partial}{\partial t} \phi_w \rho_w dV_{pm}. \quad (4.46)$$

Note, the void space is saturated by the water phase, therefore the volume fraction is equal to the porosity, $\phi_w = \phi$. Adopting this, the rate of change of the mass enclosed by an infinitesimal PM volume can be written as,

$$\frac{\partial}{\partial t} \rho_{pm} = \frac{\partial}{\partial t} \phi_s \rho_s + \frac{\partial}{\partial t} \phi \rho_w. \quad (4.47)$$

The two terms on the right hand side can be refined by employing the L-E conservation principle, i.e. substituting equation 4.35 and 4.41 in the latter expression (see chapter 3, subsection 4.2.4 and 4.2.5), which yields,

$$\begin{aligned} \frac{\partial}{\partial t} \phi_s \rho_s + \frac{\partial}{\partial t} \phi \rho_w &= -\text{div} [\phi_s \rho_s \mathbf{v}_{rel,s}] - \text{div} [\phi_s \rho_s \mathbf{v}_{\partial V}] \\ &\quad - \text{div} [\phi \rho_w \mathbf{v}_{rel,w}] - \text{div} [\phi \rho_w \mathbf{v}_{ws}]. \end{aligned} \quad (4.48)$$

We have shown that each of the two L-E conservation principles can be written after employing some algebraic manipulations, in a "volume fraction centred" form, given respectively by (equation 4.38 and 4.44),

$$\frac{1}{\phi_s^\#} \frac{d}{d\partial V t} \phi_s = -\frac{1}{\rho_s^\#} \frac{d}{d_s t} \rho_s - \frac{1}{\phi_s^\#} \text{div} [\phi_s \mathbf{v}_{rel,s}] - \text{div} [\mathbf{v}_{\partial V}], \quad (4.49)$$

and,

$$\frac{1}{\phi^\#} \frac{d}{d_w s t} \phi = -\frac{1}{\rho_w^\#} \frac{d}{d_w t} \rho_w - \frac{1}{\phi^\#} \text{div} [\phi \mathbf{v}_{rel,w}] - \text{div} [\mathbf{v}_{ws}]. \quad (4.50)$$

The solid phase and the water, for the scope of dV_{pm} , are explicitly coupled in two manners, a.) through the porosity as explicated by equation 4.16, and b.) by means of the water-solid interface velocity \mathbf{v}_{ws} . The porosity is related to the solid volume fraction as $\phi_s = 1 - \phi$. Substituting this in to the former equation yields,

$$-\frac{d}{d\partial V t} \phi = -\frac{(1 - \phi^\#)}{\rho_s^\#} \frac{d}{d_s t} \rho_s - \text{div} [(1 - \phi) \mathbf{v}_{rel,s}] - (1 - \phi^\#) \text{div} [\mathbf{v}_{\partial V}]. \quad (4.51)$$

Since we deal with a PM which we assume to be saturated at all times, we noted in subsection 4.2.5 that for the total derivative of the porosity in 4.50 $\mathbf{v}_{ws} = \mathbf{v}_s$, for the scope of dV_{pm} . However, in general it seems that this should be an approximation, which follows from inspecting the corresponding divergence term of the water-solid interface velocity. The approximation is there due to that \mathbf{v}_{ws} entails a contribution due to the motion of the solid phase and one due to compressing the solid phase. Which implies that when the solid phase is incompressible $\mathbf{v}_{ws} = \mathbf{v}_s$. Currently we want to retain the solid phase compressibility, therefore our approximation is founded on the assumption that the contribution to the interface velocity due to the compressibility of the solid phase is very small in comparison to \mathbf{v}_s . Note, this velocity \mathbf{v}_s differs from the solid flux velocity crossing the boundary of dV_{pm} , it describes the velocity within dV_{pm} of the water solid interface which, by definition, will not reach beyond dV_{pm} , i.e.

for the duration of a deformation step this velocity is smaller or equal to $\mathbf{v}_{\partial V}$. In subsection 4.2.2, 4.2.4 and 4.2.5, the integrals are with respect to the integrands dV_{pm} . This means that we do not care about the convective details within dV_{pm} if they do not manifest themselves at the scale of dV_{pm} . In other words, we are only interested in that part of the water-solid interface which forms part of the boundary of dV_{pm} , although strictly speaking this is the water-”environment” interface. Hence, \mathbf{v}_{ws} can be interpret as being equal to the velocity of the skeleton $\mathbf{v}_{\partial V}$, which dictates the boundary velocity of the dV_{pm} as a whole. Remark, this interpretation refrains us from having to worry about the validity of the former ”relative magnitude of the velocity” assumption. By invoking these considerations on equation 4.50 we will obtain,

$$\frac{d}{d\partial V t} \phi = -\frac{\phi^\#}{\rho_w^\#} \frac{d}{d_w t} \rho_w - \text{div} [\phi \mathbf{v}_{rel,w}] - \phi^\# \text{div} [\mathbf{v}_{\partial V}]. \quad (4.52)$$

The latter two equations are symmetrical to equations 4.49 and 4.50 respectively. Hence, we can simply add them as dictated by 4.45 to obtain an expression for the evolution of the mass of a PM, i.e.,

$$0 = -\frac{(1-\phi^\#)}{\rho_s^\#} \frac{d}{d_s t} \rho_s - \frac{\phi^\#}{\rho_w^\#} \frac{d}{d_w t} \rho_w - \text{div} [(1-\phi) \mathbf{v}_{rel,s}] - \text{div} [\phi \mathbf{v}_{rel,w}] - (1-\phi^\#) \text{div} [\mathbf{v}_{\partial V}] - \phi^\# \text{div} [\mathbf{v}_{\partial V}]. \quad (4.53)$$

The two last terms can be taken together and form the whole boundary of dV_{pm} ,

$$0 = -\frac{(1-\phi^\#)}{\rho_s^\#} \frac{d}{d_s t} \rho_s - \frac{\phi^\#}{\rho_w^\#} \frac{d}{d_w t} \rho_w - \text{div} [\mathbf{v}_{\partial V}] - \text{div} [(1-\phi) \mathbf{v}_{rel,s}] - \text{div} [\phi \mathbf{v}_{rel,w}]. \quad (4.54)$$

This last equation is a general L-E conservation principle for the mass of a PM, the objective of this section. It states the five kinematic processes which a PM can be subjected to, which manifest themselves at the scale of dV_{pm} , with the roman numerals referring to the respective term in 4.62,

- | | | |
|---|---|---------------------|
| I. Compressibility of the solid phase, | } | Storage processes |
| II. Compressibility of the water, | | |
| III. Compressibility of the porous medium its skeleton, | | |
| IV. Flux of solid mass entering the porous medium, | } | Transport processes |
| V. Flux of water mass entering the porous medium. | | |

Recall equation 4.32 from subsection 4.2.3, the general relation stating that under infinitesimal strain-ing conditions we can write the divergence of the boundary velocity of the PM as, $\frac{1}{dV_{pm}^\#} \frac{d}{dt} dV_{pm}$, which explixates its compressibility interpretation. Substituting this expression into equation 4.62 yields the variant,

$$0 = -\frac{(1-\phi^\#)}{\rho_s^\#} \frac{d}{d_s t} \rho_s - \frac{\phi^\#}{\rho_w^\#} \frac{d}{d_w t} \rho_w - \frac{1}{V_{pm}^\#} \frac{d}{dt} dV_{pm} - \text{div} [(1-\phi) \mathbf{v}_{rel,s}] - \text{div} [\phi \mathbf{v}_{rel,w}]. \quad (4.55)$$

Note, equation 4.62 can be written more compact by expanding the relative velocities, the flux terms, which are defined as $\mathbf{v}_{rel,w} = \mathbf{v}_w - \mathbf{v}_{\partial V}$ and $\mathbf{v}_{rel,s} = \mathbf{v}_s - \mathbf{v}_{\partial V}$. This yields,

$$0 = -\frac{(1-\phi^\#)}{\rho_s^\#} \frac{d}{d_s t} \rho_s - \frac{\phi^\#}{\rho_w^\#} \frac{d}{d_w t} \rho_w - \text{div} [\phi (\mathbf{v}_w - \mathbf{v}_s)] - \text{div} [\mathbf{v}_s]. \quad (4.56)$$

Although more compact, it seems to come at a cost of being more obscure and less of use in this manuscript, among others since Darcy’s law for creep flow through a PM essentially describes the flow of water relative to the solid skeleton (e.g. see p. 185 in [42], p. 204 in [13] or section 4 in [16]). Hence, we will not pursue it further.

In the specific case that the solid phase is incompressible as well as that there is no flux of solid material equation 4.62 reduces to,

$$0 = -\frac{\phi^\#}{\rho_w^\#} \frac{d}{d_w t} \rho_w - \text{div} [\mathbf{v}_{\partial V}] - \text{div} [\phi \mathbf{v}_{rel,w}], \quad (4.57)$$

which is practically equal to equation 6.3.19 on p. 205 in [13]. In the definition of the total derivative of the density of the water. This is a minor conceptual difference which we believe does not alter the physics.

4.3 Discussion, conclusion and advice on future research.

4.3.1 Discussion: On the validity of three adopted assumptions.

In this manuscript we presented the results of our research towards an as general as possible set of kinematic processes which can occur in a porous medium (PM). This set can then be employed in a process of elimination for to be of aid in the understanding of how high rate water mass injections can be facilitated by a PM. The original idea was to design an experiment to simulate the high rate water mass injection within a PM in the lab. In the light of the scarcity of the available data we concluded that this was beyond the scope of this thesis. Though, we kept this idea in mind and geared this research towards it. Moreover, the process of elimination can be in the form of lab experiments.

However, before we draw our final conclusion of this manuscript, three issues remained which we recognized as being susceptible of (relative) considerable debate and we will discuss first, briefly. The issues are: 1.) the validity of the approach we adopted; 2.) the validity of the separability of the well subsystem from the porous medium system; 3.) the computational value of our resulting differential equation describing the kinematic processes.

Regarding the first issue, the main statement we believe is questionable is the conclusion we have inferred, that we were inhibited from developing a decent experimental design due to the scarcity of the current available data. This seems to be mainly on the grounds of a difference in philosophy ("engineering" versus "scientific") and expertise as mentioned in subsection 1.4.2. We argued up on our lack of expertise, which we believe is crucial for an engineering approach. Especially since the experts in the field we were in contact with suggested that this phenomenon of high rate water mass injections is rather extraordinary, at least within hydrogeological practice and in specific the dewatering industry. Consequently we adopted the "scientific" philosophy within a classical physical paradigm. Moreover, our believe is that from classical physics we can reveal the workings of the phenomenon. Within the scope of the physical fields of fluid mechanics and deformation mechanics we thrived to be like a map maker: unfolding the possibilities/combinatorics which can occur at a certain "depth". The optimal depth we believed to be manageable was the kinematic level (see subsection 1.4.2).

Partly this was motivated by that both fields, fluid and deformation mechanics, have their common ground in kinematics. Another important consideration was the knowledge that the research on this phenomenon would continue. Our believe was that a robust research with less "risk" would be favourable within the whole scope of the research towards the phenomenon, of which this manuscript is, at best, only a small "cogwheel", though we hope one which one can rely on.

With the knowledge we have acquired now we are more confident in adopting an engineering philosophy. In particular the considerations which led to the deterministic kinematic model in chapter two we regard of great value. Among others, it provides the vocabulary to reason qualitatively regarding the dissipation of energy and hence the dynamics of a system. Moreover, it clarified our view regarding deformation mechanisms and fluid flow patterns. Although, unfortunately, it turned out to be beyond the scope of this manuscript to cash in on this acquired knowledge. Nevertheless, it has been of great aid in section 1.3 where we construed the conceptual model of the phenomenon of high rate water mass injection by means of a JSI system. Among others, it strengthened our believe that the relevant flow pattern within the affected PM is laminar, though of Forchheimer type.

The second issue is related to two major assumptions we made in this manuscript which we believe are open to debate and require additional research. We invoked them within the introduction for the purpose of narrowing down the scope of this manuscript to a tractable extend. It are a.) the relevance of the well casing interaction with the porous medium, as well as b.) that a quasi static approach would enclose the scope of seismic wave phenomena. We argued on their validity based on a literature research, within a field in which we are not comfortable: Acoustic logging and underlying the theory of seismology. Especially the latter we are uncertain about, with respect to the phenomenon of wave interference as well as resonance and their extend of influence. Moreover, can wave interference and resonance cause an initiated seismic wave to grow? However, it seems that crucial for stating anything about these two assumptions, is knowledge about the source frequency which initiates a wave phenomenon. We are not aware of any knowledge regarding a possible frequency and we are also not aware of deliberately initiating wave phenomena within the JSI methodology. When the second assumption is valid, seismic wave phenomena can be considered as a refinement of our developed framework of kinematic processes. This line of thought seems to be essentially the one followed by Biot (e.g. see [16] or p. 71 in [121]) and

roughly comprises taking in account explicitly transient effects (an "asymmetrical" refinement affecting the accuracy though revealing smaller time-scale phenomena) and further rewriting the displacement or velocity field by means of a Helmholtz decomposition (a symmetrical refinement affecting the precision). The Helmholtz decomposition let one to untangle the displacement or velocity field in a scalar potential contribution and a vector potential contribution. The first describing an irrotational vector field and the latter an divergence free (incompressible) vector field (e.g. see p. 85 in [12]).

The third and final issue is related to computational power of our developed Lagrangian-Eulerian mass balance. Its main power at the moment is of qualitative nature. However, eventually to be of use for the dewatering industry it is also desired to have a quantitative value. At the moment the solid flux term inhibits the equation to be of computational use. In other words, we are not aware of a constitutive equation by which the solid flux term can be transformed to be of quantitative value. Unlike the other terms in the equation which can be enriched, at least as a first approximation, with Darcy's law for the water flux term and Hooke's law for the compressibility terms. This seems to suggests that in order to assess the importance of the solid mass flux lab experiments are invaluable.

Further this manuscript is built around a mathematical framework. It hinges on common mathematical assumptions which render the validity of differential calculus and more specific the application of the Navier-Stokes equation to describe fluid flow and the Navier's equation to govern solid deformation, which we therefore do not question. In addition we padded the framework with interpretations/conceptualizations. However, we do not believe that any of them would destabilize the mathematical frame and the physical processes they describe. They are mere for a matter of perspective and may be of aid in understanding. However, it can be of use to remark that within experiments (lab or numerical) one might be unable to achieve the precision required to analyse the results with infinitesimal strain based theories. In that case, one may consider to explore the use of finite strain theories.

4.3.2 Conclusion: A porous medium has six elementary kinematic processes at hand to facilitate high rate water injections.

This manuscript is on the phenomenon of high rate water mass injection within a saturated porous medium (PM). Within this context we put forward in the introduction (section 1.1) the research question,

Where can the injected water mass go to?

We also stated their our rough vision, the water can go in to storage within the PM and/or it can be transported through it. We based this on the "storage equation" (equation 1.1), a well known theoretical result in hydrogeology.

Through mathematical considerations on kinematics, the fundamental theorem of deformation kinematics in chapter 2 and Reynolds transport theorem in chapter 3, we construed a Lagrangian-Eulerian (L-E) balance principle. The fundamental theorem of deformation kinematics has been in great aid in improving our understanding regarding the balance principles encountered in the literature. Moreover, we conclude that we got considerably closer to what Reynolds transport theorem essentially describes. Notable, Reynolds theorem does not describe explicitly rotative and shear straining patterns. The reason for it are the assumptions that the displacement field varies slowly, the infinitesimal strain assumption, as well as the local admissibility assumption. This latter assumption states that the mutual direction of the configuration between objects should be conserved, viz. a material cannot deform to the extend that it penetrates itself. The local admissibility assumption seems to us to be a corollary of the infinitesimal strain assumption. Besides this, it also did not pop up explicitly in our generalization of Leibniz's integral rule to three dimensional domains. It emerged when we established the connection between the three dimensional variant of the integral rule to Reynolds transport theorem. As a result we conclude that the infinitesimal strain assumption is likely of greater importance. The two assumptions together put us in the position to approximate the determinant of the deformation gradient tensor, which governs absolutely continuous deformation, as "one plus the divergence of the displacement field" (see subsection 3.3.8),

$$|\underline{\mathbf{F}}| \approx 1 + \text{div} [\mathbf{u}]. \quad (4.58)$$

The "one" is related to translational motion and the divergence to the dilatative deformation. In the context of Reynolds transport theorem, the assumptions are responsible for the "divergence of the displacement" term.

The rigorous derivation of Reynolds transport theorem let us to the insight just mentioned, the "domain" deformations it accounts for explicitly. In addition, viewing this theorem as a generalization of Leibniz's integral rule let us also conclude that Reynolds theorem essentially describes integrand variation and domain variation, no flux across the boundary. It seems to us that this interpretation is merely based on symmetry in mathematical form regarding the domain variation and the flux term, heuristic in nature. We conceptualized the flux term as a refinement of the integrand variation (see section 3.4), inferred from figure 3.1 based on physical considerations. As a result we ended up with the relatively simple form of the Lagrangian-Eulerian mass balance principle.

In subsection ?? we have shown that the L-E balance principle is a more general variant of the conservation principle mentioned by Bear ([13], section 4.2). The L-E principle fits more accurately our suggested conceptualization (see section 3.1 and subsection 4.2.5) of the water volume enclosed by a PM as a balloon, i.e. a deformable control volume, which is most clear in case of partly saturated PMs in which one can notice changes in the water table. Though, from our discussion presented in section 4.2 the L-E principle seems to be capable of refining the interaction between the solid phase and the water and how it can lead to changes in the porosity of the PM. In other words, the L-E principle seems to be also of value in conceptualizing a saturated PM. At a more abstract level, our main conclusion with respect to the L-E balance principle is, that it provides us with a more complete, physical realistic, mathematical tool to describe the change in a quantity within a domain. Moreover, we do not necessarily have to choose between a Lagrangian particle tracking approach or an Eulerian fixed control volume approach up front, they naturally merge together. This renders a pure Eulerian (fixed control volume) or else Lagrangian (particle tracking) approach as specific cases of the L-E balance principle.

Applying the L-E balance principle to the mass of a saturated PM, can be viewed as "theoretically tracing the mass of the PM". We traced the mass of the solid phase and the water under global mechanical equilibrium as implied by the stationary displacement field and neglected the presence of sources or sinks. Moreover, we considered in this theoretical experiment its more specific conserved variant. The result of applying the L-E conservation principle to the PM mass is the following differential equation (see subsection 4.2.6),

$$0 = -\frac{(1-\phi^\#)}{\rho_s^\#} \frac{d}{d_s t} \rho_s - \frac{\phi^\#}{\rho_w^\#} \frac{d}{d_w t} \rho_w - \text{div} [\mathbf{v}_{\partial V}] - \text{div} [(1-\phi)\mathbf{v}_{rel,s}] - \text{div} [\phi\mathbf{v}_{rel,w}]. \quad (4.59)$$

This equation explicates five kinematic processes which can occur within a PM, with the roman numerals referring to the respective terms,

- | | | |
|---|---|---------------------|
| <ul style="list-style-type: none"> I. Compressibility of the solid phase, II. Compressibility of the water, III. Compressibility of the porous medium its skeleton, IV. Flux of solid mass entering the porous medium, V. Flux of water mass entering the porous medium. | } | Storage processes |
| <ul style="list-style-type: none"> IV. Flux of solid mass entering the porous medium, V. Flux of water mass entering the porous medium. | } | Transport processes |

From this theoretical "experiment" we conclude that the L-E principle provides us with more realistic possible options regarding the kinematic processes which can occur within a PM as compared with the balance principle presented by Bear ([13], section 4.2). This balance principle is either employed, fundamentally, Lagrangian in nature or else Eulerian in nature. Roughly, the former variant is employed when compressibility is of interest and the latter when fluxes are of interest. The evolution of the mass of the solid phase of a PM is typically described by the Lagrangian variant and the evolution of the water mass by the Eulerian variant. However, in our opinion it leads to messy derivations of the mass balance for a PM, due to switching of observational perspectives, in comparison with the application of the L-E balance principle. Especially regarding the compressibility processes. In addition, in derivations of storage equations, based on Bear's balance principle, the possibility of a solid mass flux is neglected.

Finally, we are in the position to give an answer on the posed question. Based on the L-E mass conservation principle applied to the mass of a PM, we conclude that the injected water mass can go either in to storage or be transported through it. Moreover, we can refine these possibilities in to five different variants, three compressibility processes and two flux processes can occur in general. In addition, based on the discussion in chapter one of this manuscript we conclude that there is a sixth process which can be scheduled under the transport processes and its occurrence depends on the well subsystem, or its geometry: the process of geometric spreading. It did not reveal itself from our mathematical derivation,

which is simply due to that we considered rectangular coordinates as opposed to cylindrical or polar coordinates in which the process will emerge naturally.

Being able to answer the research question put us also in the position to refine the conceptual model, figure 1.8 in subsection 1.3.7. We can refine the possible instantaneous deformation mechanisms by accounting explicitly for the compressibility processes as well as a solid mass flux.

It is of importance to remark that we did not concern ourselves in this manuscript with the relative contributions of each process or whether they actually occur or not. These processes we regard as possible and their actual manifestation depends on the context. However, this can be assessed whenever desired by a process of elimination, whether by lab experiment or by working out theoretically the implications of more specific settings due to dynamical considerations. However, we are not aware of a constitutive equation which facilitates the computation of an estimate of the solid mass flux, which may inhibit further theoretical progress. Unlike the other processes, which rely in a basic sense on Darcy's law for creep flow through a PM and Hooke's law for a linear elastic description of compressibility.

Further we would like to note that we suggested in this manuscript to redefine the notion of "high rate" in to "high entrance velocity", about which we concluded that it is less susceptible of ambiguity as discussed in subsection 1.3.2. As a final note, a rough estimate is made on the expected flow pattern as a result of a high rate injection (high entrance velocity) in subsection 1.3.5, based on the Reynolds number for a gravel aquifer. From the resulting value we concluded that it is possible to inject water under high rate conditions as such that the flow pattern within the PM is "close to laminar creep flow".

4.3.3 Future research: steps which can be taken to obtain a robust experimental design.

4.3.3.1 Intro: Two main requirements for a design of an experiment.

The aim of this manuscript is to be of aid in the understanding of the phenomenon of high rate water mass injections in to a saturated aquifer, in the specific practical context of the Jet Suction Infiltration (JSI) methodology as employed in the dewatering industry. The origin of this manuscript was the request for an experimental setup, for the purpose of simulating the field setting of a JSI system in the lab. Roughly, for such a design, at least the theoretical part, we recognized two things to be of major interest:

- 1.) knowledge of maximum extend regarding spatial and pressure scales; and
- 2.) the possible kinematic processes which can occur.

With respect to both topics we concluded initially that we were not able to distil, from the available literature on the JSI methodology, enough information to design a robust experimental setup (see subsection 1.4.2). In other words, a setup of which we were confident that it would have the desired accuracy to capture the phenomenon and hence that it would only be a matter of tweaking the precision in order to succeed in the simulation of the phenomenon.

At the moment we believe that this manuscript has sufficiently covered the second interest. Through the application of a Lagrangian-Eulerian conservation principle to the mass of a porous medium we have theoretically traced the mass of the solid phase and the water, which resulted in five different kinematic processes: the three compressibility processes for respectively the solid-phase, the water and the skeleton of the (solid) matrix, as well as two flux processes, one for the solid phase and the other describing the water flux. We mentioned that if this analysis would have been employed within a cylindrical or polar coordinate system an additional kinematic processes would emerge explicitly, namely geometric spreading.

Consequently, if it is true that both two mentioned interests would lead to a robust experimental design, then successful future research to the scales at which the JSI system operates will result in a theoretical design for the the requested experimental setup. In the following we will briefly sketch our thoughts for a research regarding the scales of interest and consequently we shall outline a set of simple experimental scenarios of which we think that they have the potential to explain the phenomenon of high rate water injections in to a PM in the context of the JSI methodology.

Note, in this manuscript we have considered a confined saturated aquifer/PM. In the considerations we will present below it will be no different.

4.3.3.2 On investigating the scales at which a JSI system operates.

As mentioned in subsection 1.4.2, an experimental design can be considered to be framed by three kinds of similarity considerations: 1.) geometric similarity 2.) kinematic similarity, and 3.) dynamic similarity. We noted that kinematic similarity can be viewed roughly as the glue between the two other kinds and may be used to infer gaps in the knowledge concerning the other two. In subsection 1.3.2 we noted that "high rate" is improperly defined by solely a well yield value. Well screen characteristics are important and together they result in to proper kinematic conditions which characterizes the phenomenon of high rate water mass injection within a PM: the entrance velocity. The entrance velocity is central piece of information around which we will structure our advice for future research geared towards an experimental setup to investigate the JSI methodology. In the light of geometric spreading, it seems to be the highest flow velocity possibly to occur within a PM (see subsection 1.3.2). The considerations given below can be viewed to be underlain by the question: how to obtain the relevant extremal scales from the entrance velocity?

Let us start with dynamic considerations. Darcy's law is a simple and therefore intuitive law relating the discharge from a PM to the required pressure gradient. Its main shortcoming of being valid only in a very narrow scope with respect the flow patterns which can exist in a PM can be partly overcome, regarding conceptualization, by knowledge of how the pressure gradient varies with respect to discharge, in the context of the Reynolds number. For example see the schematic curve on p. 177 of [13] which can also be found in subsection 1.3.5 of this manuscript.

Darcy's law can be expressed as,

$$\mathbf{v} = \frac{\mathbf{K}}{\phi \rho_w g} \text{grad}[p], \quad (4.60)$$

with \mathbf{K} being the hydraulic conductivity tensor, ϕ the porosity, ρ_w the density of the water, g the gravitational constant, p the hydrostatic water pressure and \mathbf{v} the average flow velocity of the water over the PM.

In subsection 1.3.5 we have discussed that Darcy's law describes a laminar creep flow pattern over a PM, which is at the lower end of possible flow patterns, with respect to energy dissipation. In other words, according to Helmholtz dissipation theorem, for a given discharge a creep flow pattern requires the smallest pressure gradient relative to other flow patterns since it uses the available pressure energy optimally. In contrast, one can induce from kinematics (see subsection 1.3.5) that a turbulent flow pattern would require the highest pressure gradient, for the same PM, to achieve the same flow velocity. This trend is clearly shown in the pressure gradient versus discharge curve in subsection 1.3.5 and well known in hydrogeology.

Consequently, for a given undeformable PM, the maximum pressure gradient is related to a turbulent flow pattern over a PM. The pressure gradient provides the pressure difference and hence dictates the maximum pressures that can possibly occur for a given PM. Here the trouble starts, since it is not easy to quantify turbulent flow patterns over porous media. There are different approaches mentioned in the literature on quantifying turbulent flow patterns. In our opinion the best theoretical (rigorous) approach we are aware of is the theory proposed by Pedras in a series of articles [88, 89] and a book [71]. The theory is built on the Navier-Stokes equation and he derives from it through a double decomposition approach a general PM-scale variant of it, with Darcy's law as a specific case. However, the shortcoming of this theory is that it requires a reasonable study to construe from it, if possible, a numerical model and consequently to be of actual use for designing the experimental setup. Nevertheless its qualitative power we regard as invaluable. There are also more practical approaches available in the literature, however they come at the cost of accuracy and hence the precision they can be validly applied for. However, if one is aware of these, they can be of great value and likely be the most efficient choice for designing the experimental setup. The approaches we know of are centred around a pipe flow conceptualizations and their close relation with PM, i.e. the approach of Barr [11], Macdonald [75] or the approach of Halford [48]. The latter one is adopted in the conduit flow package compatible with MODFLOW [10].

In subsection 1.3.5 we gave a rough estimate of the flow pattern through a hypothetical PM comprising a well sorted fine gravel, based on the Reynolds number ($Re = qd\rho_w/\mu_w$) and the entrance well velocity. It predicted a Forchheimer laminar flow pattern, at the lower end of its Reynolds number spectrum, i.e. close to the creep laminar flow pattern regime.

Based on these considerations we would advise to let the Reynolds number guide in whether rigorous turbulent flow considerations are necessary or that the more practical engineering approach would likely

suffice. In case that the Reynolds number predicts a flow pattern well below the turbulent regime, we would expect that the engineering approach would be acceptable. Since the entrance velocity is guiding, in the light of the Reynolds number the uncertainty lie within the values for the porosity and the (average) grain diameter.

In conclusion regarding future research, we would advice to investigate the the shortcomings of the engineering approaches as well as what the order is of the pressure drops they.

The above mentions the relevance of knowledge about porosity values and grain diameters. Whenever, one has to rely on theoretical considerations to obtain a porosity value and grain diameter Darcy's law may be in turn of value. From Darcy's law we can infer that the PM requiring the highest pressure gradient to achieve the desired flow velocity would be the one with the lowest value for the ratio of hydraulic conductivity over porosity. For convenience let us assume for the following that the PM we consider is isotropic with respect to hydraulic conductivity as well as homogeneous regarding hydraulic conductivity and porosity (volumetric).

It is well known that permeability of a PM (and hence the hydraulic conductivity) are related to some extend to the PM its porosity (e.g. see section 5.5.1 in [13] or chapter 4 in [32]). Moreover, based on the dimensional analysis of Rumpf & Gupte (see p. 159 in [32]), permeability can be regarded to be in general a function of the porosity, the shape of the grains making up the solid matrix of a PM as well as grain diameter distribution. A wide variant of relations can be found in the literature (see e.g. the brief overview in section 5.10.1 of [13] or the more extensive review in chapter 4 of [32]), each with its own shortcomings. Two rather popular permeability-porosity relations are the Kozeny-Carman equation and the Fair & Hatch formula (respectively p. 166 and p. 134 in [13]). Kozeny-Carman's equation is known to be accurate for perfect spherical grains. For the purpose of the experimental scenarios we will present below this suffices, however future research is advised on permeability-porosity relations regarding the value of this equation when eventually one wants to compare lab data with field data.

Adopting Kozeny-Carman's equation we can rewrite the ratio of hydraulic conductivity over porosity as,

$$\frac{K}{\phi} = \frac{\rho_w g}{\mu_w} \left(\frac{\phi^2}{(1-\phi)^2} \right) \left(\frac{(d_{50})^2}{180} \right). \quad (4.61)$$

From this equation we can infer that a PM, comprising spherical grains, with the smallest porosity as well as smallest grain size would yield the smallest ratio of hydraulic conductivity over porosity and hence the largest pressure gradient is required to achieve the desired flow velocity. From typical values of the porosity and diameter for soil types, listed in tables that can be found e.g. in [13, 31, 32, 54]), one can then make an estimate of the ratio and consequently of the pressure gradient/drop.

Based on the above we suggest that further research on the correlation between soil types and the successful application of the JSI methodologies is invaluable. It is of great aid for estimating pressure scales for the purpose of designing an experimental setup. Note, alternatively to the above, one can also define an upper limit of the order of the pressure difference expected by considering compressibility of the materials. Finally, in relation to pressure, it is of use to investigate how the knowledge of the order of the pressure difference can be related to horizontal stresses (within the solid), e.g. through the concept of lateral earth pressure. The reason for it is that one does not want an experimental to fail in shear.

In order to get insight in the geometric scales on which a JSI system operates we advice to investigate well equations in order to infer, at least, first approximations. Roughly, for confined aquifers, one can start with Thiem's well equation for steady state flow away or towards a fully penetrating well to obtain an idea of the lateral extend, i.e. the zone of influence of the well. Regarding Thiem's equation the zone of influence can be estimated when one knows the well discharge, the hydraulic conductivity of the aquifer, the thickness of the aquifer and the accepted "negligible drawdown" or "drawup", e.g. one per cent of the initial level of the piezometric surface. For the hydraulic conductivity one should take the largest value, e.g. for gravel aquifers. The larger the hydraulic conductivity, the lower the resistance to flow, the farther the effect of the well penetrates in to the aquifer. The main uncertainty lies within the value of D . To obtain an estimate one may investigate the statistics of the aquifers in which JSI systems are successfully installed.

In the absence of sufficient statistical data, this immediately reveals, in our current understanding, the main difficulty in the theoretical framing of an experimental setup, namely determining the vertical extend. We can think of two manners which may provide a physically based vertical scale. The first one, is in reference to the scale of the pressure difference and its hydraulic head representation. The

second option, would be to investigate the effect of vertical induced geometric spreading (see subsection 1.3.6) by a partially penetrating well. We would be interested in the thickness a confined aquifer should have, in order to initiate a vertical influence zone free from boundary effects for a partially penetrating well screen positioned at the middle (vertically). We inferred this possibility from Huisman's analytical equation for a partially penetrating well in a confined aquifer (chapter 10 in [69]).

Thus, regarding geometrical scales, as a direction for future research we would advice to investigate the analytical well equations, in particular the partially penetrating solution of Huisman.

4.3.3.3 Experimental scenarios to investigate the kinematic processes.

The experiments we have in mind, have the purpose of investigating the relevance of the six kinematic processes we have identified within this manuscript. Suppose that these six kinematic processes are the fundamental building blocks and that any other kinematic process is simply a combination of them, analogous to the three fundamental modes of motion Helmholtz fundamental theorem of deformation kinematics dictates (see chapter 2). Consider the equation we obtained, explicating five of the six identified kinematic processes,

$$0 = -\frac{(1-\phi^\#)}{\rho_s^\#} \frac{d}{d_s t} \rho_s - \frac{\phi^\#}{\rho_w^\#} \frac{d}{d_w t} \rho_w - \operatorname{div} [\mathbf{v}_\partial V] - \operatorname{div} [(1-\phi) \mathbf{v}_{rel,s}] - \operatorname{div} [\phi \mathbf{v}_{rel,w}]. \quad (4.62)$$

The equation states that the kinetic processes are (linear) superposable. Which suggests that as a first approximation we can design experimental scenarios in which each process can be investigated individually with respect to a common reference. From the experiments we may try to assert the relative extend of each processes under certain conditions, specifically the high injection rate conditions. In the best case we may conclude that not all processes are relevant for the high rate conditions and that we end up with a smaller set of kinematic processes which go through to the next round of experiments. The second set of experimental scenarios we would suggest to have the purpose to investigate combinations of the set of relevant kinematic processes on if and how they interact. Of specific interest we think is the relative contribution of the two classes of processes, storage versus transport. Our current believe is that from the understanding of the extend of the individual processes as well as their interaction, it would be a matter of finding the right combination in order to come up with an explanation for the workings of the JSI system.

Two kinematic processes can be highly questioned whether they are relevant, the compressibility of the solid phase as well as the water. However, the compressibility of water plays an important role in Wills' theory on the workings of the JSI methodology (e.g. see p. 6-7 in [127] or [126]). We would suggest to assess the relevance of these compressibility processes in a theoretical manner, by simply considering the compressibilities in the light of the expected pressure differences.

With regards to the other processes we would be interested in investigating the behaviour of a very simple PM with respect to high rate water injections, or actually entrance velocities. The simple PM we have in mind is composed of perfectly spherical grains, among others for mathematical tractability. Other shapes and their relevance can be investigates in future "future" research when desired. The flow we would propose to as the reference case would be radial flow in a confined aquifer, without deformation of the solid matrix. As such we imagine an experimental setup comprising a container which is a segment of a cylinder in which we should be able to simulate flow induced due to water injected through a fully penetrating well and which can be sealed at the top to mimic confinement (see figure 4.7 for a sketch of a possible experimental setup). Further the PM "filling" of the container should be a PM in which the grains are fixed.

Of main interest for us in the moment is the behaviour of vertical geometric spreading and the deformation of the skeleton of the PM with respect to different injection rates and relative to the sketched reference case. As such as a first estimate we are interested in how a PM composed out of uniform sized spheres behaves. For the reference case we would like to closely document the behaviour of a PM in which the spheres are fixed in the two extreme packings ([54], p. 76), 1.) a simple cubic packing, and 2.) a tetrahedral packing.

To acquire a better understanding about the process of vertical geometric spreading we hypothesise that it is of value to see how an undeformable PM behaves, the two packings of uniform spheres, when subjected to water injections at different rates through a partially penetrating screen, for different screen sizes as well as at different depths. To make it insightful we would suggest experimenting with

conservative tracers to get an idea of the zone of influence. In addition we would be interested in the spatial evolution of the flow velocity.

To investigate the deformation of the skeleton of the PM, one should relax the fixation of the grains. Inspired by the experiments of Mayer and Stowe [77], we are very interested to investigate if and how a water injection can deform a close tetrahedral packing to a simple cubic packing. As a reference case we suggest to consider first injections through a fully penetrating screen.

Subsequently we would be interested when we allow both processes to occur, i.e. injections through a partially penetrating screen, of different size and at different depths, through the loose packing of uniform spheres initially tetrahedral packed.

To investigate the kinematic process of a solid flux, we would suggest to relax the requirement of that the PM should comprise uniform spheres. In other words we think of a PM composed out of multiple sizes spheres. The reference case would in turn be fixing all the spheres in the equivalent of the simple cubic packing and tetrahedral packing, only then for multiple sizes spherical grains (e.g. see the figures in section 4.2), and subject them to water injections at different rates through a fully penetrating screen. Then, keep the spheres of the largest diameter fixed, they form an undeformable skeleton, and relax the fixation for the smaller grains and observe what happens for different rates.

We can combine the scenario for the solid flux process with the vertical geometric spreading effect by injecting the water at different depths through partially penetrating screens of different sizes. By relaxing the fixation of the largest grains we can investigate deformation of the skeleton and a possible solid flux induced by water injections through a fully penetrating screen. Finally we explore the situation in which all three processes are allowed to occur when subjecting the PM to injections, by injecting through partially penetrating screens of different sizes and at different depths.

The kinematic process of geometric spreading we personally would be most interested in. The vertically induced geometric spreading by a partially penetrating well is a rather simple process though we believe it has high potential to explain for a considerable part the workings of a JSI system. The reason for it is that it seems to be a process through which we can contain a high pressure region in a relatively small region. As a result of this localization it may explain why the JSI methodology has negligible environmental effects, which is a highly advantageous characteristic over other recharge methodologies. We suspect that the facilitation of high rate injections, i.e. entrance velocities is then a favourable combination of at least the geometric spreading and the deformation of the skeleton of a PM. The above given experimental scenarios may give considerable insight in whether these two hypothesis make sense or not.

4.3.3.4 A sketch of a possible experimental apparatus

In figure 4.7 we presented a simple sketch of the experimental apparatus we have in mind. We have no idea yet about boundary effects and as a result we have given it the shape of the segment of a cylinder. It may be of use to investigate by means of a computer model whether different sized segments, with respect to the angle, show different flow behaviour.

Roughly the apparatus consists of a container or PM system, padded on the outside by a discharge channel to mimic "endless world" conditions. The face of the container separating the PM from the discharge channel should be construed from a combination of meshes and for sake of robustness, should be adjustable regarding the mesh sizes. This in order to be able to change the PM filling of the container and be able to reduce the boundary effect induced by this interface. We require the PM container to be sealed with a rubber cap in order to mimic a confined PM.

At the point of the cylindrical segment we mimic a borehole system. We imagine that it is compatible with two kinds of "walls". One which resembles the characteristics of a fully penetrating well and one wall with openings at certain positions which can be sealed. The openings represent the different positions at which one can connect an adapter which should be able to mimic the partially penetrating well screen. Both walls are connected to a adjustable pump in order to be able to control the flow rate.

This seems to be a relatively easy setup. We anticipated that the extends can be determined theoretically as we suggested above. Alternatively, a descriptive statistical analysis of the relevant data of field settings of successful JSI applications may be of aid. In the worst case one has to rely on a trial and error approach guided by a numerical model. An obvious shortcoming of this apparatus is off course that the screen size of the partially penetrating well are limited in extend as well as the discrete positioning. A continuous positioning is undoubtedly more difficult and should require further investigations in how

to conceptualize it. However, it is relevant to investigate since one may then be able to simulate the process of locating an infiltration point.

The main measurements of interest are those of tracer concentrations and the pressure distribution. We have no idea at the moment of the influence of a piezometer configuration and it might be useful to investigate this also.

An investigation by means of a computer model on the effect of the shape of the container may be of additional interest in order to find out the capabilities of a "rectangular" flow domain. Such a container is present at the university of Utrecht and has glass walls. If it turns out to be of use one may actually see directly which kinematic processes occur.

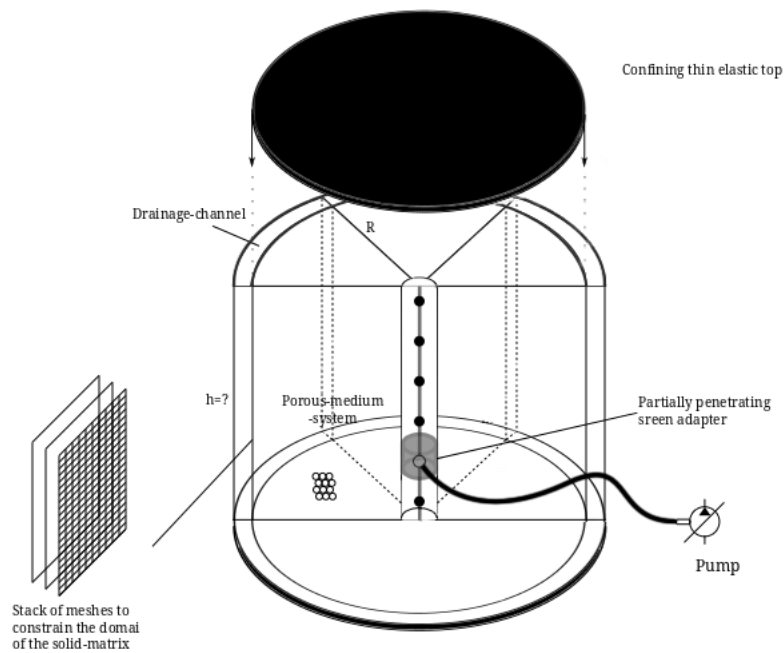


Figure 4.7: A sketch on an experimental apparatus to investigate the workings a JSI system.

Bibliography

- [1] Differential-pressure pipe sticking. PetroWiki, 2013.
- [2] Michael B. Abbott and Jens Christian Refsgaard. *distributed hydrological modelling*, volume 22. Springer Science & Business Media, 1996.
- [3] D. J. Acheson. *Elementary Fluid Dynamics*. Oxford Applied Mathematics and Computing Science Series. Oxford University Press, 2006.
- [4] K. Aki and P. G. Richards. *Quantitative Seismology*. University Science Books, 1980.
- [5] Howard Anton, Irl Bivens, and Stephens Davis. *Calculus, early transcendentals*. John Wiley & Sons, Inc, 7th edition, 2002.
- [6] T. M. Apostol. *Calculus*, volume 2. John Wiley & Sons, Inc, 1969.
- [7] Tom M. Apostol. *Calculus*, volume 1. John Wiley & Sons, Inc, 1967.
- [8] Rutherford Aris. *Vectors, tensors and the basic equations of fluid mechanics*. Dover Publications, Inc., 1962.
- [9] Y. Bachmat and J. Bear. Macroscopic modelling of transport phenomena in porous media. 1: The continuum approach. *Transport in Porous Media*, 1(3):213–240, 1986.
- [10] W. Barclay Shoemaker, Eve L. Kuniatsky, Steffen Birk, Sebastian Bauer, and Eric D. Swain. *Documentation of a conduit flow process (CFP) for MODFLOW-2005*. U.S. Geological survey, 2007.
- [11] Douglas W. Barr. Turbulent flow through porous media. *Ground Water*, 39(5):646–650, 2001.
- [12] G. K. Batchelor. *An introduction to fluid dynamics*. Cam, 1967.
- [13] Jacob Bear. *Dynamics of fluids in porous media*. Dover Publications, Inc., 1988.
- [14] M. A. Biot. Theory of propagation of elastic waves in a fluid saturated porous solid i: Low frequency range. *Journal of the Acoustical Society of America*, 28(2):168–178, 1956.
- [15] M. A. Biot. Theory of propagation of elastic waves in a fluid saturated porous solid ii: Higher frequency range. *Journal of the Acoustical Society of America*, 28(2):179–191, 1956.
- [16] Maurice A. Biot. Mechanics of deformation and acoustic propagation in porous media. *Journal of Applied Physics*, 33(4):1482–1498, 1962.
- [17] Mary L. Boas. *Mathematical methods in the physical sciences*. John Wiley & Sons, Inc, 3rd edition, 2006.
- [18] J. M. R. Bolton, M. D. & Wilson. *Structural dynamics*, chapter Soil stiffness and damping, pages 209–216. Balkema, 1990.
- [19] Rebecca Brannon. Kinematics: The mathematics of deformation. Chapter draft, December 2008.
- [20] J. Brain Cantwell. Organized motion in turbulent flow. *Annual reviews of fluid mechanics*, 13:457–515, 1981.

- [21] Eduardo W. V. Chaves. *Notes on Continuum Mechanics*. Lecture Notes on Numerical Methods in Engineering and Sciences. Springer, 2013.
- [22] Chuen Hon Cheng, M. Nafi Toksz, and Mark E. Willis. Determination of in situ attenuation from full waveform acoustic logs. *Journal of Geophysical Research*, 87(B7):5477–5484, 1982.
- [23] E. G. D. Cohen. Kinetic theory: Understanding nature through collisions. *American Journal of Physics*, 61(6):524–533, 1993.
- [24] E. R. Crain. How many acouscan dance on the head of a sonic log? *Canadian Well Logging Society*, 2004.
- [25] de la V. Cruz and T. J. T. Spanos. Thermomechanical coupling during seismic wave porpagation in a porous medium. *Journal of geophysical research*, 94(B1):637–642, 1989.
- [26] de la V. Cruz and T. J. T. Spanos. Thermodynamics of porous media. *Proceedings of the Royal Society A*, 443:247–255, 1993.
- [27] Gedeon Dagan and Shlomo P. Neuman, editors. *Subsurface flow and transport: a stochastic approach*. International hydrology series. Cambridge University Press, 1997.
- [28] Braja M. Das. *Theoretical foundation engineering*, volume 47 of *Developments in Geotechnical Engineering*. El, 1987.
- [29] Michael Davis. Avoid getting differentially stuck drilling depleted zones. *Drill Science Corp, SPE*.
- [30] Hefeng Dong and Jens M. Hovem. *Waves in Fluids and Solids*, chapter Interface Waves, pages 153–176. InTech, 2011.
- [31] Fletcher G. Driscoll. *Groundwater and Wells*. Johnson Filtration Systems Inc., 3rd printing edition, 1989.
- [32] F. A. Dullien. *Porous media, fluid transport and pore structure*. Academic Press, 1979.
- [33] Franz Durst. *Fluid Mechanics: An introduction to the theory of fluid flows*. Springer, 2008.
- [34] Maurice Dusseault, Brett Davidson, and Tim Spanos. Pressure pulsing: the ups and downs of starting a new technology. *Journal of Canadian Petroleum Technology*, 39(4), 2000.
- [35] Maurice B. Dusseault, Darrell Shand, Tor Meling, Tim Spanos, and Brett C. Davidson. Field applications of pressure pulsing in porous media. In *Poromechanics II, Proceedings of the Second Biot Conference on Poromechanics*, 2002.
- [36] Stefan Ebneith. Groundwaterpreservation using dsi-infiltration: A new approach for pipeline de-watering campains. *Wasserhaltung Brunnenbau Umwelttechnik*, 2010.
- [37] Robert Ecke. The turbulence problem: An experimentalist view. *Los Alamos Science*, (29):124–141, 2005.
- [38] Darwin V. Ellis and Julian M. Singer. *Well logging for Earth scientists*. Springer Science & Business Media, 2007.
- [39] Charles F. Fitts. *Groundwater Science*. Academic Press, 2002.
- [40] Harley Flanders. Differentiation under the integral sign. *The America Mathematical Monthly*, 80(6):615–627, 1973.
- [41] Esteban Flores-Mendez, Manuel Carbajal-Romero, Norberto Flores-Guzmn, Ricardo Snchez-Martinez, and Alejandro Rodriguez-Castellanos. Rayleigh’s, stoneley’s and scholte’s interface waves in elastic models using a boundary element method. *Journal of Applied Mathematics*, 2012.
- [42] D. J. Furbish. *Fluid Physics in Geology: An introduction to fluid motions on Earth’s surface and within its crust*. Oxford University Press, 1997.

- [43] M. B. Geilikman, T. J. T. Spanos, and E. Nyland. Porosity diffusion in fluid-saturated media. *Tectonophysics*, 217:111–115, 1993.
- [44] Herbert Goldstein, Charles Poole, and John Safko. *Classical Mechanics*. Addison Wesley, third edition edition, 2000.
- [45] W. G. Gray and P. C. Y. Lee. On the theorems for local volume averaging of multiphase systems. *International Journal for Multiphase Flow*, 3:333–340, 1977.
- [46] William G. Gray and George F. Pinder. On the relationship between the finite element and the finite difference methods. *International Journal For Numerical Methods in Engineering*, 10:893–923, 1976.
- [47] Allan Gut. *An intermediate course in probability*. Springer Texts in Statistics. Springer, 2nd edition, 2009.
- [48] K. J. Halford. Simulation and interpretation of borehole flowmeter results under laminar and turbulent flow conditions. In *Seventh International Symposium on Logging for Minerals and Geotechnical Applications*, pages 157–168, 2000.
- [49] Gang Han and Maurice B. Dusseault. Description of fluid flow around a wellbore with stress dependent porosity and permeability. *Petroleum Science & Engineering*, 40:1–16, 2003.
- [50] S. M. Hassanizadeh. High velocity flow in porous media. *Transport in Porous Media*, 2:521–531, 1987.
- [51] S. M. Hassanizadeh and William G. Gray. General conservation equations for multi-phase systems. *Advances in Water Resources*, 2:131–144, 1979.
- [52] Jasper Havik. Research into the physical processes that define the occurrence of a dsi effect. Internship report, O2DIT, 2012.
- [53] von Herman Helmholtz. On integrals of the hydrodynamic equations that correspond to vortex motions (uber integrale der hydrodynamischen gleichungen, welche der wirbelbewegung entsprechen). *J. fur die reine und angewandte Mathematik*, 55:25–55, 1858.
- [54] Daniel Hillel. *Introduction to Environmental Soil Physics*. Elsevier Academic Press, 2004.
- [55] M. Hillert and Agren J. Extremum principle for irreversible processes. *Acta Materialia*, 54:2063–2066, 2006.
- [56] M. H. Holmes. *Introduction to the foundations of applied mathematics*. Springer Science & Business Media, 2009.
- [57] Ekkehard Holzbecher, Yulan Jin, and Stefan Ebneht. Borehole pump & inject: an environmentally sound new method for groundwater lowering. *International Journal of Environmental Protection*, 1(4):53–58, 2011.
- [58] Frederick A. Howes and Stephen Whitaker. The spatial averaging theorem revisited. *Chemical Engineering Science*, 40(8):1387–1392, 1985.
- [59] M. King Hubbert and David G. Willis. Mechanics of hydraulic fracturing. *Transactions of Society of Petroleum Engineers of AIME*, 210:153–168, 1957.
- [60] H. Hlscher, S. Ebneht, M. Sauter, E. Holzbecher, and Y. Jin. Innovative dsensauginfiltration zur energieeffizienten sowie umwelt und ressourcen schonenden grundwasserabsenkung. Technical Report Phase 2, Hlscher Wasserbau GmbH, 2013.
- [61] H. Hlscher and M. Sauter. Innovative dsensauginfiltration zur energie effizienten sowie umwelt und ressourcen schonenden grundwasserabsenkung. Technical Report Phase 1, Hlscher Wasserbau GmbH, 2012.
- [62] Fridtjov Irgens. *Rheology and Non-Newtonian Fluids*. Springer, 2014.

- [63] Isao Ishibashi and Xinjian Zhang. Unified dynamic shear moduli and damping ratios of sand and clay. *Soils and foundations*, 33(1):182–191, 1993.
- [64] Slavik V. Jablan. *Theory of symmetry and ornament*. Mathematical Institute of Belgrade, electronic edition edition, 1995.
- [65] Julia A. Jackson, James P. Mehl, and Klaus K. E. Neuendorf. *Glossary of Geology*. Springer Science & Business Media, 2005.
- [66] John Conrad Jaeger, Neville G. W. Cook, and Robbert Zimmerman. *Fundamentals of Rock Mechanics*. John Wiley & Sons, Inc, 4th edition, 2007.
- [67] A. N. Kolmogorov and S. V. Fomin. *Introductory Real Analysis*. Dover Publications, Inc., 1970.
- [68] V. V. Kozlov, G. R. Grek, M. V. Litvinenko, and G. V. Kozlov. Visualization of the processes of development and turbulent breakdown of a low speed round jet. *Visualization of Mechanical Processes*, 1(2), 2011.
- [69] G. P. Kruseman and de N. A. Ridder. *Analysis and evaluation of pumping test data*, volume Publication 47. ILRI, 2nd edition edition, 1989.
- [70] Horace Lamb. *Hydrodynamics*. Cambridge University Press, 1895.
- [71] de Marcelo J. S. Lemos. *Turbulent Impinging Jets into Porous Materials*, volume SpringerBriefs in Applied Sciences and Technology of *Computational mechanics*. Springer, 2012.
- [72] William F. Lichtler, David I. Stannard, and Edwin Kouma. Investigation of artificial recharge of aquifers in nebraska. Technical report, U.S. Geological Survey, Water Resources Division, 1980.
- [73] William Lowrie. *Fundamentals of Geophysics*. Cambridge University Press, 2007.
- [74] Volkert Lubbers. Innovatieve methode voor retourbemalen voorkomt bouwvertraging. *Fugro Info*, (1):1–9, 2010.
- [75] I. F. Macdonald, M. S. El-Sayed, K. Mow, and F. A. Dullien. Flow through porous media — the ergun equation revisited. *Industrial & Engineering Chemistry Fundamentals*, 18(3):199–208, 1979.
- [76] Jerrold E. Marsden and Anthony J. Tromba. *Vector Calculus*. Freeman, 5th edition, 2003.
- [77] Raymond P. Mayer and Robert A. Stowe. Mercury porosimetry — breakthrough pressure for penetration between packed spheres. *Journal of Colloid Science*, 20:893–911, 1965.
- [78] Radoslaw L. Michalowski. Coefficient of earth pressure at rest. *Journal of geotechnical and geoenvironmental engineering*, pages 1429–1433, 2005.
- [79] Gerard V. Middleton and Peter R. Wilcock. *Mechanics in the Earth and Environmental Sciences*. Cambridge University Press, 1999.
- [80] Thomas J. Miller. *ASR in Wisconsin Using the Cambrian-Ordovician Aquifer*. Technology & Engineering. American Water Works Association, 2001.
- [81] Phoolendra K. Mishra and Kristopher L. Kuhlman. Unconfined aquifer flow theory — from dupuit to present. *arXiv:1304.3987v1 [physics.flu-dyn]*, 2013.
- [82] S. P. Neuman. Theory of flow in unconfined aquifers considering delayed response of the water table. *Water Resources Research*, 8(4):1031–1045, 1972.
- [83] F. L. Paillet and C. H. Cheng. *Acoustic waves in boreholes*. CRC Press, 1991.
- [84] F. L. Paillet, C. H. Cheng, and W. D. Pennington. Acoustic waveform logging — advances in theory and application. *The Log Analyst*, pages 7–44, May 1992.
- [85] Athanasios Papoulis. *Probability, random variables, and stochastic processes*. McGraw-Hill Inc., 1991.

- [86] s Park Seismic. What are seismic waves? Web page.
- [87] Linus Pauling. *General Chemistry*. Dover Publications, Inc., 1988.
- [88] Marcos H. J. Pedras and de Marcelo J. S. Lemos. On the definition of turbulent kinetic energy for flow in porous media. *International Communications in Heat and Mass Transfer*, 27(2):211–220, 2000.
- [89] Marcos H. J. Pedras and de Marcelo J. S. Lemos. Macroscopic turbulence modeling for incompressible flow through undeformable porous media. *International Journal of Heat and Mass Transfer*, 44:1081–1093, 2001.
- [90] A. E. Perry and M. S. Chong. On the mechanism of wall turbulence. *Journal of fluid mechanics*, 119:173–217, 1982.
- [91] Thirapong Pipatpongsa, Sokbil Heng, Atsushi Iizuka, and Hideki Ohta. Rationale for coefficient of earth pressure at rest derived from prismatic sand heap. *Journal of Applied Mechanics*, 12:383–394, 2009.
- [92] Paolo Podio-Guidugli. *A primer in Elasticity*. Springer Science & Business Media, 2000.
- [93] J. Patrick Powers, Arthur B. Corwin, Paul C. Schmall, and Walter E. Kaeck. *Construction dewatering and groundwater control: New methods and applications*. John Wiley & Sons, Inc, 2007.
- [94] M. Rahrah. Modeling interactions between turbulence induced mechanical vibrations and subsurface flow of water. Master’s thesis, Delft Institute of Applied Mathematics, 2012.
- [95] Dieter Rauch. Seismic interface waves in coastal waters: a review. Technical report, SACLANT-CEN, 1980.
- [96] J. W. Rayleigh. *The theory of sound*, volume Volume 1. MacMillan and Co., 1877.
- [97] Harold G. Reading, editor. *Sedimentary Environments: Processes, facies and stratigraphy*. John Wiley & Sons, Inc, 3 edition, 2009.
- [98] J. N. Reddy. *An introduction to continuum mechanics: With applications*. Cambridge University Press, 2008.
- [99] Wan Renpu. *Advanced well completion engineering*. Elsevier, 3rd edition, 2011.
- [100] Joe Rosen. *Symmetry Rules: How Science and Nature are founded on Symmetry*. Springer Berlin Heidelberg, 2008.
- [101] J. S. Rowlinson and B. Widom. *Molecular Theory of Capilarity*. Dover Publications, Inc., 4th edition, 2002.
- [102] G. Robello Samuel. *Formulas and calculations for Drilling operations*. Scrivener Publishing, 2010.
- [103] Florian Scheck. *Mechanics, from Newton’s laws to deterministic chaos*. Springer, 5th edition edition, 2010.
- [104] Meinhard T. Schobeiri. *Fluid mechanics for engineers*. Springer, 2010.
- [105] Leslie Scott. The game jenga.
- [106] Zekai Sen. *Applied hydrogeology for Scientists and Engineers*. CRC Press, 1995.
- [107] P. M. Shearer. *Introduction to seismology*. Cambridge University Press, 1999.
- [108] J. C. Slattery. Flow of viscoelastic fluids through porous media. *AIChE Journal*, 13:1066–1072, 1967.
- [109] Roel Snieder. *A guided tour of mathematical methods for the physical sciences*. Cam, 2006.

- [110] Seth Stein and Michael Wysession. *An Introduction to seismology earthquakes and earth structure*. Blackwell Publishing, 2007.
- [111] Robert S. Strichartz. *A guide to distribution theory and fourier transforms*. CRC Press, 1994.
- [112] Werner Stumm and James J. Morgan. *Aquatic Chemistry*. Wiley-Interscience, 1970.
- [113] X. M. Tang, C. H. Cheng, and M. N. Toksöz. Dynamic permeability and borehole stoneley waves: A simplified biot-rosenbaum model. *The Journal of the Acoustical Society of America*, 90, 1991.
- [114] Xiao-Ming Tang and Chuen Hon Arthur Cheng. *Quantitative borehole acoustic methods*, volume 24 of *Handbook of geophysical exploration series*. Gulf Professional Publishing, 2004.
- [115] Ikuo Towhata. *Geotechnical earthquake engineering*. Springer, 2008.
- [116] C. Truesdell. *Six lectures on modern natural philosophy*. Springer-Verlag, 1966.
- [117] C. Truesdell and K. R. Rajagopal. *An introduction to the mechanics of fluids*. Birkhuser, reprint of the 1999 edition edition, 2009.
- [118] Arkady Tsinober. *The essence of turbulence as a physical phenomenon: with emphasis on issues of paradigmatic nature*. Sprin, 2014.
- [119] G. Della Vecchia. An analytical expression for the determination of in situ stress state from borehole data accounting for breakout size. *International Journal of Rock Mechanics & Mining Sciences*, 66:64–68, 2014.
- [120] A. Verruijt. *An introduction to soil dynamics*, volume 24 of *Theory and Applications of Transport in Porous Media*. Springer, 2010.
- [121] Herbert F. Wang. *Theory of linear poroelasticity: with applications to geomechanics and hydrogeology*. Princeton University Press, 2000.
- [122] Eric W. Weisstein. Boxcar function.
- [123] J. R. Welty, C. E. Wicks, R. E. Wilson, and G. L. Rorrer. *Fundamentals of momentum heat and mass transfer*. John Wiley & Sons, Inc, 2008.
- [124] S. Whitaker. Diffusion and dispersion in porous media. *AIChE Journal*, 13:420, 1967.
- [125] E. B. Williams. Fundamental concepts of well design. *Ground Water*, 19(5):527–542, 1981.
- [126] Werner Wils. *Fliessen Stroemen und Turbulenz*. Wils, Andrea, 2010.
- [127] Werner Wils. *Dsensauginfiltration system Werner Wils*. Wils, Andrea, 2011.
- [128] Werner Wils. Jet suction infiltration system werner wils. 2011.
- [129] H. J. G. W. A. Wolfs, B. Snacken, R. J. Schotting, C. Snaterse, and de T. Vet. 15-10-2013. personal communications.
- [130] Jie-Zhi Wu, Hui-Yang Ma, and Ming-De Zhou. *Vorticity and vortex dynamics*. Springer-Verlag, 2006.
- [131] Hugh D. Young and Roger A. Freedman. *University Physics, with modern physics*. Pearson, Addison Wesley, 11th edition, 2004.
- [132] Arno Zang and Ove Stephansson. *Stress field of the Earth's crust*. Springer Science & Business Media, 2010.
- [133] J. Zruba. *Water Hammer in Pipe-Line Systems*, volume 43 of *Developments in Water Science*. Elsevier, 1993.